Chapter 1
INTRODUCTION

Catalysis Today

Scientific research has been changing its emphasis every decade and accordingly the manufacturing and processing sectors have been adopting new materials and concepts in their manufactured products. The developments in design strategy and introduction of new synthetic methodologies have thrown open a number of choices and it has become a tough proposition to select the material for a given application. One such area, where material selection has been a demanding proposition in the last four to five decades is the selection appropriate anode material for the photoelectrochemical cells [1] for the following:

1.Eespecially for the decomposition of water [2]

2. Reduction of carbon dioxide [3]

3 Photo-catalytic reduction of dinitrogen

4 Decontamination of water and air and pollutants removal

Are a few reactions of great relevance in the context of energy carrier or conversion. Even though the governing principles [4] for each of these reactions have been postulated and their applicability established beyond doubt, the selection and application of the most appropriate material that can be employed for commercial endeavour for these reactions so as to be economically viable is still eluding [5]. The primary purpose of this monograph is to address this aspect even though it is the realized that a complete and fully satisfactory solution may not evolve so easily, at least one can formulate a path in finding the solution.

Catalysis has been the corner stone of chemical manufacturing industry. The corner stone of a successful catalyst development depends on the identification and generation of adequate number of so-called active sites [6]. A simple one component catalyst system itself can give rise to a variety of sites (both active and possibly inactive sites on the surface (refer to Fig.1 for a typical conceived defect surface) and this so-called heterogeneity makes the catalyst selection most often cumbersome.

Figure 1.: Representative model of a one component surface with possible active sites indicated.

Among the various manifestations of catalysis, Photocatalysis has taken a dramatic revolution these days. In simple terms a catalyst (usually a semiconductor or possibly an insulator) is irradiated with light of suitable wavelength corresponding to the energy of the band gap, electrons normally present in the usually or mostly filled energy levels of the valence band will be transferred to the allowed unoccupied energy levels of the conduction band and thus creating a hole in the valence band and an active electron in the conduction band. This photo-generated electron-hole pair can be directed to perform both reduction and oxidation reactions simultaneously and in doing so the photon is technically consumed in the reaction. The photon can also be absorbed by the substrate, thus generating an excited state of the substrate and the science that follows is conventionally termed photochemistry. It may become obvious that the term photocatalysis is possibly misleading since catalysis means the catalyzing species has to be regenerated at the end of the catalytic reaction. A simple pictorial representation of photocatalytic decomposition of water (the details of this process will be considered subsequently) is shown in Fig.2.

Figure 1.2: Schematic representation of charge transfer across a semiconductor-substrate interface indicating both reduction and oxidation reactions taking place [7]

The advent of this possibility has given rise to a change in face of the field of catalysis. It is generally considered that the energy position of the bottom of the conduction band and the top of valence band of the semiconductor respectively denote the reducing and oxidizing power of the semiconductor and thus facilitating the selection of appropriate substrates that can undergo decomposition. This interesting reaction sequence as a result of photon absorption by the semiconductor has been exploited in a number of ways like

decontamination of water and air, [8] or generation of chemicals by p8otocatalytic routes [9]. A typical general scheme is shown in Fig.3 for the use of photocatalysis for pollutant removal.

Heterogeneous photo-catalysis is thus evolving as a versatile low cost, environmentally benign technology and these applications can be expected to be exploited in many ways in the coming days.

This changing face of catalysis not only introduced a new branch of science called photocatalysis but also added new challenges in addition to the various challenges that are already present in the field of catalysis like the use of alternate feed stocks for the production of value-added chemicals [10]. The main challenge of this new face of catalysis namely photocatalysis is to provide the governing principles for the selection of catalysts.

Figure 1.3: A typical representative scheme of pollutant removal by a photocatalysis; Reproduced from A.O.Ibhadon and P.Fitzpatrick, Catalysts, 3,189 (2013).

1.2 Photocatalysis Today

For some obvious reasons, like the possibility of utilizing the solar radiation and the amount acquired knowledge on the physics, semiconductors (among them TiO_2 based systems especially) have been the material of choice, though of late nano metals have also been proposed as possible candidates for the new phenomenon called Plasmonic Catalysis [11]. The motivation for modifying semiconductors [like doping (both anionic and cationic sites), coupling (two or more semiconductors and inclusion of co-catalysts), and compounding (generating ternary and other quaternary systems) is probably to mimic natural photosynthesis and also the anxiety to utilize major portion of the available solar radiation which is nearly in the visible region. Even though nearly four decades of research has been expanded in search for the suitable and viable semiconductor material and nearly more than 400 semiconductors with all possible modifications have been screened, it must be admitted that still the appropriate material which can satisfy all the desired characteristics is yet to be identified.

This presentation therefore attempts to address this particular question. This possibly requires an understanding of the physics of semiconductor-electrolyte interface. Interested readers can refer to authoritative documents on this topic elsewhere [12]. There are also other questions relating to this topic which requires careful examination of the possibilities. Some of them are:

1.Is it necessary to look for materials which will absorb photons in the visible region or is it sufficient or is it advisable to try other materials which will absorb only in the UV region? This question arises due to the fact that the energy available in the UV region of the solar radiation may be more than sufficient for the requirements of earth.

2, In photoelectrochemical cells, thin films and in photocatalysis, powdered polycrystalline samples are normally employed. It may be worthwhile to examine if these are the appropriate geometry for harnessing maximum efficiency?

3. In the modification of the semiconductors, doping is most often resorted to and it may be necessary that these methods of alteration of the electronic properties of the semiconductors have been standardized so that interpretations can be within one framework.

4. The selection of the semiconductor is mostly based on the value of the band gap, nature of the semi-conductivity (direct or indirect) and possibly photon absorption coefficient but it is not clear all these parameters are enough and how weightage has to be given to each of these parameters.

References

1.F.E. Osterloh, Inorganic nanostructures for PEC and photocatalytic water splitting, Chem. Soc. Rev., 42,2294-2340 (2013); Inorganic materials as catalysts for photochemical splitting of water, Chem. Mater., 20,35-54 92008).

2. X. Chen, S. Shen, L. Guo and S.S. Mao, Semiconductor based photocatalytic hydrogen generation, Chem. Rev., 110,6503-6570 (2010); Y. Wu, P. Lazic, G. Hautier, K. Persson and G. Ceder, First principles high throughput screening of oxynitrides for water splitting photocatalysts, Energy and Environmental Science, DOI10.10391(2ee2348c.(2012).

3.S. Kohtani, E. Yoshioke and H. Miyabe, Photocatalytic hydrogenation on semiconductor Particles, chapter 12 (http://dx.doi.org/10.5772/45732

4. K. Rajeshwar, Fundamentals of semiconductor electrochemistry and photo-electrochemistry, Encyclopedia of Electrochemistry Semiconductor Electrodes and Photo-electrochemistry, Vol-6, Wiley (2002)

5.I.E.Castelli, D.D. Landis, K.S. Thygesen, S. Dahl, Ib Chorkendorff, T.F. Jaramillo and K.W. Jacobsen, New Cubic perovskites for one- and two photon water splitting using the computational materials repository, Energy and Environmental Science, 5,90349043 (2012)

6. B. Viswanathan, The concept of active sites in Catalysis, in Catalysis Principles and applications, Narosa Publishing House, New Delhi, (2007) pp.384-389.

7. P.V. Kamat, Manipulation of charge transfer across semiconductor interface: a criterion that cannot be ignored in photocatalyst design, J. Phys. Chem. Lett., 3,663-672 (2012).

8. J.A. Byrene, P A Fernandez-Ibanez, P.S.M. Dunlop, D.M.A. Alrousan and J.W.J. Hamilon, Photocatalytic Enhancement for solar disinfection of water: A review, International Journal of Photoenergy, volume 2011 Article ID 798051 (2011) DOI:10.1155/2011/798051

9. B. Viswanathan, and M.Aulice Scibioh. Photo-electrochemistry Principles and Practice, Narosa Publishing House, New Delhi, (2013)

10.B. Viswanathan, The changing face of Catalysis, Chemical Industry Digest, 100-104, October, 2013.

11. P. Wang, B. Huang, Y. Dai and M.H. Whanbo, Plasmonic Photocatalysis: Harvesting visible light with noble metal nanoparticles, Phys. Chem. Chem. Phys., 14, 9813-9825 (2012); N. Serpone and A.V. Emeline, Semiconductor photocatalysis - past, present and Future outlook, J. Phys. Chem. Lett., 3.673-677 (2012)

12. M.X. Jan, P.E. Laibinis, S.T. Nguyen, J.M. Kesselman, C.E. Stanton and N.S. Lewis, Principles and Applications of semiconductor Photochemistry, Progress in Inorganic Chemistry, 41,21-144 (1994); Z. Zhang, and J.T. Yates, Band bending in semiconductors: Chemical and Physical consequences at surfaces and interfaces, Chem. Revs., (2012)

Chapter 2
AN OVERVIEW OF PHOTOCATALYSIS

1.1 Introduction

There is generally a conception that Photo-catalysis originated with the discovery of Photo-electrochemical decomposition of water by Fujishima and Honda [2] in the 70s. Photo-catalysis which is a phenomenon where in an acceleration of a chemical reaction in the presence of photons and catalyst has been reported in the literature in 50s (possibly even earlier to this) by Markham and Laidler [20]. Sister Markham followed this with a publication in chemical education [19] wherein she reported the photo-catalytic properties of oxides. In fact, Sister absorption of photons by the solid which generate electron hole pair which are utilized in the generation free radicals (hydroxyl radicals (.OH)). The chemical consequence of this process today goes with the name of advanced oxidation process (AOP; which may or may not involve TiO2 and Photons). Markham had a number of subsequent publications on the photo-catalytic transformations on irradiated zinc oxide [12]. Photo-catalysis deals with the Photochemistry has been an integral part of life on earth. One often associates photo-catalysis with photosynthesis. However, the term photo-catalysis found mention in an earlier

work by Plotnikov in the 1930's in his book entitled Allaemeine photochemie. The next major systematic development as stated in the previous paragraph was in the 1950's when Markham and Laidler performed a kinetic study of photo oxidation on the surface of zinc oxide in an aqueous suspension. By the 1970's researchers started to perform surface studies on photo-catalysts like Zinc Oxide and Titanium dioxide. The most commonly employed photo-catalyst is Titanium dioxide. TiO2 exists mainly in three crystallographic forms, namely Brookite Anatase and Rutile. There have been a number of studies on the three modifications of titania. The energetics of the titania polymorphs were studies by high temperature oxide melt drop solution calorimetry. It has been shown that relative to bulk rutile, bulk brookite is 0.71±0.38 kJ/mol and bulk anatase is 2.61±0.41 kJ/mol higher in enthalpy. [21]. The effect of particle size on phase stability and phase transformation during growth nanocrystalline aggregates and has been shown that mixed phases transforms to brookite and/or rutile before brookite transforms to rutile. [13] Among these three forms, the most often used photo-catalyst is the anatase phase either in pure form or in combination with rutile form. There are various reasons for this preference of TiO2 as photo-catalyst. These reasons include that it was the first system studied by Fujishima and Honda and TiO2 exhibits possibly maximum photon absorption cross section (i.e., it absorbs maximum number of photons of correct wavelength). This preference over TiO2 is seen from the data given in Table 1.

Table 1 Statistical distribution of scientific publications focused on nanomaterials for PEC/Photo-catalysis hydrogen production [15]

Materials	percentage of study
TiO_2	36.2
Non-TiO_2Oxides	10.9
Oxy-sulphides	18.8
Oxy-nitrides	5.1
Other semiconductors	5.8
Composites and Mixtures	17.4
Non-semconductors	5.8
Total	100

Degussa P25 Titanium dioxide generally employed as catalyst in many of the studies reported in literature and hence, considered as standard for photocatalytic activity comparison, contains both anatase(about 80 percent) and rutile (about 20 percent). It is in general impossible to completely trace the history of Photo-

catalysis. Even Fujishima and his coworkers [3] have expressed concern on completely outlining the history of photo-catalysis. The main difficulty appears to be that photo-catalysis unlike other chemical reactions involves simultaneously both oxidation and reduction reactions on a surface possibly assisted by photons of appropriate wavelength corresponding to the band gap of the semiconductor employed as catalyst. In 1921 Renz reported that titania was partially reduced when it was illuminated with sunlight in the presence of organic substrates like glycerol. [24] In 1924, Baur and Perret [?] probably were the first to report the photo-decomposition of silver salt on ZnO to produce metallic silver. Probably Baur and Neuweiler [5] were the first to recognize that both oxidation and reduction are taking place simultaneously on the production of hydrogen peroxide on ZnO. This was followed by the work of Renz in 1932 [25] who reported the photocatalytic reduction of silver nitrate and gold chloride on TiO2. Goodeve and Kitchener [6] studied the photo-catalytic decomposition of dye on titania surfaces and even reported the quantum yields. In 1953, it has been recognized that the organic substrate was oxidized and oxygen was reduced. Unfortunately, these studies have been carried out on ZnO surfaces and hence could have been hampered because of the inevitable problem of photo corrosion of ZnO. [20] There were few attempts in between for the production of hydrogen peroxide and decomposition of dyes on illuminated semiconductor surfaces. There were attempts to study the photo-catalytic oxidation of organic substrates on a variety of oxide surfaces from other parts of the world in and around this period. In the 1960s photo-electrochemical studies on ZnO with various redox couples were started. All these studies culminated in the photo-electrochemical decomposition of water by Fujishima and Honda which opened up means for solar energy conversion and also for the generation of hydrogen fuel. Subsequently Bard and his coworkers [16] have demonstrated that illuminated TiO_2 could be used for the decontamination of water by photo-catalytic decomposition. This has led to new photo-catalytic routes for environmental clean-up and also for organic synthesis. These aspects will be dealt with in separate chapters in this monograph. Fujishima et al., have provided a more detailed and authentic write-up on the history of photo-catalysis. [3]

1.2 Basic Principle of Photocatalysis

According to the glossary of terms used in photochemistry [IUPAC 2006 page 384] photo-catalysis is defined as the change in the rate of a chemical reaction or its initiation under the action of ultraviolet, visible or infra-red radiation in the presence of a substance the photo-catalyst that absorbs light and is involved in the chemical transformation of the reaction partners. When a semiconductor (or

an insulator) is irradiated with light of suitable wavelength corresponding to the energy of the band gap, electrons occupying the usually or mostly filled energy levels in the valence band will be transferred to an allowed energy state in the normally empty conduction band thus creating a hole in the valence band. This electron-hole pair is known as exciton. These photo-generated electron-hole pairs promote the so-called redox reaction through the adsorbed species on the semiconductor or insulator surface. However, the band gap of the insulators will be usually high and as such generating of such high energy photons will not be comparatively easy and hence insulators are not considered as possible candidates for Photo-catalysis. Generally, metals cannot be employed as photo-catalysts since their occupied and unoccupied energy states are overlapping with respect to energy and hence the recombination of electron-hole pair will be the most preferred process and hence the conversion of photon energy to chemical energy using metals will not be advantageous. It is generally considered that the energy position of the top of the valence band of a semiconductor is a measure of its oxidizing power and the bottom of the conduction band is a measure if its reducing capacity. It is therefore necessary one has to know with certain level of certainty the energy positions of the top of the valence band and bottom of the conduction band so that the reactions that these excitons can promote can be understood. One such compilation is given later in this chapter in Table 3 and more extensive data are given in Appendix. Photo-catalytic destruction of organic pollutants in water is based on photochemical process involving semiconductors. When a semiconductor is irradiated with UV (usually but it can be any other radiation as well) light of wavelength appropriate for excitation from valence band to the conduction band of the chosen semiconductor an exciton is created. The photochemical oxidation of the organic substrate normally proceeds by the adsorption of the substrate on the surface of the semiconductor with transfer of electrons with the hole generated. However other possible oxidation processes can also take place with radicals generated (OH radical if the solvent is water) at the surface of the semiconductor surface. Thus a variety of surface reactions will take place on the photo-excited semiconductor surface, the preferred reaction depends on the nature of the substrate under consideration and its nature of adsorption and activation on the semiconductor surface. In Fig 1 a simple representation of these possible processes are shown by considering simple general reactions water giving hydroxyl radicals and organic substrate being oxidized all the way to carbon dioxide and water in order to get an idea of what can takes place on the surface of semiconductor as a result of photoexcitation and catalysis. Since it is possible that the organic substrate can

be completely degraded to carbon dioxide and water, this process has been considered to be a viable method for the decontamination of water. In addition, it should be kept in mind that hydroxyl radical is a powerful oxidizing agent as compared to other common oxidizing agents as can be seem from the data given in Table.2. It is clear from the data given in Table.2 that the aqueous phase reactions will still be preferred in Photo-catalysis.

Figure 1.1: Schematic representation of the principle of photocatalysis showing the energy band gap of a semiconductor particle. Typical reactions considered are: water → hydroxyl radical; organic substrate + hydroxy radical→ carbon dioxide + water + mineral acid/

Table 2 Oxidizing power of some of the commonly employed oxidizing agents.

Oxidant	Oxidation Potential(V)
Hydroxy Radical	2.80
Ozone	2.07
Hydrogen Peroxide	1.77
ClO_2	1.49
Chlorine (Cl_2)	1.35

1.3Limitations of photo-catalysis

Though Photo-catalytic technology has been emerging as a viable technology for the remediation of pollutants from water, it can be applied to a variety of compounds. One of the factors to be considered is the possibility of mass transfer limitations due to the characteristics imposed in the reaction chamber by the existence of the catalyst in various forms in dispersed state. In fact the construction of a appropriate photo-chemical reactor itself has been a major issue and various designs have been proposed in literature. A simple reactor design conventionally employed is shown in Fig.2. Sclafani et al. [4] postulated external

mass transfer limitations to interpret their results in a packed bed reactor filled with spheres of semiconductor catalyst (in this case pure titanium dioxide (ca. 0.12 cm in diameter)). Chen and Ray [8] studied internal and external mass transfer limitations in catalytic particles of photo-catalytic reactors and concluded only mild mass transfer restrictions since the effectiveness factor observed was near 0.9 and hence rotating disc photo reactor when the spherical particles of the semiconductor fixed on a solid support. The specific role of mass transfer was analyzed in terms of one of the dimensionless Damkhler numbers. In other reactor configurations, particularly films and membrane reactors other quantitative observations of internal mass transfer limitations have been published. [9], [7] and many others (see for example one of the reviews on this topic in Legrini et al. [22]. Unfortunately, these limitations have not been examined with other type of reactors like slurry reactors. In addition, since photons are coupling with a heterogenous system, this can result in gradients in concentration or the coupling of the photon field with the scattering particles. The points that emerge from the data presented in these two tables are that the top of the valence band is nearly the same for the oxide semiconductors and the bottom of the conduction band depends on the cation involved and hence the oxide semiconductors will be more or less behaving in a similar manner. The other chemical limitations involved in the photo-catalytic degradation of pollutants from water are: The adsorption of the pollutant species on the surface of the semiconductor. This fact has been recognized in the literature but still not many quantitative relationships have emerged indicating the importance of this step in the photo-degradation processes. However, the importance of this step is apparent since the charge transfer from the semiconductor to the substrate and hence cause their degradation is possible only in the adsorbed state of the substrate since charge transfer has restrictions with respect to distances involved. In addition the adsorption is directly related to the surface area of the photo-catalyst and hence it is conventional to optimize the surface area of the photo-catalyst. The pH may also have an effect on the photo-degradation of organic pollutants since the nature of the species involved can change with respect to pH. In addition in aqueous medium the potential changes by 59 milli-volts per pH unit and this also can affect the process of degradation. In solution phase, the presence of both type of counter ions namely, anions and cations can affect the photo-degradation process due to reasons like photon absorption by the ions and also the type of species that will be generated as a result of photon absorption. When the composite solar radiation is employed for photo-degradation process, the temperature of the system can affect all the reactions (normally increase is

noticed) except for the electron hole creation step. However, the solubility of oxygen will decrease with increase in temperature and this can also affect the rate of photo-degradation reaction. In a separate chapter, the studies reported on the application of photo-catalysis for the decontamination of water will be considered. This field seems to assume importance in these days due to various reasons. However, the studies reported in this area have to be considered with care since the products of oxidation and their effects have not yet been established though it is generally assumed to be carbon dioxide. As seen earlier that one of the areas in which photocatalysis has been extensively employed is the decontamination of water. Water covers over tow thirds of earth's surface and less than a third is the land area. Oceans, rivers and other inland waters are continuously polluted by human activities leading to a gradual decrease in the quality of water. There are specified limits of concentration beyond which the presence of some substances is considered as polluting water. In Table 5, the recommended tolerance limits of pollutants are given. The common pollutants in water are classified as inorganic contaminants and organic pollutants. The main inorganic contaminants are the metal ions, nitrates, nitrites, nitrogen dioxide, ozone, ammonia, azide and halide ions. There are various studies reported in literature that deal with the photocatalytic decomposition or transformation of these inorganic contaminants. This will be dealt with in a separate chapter. Photocatalytic decomposition (mostly oxidation) of organic pollutants has been of great interest. In these studies, the reaction is carried out in presence of molecular oxygen or air for complete oxidation to carbon dioxide and water and possi bly inorganic mineral acids as the final products.It has been shown that man of the organo-chlorides, pesticides, herbicides and surfactants are completely oxidized to carbon dioxide, water and hydrochloric acid. It may be worthwhile to realize the effect of some of the pollutants on human health. The data collected from literature are given in Table.6. It is to be remarked the effects of pollutants generally affect the human health in a variety of ways basically affecting the nervous system.

Figure 1.2: Typical reactor design conventionally employed for the photo-splitting of water.

Table.3. Electro-negativity, [χ], Band gap,(Eg) energy levels of the conduction band bottom (ECB) and energy position of the top of valence band (E V B) [data extracted from Y.Xu and M.A.A. Schoonen, American Mineralogist, 85, 543-556 (2000)]

Substance oxide	Electronegativity (χ)	Band gap (E_g)	Conduction band E_{CB}	Valence Band E_{VB}
$BaTiO_3$	5.12	3.30	-4.58	-7.88
Bi_2O_3	6.23	2.80	-4.83	-7.63
$CoTiO_3$	5.76	2.25	-4.64	-6.89
CuO	5.81	1.70	-4.96	-6.66
Fe_2O_3	5.88	2.20	-4.78	-6.98
Ga_2O_3	5.35	4.80	-2.95	-7.75
$KNbO_3$	5.29	3.30	-3.64	-6.94
$KTaO_3$	5.32	3.50	-3.57	-7.07
$MnTiO_3$	5.59	3.10	-4.04	-7.14
Nb_2O_5	6.29	3.40	-4.59	-7.99
NiO	5.75	3.50	-4.00	-7.50
$NiTiO_3$	5.79	2.18	-4.70	-6.88
PbO	5.42	2.80	-4.02	-6.82
SnO_2	6.25	3.50	--4/50	-8.00
$SrTiO_3$	4.94	3.40	-3.24	-6.64
TuO_2	5.81	3.20	-4.21	-7.41
V_2O_5	6.10	2.80	-4.70	-7.50
WO_3	6.59	2.70	-5.24	-7.94
ZnO	5.79	3.20	-4.19	-7.39
ZrO_2	5.91	5.00	-3.41	-8.41

Table.4. Band positions of some semiconductor photo-catalysts in aqueous solution at pH =1 and positions are given in volts versus NHE.

Semiconductor material	Valence Band V vs NHE	Conduction band V vs NHE	Band Gap (eV)	Band gap (wavelength)
TiO_2	+3.1	-0.1	3.2	387
SnO_2	+4.1	+0.3	3.9	318
ZnO	+3.0	-0.2	3.2	387
ZnS	+1.4	-2.3	3.7	337
WO_3	+3.0	+0.2	2.8	443
CdS	+2.1	-0.4	2.5	490
CdSe	+1.6	-0.1	1.7	729

In addition, there are some Persistent Organic Pollutants (POP) like aldrin, chlordane DDT, hexachlorbenzene, furans, polychlorinated biphenyls, Polycycic aromatic hydrocarbons (PAHs) and so on. These substances some of which are called the dirty dozen cause many disorders including cancer breast cancer, damage to reproductive system, neuro-behavioural disorders and health related concerns.

Table 5 Recommended tolerance limits of pollutants in water [Data collected from K.C.Agarwal, Industrial power engineering and Applications, Butterworth-Heinemann, pp.565 (2001)

S.No	Parameter	Recommended Tolerance level
1	Biological Oxygen Demand (BOD)	30 mg/l
2	Chemical Oxygen Demand (COD)	250 mg/l
3	Alkali traces	maximum upto pH 9
4	Acid	Not less than pH 5.5
5	Total suspended solids	100 mg/l
6	Oil and Grease	10 mg/l
7	Dissolved phosphates as P	5 mg/l
8	Chlorides as Cl	600 mg/l
9	Sulphates (as SO_4)	1000 mg/l
10	Cyanides as (CN)	0.2 mg/l
11	Total Chromium	2 mg/l
12	Hexavalent chromium	0.1 mg/l
13	Zinc as Zn	0.25 mg/l

14	Iron	3 mg/l
15	Total heavy metals	7 mg/l
16	Total Phenolic compounds	1 mg/l
17	Lead (Pb)	0.1 mg/l
18	Copper as Cu	2 mg/l
19	Nickel as Ni	2 mg/l
20	Bioassay test	89% survival after 96 hours

1.4. Advanced Oxidation Processes

Irrespective of the method of generation of hydroxyl radicals, the methods which utilize hydroxyl radicals for carrying out the oxidation of the pollutants are grouped as Advanced Oxidation Processes. Hydroxyl radicals are extraordinarily reactive species and have one of the highest oxidation potential (2.8 V). The values of rate constants in reactions with organic substrates are in the range of 106 - 109 $M^{-1} s^{-1}$ [23][1] [14] (Table 7). In addition, hydroxyl radicals do not show any selectivity with respect to the position of attack on the organic substrates which is useful aspect for the treatment of water. The fact that the production of hydroxyl radicals can be made by a variety of methods adds to the versality of Advanced Oxidation Processes thus allowing a better compliance with the specific treatment requirements. An important consideration to be made in the application of AOP to waste water treatments is the requirement of expensive reactants like hydrogen peroxide and /or ozone. Hence, AOP cannot replace the application of more economical treatments methods such as biological degradation whenever possible. A list of the different possibilities offered by AOP are briefly given in Table 8.

Table 6 Possible pollutants in water and their effect on human health

Pollutant	Adverse effect on human health
Atrazine	Cancer, damage to nervous system
Benzene	Cancer anemia
Pentachlorophenol	Liver and Kidney damage and Cancer
Trichloroethylene	Cancer
Trichloroethane	Damage to Kidney, liver and nervous system
Bromoform	Damage to nervous system and muscle
Carbofuran	Damage to nervous system, kidney reproductive system
Carbon tetrachloride	Cancer
Chlorobenzene	Damage to nervous system, kidney and liver

Dibrinichloroethane	Damage ti nervous system muscle and cancer
Eridriin	Damage to nervous system, kidney, liver anemia and cancer
Ethylbenzene	Damage to nervous system, liver and Kidney
Heptachlor	Cancer
Heptachlor epoxide	Cancer
Hexachlorocyclopentadiene	Damage to Kidney and stomach
Lindane	Damage to nervous system liver and kidney
Simazine	Damage ti nervous system, Cancer
Styrene	Damage to nervous system, liver
Tetrachloroethylene	Damage to nervous system, Cancer
1,2,4-trichlorobenzene	Damage to liver and Kidney
Xylene pesticides	Damage to nervous system kidney lungs and membranes
Toluene	Damage to nervous system, liver and kidney

,

Table.7. Values of second order rate constants for the oxidation by ozone and hydroxyl radical for a variety of compounds [data from [23]]

Organic compound	value of rate constant M−1 s −1	
	Ozone[a]	OH radical[b]
Benzene	2	7.8 X 10^9
n-butanol	0.6	4.6 X 10^9
t-butanol	0.3	0.4 X 10^9
Chlorobenzene	0.75	4 X 10^9
Tetracholoroethylene	<0.1	1.7X 10^9
Tolunene	14	7.8X10^9
Tricholorethylene	17	4.0X10^9
		a.

a- from Hoigne and Bader, 1983; b- from Farhataziz and Ross, 1977.

Table 8 Sources involved in the various Advanced Oxidation Processes

Source of Oxidants	Name of the processes
$H_2O_2/Fe^{2=}$	Fenton
H_2O_2/Fe^{3+}	Fenton like
H_2O_2/Fe^{2+}, Fe^{3+}/UV	photo-assisted Fenton
TiO_2 hν/O_2	Photocatalysis
O_3 or H_2O_2/UV	Photo-assisted oxidation

Heterogeneous Photo-catalysis

Among the AOPs mentioned, photo-catalysis is the promising method. This is attributed to its potential to utilize energy from the sun without the addition of others forms of energy or reagents. The reactions carried out by the photo-catalysts are classified into two categories namely homogeneous or heterogeneous photo-catalysis. Heterogeneous photo-catalysis is based on the semiconductors which are employed for carrying out various desired reactions in both liquid and vapour phases. Photo-catalysis involve the formation of highly reactive electrons and holes in the conduction and valence bands respectively. The electrons are capable of carrying out reduction reactions and holes can carry out oxidation reactions. There are also other processes that take place in the semiconductor. The electron and hole can react with acceptor or donor molecules respectively or recombine at surface trapping sites. They can also be trapped at bulk trapping sites and recombine with the release of heat. The electron hole can be exploited in a number of ways:(i) For producing electricity(solar cells)-Photo-voltaics; (ii) For decomposing or removing pollutants-Photo-oxidation;(iii) For the synthesis and production of useful chemicals-Photo-catalysis;(iv) For the photo-electrolysis of water-photo-electro-chemistry. As the recombination of the photogenerated electron and hole occurs on a pico-second time scale, electron transfer at the interface can kinetically compete with recombination only when the donor or acceptor is adsorbed on the surface of the semiconductor before irradiation. Hence adsorption of the substrate prior to irradiation is important for efficiency of the heterogeneous photo-catalytic process. [18]. Hydroxyl groups or water molecules adsorbed on the surface can serve as traps for the photogenerated hole, leading to the formation of hydroxyl radicals in the case of metal oxide suspensions. Strong adsorption of acetone and 2-propanol on ZnO has been observed during temperature programmed desorption [17]. Metal oxide surfaces have asurface density of about 4-5 hydroxy groups /nm2 as has been shown by the continuous distribution of adsorption energies in the Freundlich

isotherm. Many organic substrates were found to play the role of adsorbed traps for the photo-generated holes. For example, in a colloidal suspension of TiO2 in acetonitrile, radical ions are detected directly during flash excitation [17]. Apart from materials derived from TiO2 by modifications like doping, coupling with an additional phase or morphological changes different compounds with distinct composition and structure have also been examined. Various tantalates, [10] [11],niobates [26], Oxides of bismuth like Bi2W2O9, Bi2MoO6, Bi2Mo3O12 and oxides of Indium as In2O3,Ba2In2O5,MIn2O4 (M=Ca,Sr) were found to be capable of photosplitting water. Tantalum nitride and tantalum oxynitriede were also found to be effective catalysts for water splitting.

Bibliography

[1] A.Farhataziz and B.Ross. Selective specific rates of reactions of transients in water and aqueous solutions part iii hydroxyl radical and perhydroxyl radical and their radical ions. Natl.Stand.Ref.Data Ser.,USA (National Bureau of standards), 59:22–67, 1977.

[2] A.Fujishima and K.Honda. Electrochemical photolysis of water at a semiconductor electrode. Nature, 238:37–38, 1972.

[3] A.Fujishima, X. Zhang, and D.A.Tyrk. Tio2 photo-catalysis and related surface phenomena. Surface Science Reports, 63,515–582, 2008.

[4] A.Sclafani, L.Palmisano, and E.Davi. Photocatalytic degradation of phenol in aqueous titanium dioxide dispersion: The influence of iron 3+ and iron 2+ and silver 1+ on the reaction rate. J.Photochem.Photobiol A: Chemistry, 56:113, 1991.

[5] E. Baur and C. Neuweiler. Helv. Chim. Acta, 10:901–907, 1927.

[6] J.A. Kitchener C.F. Goodeve and. Trans. Faraday Soc. 34, 34:570–579 and 902–908, 1938. [7] J Chen, D.F. , Ollis, and H. 1173. Rulkens, W.H.and Bruning. Kinetic processes of photocatalytic mineralization of alcohols on metallized titanium dioxide. Water Res., 33.:1173, 1999.

[8] D.Chen and A.K. Ray. Photodegradation kinetics of 4- nitrophenol in tio suspension. Water Res., 32:3223., 1998.

[9] M.F.J Dijkstra, H. ., Buwalda, A.W.F. de Jong, A. Michorius, J.G.M. Winkelman, and A.A.C.M. Beenackers. Experimental comparison of three reactor designs for photocatalytic water purification. Chem.Eng.Sci., 56:547., 2001. 15

[10] F.E.Osterloh. g into h2 and o2 over lanthanum doped natio3 photocatalyst with high crystallinity and surface nanostructure. J.Am.Chem.Soc., 125:3082–3089, 2003.
[11] F.E.Osterloh. Inorganic materials as catalysts for photochemical splitting of water. Chem. Mater., 20:35–54, 2008.
[12] J.C.Kuriacose and M.C.Markham. J. Catal., 1:498–507, 1962.
[13] H.Zhang &J.F.Banfield. Undeerstanding polymorphic phase transformation behaviour during growth nanocrystalline aggregates: Insights from tio2. Journal of Physical Chemistry B, 104:3481–3487, 2000.
[14] J.Hoigne and H.Badar. Rate constants of reaction of oxzone with organic and inorganic compounds in water part ii dissociating organic compounds. Water Resour., 17:185–194, 1983.
[15] J.Zhu and M. Zach. Nanostructured materials for photo catalytic hydrogen production. Current opinion in colloid and interface Science, 14:260–269, 2009.
[16] B. Kraeutler and A.J. Bard. J. Am. Chem. Soc.., 100:4317–4318. ., 1978.
[17] M.A.Fox, C.C.Chen, and R.A.Lindig. Transients generated upon photolysis of colloidal titanium dioxidein acetonitrile containing organic redox couples. J. Am.Chem.Soc., 104:5828–5829, 1982.
[18] M.A.Fox and M.T.Dulay. Heterogeneous photocatalysis:. Chem. Rev., 93:341–357, 1993.
[19] M.C.Markham. Photocatalyic propertiesof oxides. J. Chem. Educ., pages 540–543, 1955. [20] M.C.Markham and K.J.Laidler. A kinetic study of photo-oxidations on the surface of zinc oxide in aquesou suspensions. J. Phys. Chem., 57:363–369, 1953.
[21] M.R.Ranade, A.Navrotsky, H.Z.Zhang, J.F.Banfield, S.H.Elder, A.Zaban, P.H.Borse, S.K.Kulkarni, G.S.Doran, and H.J.Whitfield. Energtics of nanocrystalline tio2. PNAS, 99:6476–6481, 2002.
[22] O.Legrini, E.Oloveros, and A.M.Braun. Photochemical processes for water treatment. Chem.Rev, 93:671–698, 1993.
[23] R.Andreozzi, V.Capiro, A.Insola, and RMarotta. Advanced oxidation processes (aop) for water purification and recovery. Catal. Today, 53:51– 59, 1999.
[24] C. Renz. Helv. Chim. Acta, 4:961–968, 1921.
[25] C. Renz. Helv. Chim. Acta, pages 1077–1084, 1932.
[26] Y.Ebina, N.Sakai, and T.Sasaki. Photocatalyst of lamellar aggregates of ruo2 loaded perovskite nanosheets for overall water splitting, J.Phys.Chem.,B, 109:17212–17216, 2005.

Chapter 3

GENERAL PRINCIPLES OF PHOTOCATALYSIS

The scope of photocatalysis is increasing day by day. However, the field of decontamination of pollutants (including some drug and dye molecules) has received considerable attention. This aspect will be dealt with in detailed manner in a separate chapter. The activation and conversion of stable molecules lie water. Carbon dioxide and dinitrogen still attract the attention of scientific community. In Figure 1, the various promoted by photocatalysis by semiconductors are shown.

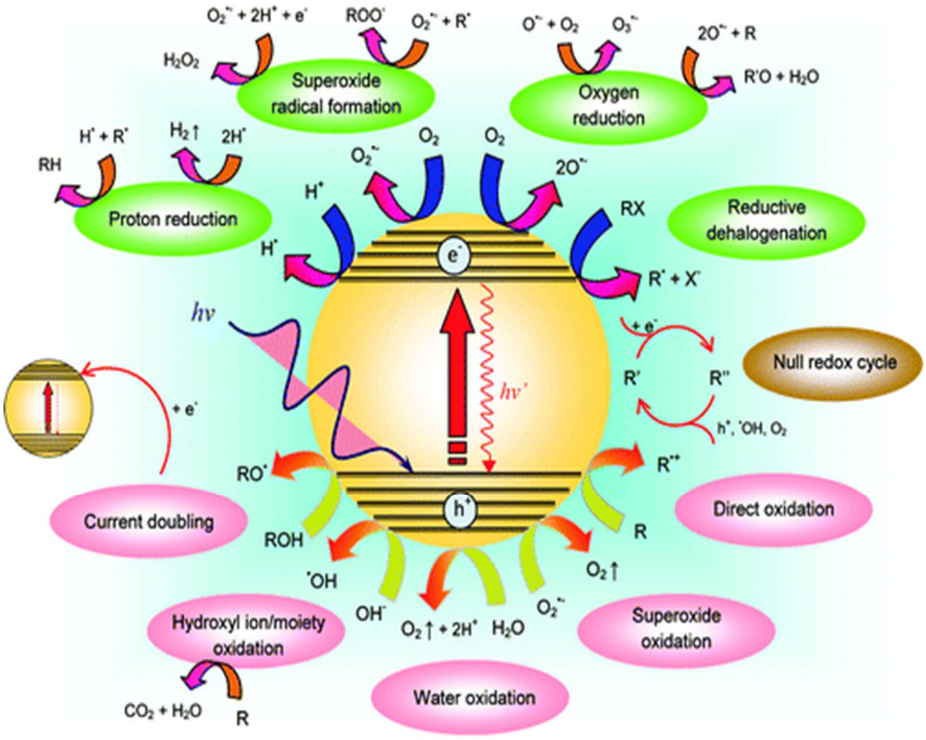

Figure 1 Various light induced reactions involved in semiconductor photocatalysis [Reproduced from reference Tech et al., J. Phys. Chem. Lett., 3, 629-639 (2012)].

It is seen a variety of oxidation and reduction reactions can be carried out as a result of photo-catalysis. In addition, a host of organic reactions and radical induced inorganic transformations can be promoted in this field. The basic principles involved in this type of photocatalytic reactions are shown in Figure 2 using TiO_2 as a typical photocatalyst. The photon absorption gives rise to an energic electron in the conduction band which can be utilized for the reduction (acceptor) reaction and the hole created in the valence band can be utilized in the oxidation (donor) reaction.

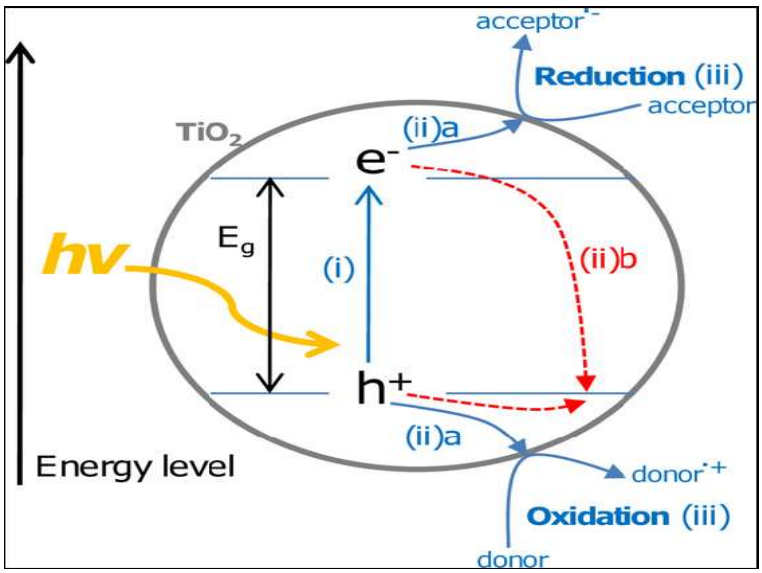

Figure 2. Various processes involved in semiconductor photocatalysis. (i) Photon absorption and electron–hole pair generation. (ii) Charge separation and

migration; (ii)a to surface reaction sites or (ii)b to recombination sites. (iii) Surface chemical reaction at active sites.[Leary et al carbon, 49. 741-772 (2011)]

Various Methods for Improving the Efficiency of Photocatalyst

These attempts are mainly concerned with facilitating the charge transfer efficiency/ This can be achieved in many ways. Among them is to alter the energy position of Fermii level of the semiconductor. In addition. It is possible to introduce the electron transfer agents or hole trapping species. For electron transfer process, one has to use agents which have high electron affinity and these are mostly noble metals. Like Au, Pt and so on. This situation is pictorially shown in Figure 3.

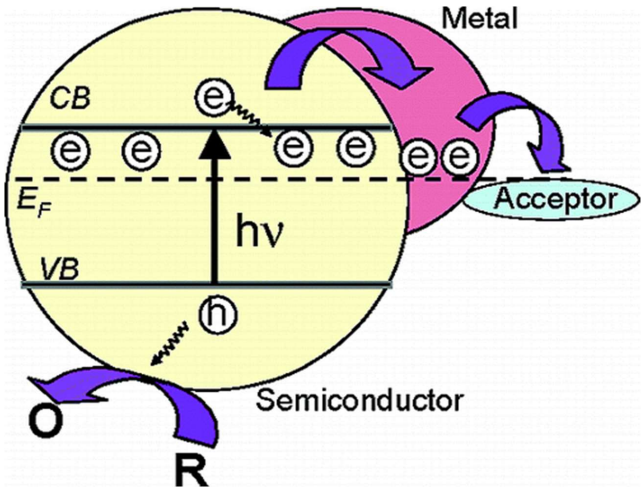

Figure 3 Metal deposited semiconductor to facilitate electron transfer to the acceptor species. Refer ti Subramanian et al., J. Am. Chem. Soc. 2004, 126, 4943-4950

2. Coupling of two semiconductors:

Another way to achieve efficient electron traanfer and decrease recombination of charge carriers is coupling two semiconductors. This can also be useful to use longer wavelenth radiaation that is shifting the photon source from UV to visible range. This has to satisfy that interfacial electron transfer between two

semiconductors with different conduction band edges will facilitate and also minimize electron-hole recombination. The possibilityis illustrated in Figure 4.

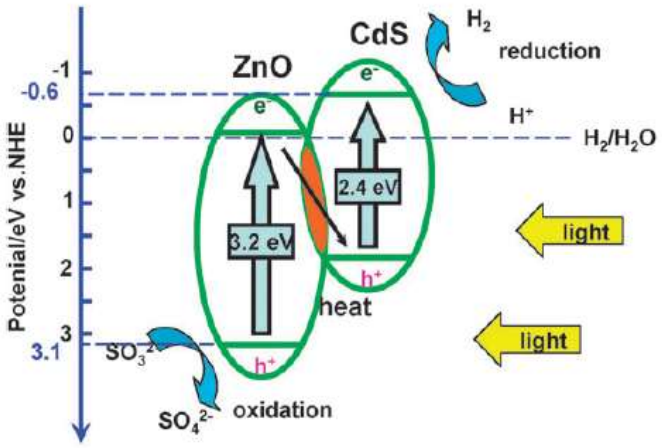

Figure 4 Coupling of two semiconducotrs Note the relative postions of the conduction band minima of the two semiconductors. See for example Wang et al. *Chem. Commun.,* **2009**, 3452–3454.

3.Sensitiization

Usually this is done by employing substances (Dyes) which will absorb radiations. The separation and transfer of the charges like in splitting of pure water was achieved with dye-coated photocatalyst which is attributed to good electronic contact between dye and photocatalyst. This is pictorially shown in Figure 5.

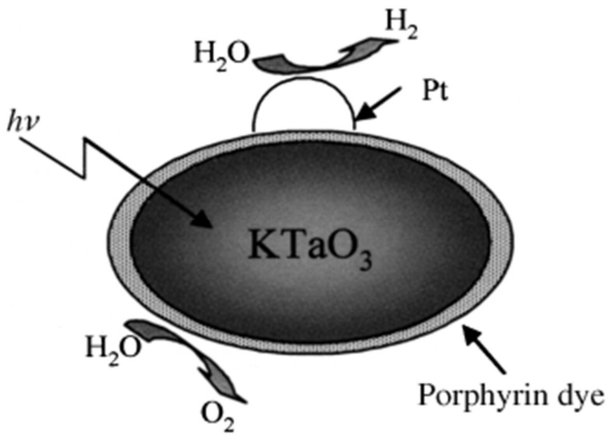

Figure 5 Dye coated semiconductor and the dye absorbs radiation or facilitate the charge transfer See for example Hagiwara et al. *Angew. Chem. Int. Ed*., 2006, 45, 1420–1422.

Doping with metal ions (Fe^{3+}, V^{5+} etc.) and non-metals (N, C, S etc.)

The doping process helps to introduces additional states in the semiconductor eg.TiO_2 there-by reducing the band gap and improving the visible light absorbing properties. The main drawbacks of these systems are (1) The new energy states introduced into the composite material can also act as recombination center for excitonic species especially when dopant concentration is high and (2) the thermal stability of the material will be affected.

There are other possibilities of activating and facilitating charge transfer process which will be taken up subsequently.

CHAPTER 4

PHOTOCATALYSIS – WHY SEMICONDUCTORS AND WHAT TYPE OF SEMICONDUCTORS

This branch of science has become popular since 1970s due to the possibility of generating fuel hydrogen from water by the action of photons and on a surface of a semiconductor (TiO_2). The photon energy is utilized in altering the reduction potential of electrons and the oxidation potential of the positive holes of semiconductor.

A band gap is the energy difference between the electrons of the valence band and the conduction band. Essentially, the band gap represents the minimum energy that is required to excite an electron to a state in the conduction band where it can participate in conduction. The lower energy level is the valence band, and thus if a gap exists between this level and the higher energy conduction band, energy must be input for electrons to change its potential. The size and existence of this band gap allow one to visualize the difference between conductors, semiconductors and insulators. These distances can be seen in diagrams known as *band diagrams*, shown in Figure 1. For more detailed account

how the bands are formed and other details, one should refer to a text book on solid state Physics [1].

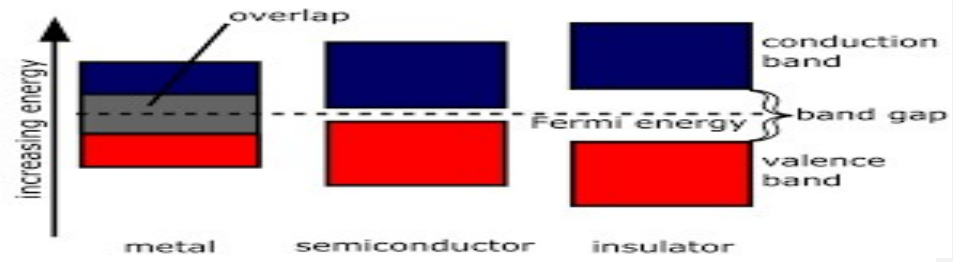

Figure 1. A band diagram with different values of band gaps for conductors (~0 eV), semiconductors (0-3 eV), and insulators (>4eV)

The energy positions of the bottom of the conduction band should be more positive with respect to the reduction potential of the substrate and the top of the valence band should be more positive with respect to the oxidation potential of the substrate. Here the potential scale used is the electrochemical scale not with respect to the absolute scale. This is pictorially shown in Figure.2.

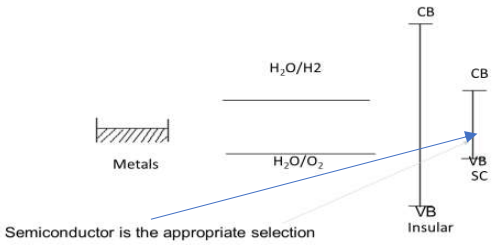

Figure 2 Water decomposition reaction and metals, semiconductors and insulators – why semiconductor band positions are favourable for this reaction.

Among the various semi-conductors, for water decomposition reaction which ones are suitable or not is shown in Fig.3.

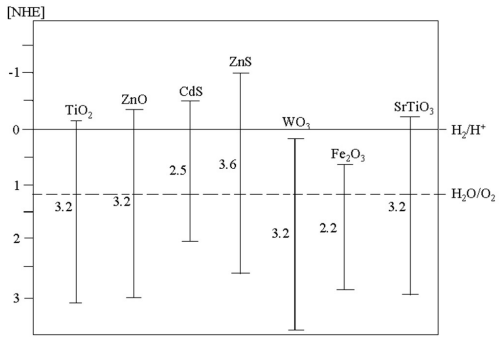

Figure 3 For water decomposition only those semiconductors whose conduction band bottom is more negative with respect to hydrogen evolution reaction and valence band maximum must be more positive with respect to oxygen evolution reactio. On this basis, the known semiconductors can be clasified as reuction (R) type oxidation (O) type or OR type or X type where both the reactions are not possible.

This leads one to classify the known semiconductors into 4 different types, namely the ones that will promote both oxidation and reduction reactions simutaneously designated as OR type. If the chosen semiconductor promotes either of the reaction, then they are termed as O or R type and the systems that cannot promote either of the reactions is called X type. This classification is based on the relative positions of the redox potentials and the bottom of the conduction band and the top of the valence band. A pictoral representation of these 4 different types of semiconductors is shown in Figure 4.

Figure 4 Types of semiconductors reduction (R) type; Oxidation type (O) Both reactions (OR) and niether of them (X) type

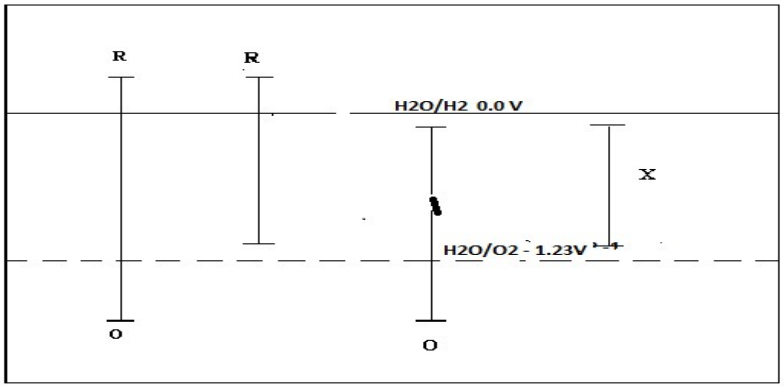

There can be competing reactions and instead of the water decomposition reactions these reactions will take place. For example, the case of ZnO semiconductor is considered here. If the dissolution potential of Zn^{2+} were to me more positive to hydrogen evolution reaction then this reaction will occur in preference to the hydrogen evolution. This process is called photo-corrosion and thus the material loss will take place. To prevent this type of degradation some deposits may be coated but it may adversely affect the photon absorption capacity of the semiconductor. These situations are shown in Figure 5 with respect to the energy scale with respect to Normal Hydrogen Electrode (NHE).

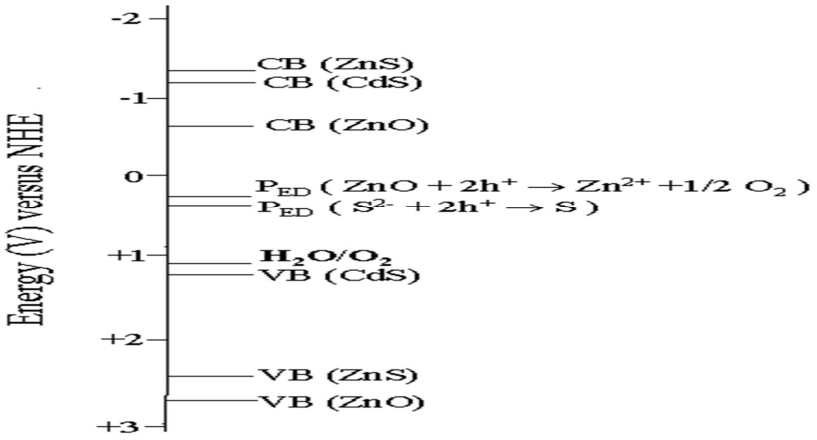

Figure 5 The energy scale for conduction band and valence band for a few semiconductors and the preferred photo corrosion reactions

When a semiconductor is irradiated with light whose wave length is equal to or shorten than the band gap value, an electron from the valence band will be excited and occupy an energy state in the conduction band. The positively charged state will remain in the valence band. Both these charged states can be utilized to promote a reduction reaction (electron) and an oxidation reaction (positive charged state) But for these reactions to take place, the charged states have to migrate to the surface. During this process, the charge states can recombine and thus not suitable for promoting the redox reaction. This recombination can take place in the bulk of the semiconductor or at the surface of the semiconductor.
These processes are pictorially shown in Figure.6.

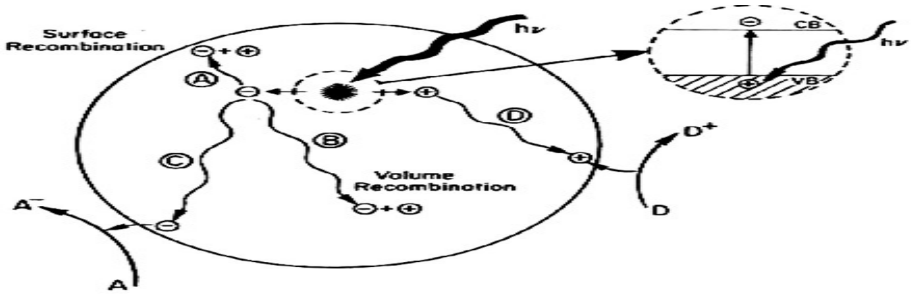

Figure 6. Creation of exciton and their process in the semiconductor and the donor and the acceptor reactions with the substrate [reproduced from ref A. Millis and S. L. Hunte *J. Photochem. Photobiol.* A: *Chem* 180 (1997) 1; ref 2]

Many types of sensitization are possible to facilitate the charge separation and utilizing the charged states in the proposed redox reactions. One of the methods goes with the name "*doping*" which can be incorporation or inclusion of alter valent ionic species in the semiconductor. For example, if in ZnO semiconductor. if either Li_2O creating positive charged state and termed as p-type or Ga_2O_3 (creates excess electronic states to facilitate the reduction reaction) and is termed as n-type doping.

One another striking way of sensitization, is called coupling of semiconductors. To make use of the radiation whose wavelength is longer than that is suitable for the semiconductor, then one can use a semiconductor whose band gap is suitable

for the light radiation available the charge states can be created in the second semiconductor and if the energy positions of the excitation states are suitable for transfer to the original semiconductor then these charged states can be utilized in the redox reaction. The situation considered is shown in Figure 7.

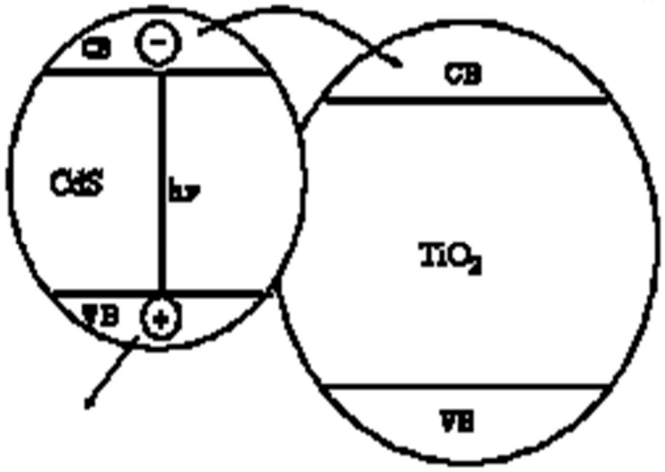

Figure 7. Coupling of semiconductors and the energy levels of the valence band and the conduction band positions facilitate the excited charged states to transfer to the original semiconductor.

For conventional redox reactions, one is interested in either reduction or oxidation of a substrate. In water decomposition, both the reactions have to take place at the rates corresponding to the stoichiometry of the molecule, namely for every mole of hydrogen evolved, half a mole of oxygen has to evolve.

For example, consider that one is interested in the oxidation of Fe^{2+} ions to Fe^{3+} ions then the oxidizing agent that can carry out this oxidation is chosen from the relative potentials of the oxidizing agent with respect to the redox potential of Fe^{2+}/Fe^{3+} redox couple.

The oxidizing agent chosen should have more positive potential with respect to Fe^{3+}/Fe^{2+} couple so as to affect the oxidation, while the oxidizing agent undergoes reduction spontaneously. This situation throws open a number of possible oxidizing agents from which one of them can be easily chosen.

Water splitting - carry out both the redox reactions simultaneously - reduction of hydrogen ions ($2H^+ + 2e- \rightarrow H_2$) as well as ($2OH^- + 2h+ \rightarrow H_2O + 1/2O_2$) oxygen evolution from the hydroxyl ions. The system that can promote both these reactions simultaneously is essential**.**

Since in the case of metals the top of the valence band (measure of the oxidizing power) and bottom of the conduction band (measure of the reducing power) are almost identical they cannot be expected to promote a pair of redox reactions separated by a potential of nearly 1.23 V.

Where the top of the valence band and bottom of the conduction band are separated at least by 1.23V in addition to the condition that the potential corresponding to the bottom of the conduction band has to be more negative with respect to the reduction reaction namely hydrogen evolution reaction, while the potential of the top of the valence band has to be more positive to the oxidation potential of the reaction $2OH- + 2h+ \rightarrow H_2O + ½ O_2$.

This situation is obtainable with semiconductors as well as in insulators.

Insulators are not appropriate due to the high value of the band gap which demands high energy photons to create the appropriate excitons for promoting both the reactions. The available photon sources for this energy gap are expensive and again require energy intensive methods. Hence insulators cannot be employed for the purpose of water splitting reaction.

Therefore, it is clear that semiconductors are alone suitable materials for the promotion of water splitting reaction.

Selection of the semiconductor materials

Essentially for photo-catalytic splitting of water, the band edges (the top of valence band and bottom of the conduction band or the oxidizing power and reducing power respectively) have to be sifted in opposite directions so that the reduction reaction and the oxidation reactions are facile.

Ionic solids (for example oxides) as the ionicity of the M-O bond increases, the top of the valence band (mainly contributed by the p- orbitals of oxide ions) becomes less and less positive (since the binding energy of the p orbitals will be decreased due to negative charge on the oxide ions) and the bottom of the conduction band will be stabilized to higher binding energy values due to the

positive charge on the metal ions which is not favourable for the hydrogen reduction reaction.

More ionic the M-O bond of the semiconductor is, the less suitable the material is for the photo-catalytic splitting of water. The bond polarity can be estimated from the expression

Percentage ionic character (%) = $(1-e^{-\frac{(\chi_A-\chi_B)^2}{4}})X100$

Table 1 Percentage ionic characters of some of the commonly employed semiconductors

Semiconductors	M -X	Percentage ionic character
TiO_2	Ti-O	59.5
$SrTiO_3$	Ti-O-Sr	68.5
Fe_2O_3	Fe-O	47.3
ZnO	Zn-O	55.5
WO_3	W-O	57.5
CdS	Cd-S	17.6
CdSe	Cd-Se	16.5
$LaRhO_3$	La-O-Rh	53.0
$LaRuO_3$	La-O-Ru	53.5
PbO	Pb-O	26.5
ZnTe	Zn-Te	5.0
ZnAs	Zn-As	6.8
ZnSe	Zn-Se	18.4
ZnS	Zn-S	19.5
GaP	Ga-P	3.5
CuSe	Cu-Se	10.0
$BaTiO_3$	Ba-O-Ti	70.8
$BaMoS_2$	Ba-S-Mo	4.3
$FeTiO_3$	Fe-O-Ti	53.5
$KTaO_3$	K-O-Ta	72.7
$MnTiO_3$	Mn-O-Ti	59.0
SnO_2	Sn-O	42.2
Bi_2O_3	Bi-O	39.6

It is seen that we have semiconductors of high ionic character (>40%) or of low ionic character (,20%) and the suitable semiconductor may be those that lie in between since high ionic character has large value of band gap and require ultra violet light and low ionic character systems will lead to more recombination.

The oxide semiconductors though suitable for the photo-catalytic water splitting reaction in terms of the band gap value which is greater than the water decomposition potential of ~1.23 V.

Most of these semiconductors have bond character more than 50-60 % and hence modulating them will only lead to increased ionic character and hence the photo-catalytic efficiency of the system may not be increased.

Therefore, from the model developed, the following postulates have been evolved.

The photo-catalytic semiconductors are often used with addition of metals or with other hole trapping agents so that the life time of the excitons created can be increased. This situation is to increase the life time of the excited electron and holes at suitable traps so that the recombination is effectively reduced. In this mode, the positions of the energy bands of the semiconductor and that of the metal overlap appropriately and hence the alteration can be either way and also in this sense only the electrons are trapped at the metal sites and only reduction reaction is enhanced.

Hence, we need stoichiometrically both oxidation and reduction for the water splitting and this reaction will not be achieved by one of the trapping agents namely that is used for electrons or holes. Even if one were to use the trapping agents for both holes and electrons, the relative positions of the edge of the valence band and bottom of the conducting band may not be adjusted in such a way to promote both the reactions simultaneously.

Normally the semiconductors used in photo-catalytic processes are substituted in the cationic positions so as to alter the band gap value.

Even though it may be suitable for using the available solar radiation in the low energy region, it is not possible to use semiconductors whose band gap is less

than 1.23 V and anything higher than this may be favourable if both the valence band is depressed and the conduction band is destabilized with respect to the unsubstituted system. Since this situation is not obtainable in many of the available semiconductors by substitution at the cationic positions, this method has not also been successful.

In addition, the dissolution potential of the substituted systems may be more favourable than the water oxidation reaction and hence this will be the preferred path way. These substituted systems or even the bare semiconductors which favour the dissolution reaction will undergo only preferential photo-corrosion and hence cannot be exploited for photo-catalytic pathway. In this case ZnO is a typical example.

Low value of the ionic character also is not suitable since these semiconductors do not have the necessary band gap value of 1.23 V. - the search for utilizing lower end of the visible region is not possible for direct water splitting reaction. If one were to use visible region of the spectrum, then only one of the photo-redox reactions in water splitting may be preferentially promoted and probably this accounts for the frequent observation that non-stoichiometric amounts of oxygen and hydrogen were evolved in the photo-assisted splitting of water. At this point it is necessary to find the available photon sources. As is known the solar radiation is the best source of irradiation in terms of availability and also economic point of view. The available solar spectrum is shown in Figure 8. It is seen that only 5-7% radiation is in ultraviolet region and nearly about 40% is in the visible region. This is the factor for the anxiety to utilize the visible portion of solar radiation. Though this may be true. It has to be considered whether the available ultra-violet region is enough to harness for the consumption of earth's requirement. This is a question to ponder and evolve a solution. This Will be taken up in some subsequent section.

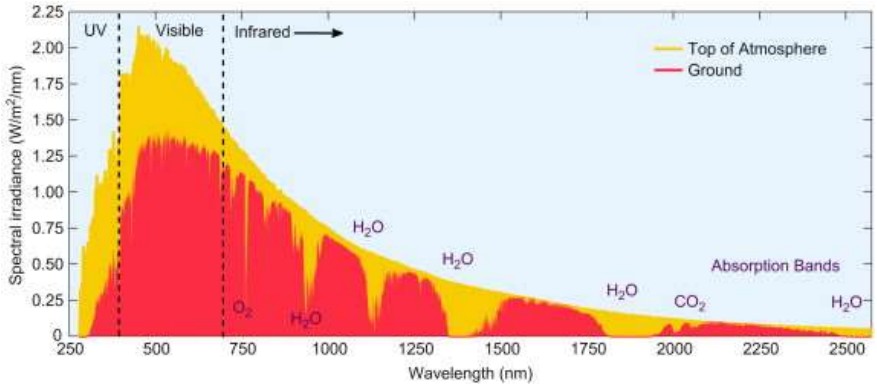

Figure 8 The solar spectrum as a function of wavelength [3]

There essentially a few reactions that are relevant to the wociety and which can be promoted by photons. These can be listed as follows:

(1) Photo-assisted decomposition of water for the production of fuel hydrogen [4]
(2) Photo-catalytic reduction of carbon dioxide to value added products [5]
(3) Photo-catalytic reduction of dinitrogen to ammonia [6]
(4) Photocatalytic process in pollution abatement [7]
(5) Photocatalytic production of fine chemicals [8]

The listed are indicative and in each category there can be many manifestations and these will be considered in subsequent chapters.

References

[1] Introduction to Solid State Physics by Charles Kittel.

[2] A.Mills and S, L. Hunte *J. Photochem. Photobiol.* A: *Chem* 180 (1997) 1.

[3] https://www.sciencedirect.com/topics/engineering/solar-spectrum

{4] Meng Ni, Michael K.H. Leung, Dennis Y.C. Leung, K. Sumathy. A review and recent developments in photocatalytic water-splitting using TiO2 for hydrogen production. Renewable and Sustainable Energy Reviews. 11.401-425 (2007).

[5] S. R. Lingampalli. Mohd Monis Ayyub and C.N.R.Rao, Recent Progress in the Photocatalytic Reduction of Carbon Dioxide, A*CS Omega*, 2, 6, 2740–2748(2017).
[6] Songmei Sun, Qi An, Wenzhong Wang, Ling Zhang, Jianjun Liu and William A. Goddard III Efficient photocatalytic reduction of dinitrogen to ammonia on bismuth monoxide quantum dots, J. Mater. Chem. A, 5, 201 (2017).

[7] P Venkata Laxma Reddy, Ki-Hyun Kim, Beluri Kavitha and Sudhakar Kalagara, Photocatalytic degradation of bisphenol A in aqueous media: A review, Journal of Environmental Management,213, 189-205 (2018).

[8] G.Maghesh, B.Viswanathan, R.P.Viswanath & T.K Varadarajan, PEPEEF, Research Signpost (2007)pp.321-357).

CHAPTER 5

Photo electrolysis of Water-Holy Grail of Electrochemistry

Historically, the discovery of photo-electrolysis of water directly into oxygen at a TiO_2 electrode and hydrogen at a Pt electrode by the illumination of light greater than the band gap of TiO_2 [~3.1 eV] is attributed to Fujishima and Honda [1] though photo catalysis by ZnO and TiO_2 has been reported much earlier by Markham in 1955. For more details of the origin of photocatalysis refer to ref.2.

In simple terms the essential reactions taking place are shown schematically in Fig.1.

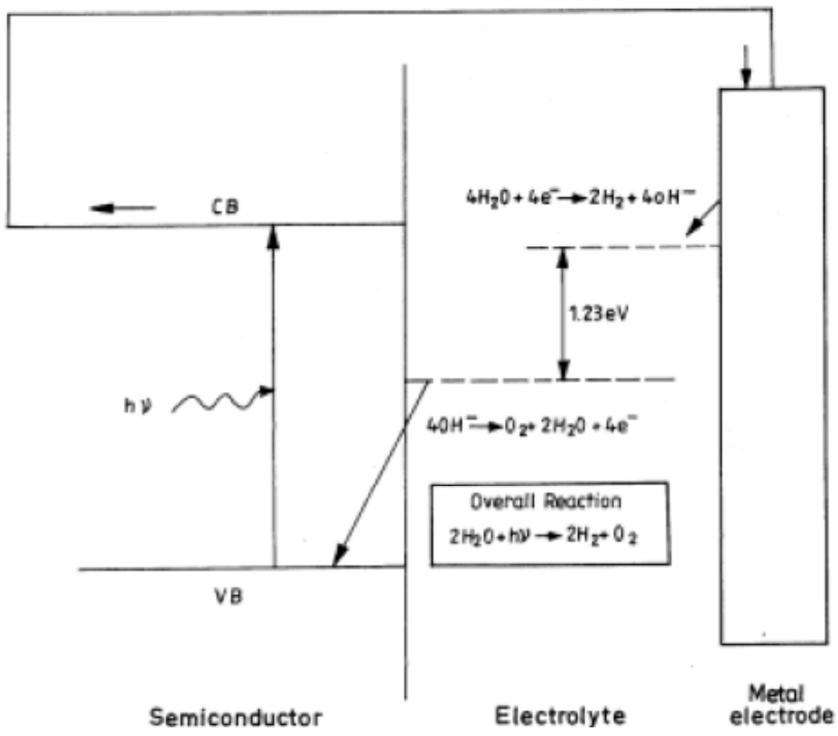

Figure 1 Schematic representation of photo-electrolysis of water

Using these postulates the known semiconductors and the possibility of water splitting reaction taking place on their surfaces are pictorially shown in Figure 2.

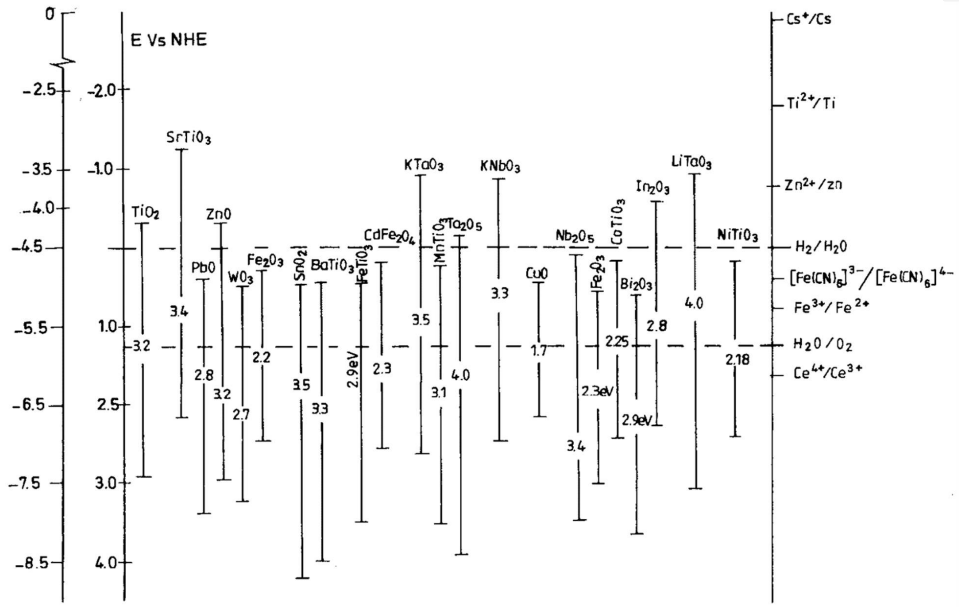

Figure 2 Some of the well-known semiconductors, their band gap values and hydrogen and oxygen evolution potential are shown. From these, one can make a choice of semiconductors which can decompose water. On the right side some other common redox potential values are also given to indicate which other redox reactions are possible. The left -hand side scale is the absolute energy scale and the electrochemical scale is also shown as second vertical axis in the left =hand side. On the right hand the redox potential values of selected redox reactions are given.

The H_2 production rate is normally measured in the units of micromoles of H_2 evolved per hour per gram of the catalyst employed and the photon current density in terms of mA cm^{-2}. The wavelength and intensity of the incident radiation are a few of the other parameters of relevance. However, the set up used to measure these data are mostly home made and different from each other, varied results are obtained and hence, it is necessary to report the results in a consistent manner. In order to compare the results from different sources two parameters are often employed namely the quantum yield (QY) or apparent quantum Yield (AQY) and they are defined as follows:

(QY) % = (Number of electrons reacted / Number of photons absorbed) X 100... (1)

AQY%-(No of electrons reacted/No of incident electrons) X 100 ……(2)

AQY% = (No of evolved hydrogen moleculesX2/ no of incident photons) X 100 .(3)

However, in the solar water splitting reaction, the incident radiation creates and electron and hole pairs and if these were to take part in the surface reaction, then the efficiency will be desirable. However, in this transport of charge carriers, there can be recombination and so the solar to hydrogen conversion efficiency may be different. Hence, another parameter is often used namely the solar to hydrogen conversion efficiency (STH) defined as follows:

STH% - (Output energy of hydrogen /energy of input solar light) $AM_{1.5G}$ X 100 ..(4)

= [(m moles of hydrogen/s x 237kJ/mol)/($P_{incident}$(mW.cm^2) X Area(cm^2)] $AM_{1.5G}$ X100

Various conceptual principles have been incorporated into typical TiO_2 catalyst system so as to make this system responsive to longer wavelength radiations. These efforts can be classified as follows:

- Dye sensitization
- Surface modification of the semiconductor to improve the stability
- Multi -layer systems (coupled semiconductors)
- Doping of wide band gap semiconductors like TiO_2 by nitrogen, carbon and Sulphur
- New semiconductors with metal 3d valence band instead of Oxide 2p contribution
- Sensitization by doping.

All these attempts are some kind sensitization and hence the route of charge transfer has been extended and hence the efficiency could not be increased

considerably. Sensitization of semiconductors will be taken up in a subsequent chapter.

The available opportunities include:

(1) Identifying and designing new semiconductor materials with considerable conversion efficiency and stability
(2) Constructing multilayer systems or using sensitizing species including dyes – increase of absorption of solar radiation
(3) Formulating multi-junction systems or coupled systems - optimize and utilize the possible regions of solar radiation
(4) Developing nano-size systems to efficiently dissociate water

These are mostly tried possibilities and there can be other avenues and these will come up in subsequent chapters. In these opportunities, the attempts so far made include:

- Deposition techniques have been considerably perfected and hence can be exploited in various other applications like in thin film technology especially for various devices and sensory applications.
- The knowledge of the defect chemistry has been considerably improved and developed.
- Optical collectors, mirrors and all optical analysis capability have increased which can be exploited in many other future optical devices.
- The understanding of the electronic structure of materials has been advanced and this has helped to our background in materials chemistry.
- Many semiconductor electrodes have been developed, which can be useful for all other kinds of electrochemical devices.

In spite of all these concerted attempts, there is only limited success in developing a viable semiconductor with maximum efficiency for the decomposition of water. The main reasons for this limited success in all these directions are due to:

- The electronic structure of the semiconductor controls the reaction and engineering these electronic structures without deterioration of the stability of the resulting system appears to be a difficult proposition.
- The most obvious thermodynamic barriers to the reaction and the thermodynamic balances that can be achieved in these processes give little

scope for remarkable improvements in the efficiency of the systems as they have been conceived and operated. Totally new formulations which can still satisfy the existing thermodynamic barriers have to be devised.

- The charge transfer processes at the interface, even though a well- studied subject in electrochemistry, has to be understood more explicitly, in terms of interfacial energetics as well as kinetics. Till such an explicit knowledge is available, designing systems will have to be based on trial and error rather than based on sound logical scientific reasoning.
- Nanocrystalline (mainly oxides like TiO_2, ZnO, SnO and Nb_2O_5 or chalcogenides like CdSe) mesoscopic semiconductor materials with high internal surface area and can be made in nano scale and thus effectively absorb solar radiation.
- If a dye were to be adsorbed as a monolayer on the semiconductor surface, enough can be retained on a given area of the electrode so as to absorb the entire incident light.
- Since the particle sizes involved are small, there is no significant local electric field and hence the photo-response is mainly contributed by the charge transfer with the redox couple.
- Two factors essentially contribute to the photo-voltage observed, namely, the contact between the nano crystalline oxide and the back contact of these materials as well as the Fermi level shift of the semiconductor as a result of electron injection from the semiconductor.
- Another aspect of the nano crystalline state is the alteration of the band gap to larger values as compared to the bulk material which may facilitate both the oxidation/reduction reactions that cannot normally proceed on bulk semiconductors.
- The response of a single crystal anatase can be compared with that of the meso-porous TiO_2 film sensitized by ruthenium complex (cis $RuL_2(SCN)_2$, where L is 2-2'bipyridyl-4-4'dicarboxlate).
- The incident photon to current conversion efficiency (IPCE) is only 0.13% at 530 nm (the absorption maximum for the sensitizer) for the single crystal electrode while in the nano crystalline state the value is 88% showing nearly 600-700 times higher value. This increase is due to better light harvesting capacity of the dye sensitized nano crystalline material but also due to mesoscpic film texture favouring photo-generation and collection of charge carriers.

- It is clear therefore that the nano crystalline state in combination with suitable sensitization is one another alternative which is worth investigating.
- The second option is to promote water splitting in the visible range using Tandem ells. In this a thin film of a nanocrystalline WO_3 or Fe_2O_3 may serve as top electrode absorbing blue part of the solar spectrum. The positive holes generated oxidize water to oxygen

  $4h+ + 2H_2O \text{ ---}\rightarrow O_2 + 4\ H^+$

- The electrons in the conduction band are fed to the second photo system consisting of the dye sensitized nano crystalline TiO_2 and since this is placed below the top layer it absorbs the green or red part of the solar spectrum that is transmitted through the top electrode. The photo voltage generated in the second photo system favours hydrogen generation by the reaction

  $4H+ \ + \ 4e- \text{ ---}\rightarrow \ 2H_2$

- The overall reaction is the splitting of water utilizing visible light. The situation is similar to what is obtained in photosynthesis.
- Dye sensitized solid hetero-junctions and extremely thin absorber solar cells have also been designed with light absorber and charge transport material being selected independently so as to optimize solar energy harvesting and high photovoltaic output. However, the conversion efficiencies of these configurations have not been remarkably high.
- Soft junctions, especially organic solar cells, based on interpenetrating polymer networks, polymer/fullerene blends, halogen doped organic crystals and a variety of conducting polymers have been examined. Though the conversion efficiency of incident photons is high, the performance of the cell declined rapidly. Long term stability will be a stumbling block for large scale application of polymer solar cells.

Thus, this field has given rise to new opportunities in science and these can be listed as follows:

1. New semi-conducting materials with conversion efficiencies and stability have been identified. These are not only simple oxides,

sulphides but also multi-component oxides based on perovskites and spinels.

2. Multilayer configurations have been proposed for absorption of different wavelength regions. In these systems the control of the thickness of each layer has been mainly focused on.
3. Sensitization by dyes and other anchored molecular species has been suggested as an alternative to extend the wavelength region of absorption.
4. The coupled systems, thus giving rise to multi-junctions is another approach which is being pursued in recent times with some success
5. Activation of semiconductors by suitable catalysts for water decomposition has always fascinated scientists and this has resulted in various metal or metal oxide (catalysts) loaded semiconductors being used as photo-anodes.
6. Recently a combinatorial electrochemical synthesis and characterization route has been considered for developing tungsten based mixed metal oxides and this has thrown open yet another opportunity to quickly screen and evaluate the performances of a variety of systems and to evolve suitable composition-function relationships which can be used to predict appropriate compositions for the desired manifestations of the functions.
7. It has been shown that each of these concepts, though have their own merits and innovations, have not yielded the desired levels of efficiency. The main reason for this failure appears to be that it is still not yet possible to modulate the electronic structure of the semiconductor in the required directions as well as control the electron transfer process in the desired direction.

In spite of all these efforts, there is still no economically viable semiconductor identified for the decomposition of water. The success in this attempt will give a boost to the energy needs of this universe.

References

[1] A. Fujishima and K.Honda, Electrochemical photolysis of water at a semiconductor electrode, Nature, 238 (1972).http://doi.org/10.1038/238037a0.

[2] B. Viswanathan and M. Aulice Scibioh, Photo-electrochemistry, Principles and practices, Narosa Publishing House, New Delhi (2014).

Semiconductors with high ionicity are stable against corrosion and passivation. However, they require the ultra violet region of the electromagnetic spectrum. As stated earlier, threshold behaviour is important in photo-electrochemistry to maximize the use of solar spectrum. In this sense, for water decomposition materials with band gap between 1.3 to 1.8 are the optimum type of semiconductors for maximizing the efficiency of the water decomposition reaction. This means one wishes to make useof the visible range of the solar spectrum.

Light absorption by a semiconducting solid is governed by Beer's law

$A = \ln (I/I_o) = \alpha l$ or $T = (I/I_0) = \exp(-\alpha l)$

Where I and I_0 – transmitted and incident light intensity and α is called the absorption coefficient. Semiconductors can be classified as direct or indirect band semiconductors. Direct band gap semiconductors have large absorption coefficient (10^4 -10^5 cm^{-1}).

The absorption coefficient for these materials are given by the equation,

$$\text{Alpha } \alpha = [A(h\nu - E_g)^m] / h\nu$$

In this equation m is a constant which depends on the optical transition, m=2 for an indirect band gap semi-conductor and ½ for a direct band gap semi-conductor.

Intrinsic carrier concentration in semiconductors is normally low and the equation concerning this parameter is given by

$$N_j p_i \alpha \exp(-E_g/kT)$$

Doping generally increases the conductivity of the semiconductor and able to control other electronic properties. Doping with other valent ions or even the crystal defects can also behave as dopants. Therefor conductivity can be controlled by doping and is given by the expression

$$\text{Sigma} = \sigma = qn\mu_n + qp\mu_p$$

Where μ_n and μ_p are the charge carrier mobilities

The processes that take place on a semiconductor powdered material can be visualized as follows:

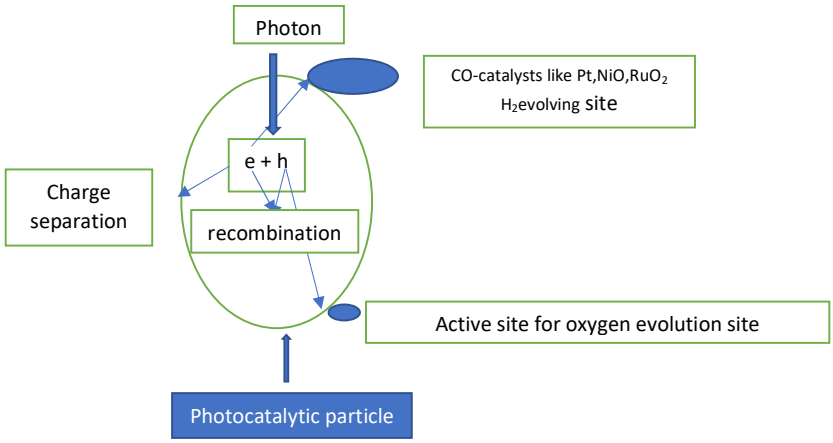

At this stage, we need to understand the structure of electrode-electrolyte interface and the possibility of charge transfer when the electrode happens to be

a semiconductor. The charge transfer depends on the relative energy positions of the donor and that of the acceptor. Flat band potential is defined no band as Flat bending situation and for highly doped semiconductors, this equals the bottom of the conduction band. This is defined by the following equation:

$V_{fb} = E_0 - \chi + (1/2) E_g$ where χ is the value of electronegativity in Mulliken's scale.

Typical model calculation is shown below

The charge transfer abilities of a semiconductor electrode depends on whether there is an accumulation or depletion layer. If there is an accumulation layer – behaves as metallic electrode-since excess of majority charge carriers available for charge transfer.

If there is a depletion layer - there are few charge carriers available and the electron transfer reaction occur slowly. However, if the electrode is exposed to radiation of sufficient energy electron hole pairs are produced. If the processes occur within the interior of semiconductor, the heat and recombination take place. If it occur in the space charge region, the electric field in this region will cause the separation of the charge.

1, Sufficiently high (visible) light absorption

2. High stability in dark and under illumination (no photo corrosion)

3. Suitable band edge positions to enable the reduction/oxidation of water by the photo generated holes /electrons

4.Efficient charge transport in the semiconductor

5. Low over potentials for the reduction/oxidation reaction (high catalytic activity).

Stability against photo corrosion

Most important property which limits the usefulness of many photo-active materials. Many non-oxide semiconductors (Si, Ga As, GaP, and so on) either dissolve or form a thin oxide film which prevents the electron transfer across the interface.

Almost all M-O photo anodes are thermodynamically unstable!

Eg: TiO_2 and SnO_2 show excellent stability over a wide range of pH and applied potential. ZnO always decomposes, Fe_2O_3 shows an intermediate case (pH and oxygen stoichiometry)

Requirement of band positions:

Conduction and valence band edges should straddle the reduction and oxidation potential of water Specifically E_{CB} should be above or less in numerical value E_{red} and E_{VB} should be below or more numerical value of E_{ox}.

The exciton life time is a very important criterion is the hole transfer across the n type semi-conductor-electrolyte interface. It should be fast enough to compete with photo-corrosion and to avoid accumulation.

Loading of metals like Cu, Ag, Au, Ni, Pd, Rh and Pt over a variety of metal oxide semiconductors results efficient charge separation!

Pt is well known as an excellent co catalyst for hydrogen evolution

The addition of carbonated salts or other electron mediators enhance the hydrogen production by preventing backward reaction.

Mixed metals oxide semiconductors ⎪ NiO over SrTiO3 – NiO(H2), SrTiO3 (O2) RuO2 over TiO2 -30 times bigger activity than TiO2 alone ⎪ But if the concentration of RuO2 exceeds a limit- act as electron hole recombination centers !!! ⎪ In the presence of co - catalysts such as NiO –highly active niobates , titanates and tandalates are reported (NiO/NaTaO3).

Visible light activity

There are methods by which photocatalysts can be fabricated, by which they respond in the visible light ♣ Valence band formation using elements other than oxygen [BiVO4 , AgNbO3 ,Ag3 VO4 ,Ca2 Bi2 O4 .....]

Ion doping

Cation doping - transition metals (V, Cr, Fe, Mo, Ru, Os, Re, Rh, V, etc.) -rare earth metals doped ion create new (impurity) energy levels. metal ion dopants act as electron or hole traps

Doping of anions such as N, F, C, Si in metal oxides or mixed metal oxides can shift in photo response into the visible region ¬ little tendency to form recombination centers-remarkable thing Z-scheme construction Dual semiconductor system Dye-sensitization Dye molecules absorb light with the transfer of an electron from the ground state to excited state. The excited electron goes to the conduction band of an appropriate metal oxide.

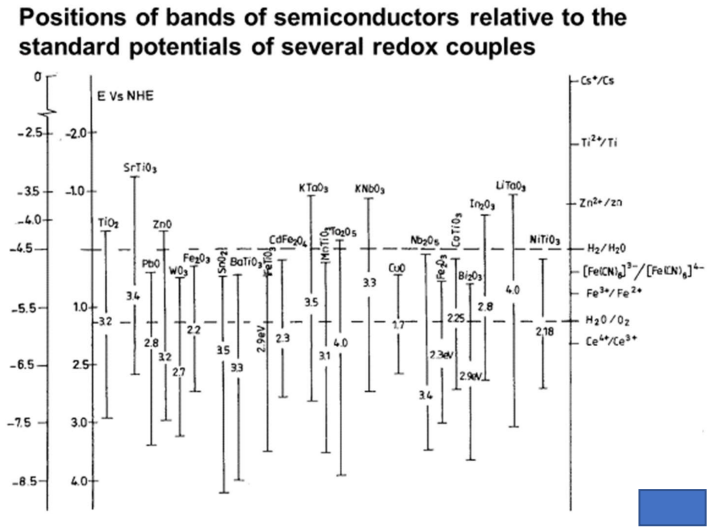

[1] C H Henry, J. Appl. Phys.,51, 4494 (1980)

[2] W. Shockley and H J Queisser, J. Appl. Phys., 32, 510 (1981)

CHAPTER 6

Photo-catalytic Degradation of Dyes: An Evaluation

1. Introduction

Photo-catalytic degradation of dyes or other organic pollutants is a recent research exercise intensively pursued [1-7]. Synthetic dyes are nowadays extensively used in the products like clothes, leather accessories, furniture, and plastic products. However, nearly 12% of these

dyes are wasted during the dying process and ~ 20% of this wastage enters the environment [8]. Dye degradation is a process in which the large dye molecules are broken down chemically into smaller molecules. The resulting products are water, carbon dioxide, and mineral byproducts that give the original dye its color. During the dyeing process, not all of the dye molecules are used. The water waste that the industry releases contains a percentage of these dye molecules.

Heterogeneous photo-catalysis is one of the modern methods widely employed for the degradation or bleaching of the dyes [9]. The process mainly involves transfer of electrons from the valence band to the conduction band of a semiconductor surface (mostly oxides and sulfides) on illumination with appropriate wavelength of light. These generated excitons react with oxygen or water to yield superoxide anions and hydroxide radicals. These species have increased oxidizing and reducing power to degrade numerous molecules including those present in industrial dyes. The decontamination processes by these species and some other species like various forms of Fenton processes are called in scientific parlor Advanced Oxidation Process (AOP). Even though AOP is an important research area in the contemporary literature, we shall restrict only to those processes dye degradation processes promoted by semiconductors photo-catalytically [10-12].

It is necessary at this stage to point out the need for a review on this topic at this stage. The reasons include [13]:

(1) There are number of research groups working on this area and it is better to assimilate the literature at frequent periodicity

(2) Photo-catalytic degradation of pollutants is one of the methods which has some advantages including total degradation and possibly the less expensive method.

(3) The degraded components like water and carbon dioxide are non-toxic.

(4) The feasibility of degradation of any pollutant can be *a priori* decided from the numerical values of the oxidation potential of the pollutant and the reagent (like $OH^{\bullet}$ radical; standard reduction potential value is around 2 V [14]).

There are various kinds of dyes that are employed for coloring objects. These materials are classified according to the structure of the molecule component, color, the method that is adopted to apply these dyes to objects. The chromophore group attached to the dye molecule specifies the group to which the dye belongs and these can mainly be classified as acridine dyes, azo dyes, anthroquinone dyes, nitro dyes, xanthene dyes and quinine-amine dyes and so on [7]. The studies reported on photocatalytic dye degradation mainly concerned with the variables like concentration of the dye, the amount of catalyst employed, the effect of the intensity of the light irradiation and the time of irradiation and the effect of dissolved oxygen and other species. The kinetics of photocatalytic degradation of dyes are usually considered to

be a pseudo first order reaction with the kinetic data fitted to the equation -ln (C/C_0) = kt. The relevance of this kinetic data fit will be considered separately in a subsequent section.

Though extensive studies are reported on the photo-catalytic degradation of pollutants in water, there are certain aspects that have not yet received careful attention. The purpose of this presentation is to focus on these issues and to point out what is required in this direction. The literature in this area is increased five times or more during the last 10 years as seen from the data shown in Table 1. It is noticed that the number of publications is doubling or more every five-year period. It is therefore natural that people attempt to review the literature at periodic intervals [5-7]. However as said earlier, the research is pursued mostly around oxides (especially TiO_2) and the variables studied are mostly the same, whether it is required or not.

Fig.1.Number of publications falling under the category of Photo-catalytic degradation of dyes (source: Web of Science)

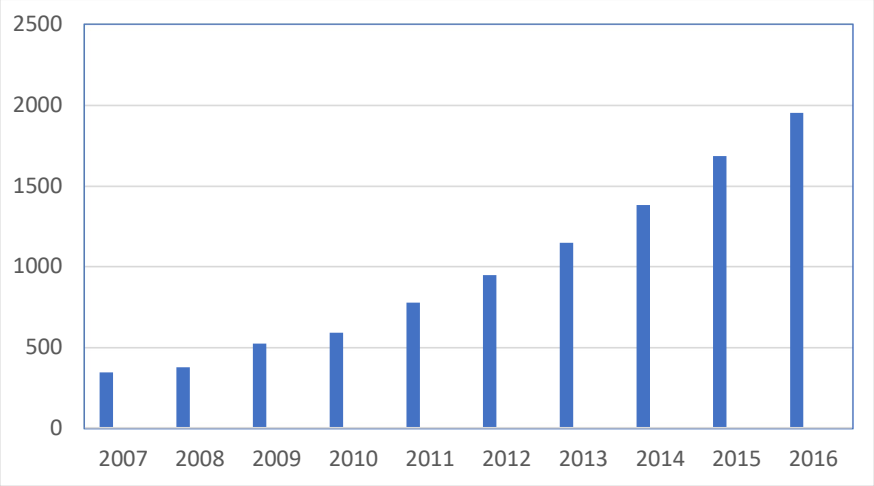

Before we embark on the limitations of the studies so far reported, it is necessary to briefly review the available literature though not comprehensively but representatively. A few selected publications from literature is summarized in Table 1. Majority of the studies reported in literature deal with the effect on degradation activity on variables like the amount of the catalyst, the concentration of the dye employed, pH, effect of the radiation source and time of irradiation and also the effect of dissolved oxygen and others**.** The kinetics of degradation of dyes on most of the catalyst systems studied follows first order [15].

Conventional chemical, physical and biological processes have been extensively employed for treating waste water containing dye molecules. These methods have the following disadvantages like high cost, requirement of high energy, generation of secondary pollutants

in the treatment process. The Advanced Oxidation Process (AOP) has received considerable attention in recent times for the decomposition of organic dyes [16].

2. The literature so far

This is an area of research which is carried out throughout the world unlike other areas of science. Research in certain areas of science are confined to certain regions of the world but degradation of dyes has been studied in almost all the countries and regions including almost all the developing countries around the world. This is reflected in the data assembled in Table 1**.** Scientifically the process involved in the degradation of dyes can be pictorially represented as shown in Fig2**.**

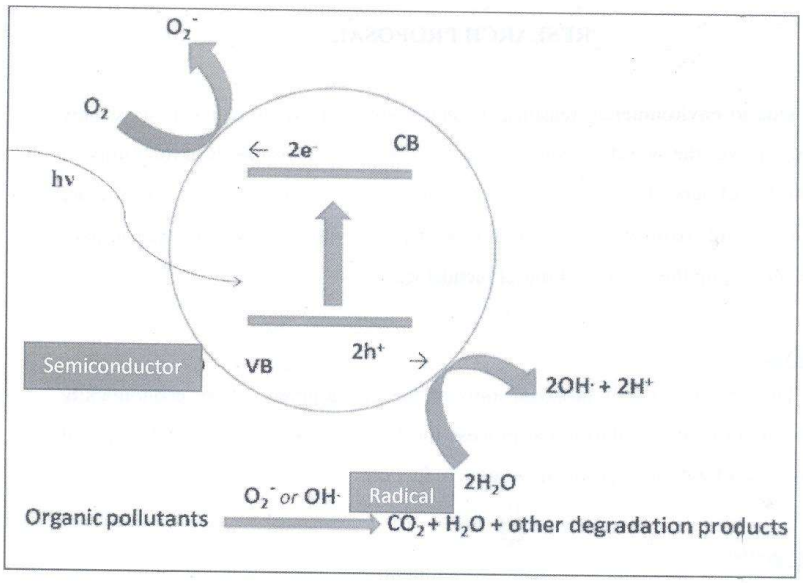

Fig.2. Pictorial representation of the process taking place in the photocatalytic degradation of dyes on semiconductor surfaces.

Most of the photocatalytic dye degradation studies reported have been with Titanium dioxide as photo-catalyst. However, the major disadvantage of TiO_2 that it absorbs only in the UV regions since it has a band gap of around 3.2 eV. Among the different phase of TiO_2, anatase form of TiO_2 is mostly employed due to its higher photon absorption characteristics. It is clear that the phase composition of TiO_2 has a role to play in degradation of dyes. Among the most prominent phases of TiO_2 namely Anatase, rutile and Boookite, the first two phases are most studied systems as seen from the data given in Table.1. The position of oxygen ions on the anatase surface possesses a triangular arrangement which allows significant absorption of organic molecules,. whereas, the orientation of titanium ions in the anatase phase creates an

advantageous reaction condition with the absorbed organic pollutants [17-24]. Interestingly, these favorable structural arrangements of oxygen and titanium ions are not present in the rutile phase. It is also believed that pure anatase with small proportion of rutile phase is conducive for meso-porosity and thus favourable for dye adsorption [17-28].

Mechanistically, the photon excites an electron from valence to the conduction band and the excitons (free electron in the conduction band and hole in the valence band) generate radical species which is responsible for the degradation of organic dyes carbon dioxide and water and other degradation species.

Even though large surface area is recommended for effective dye degradation, (P-25 Degussa TiO_2 is a mixture of 80% anatase + 20% rutile phase and this combination alone makes this system active and in most cases used as standard for comparison), dye adsorption may precede the degradation and this can affect the interpretation of the kinetics of degradation of dye. This aspect will be taken up subsequently.

Among the various waste water treatment procedures, dye removal has occupied a prominent place. Because of aesthetic and environmental concerns, the degradation of dyes in the effluent water of textile dyeing and finishing industry has been most important [29]. The semiconductors especially TiO_2 and ZnO are employed as nanorods, nano-spheres, thin porous films, nanofibers and nanowires or supported on polymeric films [30]. These systems exhibit high activity, low cost and environmentally acceptable [31-33].

Apart from TiO_2 and ZnO, various other semiconducting systems like CdS, ZrO_2 and WO_3 systems have been employed in the photocatalytic degradation of dyes. These studies and other reports on ternary oxides are included in the listing in Table.1. The drawback of most of these systems like TiO_2 is the high value of band gap and they require UV photon sources to be able to decolourize waste-water.

Table 1. Representative literature data on the photocatalytic degradation of dyes

Catalyst systems studied	Dyes employed	Conditions and variables studied	Reference
Graphene – gold Nano composite (GOR/Au)	Rhodamine B Methylene blue Orange H	Visible light - Rate of degradation of methylene blue is greater than Rhodamine B even though the redox potential is highest among these three dyes. Adsorption is identified as the reason	A1
Nanocrystalline anatase and rutile TiO_2	Acetophenone Nitrobenzene Methylene blue Malachite green	The activity of Anatase is higher than that observed with Rutile. The reason for this difference is not indicated in this communication	A2
TiO_2, ZnO, SnO_2	Crystal Violet Methyl Red	ZnO exhibited highest activity. Even better than Degussa P-25 and loading silver on ZnO resulted in	A3

		20% increase in photocatalytic activity	
Mg^2-TiO_2	Methyl Orange	The catalyst has better activity than the undoped TiO_2- Dye sensitization and injection of the excited electron is considered as the cause	A4
TiO_2 Impregnated ZSM-5 (TiO_2-ZSM = 0.15:1)	Reactive Black-5	This ratio system shows high adsorption capacity and degradation activity	A5
ZnO-nanoflowers	Methyl Orange Congo Red Eosin B Chicago Sky Blue	The catalyst prepared from asymmetric Zn(ii)dimeric complex showed good photocatalytic activity towards methyl Orange to compared to other dyes	A6
ZnO Nano powder	Rhodamine B	95% degradation of the dye was observed under solar light irradiation	A7
TiO_2	Methyl Orange Methylene Blue	The photocatalytic activity is found to be greater in the presence of solar light than in UV.	A8
Nano-sized $GdCoO_4$	Rhodamine B Rhodamine Blue(RBL) Orange G(OG) Remazol Brilliant Blue (RBBR)	The catalyst (3nm) is more efficient than P-25. Size dependence is shown. The intermediates in both $GdCoO_4$ andP-25 are the same	A9
TiO_2	Methylene Blue Methyl Orange Congo Red	The size and Phase (Anatase) are important. Adsorption of the dye on the catalyst surface is also important (Freundlich isotherm)	A10
TiO_2	Indigo Indigo Carmine	Complete mineralization of the dyes Irradiation with visible light only produced color removal	A12
TiO_2 immobilized on polyvinyl alcohol (PVA) or polyacrylamide (PA)	Methylene Blue, Anthraquinone, Remazol Brilliant Blue R (RBBR), Reactive Orange (RO16).	TiO_2 loaded on PVA appears to be better than that loaded on PA	A11
Nanostructured TiO_2	Mono, di and tri azo class of dyes.	Degradation depends on the chemical structure of the dye, the	4

	Classes of indigoid, anthraquinone triaryl methane and xanthene dyes	nature of functional groups. Mono-azo dyes degrade faster than anthraquinone dyes. Presence of nitrite group promote the degradation activity.	
High surface area TiO_2	Methylene Blue Congo Red	Sol-gel method preparation of TiO_2 is suitable for degradation of Dyes. Freundlich Isotherm is employed.	2
N-doped TiO_2	Methylene Blue Methyl Orange	Visible light source was employed and depends on nitrogen content of the catalyst	1
Nanometer sized TiO_2	Acid Orange 10(AO10) Acid Red 14 14ARI14)	The azo and sulphonate groups determining factor for degradation	A13
SiO_2 nanoparticle dopes with Ag and Au	Methyl Red	OH radical produced initiates and also sustains the degradation of the dye	A14
Titanium dioxide	Emerald Green	Degradation rate constant depends on pH	A15
ZnO and TiO_2	Rhodamine B Methylene Blue Acridine Orange	ZnO dissolves as $Zn(OH)_2$ and hence shows lower activity as compared to TiO_2	A16
TiO_2 (UV/Solar/pH)	Procion Yellow	TiO_2 in presence of solar irradiation is better	A17
TiO_2	Reactive Red 2	Degradation in presence of $H2O_2$ and persulphate ion.	A18
Thermally activated ZnO	Congo Red	Pseudo second order Kinetics was observed	A19
Sol-gel TiO_2 films	Lissamine Green B	The film prepared in presence of Polyethylene glycol is better	A20
ZnO	Mythylene Blue	Decoloured of actual industrial waste water	A21
Ag-TiO_2 core shell particle	Reactive Blue 220	the core shell system was better catalyst under solar light	A22
Anatase Nano-TiO_2	Reactive Blue 4 (anthraquinone dye	In presence of H_2O_2 the dye degradation increased	A23
TiO_2/ZnO Photo catalyst	Methylene Blue	ZnO appeared to be better than Pure TiO_2	A24

P160 TiO_2	C! Basic Yellow – 28	Better degradation in weak acidic conditions, carbonate ion increased degradation activity	A25
Ferrihydrite modified Diatomite with TiO_2 /UV	Vat Green 03	A composite catalyst with P-25 with co-adsorbent removed colour over 98%	A26
Orthorhombic WO_3	AO7 dye	Phenol, humic acid and EDTA inhibited decolouring but oxalic acid increased	A27
Fe^{3+}/C/S/-TiO_2	Mono and Di-azo dyes	Mono azo dye is better than diazo dyes. Decolurization under visible light	A28
Ni doped TiO_2	Malachite Green	Hydroxyl ion as the oxidizing species	A29
TiO_2	Solo phenyl Red 3BL	Concentration of OH^* and O^* radical determines the rate	A30
TiO_2	Mono Azo Orange 7 (AO&) Reactive Green 19 (RG19)	Mono azo dye (AO7) than the binary azo dye (RG19) under solar light	A31
TiO_2	Azo dye and disperse dye	A modelling exercise on governing parameters	A32
TiO_2	Methyl Orange Methylene Blue	Degradation under UV irradiation	A33
TiO_2 Photo-catalyst	Indigo Carmine dye	UV irradiation optimum conditions pH =4 and dye concentration 25 ppm 98% colour removal	A34
ZnO photo-catalyst	Methylene Blue	Basic solution is better.	A35
TiO_2 Photo-catalyst	Methylene Blue	Basic medium is better	A36
Carbon doped TiO_2	Amido Black-10B	Active oxygenated species is responsible for decolourization.	A37
ZnO photocatalyst	Direct Red-31 (DR-31) dye	Effect of annealing temperature (500-800C)- UV irradiation	A38
Sol-gel TiO_2 films	Methyl orange, Congo Red	TiO_2 films with dip coating with Polyethylene glycol (better) 254 UV is better than UV 365 nm	A39
Undoped and Fe doped CeO_2	Methyl Orange	1.5 % doping of Fe^{3+} was optimal	A40
Immobilized TiO_2	Methylene Blue	Deposition of Photosensitive hydroxides decreased the activity	A41
Ni/$MgFe_2O_4$	Malachite Green	Visible light active	A42
TiO_2	Methyl Orange	Superoxide anion radicalPolytetrafluoroethyle-A1	A43

		based triboelectric nanogenerator (TENG) assisted the process	
Crosslinked Chitosan/nano CdS	Congo Red	Acidic Medium is better, Presence of No_3^- accelerated Br^-, Cl^-, SO_4^{2-}, inhibit decolourization	A44
TiO_2/UV	Methylene Blue	Mineralization of carbon, nitrogen and Sulphur into CO_2, NH_4^+,SO_3^{2-}	A45
Cu impregnated P-25	Azo dye Orange II	Cu Impregnated TiO_2 is better then H_2O_2/UV homogeneous reaction.	A46
Ag-Ni/TiO_2 synthesized by gamma irradiation	Methyl Red	Bimetallic co-doped is better than bare TiO_2	A47
Cr doped TiO_2	Methylene Blue Congo Red	Cr doped promoted Anatase to Rutile phase transition	A48
ZnS Quantum dots doped with Au and Ag	Methylene Blue	Metal loading favours degradation; accounted in ,terms increased life time of charge carriers, Opto electronic characteristics and isoelectric point need to be considered in proposing photo-catalyst	A49
Mesoporous CeO_2	Rhodamin B	Hydroxyl radicals are the active species	A50
ZnS	Rose Bengal	Hydroxyl radicals are shown as the active species	A51
C-TiO_2 films	Azorubine	Photo-degradation and adsorption dual effect is the reason for better decolourization	A52
La-Y/TiO_2	Methylene Blue	Optimum dose 4 g/L	A53
Ag-TiO_2	Direct Red 23	Optimum dose 3 g/L	A53
ZnO	Remazol Brilliant Blue dye (RBB)	The degradation follows first order kinetics	A54
TiO_2 Degussa P-25	2,4-dimethylphenol, 2,4-dichlorophenol, 2-chlorophenol and phenol	pH 5 was found suitable	A55
ZnO	Crystal Violet	high specific surface area (56.8 m^2/g), high crystallinity and better optical property are	A56

		responsible for the better activity of ZnO nanonails.	
In/ZnO nano particles	Methylene Blue	In is well dispersed on ZnO	A57
TiO2 Degussa P25 and ZnO	Methylene Blue	Visible light is better and ZnO better than TiO_2	A 58
TiO_2 nano particles	Methylene Blue	Basic medium is better	A59
ZnO	Reactive Blue	Reactor design and optimum time	A60
Magnetite+H2O2+UV	Methylene Blue	Process parameter optimization	A61
$Bi_{24}O_{31}Cl_{10}$	Rhodamine B	compatible energy levels and high electronic mobility	A62
BiOI	Rhodamine B anionic reactive blue KN-R	h^+ is the dominant specie for the degradation of dyes.	A63
TiO_2	Alizarin yellow	of Cl^-, SO_4^{2-} inhibit dye removal, depends on TiO_2 source	A64
TiO_2, ZnO	Polycyclic aromatic hydrocarbons (AH)	Surface to volume ratio appears to be relevant	A65
ZnS doped with Mn	Malachite green	UV/ZnS, UV/ZnS/H2O2, UV/doped ZnS systems studied	A66
TiO_2 and Cu-doped TiO_2	reactive blue 4, reactive orange 30, reactive red 120and reactive black 5	Cu-doped TiO2 nanoparticles are very effective in degrading the dye pollutants	A67
Mn_3O_4 nano particles	amido black 10B	peroxomonosulfate (PMS), peroxodisulfate (PDS) and hydrogen peroxide (HP) enhanced degradation	A68
Photo-Fenton system	Reactive orange M2R dye	Acidic pH favours; a mechanism is proposed	A69
TiO2 catalyst with a very low level of Pt	Phenol	Eosin Y sensitized TiO_2	A70
TiO_2	Methylene Blue	p-n junction heterostructure CuO-TiO2 enhance photoactivity	A71
TiO_2 coated Cotton fabric	amaranth dye	prepared fabric showed enhanced dye degradation capabilities	A72
titanium dioxide TiO2 and zinc phthalo cyanine (ZnPc)	4-Nitrophenol	Efficiently degrade nitrophenol	A73

Silver phosphate	Methylene Blue	visible-light-driven photodegradation of dye pollutants	A74
$CeCrO_3$	Fast Green dye	First order kinetics,	A75
ZnO	Acid Green 25	Both acidic and basic medium	A76
Anatase TiO_2	Methylene Blue Phenol	pH = 6.4 is optimum	A77
CeO_2-ZnO	Methylene Blue 4'-(1-methyl-benzimidazoyl-2)-phenylazo-2"-(8"-amino-1"-hydroxy-3",6"-disulphonic)-naphthalene acid	50-80 nm with large defects	A78
Al_2O_3-TiO_2 and ZrO_2-TiO_2 Nanocomposites	Methylene Blue Rhodamine B Methyl Orange	both the composites degrade methylene blue and rhodamine B effectively under UV-A light the photodegradation of methyl orange is slow	A79
MgO	Methylene Blue	Over 90% degradation	A80
TiO_2	Acid Orange 67	light source is UV is better in comparison to Visible.	A81
TiO_2 on Polyethele film	Crystal Violet Methylene Blue Basic Fuchsine	Sun light degradation Undergraduate experiment	A82
Mo doped TiO_2	Toluidine blue-o	degradation of the dye follows pseudo-first order kinetics	*A83*
Copper Ferrite	Methylene blue	In Glycerol it is not effective H_2O_2 is better	A84
TiO_2 as photo-catalyst	Tatrazine (azo dye)	Influence of addition of other salts studied	A85
$Ni_{o.6}Co_{0.4}Fe_2O_4$	Congo Red	Photo-catalytic degradation maximum at pH 3	A86
Zn-TiO2	Direct Blue 71 dye	Zn Doped system is better than bare TiO_2	A87
Ag modified ZnO	Reactive Orange *16*	Ag modified system was better than pure ZnO	A88
TiO_2	Reactive Orange 16 Dye (RO16)	Effect of the amount of TiO_2 studied	A89
ZnO-CuO	Reactive black5 (RB5)	This system is suitable technique for degradation of dyes and	A90

		environmental pollution from effluents.	
TiO_2 on polyethylene glycol	Methyl Orange Congo Red	Under UV irradiation higher efficiency observed	A91
g-C3N4 thermally Modified with Calcium Chloride	Rhodamine B	The photo-generated hole and the superoxide radical are the main active species in the degradation process. 50 times more active than unmodified system	A92
CdO/TiO_2 coupled semiconductor	Reactive Orange 4 (RO 4)	best photocatalytic activity in the degradation of RO 4 compared with bare TiO_2	A93
ZnO	Remazol Brilliant Blue R, Remazol Black B, Reactive Blue 221 and Reactive Blue 222	A synergistic effect in the coupled TiO2-ZnO system was not observed	A94
CdS/SL g-C_3N_4) SL= Single Layer)	Rhodamine B	visible-light-responsive and environmentally friendly photo-catalyst for the degradation of dye	A95
BiOCl	Rhodamine B and other dyes	Visible light degradation may be complicated. The use of multitude of dyes is necessary to assess the degradation activity	A96
Cr doped ZnS	Methyl Orange	Visible light is better than UV	A97
Nano TiO_2(C-Fe doped)	C.I. Basic blue 9 C.I. Acid orange 52	Real waste water treatment	A98
CeO_2-SnO_2	Direct Black 38	Activity is comparable with TiO_2-P25	A99
Z-scheme SnO_{2-x}/g-C_3N_4 composite	Rhodamine B	Z-scheme mechanism to enhance photo-degradation activity	A100
BiOCl-Au-CdS	Methyl Red Rhodamine B	Z-scheme BiOCl-Au-CdS exhibited excellent sunlight-driven photocatalytic activity toward the degradations of organic dyes and antibiotics	A101
TiO_2-ZnO	RB 21 dye	UV photoreactor and TiO_2 is the best	A102

CaO	indigo carmine dye	pH 9 was suitable	A103
g-C_3N_4/oxygen vacancy-rich zinc oxide	Methyl Orange	deactivated after five cycles of methyl orange degradation	A104
$CoFe_2O_4/C_3N_4$ hybrid	Rhodamine B	Typical Z-scheme system in environmental remediation	A105
α-$Bi_4V_2O_{11}$; γ-$Bi_4V_2O_{11}$	Rhodamine B Methylene Blue	Surface to Volume ratio is responsible	A106
BiVO4-rGO	Rhodamine B	Better than pure BiVO4 and P-25	A107
Flower like N-doped MoS_2	Rhodamine B	27 times better than bare MoS_2 and 7 times better than P-25	A108
$H_3PW_{12}O_{40}/SiO_2$	Rhodamine B	under simulated natural light irradiation	A109
$SrTiO_3$	Methylene Blue Rhodamine Methyl Orange	Non-selective process	A110
CuO/Ag_3AsO_4/GO	Phenol	Photo-stability and reusability	A111
TiO_2/diatomite	Rhodamine B, Methyl orange, Methylene blue	wastewater treatment -good photocatalytic property and reusability.	A112
Cr(VI) using Ag/TiO2	4-chlorophenol	stability and reusability of catalysts	A113
PbCrO4/TiO2	Rhodamine B	good visible light-sensitive photocatalyst for removing Rh B	A114
$WO_3/SnNb_2O_6$	Rhodamine B	Z-scheme charge transfer mechanism was proposed for the elimination of organic contaminants under irradiation of visible light.	A115
ZnO	Acid Red 27	H_2O_2, $K_2S_2O_8$, $KBrO_3$ due to concentration increases the rate	A116
CuS	methylene blue, rhodamine B, eosin Y and congo red	photodegradation rates of dyes usually follow pseudo-first-order kinetics for degradation	A117
Cobalt Hexacyanoferrate(II)	Neutral Red dye	Degradation under UV light and photo-catalyst	A118
N-doped ZnO	Azure A	N-doped zinc oxide has been used as an effective catalyst for carrying out number of chemical reactions	A119
Al_2O_3-TiO_2, ZrO_2-TiO_2	methylene blue rhodamine B	Methylene blue degradation is slow	A120

		Visible light degradation of rhodamine B	

The percentage degradation of dyes in waste water improved with increasing intensity of exposed light. With high intensity irradiation, the recombination may not be significant, but when the intensity is low the recombination of the electron hole formed predominates. The photocatalytic activity depends on the thermal history of the semiconductor and the chemical nature of the semiconductor. The choice of the semiconducting systems are based on parameters like physical form of the semiconductor, their stability under the reaction conditions. Environmentally acceptable, cost effectiveness, less toxicity and in all these counts titanium dioxide appears to be the best choice. Comparing various systems for use of actual waste water treatment the following order has been proposed Degusa P-25 > TiO_2 (Anatase) > TiO_2 (Rutile). However, the amount of catalyst employed depends on the chemical nature of the semiconductor.

The photocatalytic activity can be altered with modification of the semiconductor. The modification can be with various aims like shifting the irradiation wavelength to the visible region and also coupling semiconductors for effective use of the excited electron-hole pair. Recently g-carbon nitride (g-C_3N_4) has been modified with calcium chloride and the mechanism of degradation of Rhodamine B dye itself is modified. The proposed schematic diagram is shown in Fig.3.

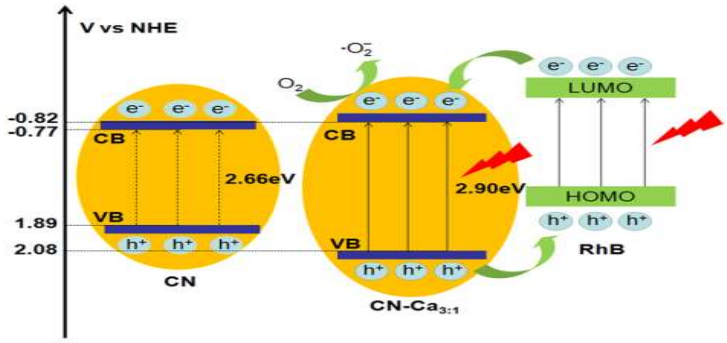

Fig.3. Energy level diagram of CN and CN modified with $CaCl_2$ and how the degradation activity of Rhodamine B is enhanced with modification of CN [reproduced from ref. A92].

The valence band level in modified system is shifted to more positive value and thus enhances the oxidation ability. Simultaneously the dye is also photoexcited and transfers the electrons to the conduction band of the modified g-C_3N_4. This route predominates when visible light is employed.

Apart from these inherent modifications to the semiconductors, (so called doping), coupling of semiconductors have also been tried for shifting the wavelength to the visible region and this is called Z-scheme.

Mechanism of Photo-catalytic Degradation of Dyes

It has been stated that radical species generated during photoexcitation of the semiconductor is responsible for the degradation of dyes. The essential steps involved can be visualized as the following steps [34-36]**.**

Semiconductor + photons (hv) → e^- (CB) + h^+(VB) (1)

$h^+ + H_2O \rightarrow H^+ + OH^-$ (2)

$h^+ + OH^- \rightarrow OH\bullet$ (3)

$e^- + O_2 \rightarrow O_2\bullet$ (4)

$2e^- + O_2 + H_2O \rightarrow H_2O_2$ (5)

$e- + H_2O_2 \rightarrow OH\bullet + OH^-$ (6)

Organic pollutant + $OH\bullet + O_2 \rightarrow CO_2 + H_2O$ + other degradation products (7)

The pictorial representation of this process is shown in Fig.2. The excited electron and hole in the semiconductor is responsible for the degradation of the dye. Variety of semiconductors have been employed and most of them are employed in the nano-state due to increased surface area and also due to favourable quantum size effect [37-40].

TiO_2 in various forms with metal and non-metal doping have been employed for the degradation of a variety of dyes owing to its stability, degradation capability, and also non-toxic nature [41,42]. However, the possible experimental variables including the wavelength of the light to be used and separation technology of the solid in treatment process restricts the employment of TiO_2 for commercial dye degradation process. More advanced level research is at present required to find suitable alternative to TiO_2 for this application. Other than TiO_2 the other system that is mostly employed is ZnO and other semiconducting oxides as stated above [ ].

Experimental Variables Studied:

In addition to the chemical nature of the semiconductor employed, the wave length of irradiation employed based on the band gap of the semiconductor, the effect on the degradation of dyes on a number of other experimental variables have been studied**.** Typical semiconductors studied and the band gap values of each of them are assembled in Table.2.

Table.2. Typical Semiconductors [Refer to Table 1] used for Photo-catalytic Degradation of Dyes and the Band gap (eV) Values of these Materials.

Semiconductors studied for photodegradation of dyes	Band gap values (eV) (wavelength [nm] of irradiation)
TiO_2(Anatase form)	3.2(387)
TiO_2 (Rutile form)	3.0 (415)
TiO_2 (Brookite form)	3.14(395)
ZnO	3.36(370)
WO_3	2.76(450)
CdS	2.42(515)
CuO	1.2 (1035)
Cu_2O	2.2 (565)
MgO	5.90
Mn_3O_4	3.28(380)
ZnS	3.6(345)
CeO_2	3.19(390)
Fe_2O_3	2.3(540)
Fe_3O_4	2.25(550)
ZrO_2	3.87(320)
g-C_3N_4	2.66(465)
Ag_2O	1.4(885)
$SrTiO_3$	3.25(380)
Bi_2WO_6	3.13(395)
BaTiO3	3.30
Bi_2O_3	2.80
CdO	2.20
CoO	2.01
Cr_2O_3	3.50
HgO	1.90
In_2O_3	2.80
MnO	3.60
Nb_2O_5	3.40
NiO	3.50
PbO	2.80
PdO	1.00
Sb_2O_3	3.00
SnO	4.20
SnO_2	3.50
V_2O_5	2.80

Effect of pH on the Photo-catalytic Degradation of Dyes

As seen from Table 2, each of the degradation studies is efficient at a particular pH. The reason for this observation is the change in the value of the oxidation potential (approximately 59 mV

per pH) of the species involved in the experimental system studied. Since the oxidation potential of hole and reduction power of the electron generated due to irradiation are dependent on the positions of the top of the valence band and bottom of the conduction band and these are critical for the degradation of dyes on semiconducting systems employed.

The Issues on Hand

Most of the published literature covers as variables, the light source, its intensity, pH of the medium, the amount of the catalyst employed. The initial concentration of the dye taken for study, the irradiation time and the other species like oxygen present in the reaction medium. Almost all the publications have been following these variables invariably. It is recognized that the study of these variables is important for assessing the utility of this method for pollutant removal (textile dye industry) from waste water stream. The purpose of this presentation is to examine on what other aspects of these parameters can be intrinsically examined.

Kinetics of photodegradation of Dyes

Generally, the kinetics of photocatalytic degradation of organic pollutants and dyes by semiconductors has most often treated as first order kinetics. This is most common in literature and as an example one of the recent references [15] is provided. The purpose is to analyze some of the consequences of treating the kinetic data on the removal of pollutants and other organic species especially under photo-catalytic conditions generally under first order kinetic equation. The first order kinetic equation generally employed in such circumstances [41] can be written as $- \ln (C/C_0) = kt$; where C is the concentration at any time t seconds and C_0 is the value of concentration of the species that is undergoing degradation at zero time (initial concentration taken) and k is the value of the rate constant, this may be a lumped parameter including the value of the intrinsic rate constant, adsorption equilibrium constant and so on. Typical kinetic data analyzed according to first order kinetic equation of the photo catalytic decomposition of Rhodamine B from ref 15 is given as an example.

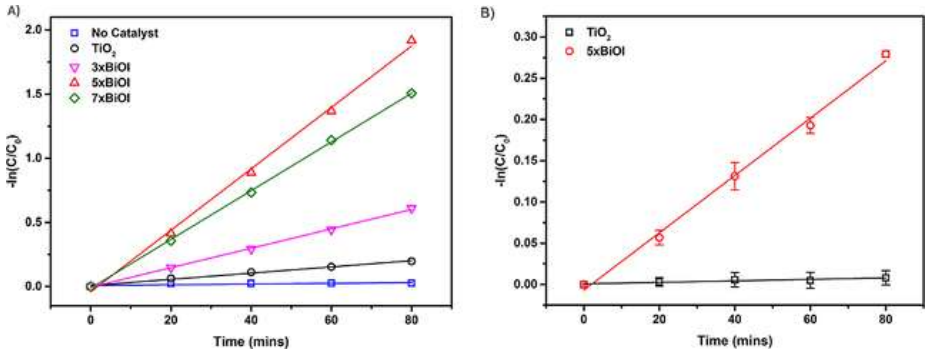

Fig 1 Photocatalytic degradation kinetics of Rhodamine B on various photo-catalysts treated according to first order kinetic equation [data reproduced from ref.15. There are any number of this kind of analysis reported in literature on photocatalytic decomposition of dyes and they are referred to in this article at other places] as an example.

The main conclusion of this study is that the inherent rate consists of the photo-catalytic and also photo-induced self-degradation of the dye follows first order kinetics. If this argument were to be accepted then the treatment of kinetic data according to first order is only grossly approximate and the apparent rate constant in the equation is only a lumped parameter consisting of mostly the value of the intrinsic rate constant and the rates of other parallel reactions that would have taken place on the surface of the catalyst and many other accompanying non-elucidated rates of degradation. Possibly, the value of the apparent rate constant cannot be taken as a measure of the activity of the catalyst for comparison since the process taking place on the two or more catalysts are not identical or not even similar. This will have serious misconceptions for comparison purposes.

In the example given, the authors report the apparent rate constant on the most active catalyst as 23.9 min^{-1} while the value of the apparent rate constant for the degradation of chlorophenol (where the photon induced degradation is assumed to be nearly negligible) is 3.47 min^{-1} which can be assumed in this case as the value of the intrinsic rate constant. May be caution has to be exercised while comparing two or more catalytic systems on the basis of the rate constant values of the kinetic data treated as first order since on all catalyst systems the reaction may not follow the same kinetics though the treatment according to first order kinetics may apparently satisfy the first order kinetics. The statements given may be applicable to all general reactions which can involve multiple steps like preceding or succeeding surface reactions which are more often treated with first order kinetics. However, it is not our intention to make a general treatment.

Dye degradation can have many preconditions, one of them is the adsorption of the dye on the catalyst surface and this equilibrium constant should be reflected in the value of the rate constant

evaluated from the data. The values of the equilibrium constants of adsorption on various catalyst surfaces can give same or different order of reactivity of adsorbents and this has to be considered while choosing the material for wastewater treatment.

The catalyst loading

Another observation invariably recorded in literature is that the rate increases with catalyst loading till certain weight and above this the rate of degradation of the dye decreases with increase in weight. This is not an unusual result since the exposed surface area of the catalyst will not be directly proportional to the amount of catalyst loaded in solution phase reactions. Since dye degradation is proportional to the amount that is adsorbed on the surface of the solid, there can be a saturation point beyond which the solid amount may not have a direct relationship to the degradation extent. In most of the studies reported the maximum amount of the solid loaded for maximum activity is 3-4 mg per litre [3] of the dye solution. This weight of the solid probably indicates the saturation limit of adsorption of the dye and possibly limits the concentration of the dye solution that can be employed for degradation and thus the industries polluting waterways must restrict their pollution limits to this level. This may be a mark for pollution control authorities to note and it must restrict pollution to this level.

1. Olga Sacco, Marco Stoller, Vincenzo, Vaiano, Paolo Ciambelli, Angelo Chianese, and Diana Sannino, Photocatalytic degradation of organic dyes under visible light on N-doped TiO_2 photo-catalysts, International Journal of Photoenergy, vol.2012, pp.1-8 (2012) Doi:10.1155/20121626759.
2. M.Z.B. Mukhtish, F. Najnin, M.M. Rahman, and M.J. Uddin, Photocatalytic degradation of different dyes using TiO2 with high surface area: A kinetic study, J. Sci. Res., 5(2) 301-314 (2013).
3. Khan Mamum Reza, A S W Kurney and Fahmida Gulshan, Parameters affecting the photocatalytic degradation of dyes using TiO_2: a review, Appl. Water. Sci., 7, 1569-1578 (2017), DOI:10.1007/s13201-015-0367-y.
4. A.K. Khataee and M.B. Kasiri, Photocatalytic degradation of organic dyes in the presence of nanostructured titanium dioxide: influence of the chemical structure of dyes, Journal of Molecular Catalysis A: Chemical, 328, 8-26 (2010); DOI:10.1016/j.monicata2010.05.023.
5. U.G. Akpan and B.H. Hameed, Parameter affecting he photocatalytic degradation of dyes using TiO_2 photo-catalysts: A review, Journal of Hazardous Materials, 170, 520-529 (2009); DOI:10.1016/jhazmet.3009.05.030.
6. M.A. Rauf and S. Salman Ashraf, Fundamental Principles and application of heterogeneous photocatalytic degradation of dyes in solution, Chemical Engineering journal, 151,10-18 (2009); doi:10.1016/j.cej 2009.02.026

7. M.A. Rauf, M.A. Meetani and S. Hisaidee, An overview on the photocatalytic degradation of azo dyes in the presence of TiO_2 doped with selective transition metals, Desalination276,13-27 (2011);doi:10.1016/j.desal 2011.03.071.
8. https://en.wikipedia.org/wiki/Industrial_dye_degradation.
9. Pandit, V.K.; Arbuj, S.S.; Pandit, Y.B.; Naik, S.D.; Rane, S.B.; Mulik, U.P.; Gosavic, S.W.; Kale, B.B. Solar Light driven Dye Degradation using novel Organo–Inorganic (6,13-Pentacenequinone/TiO2) Nanocomposite". RSC Adv. 2015, 5, 10326-10331.
10. T.M. Elmorsi, Y.M. Riyad, Z.H. Mohamed, H.M.H Abid, E. Bary, Decolorization of mordant red 73 azo dye in water using H_2O_2/UV photo Fenton treatment, Journal of Hazardous Materials, 174, 352-356 (2010).
11. S. Gul, O. Ozcan Yildlrln, Degradation of Reactive Red 194 and reactive yellow 145 azo dyes by O_3 and H_2O_2/UV-C process, Chemical Engineering Journal, 155,684-690 (2009)
12. F.H. AlHamedi and M.A. Rauf and S.S. Asraf, Degradation of Rhodamine B in the presence of UV/H_2O_2, Desalination 239, 159-166 (2009).
13. Y.B. Xie an X.Z. Li, Interactive oxidation of photo-electro-catalysis and electro-Fenton for azo- dye degradation using TiO_2-Ti mesh and reticulated Vitreous carbon electrode, Materials Chemistry and Physics, 95,39-50 (2006).
14. https://www.researchgate.net/post/What_is_the_Reduction_oxidation_Redox_Potential_of_Sulfate_Radicals_and_Hydroxyl_Radicals.
15. Gylen Odling and Neil Robertson, SILAR BiOI-Sensitized TiO_2 Films for Visible-Light Photocatalytic Degradation of Rhodamine B and 4-Chlorophenol, ChemPhysChem, 18, 728 – 735 (2017); DOI: 10.1002/cphc.201601417.
16. Khan Mamun Reza, A S W Kurny and Eahmida Gulshan, Parameters affecting the photo-catalytic degradation of dyes using TiO_2: A review, Applied Water Science, 7, 1569-1578 (2017).
17. Mo S-D, Ching WY. (1995) Electronic and optical properties of three phases of titanium dioxide: Rutile, anatase, and brookite. Physical Review B 51(19), 13023-32.
18. Iskandar F, Nandiyanto ABD, Yun KM, Hogan CJ, Jr. KO, Biswas P. Enhanced photocatalytic performance of brookite TiO2 macroporous particles prepared by spray drying with colloidal templating. Advanced Materials 19(10), 1408–12.(2007).
19. Bavykin DV, Friedrich JM, Walsh FC. Protonated titanates and TiO2 nanostructured materials: Synthesis, properties, and applications. Advanced Materials 18(21), 2807-24 (2006).
20. M. Koelsch, S. Cassaignon, J.F. Guillemoles, J.P. Jolivet.Comparison of optical and electrochemical properties of anatase and brookite TiO2 synthesized by the sol-gel method Thin Solid Films 403:312–9(2002).

21. Morgan BJ, Watson GW. (2010) Intrinsic n-type Defect Formation in TiO2: A Comparison of Rutile and Anatase from GGA plus U Calculations. Journal of Physical chemistry 114(5), 2321-8 (2010).
22. Qamar M, Yoon CR, Oh HJ, Lee NH, Park K, Kim DH, Preparation and photocatalytic activity of nanotubes obtained from titanium dioxide Catalysis Today 131(1-4), 3-14(2008).
23. Sclafani A, Herrmann JM. Comparison of the photoelectronic and photocatalytic activities of various anatase and rutile forms of titania in pure liquid organic phases and in aqueous solutions Journal of Physical Chemistry 100(32), 13655-61(1996).
24. Bakardjieva S, Subrt J, Stengl V, Dianez MJ, Sayagues MJ. Photoactivity of anatase-rutile TiO2 nanocrystalline mixtures obtained by heat treatment of homogeneously precipitated anatase. Applied catalysis B:Environmental 58(3-4), 193-202(2005).
25. Ohno T, Tsubota T, Toyofuku M, Inaba R. (2004) Photocatalytic activity of a TiO2 photo-catalyst doped with C4+ and S4+ ions having a rutile phase under visible light. Catalysis Letters 98(4), 255-8 (2004).
26. Colon G, Hidalgo MC, Munuera G, Ferino I, Cutrufello MG, Navıo J A, Structural and surface approach to the enhanced photocatalytic activity of sulfated TiO2 photo-catalyst. Applied Catalysis B: Environmental 63(1-2), 45-59(2006).
27. Li H, Zhang and W, Pan W. Enhanced photocatalytic activity of electrospun TiO2 nanofibers with optimal anatase/rutile ratio. Journal of the American Ceramic Society 94(10), 3184-7(2011).
28. Ohtani B, Ogawa Y, Nishimoto S-i. Photocatalytic activity of amorphous-anatase mixture of titanium(IV) oxide particles suspended in aqueous solutions. Journal of Physical Chemistry B 101(19), 3746-52 (1997).
29. Elahee K., Heat recovery in the textile dyeing and finishing industry: lessons from developing economies Journal of Energy in Southern Africa, 21(3), 9-15 (2010).
30. Singh P, Mondal K, Sharma A. Reusable electro-spun mesoporous ZnO nanofiber mats for photocatalytic degradation of polycyclic aromatic hydrocarbon dyes in wastewater. Journal of Colloid and Interface Science, 394, 208-15, (2013).
31. Hoffmann MR, Martin ST, Choi W, Bahnemannt DW. Environmental Applications of Semiconductor Photo catalysis. Chemical Reviews, 95(1), 69-96, (1995).
32. Meng Z, Juan Z. (2008) Wastewater treatment by photocatalytic oxidation of nano-ZnO. Global Environmental Policy in Japan, 12, 1-9 (2008).
33. Hernandez-Alonso MD, Fresno F, Suareza S, Coronado JM. Development of alternative photo catalysts to TiO2: Challenges and opportunities. Energy & Environmental Science, 2(12), 1231-57, (2009).
34. Mills, A., Davies,R.H., Worsley, D., Water Purification by semiconductor photocatalysis, Chemical Society of Reviews, 22(6),417-25 (1993).
35. Hashimoto,k., Irie,H., and Fujishima, A., TiO_2 Photcatalysis: A historical overview future prospects, Japanese Journal of Applied Physics, 44(12),8269-8285 (2005).

36. Neppolian, B., Sakthivel,S., Arabindoo,B., Palanichamy, M., Murugesan,V., Degradation of textile dye by solar light using TiO_2 and ZnO photocatalysts, Journal of Environmental science and Health Part A., Toxic/Hazardous Substances and Environmental Engineering, 34(9),1829-1838 (1999).
37. Ye, M., Zhang,Q., Hu,Y., Ge,J., Lu,Z., He,L., Magnetically recoverable core shell nanocomposites with enhanced photocatalytic activity, Chemistry – a European Journal, 16(21), 6243-6250 (2010).
38. Colmenares, J.C., Luque, R., Campelo,J.M., Colmenares,F., Karpinski,Z., and Romero, A.A., Nanostructured photocatalysts and their applications in the photocatalytic transformation of lignocellulosic biomass: an Overview, Materials, 2(4),2228-2258 (2009).
39. Anpo,M., Shima,T., Kodama,S., and Kubokawa,Y., Photocatalytic hydrogenation of propyne with water on small particle titania: size quantization effects and reaction intermediates, Journal of physical Chemistry, 91(16),4305-4310 (1987).
40. Lin,H., Huang C.P., Li,W., Ni,C., Shah,S.I., and Tseng, Y-H, Size dependency of nanocrystalline TiO_2 on its optical property and photocatalytic reactivity exemplified by 2-chlorophenol, Applied Catalysis B:Environmental,68(1-2),1-11(2006).
41. Reza Sarkhanpour, Omid Tavakoli , Samira Ghiyasi, Mohammad Reza Saeb* , Rafael Borja, Photocatalytic Degradation of a Chemical Industry Wastewater: Search for Higher Efficiency, Journal of Residuals Science & Technology, 14, 44-58 (2017); doi: 10.14355/jrst.2017.1404.006.
42. Anila Ajmal , Imran Majeed, Riffat Naseem Malik, Hicham Idriss and Muhammad Amtiaz Nadeem, Principles and mechanisms of photocatalytic dye degradation on TiO_2 based photo-catalysts: a comparative overview, RSC Advances, 4,37003-37026 (2014) DOI: 10.1039/C4RA06658H
43.

A1. Zhigang Xiong, Li Li Zhang, Jizhen Ma and X.S. Zhao, Photocatalytic degradation of dyes over graphene-gold nanocomposites under visible light irradiation, Chem.Commun.,46, 6099-6101 (2010).

A2. Rajesh J. Tayade, Praveen K. Surolia, Ramachandra G. Kulkarni and Raksh V. Jasra, Photocatalytic degradation of dyes and organic contaminants in water using nanocrystalline anatase and rutile TiO_2, Science and Technology of Advanced Materials, 8, 455-462 (2007).

A3. Dnyaneshwar R. Shinde, Popat S. Tambade, Manohar G. Chaskar and Kisan M. Gadave, Photocatalytic degradation of dyes in water by analytica reagent grade photocatalysts – A comparative study, Drink.water Eng.Sci.,(under review on June2017).

A4. Balaram Kiran Avasarala, Siva Rao Tirukkovalluri and Sreeder Bojja, Magnesium doped Titania for photocatalytic degradation of dyes in visible light, Journal of Environmental and Analytical Toxicology,6,1-8 (2016).

A5. O.K.Mahadwad, P.A.Parikh, R.V. Jasra and C. Patil, Photocatalytic degradation of reactive black-5 dye using TiO_2 impregnated ZSM-5, Bulletin of Material Science, 34,551-556(2011).

A6. Akbar Mohammed, Kshipra Kapoor and Shaikh M.Mobin, Improved photocatalytic degradation of organic dyes by ZnO-nanoflowers, Chemistryselect, 1,3483-3490 (2016).

A7. R.Nagaraja, Nagaraju Kottam, C.R.Girija and B.M.Nagabhushana, Photocatalytic degration of Rhodamine B dye under UV/solar light using ZnO nano powder synthesized by solution combustion route, Powder Technology,215-216, 91-97 (2012).

A8. Meeti Mehra and T.R.Sharma, Photo-catalytic degradation of two commercial dyes in aqueous phase using photo catalyst TiO_2, Advances in Applied Science Research, 3,849-853 (2012).

A9. Partha Mahata, T. Aarthi, Gridhar Madras and Srinivasan Natarajan, Photocatalytic degradation of Dyes and Organics with nanosized $GdCoO_4$, Journal of Physical Chemistry C, 111, 1665-1674 (2007).

A10. Elvis Fosso-kaneu, Frans Waanders and Maryka Geldenhuys, 7th International conference on latest Trends in Engineering & technology, Pretoria, Nov 26-27 (2015).

A11. Jan Sima and Pavel Hasal, Photocatalytic Degradation of Textile Dyes in a TiO_2/UV system, Chemical Engineering Transactions, 32, 79-84 (2013).

A12. Manon Vautier, Chantal Guillard and Jean-Marie Herrman, Photocatalytic Degradation of Dyes in Water: Case study of Indigo and Indigo Carmine, Journal of Catalysis, 201, 46-59 (2001).

A13. S.A. Abo-Farha, Photocatalytic degradation of Monoazo and Diazo dyes in wastewater on Nanometer-sized , Researcher, 2(7) 1-20 (2010).

A14. M.A. Mahmoud, A. Poncheri, Y. Badr and M.G. Abd El Wahed, Photocatalytic degradation of methyl red dye, Aouth African Journal of Science, 105, 299-303 (2009).

A15. Morteza Montazerozohori, Masoud Nasr-Esfahani and Shiva Joohari, Environment Protection Engineering, 38,45-55(2012).

A16. M. Amini and .M. Ashrati, Photocatalytic degradation of some organic dyes under solar light irradiation using TiO_2 and ZnO nanoparticles, Nano.Chem.Res., 1 (1) 79-86 (2016).

A17. Chhoyu Ram, Ravi Kant Pareek and Varinder Singh, Photocatalytic degradation of textile dye using Titanium dioxide nanocatalyst, International Journal of Theroetical and applied Sciences, 4(2) 82-88 (2012).

A18. M.V. Shankar, B.Beppolian. S.Sakthivel, Banumadhi Arabindoo. M.Palaniswamy and V.Murugesan, Kinetics of photocatalytic degradation of textile dye reactive Red 2, Indian Journal of Engineering and Material Scince, 8, 104-109 (2001).

A19. Tapas Kumar Roy and Naba Kumar Mondal, Photocatalytic degradation of congo red dye on thermally activated Zinc Oxide, International Journal of Scientific Research and environmental Science, 2 (12)457-469 (2014).

A20. Lidija Curkovic, Davor Ljubas, Suzana Segota, Ivana Bacic, Photocatalytic degradation of Lissminw Green B dye by using Nanostructured Sol-gel TiO_2 films, Journal of Alloys and Compounds,604, 308-316 (2015).

A21. Susheela Bai Gajbhiye, Photocataltic degradation study of methylene blue solution and its application to dye industry effluent, International Journal of Modern Engineering Research, 2(3), 1204-1208 (2012).

A22. Ankita Khanna and Vidya K Shetty, Solar light induced photocatalytic degradation of Reactive Blue 220 (RB—220) dye with highly efficient Ag@TiO_2 core shell nanoparticles: A comparison with UV photocatalysts, Solar Energy, 99,67-76 (2014).

A23. Emy Marlina Samsudin, Sze Nee Guh, Ta Young Wu, Tan Tong Ling, Sharifati Bee Abd Hamid and JoonChingJean, Evaluation on the photocatalytic degradation activity of reactive Blue-4 using Pure anatase Nano-TiO_2, Sains Malaysiana 44(7),1014-1019 (2015).

A24. N.P.Mohabansi, V.B.Patil and N.Yenkie, A comparative study on Photodegradation of Methylene blue dye effluent by advanced oxidation process by using TiO_2/ZnO photocatalyst, Rasayan Journal Chemistry,4(4),814-819 (2011).

A25. Veljko Djokic, Jelena Vujovic, Aleksandar Marinkovic,Rada Petrovic, Djordje Janackovic, Antonije Onjia, and Dusanijin, A study of the photocatalytic degradation of the textile dye C1 Basic Yellow 28 in water using a P160 TiO_2 based catalyst, Journal of the Serbian Chemical Society,77(12), 1747-1757 (2012).

A26. W.Rezig and M.Hadjel, Photocatalytic degradation of Vat Green 03 textile dye using the ferrihydrite-modified Diatomite with TiO_2/UV process, Oriental Journal of Chemistry, 30(3),993-1007 (2014)).

A2. Azita Mohagheghian, Seyydeh-Amene Karimi, Jae-Kyu Yang, and Mehdi Shirzad Siboni, Photocatalytic degradation of a textile dye by Illuminated Tungsten oxide nano powder, Journal of Advanced Oxidation Technology, 18 (1) 61-68 (2015).

A28. William Wilson Anku, Samuel-Osei-Bonsu Oppong, Sudheesh Kumar Shukla and Poomani Penny Govender, Comparative photocatalytic degradation of Mono-azo and diazo dyes under simulated visible light using Fe^{3+}/C/S doped TiO_2 nano particles, Acta Chimica Slovakia, 63, 380-391 (2016).

A29. Khushnuma Parveen and Ritu Vyas, Photocatalytic degradation of Non-Biodegradable Malachite Green dye by Ni-Doped Titanium dioxide, Journal of Current Chemical and Pharmaceutical Science, 6(4) 53-62 (2016).

A30. A.Bonkhennoufu, M.Bouhelassa and Z.Zoulalidian, Photocatalytic degradation of Solo phenyl Red 3 BL an aqueous suspension of Titanium Dioxide, Journal of Advanced Chemical Engineering, 1, 1-8 (2011).

A31. Ohm-Mar Min, Li-Ngee Ho, Soon-An Ong and Yee-Shian Wong, Comparison between the photocatalytic degradation of single and binary azo dyes in TIO_2 suspensions under solar light irradiation, Journal of Water Reuse and Desalination, 13 pages (2015).

A32. Sayed Mohammad Bagner Hosseini, Narges Falish and Sayed Javid Royaee, Optimization of photocatalytic degradation of real textile dye house wastewater by response surface methodology, Water Science and Technology, (2016) In press.

A33. Nyabaro Obed Mainya, Patrick Tum and Titus M Muthoka, Photodegradation and adsorption of methyl orange and Methylene Blue dyes on TiO_2, International journal of Science and Research, 4(4)3185-3189 (2015).

A34. Ahmed Hassan Ali, Study on the photocatalytic degradation of Indigo Carmine dye by TIO_2 photo-catalyst, Journal of Kerbala University, 11(2)145-153 (2013).

A35. S.K.Pinky, Ferdush Ara,A.S.W Kurny, Fahmida Gulshan, Photo degradation of industrial dye using ZnO as photo catalyst, International Journal of Innovative Research in Science, Engineering ad Technology, 4 (10) 9986-9992 (2015).

A36. Aghareed M.Tayeb and Dina S.Hussein, Synthesis of TiO_2 nanoparticles and their photo catalytic activity for methylene Blue, American Journal of Nanomaterials, 3(2) 57-63 (2015).

A37. E.K.Kirupavasam and G.Allen Gnana Raj, Photocatalytic degradation of amido black-10B catalyzed by carbon doped TiO_2 photo-catalyst, International Journal of Green Chemistry and Bioprocess, 2(3)20-25 (2012).

A38. Neha Verma, Sunik Bhatia and R.K.Bedi, Effeict of annealing temperature on ZnO nano particles and its applications for photo-catalytic degradation of DR-31 dye, International Journal of Pure and Applied physics, 13(1)118-122 (2017).

A39. Veronika Marinovic, Davor Ljubas and Lidija Curkovic, Effects of concentration and UV radiation wavelengths on photolytic and photo-catalytic degradation of azo dyes aqueous solution by sol-gel TiO_2films, The Holistic Approach to Environment, &,3-14 (2017).

A40, D.Channei, B.Inceesungvorn, N.Wetchakun, S.Ukritnukun, A.Nattestad, J.Chen, and S.Phanichphant, Photo-catalytic degradation of methyl orange by CeO_2 and Fe-doped CeO_2 films under visible light irradiation, AP energy conference Proceedings, (2014).

A4. Siew-Teng Ong, Wai-Sim Cheong, and Yung-Tse Hung, Photodegradation of commercial dye, methylene blue using immobilized TiO_2, 4^{th} International conference on Chemical , Biological and Environmental Engineering, IPCBEE, 43,109-113 (2012).

A42. A.Abilarasu, T.Somanathan, A.Saravanan, V.Saravanan and P.Rajkumar, Enhanced photo-catalytic degradation of malachite green on spinel ferrite(nickel/magnesium ferrite) under direct sunlight, International Journal of Pharma and Bio-Sciences, 7(4),93-99 (2016).

A43.Yuanjie Su, Ya Yang, Hulin Zhang, Yannan Xie, Zhiming Wu, Yadong Jiang, Naoki Fukata, Yoshio Bando and Zhong Lin Wang, Enhanced Photodegradation of methyl orange with TiO_2 nanoparticles using a triboelectric nanogenerator, Nanotechnolgy, 24, 1-6 (2013).

A44. Huayue Zhu, Ru Jiang, Ling Xiao, Yuhua Chang, Yujiang Guan, Xiaodong Li, and Guangming Zeng, Photocatalytic decolorization and degradation of Congo Red on innovative crosslinked chitosan/nano CdS composite catalyst under visible light irradiation, Journal of Hazardous Materials,169, 933-940 (2009).

A45. Ammar Houas, Hinda Lachheb, Mohamed Ksibi, Elimame Elaloui, Chantal Guilard, Jean-Marie Herrmann, Photocatalytic degradation pathway of methylene blue in water, Applied Catalysis, B. Environmental, 3 145-157 (2001).

A46. N.Divya, A.Bansal and A.K.Jana, Photocatalytic degradation of azo dye orange II in aqueous solutions using copper impregnated titania, International Journal of Environmental Science and Technology, 10, 1265-1274 (2013).

A47. Vo Thi Thu Nhu, Do Quang Minh, Nguyen Ngoe Duy and Nguyen Quoc Hien, Photocatalytic degradation of Azo dye (methyl Red) in water under visible light using Ag-Ni/TiO_2 synthesized by γ-Irradiation method, International Journal of Environment Agriculture and Biotechnology, 2 (1), 529-538 (2017).

A48. Pei Wen Koh, Mohd Hayrie Mohd Hatta, Stew Teng Ong, Leny Yuliati and Siew Ling Lee, Photocatalytic degradation of photosensitizing and non-photosensitizing dyes over chromium doped titania photo-catalysts under visible light, Journal of photochemistry and Photobiology: A Chemistry,332, 215-223 (2017).

A49. Metwally Madkour and Fakhreia Al Sagheer, Au/ZnS and Ag/ZnS nano heterostructures as regenerated nano photo-catalysts for photo-catalytic degradation of organic dyes, Optical Materials Express, 7, 158-169 (2017).

A50. Subas K Muduli, Songling Wang, Shi Chen, Chin Fan Ng, Cheng Hon Alfred Huan, Tze Chen Sum, and Han Sen Soo, Mesoporous Cerium oxide nano spheres for the visible light driven photocatalytic degradation of dyes, Beilstein Journal of Nanotechnology, 5, 517 523 (2014).

A51. Shweta Sharma, Rakshit Ameta, R.K.Malkani and Suresh C.Ameta, Photo-catalytic degradation of Rose Bengal using semiconducting Zinc Sulphide as the photo-catalyst, Journal of the Serbian Chemical Society, 78, 897-905 (2013).

A52. Jatinder Kumar and Ajay Bansal, Dual effect of photo-catalysis and adsorption in degradation of Azorubine dye using nano-sized TiO_2 and activated carbon immobilized with different techniques, International Journal of Chemtech Research, 2(3),1537-1543 (2010).

A53. Muhammad Umar and Hamidi Abdul Aziz, Photocatalytic degradation of organic pollutants in water, Environmental Science ," Organic Pollutants Monitoring ,Risk and Treatment", book edited by M. Nageeb Rashed, 2013 and other systems referred to in Table 2 in this chapter 8 of this book.

A54. Abrar M. Algubil, Enas M. Alrobay and Ayad F. Alkaim, Photocatalytic degradation of Remazol Brilliant Blue dye by ZnO/UV process, International Journal of chemical Sciences, 13(2), 911-921 (2015).

A55. Raquel Cruz, Laura Hinojosa Reyes, Jorge L. Guzmán-Mar, Juan Manuel Peralta-Hernández and Aracely Hernández-Ramírez, Photocatalytic degradation of phenolic compounds contained in the effluent of a dye manufacturing industry, Sustainable Environmental Research, 21(5), 307 -312 (2011).

A56. Nirmalya Tripathy , Rafiq Ahmad, Jeong Eun Song, Hyun Park, Gilson Khang, ZnO nanonails for photocatalytic degradation of crystal violet dye under UV irradiation, AIMS Materials Science, 2017, 4(1): 267-276. doi: 10.3934/matersci.2017.1.267.

A57. **E.S. Baeissa,** Photocatalytic degradation of methylene blue dye undervisible light irradiation using In/ZnO nanocomposite, **Frontiers in Nanoscience and Nanotechnology,2(05)1-5 (2016).**

A58. Ouarda Brahmia, Photocatalytic Degradation of a Textile Dye under UV and Solar Light Irradiation UsingTiO2 and ZnO nanoparticles, International Journal of Advances in Chemical Engineering and Biological Sciences (IJACEBS) 3, (2), 225-227, (2016) ISSN 2349-1507 EISSN 2349-1515.

A59. Aghareed M. Tayeb, Dina S. Hussein, Synthesis of TiO2 Nanoparticles and Their Photocatalytic Activity for Methylene Blue, *American Journal of Nanomaterials, 3,(2), 57-63.(2015).*

A60. Loum Janani, Kanwezi Henry, Kamalha Edwine, **Optimization of Photocatalytic Degradation of Reactive Blue Dye Using Zinc Oxide Catalyst,** International Journal of Research and Review,2(6), 343-347 (2015).

A61. Khan M. Reza, Asw Kurny, and Fahmida Gulshan, Photocatalytic Degradation of Methylene Blue by Magnetite+H_2O_2+UV Process, *International Journal of Environmental Science and Development, 7(5),325-329(2016).*

A62. Liang Wang1, Jun Shang1, Weichang Hao, Shiqi Jiang, Shiheng Huang, Tianmin Wang, Ziqi Sun, Yi Du, Shixue Dou, Tengfeng Xie, Dejun Wang and& Jiaou Wang, A dye-sensitized visible light photocatalyst-Bi24O31Cl10, SCIENTIFIC REPORTS,(2014) DOI: 10.1038/srep07384.

A63. F U Dawei, Xie Ruyi, Zhang Linping, Xu Hong, Zhong Yi, Sui Xiafeng and Mao Zhiping, Preparation of Hallow spherical Bismuth oxyiodide and its adsorption and

Photocatalyti degradation of dyes, Chinese Journal of Applied Chemistry, 34(5), 590-596 (2017).

A64. S.Aliouche, K.Djebbar, R.Zouaghi and T.Sehili, Photocatalytic degradation of yellow Alizarin Azo Dye in the presence of TiO_2 suspension, Sciences & Tecnhologie, A; No.39 june 2014, pp.23-30.

A65. Kunal Mondal and Ashutosh Sharma, Photocatalytic Oxidation of Pollutant Dyes in Wastewater by TiO_2 and ZnO nono-materials, A Mini-review, www.nasi.org.in/Nano/3%20-20Ashutosh%20Sharma.pdf

A66. Jyoti Tolia, Mousumi Chakraborty and Z.Murthy, Photocatalytic degradation of malachite green dye using doped and undoped ZnS nanoparticles, Polish Journal of Chemical Technology, 14(2), 16-21 (2012).

A67. P. Dharmarajan, A.Sabastiyan, M.Yosuva Suvaikin, S.Titurs and C.Muthukumar, Photocatalytic Degradation of Reactive Dyes in Effluents Employing Copper Doped Titanium Dioxide Nanocrystals and Direct Sunlight, Chemical Science Transactions, 2(4),1450-1458 (2013).

A68. K. Govindan, Chandran, H. T., Raja, M., Maheswari, S. U., and Dr. Murali Rangarajan, "Electron scavenger-assisted photocatalytic degradation of amido black 10B dye with Mn3O4 nanotubes: A response surface methodology study with central composite design", Journal of Photochemistry and Photobiology A: Chemistry, vol. 341, pp. 146-156, 2017.

A69. S.Harikengaram , M.Robinson, A.Chellamani, Homogeneous Photocatalytic Degradation of Reactive Orange M2R Dye in Aqueous Medium, Journal of Environmental Nanotechnology, 3(2), 1-8, (2017).

A70. Pankaj Chowdhury, Jesus Moreira, Hassan Gomaa and Ajay K. Ray. "Visible-solar-light-driven photocatalytic degradation of phenol with dye-sensitized TiO2: parametric and kinetic study" *Industrial & Engineering Chemistry Research* Vol. 51 Iss. 12 (2012) Available at: http://works.bepress.com/pankaj_chowdhury_western_university/6/

A71. S.N.Muhith, B.D.Choudhury, M.T.Uddin and M.A.Islam, Study of Photo-catalysts for the Treatment of Dye-Contaminated Wastewater, International Journal of Integrated Sciences & Technology 2 (2016) 19-23.

A72. Jatinder Kumar, and Ajay Bansal, Photocatalytic degradation of amaranth dye in aqueous solution using sol-gel coated cotton fabric, Proceedings of the World Congress on Engineering and Computer Science 2010 Vol II, WCECS 2010, October 20-22, 2010, San Francisco, USA.

A73. Houda Ben Yahia Smida1 and Bassem Jamoussi, Degradation of Nitroaromatic Pollutant by Titanium dioxide/Zinc Phthalocyanine: Study of the Influencing Factors, *IOSR Journal of Applied Chemistry (IOSR-JAC),2(3)11-17, (2012).*

A74. Tiantian Wu, Yanping Liang and Fangyuan Deng, Study on the Degradation of Dye Pollutants Over Silver Phosphate Photocatalyst, International Conference on Advances in Energy, Environment and Chemical Engineering (AEECE-2015).

A75. Indu Bhati, Pinki B. Punjabi, and Suresh C. Ameta, Photocatalytic degradation of fast green using nonosized $CeCrO_3$, *Macedonian Journal of Chemistry and Chemical Engineering.* Vol. 29, No. 2, pp. 195–202 (2010).

A76. Mohamed A. Salem, Shaban Y. Shaban and Sherin. M. Ismail, Photocatalytic Degradation of Acid Green 25 using ZnO and Natural Sunlight, International Journal of Emerging Technology and Advanced Engineering, 5(3), 439-443 (2015).

A77. Kamila Bubacz, Julia Choina, Diana Dolat, Antoni W. Morawski, Methylene Blue and Phenol Photocatalytic Degradation on Nanoparticles of Anatase TiO2, *Polish Journal of Enviromental Studies,19 (4) 685-691(2010).*

A78. Gabriela Antoaneta Apostolescu, Corina Cernatescu, Claudia Cobzaru, Ramona Elena Tataru-Farmus, Nicolae Apostolescu, Studies on the photocatalytic degradation of organic dyes using CeO_2 – ZnO mixed oxides, *Environmental Engineering and Management Journal,14(2), 415-420 (2015).*

A79. C. Karunakaran, P. Magesan, P. Gomathisankar, P. Vinayagamoorthy, "Photocatalytic Degradation of Dyes by Al_2O_3-TiO_2 and ZrO_2-TiO_2 Nanocomposites", Materials Science Forum, Vol. 734, 325-333,(2013).

A80. Zainab Raheem and Ahmed M. Hameed, Photocatalytic Degradation for Methylene Blue Dye Using Magnesium Oxide, International Journal of Basic and Applied Science, 4(1),81-83 (2015).

A81. Rachita Mehta and Menka Surana, Photodegradation of Dye Acid Orange 67 by Titanium Dioxide in the Presence of Visible Light and UV Light, Research Reviews, 2(2), 1216 (2013).

A82. *https://www.rit.edu/affiliate/nysp2i/sites/rit.edu.../12rdsc09_report_cuny-csi.pdf.*

A83. Rakshit Ameta, Sanyogita Sharma, Shweta Sharma and Yogesh Gorana, Visible Light Induced Photocatalytic Degradation of Toluidine Blue-O by using Molybdenum Doped Titanium Dioxide, European Journal of Advances in Engineering and Technology, 2(8), 95-99(2015).

A84. Lum Sin Wan, A Study into photocatalytic degradation of methylene blue and glycerol aqueous solution over copper ferrite catalyst, Bachelor degree thesis, Faculty of Chemical & Natural Resources Engineering, Universiti Malaysia, Pahang, (2015).

A85. Valentine Rupa, A., Manikandan, D., Divakar, D., Revathi,S., Leena Preethi, M, Esther, Shanthi, K., and Sivakumar,T., Photocatalytic degradation of tatrazine dye using TiO_2 catalyst : Salt effect and kinetic studies. Indian Journal of Chemical Technology,14(1),71-78 (2007).

A86. Narde SB, Lanjewar RB, Gadegone SM, Lanjewar MR, Photocatalytic Degradation of Azo Dye Congo Red Using Ni0.6Co0.4Fe2o4 as Photocatalyst, Der Pharma Chemica, 9(7),115-120 (2017).

A87. Zahra Minaii Zangi, Hossein Ganjidoust and Bita Ayati, Analysis of photocatalytic degradation of azo dyes under sunlight with response surface method, *Desalination and Water Treatment,* 63, 262–274 (2017).

A88. Bojana Simovic´, Dejan Poleti2, Aleksandar Golubovic´, Aleksandar Matkovic´, Maja Ščepanovi , Biljana Babic´, and Goran Brankovic, Enhanced photocatalytic degradation of RO16 dye using Ag modified ZnO nanopowders prepared by the solvothermal method, Processing and Application of Ceramics 11 [1] 27–38, (2017).

A89. Khaled Mezughi, Chedly Tizaoui, and Ma'an Fahmi Alkhatib, **Effect of TiO2 Concentration on Photocatalytic Degradation of Reactive Orange 16 Dye (RO16),** *Advances in Environmental Biology, 8,(3), 692 – 695, (2014).*

A90. Salehi Kamal, Maleki Afshin, Shahmoradi Behzad, Mansouri Borhan, Gharibi Fardin, Investigation of photocatalytic degradation of reactive black5 dye suing ZnO-CuO nanocomposite, Zanko Journal of Medical Sciences, 15(46), 66-74 (2014).

A91. Veronika Marinovic, Davor Ljubas, Lidija Curkovic, Effects of concentration and UV radiation wavelengths on photolytic and photocatalytic degradation of azo dyes aqueous solutions by sol-gel TiO2 films, The Holistic Approach to Environment 7(2017)1, 3-14.

A92. Xiaozhou Long, Tingnan Yan, Tianjiao Hu, Xianghui Gong, Huaming Li, and Zengyong Chu, Enhanced Photo-catalysis of g-C3N4 Thermally Modifed with Calcium Chloride, Catalysis Letters, 147, 1922-1930 (2017). DOI 10.1007/s10562-017-2099-0.

A93. P.Dhatshanamurthi, B.Subash and M.Shanthi, Investigation on UV-A light photocatalytic degradation of an azo dye in the presence of CdO/TiO_2 coupled semiconductor, Materials Science in Semiconductor Processing, 35, 22-29 (2015).

A94. Cresus V.D.Gouvea, Fernandes Wypych, Sandra G.Moraes, Padricio Peralta-Zamora, Semiconductor-Assisted Photo-catalytic Degradation of Reactive Dyes in Aqueous Solution,Chemosphere, 40(4), 433-440 (2000).

A95. Xinshan Rong, Fengxian, Hao Zhao, Jie Yan, Xiaolu Zhu and Dongya Yang, Fabrication of Single-Layer Graphitic Carbon Nitride and Coupled Systems for the Photo-catalytic Degradation of Dyes under Visible-Light Irradiation, Eur. J. Inorg. Chem. 1359–1367 (2015).

A96. Malka Rochkind, Sagi Pasternak and Yaron Paz, Using dyes for evaluating photo-catalytic Properties: A critical Review, Molecules, 20,88-110(2015), doi:10.3390/molecules20010088.

A97. Alemseged Eyasu, O.P.Yadav, and R.K.Bachheti, Photo-catalytic degradation of methyl orange dye using Cr-doped ZnS nanoparticles under visible radiation, International Journal of chemtech Research, 5(4), 1452-1461 (2013).

A98. Raji, Jeevitha, Palanivelu, Kandasamy, Semiconductor coupled solar photo-Fenton`s treatment of dyes and textile effluent, Advances in Environmental research, 5(1) 61-77 (2016).

A99. Edson Luiz Foletto, Suellen Battiston, Gabriela Carvalho Collazzo, Mariana Moro Bassaco and Marcio Antonio Mazutti, Degradation of Leather dye using CeO_2-SnO_2 nanocomposite as photocatalyst under sunlight, water Air Soil pollutant, 223, 5773-5779 (2012).

A100. Yiming He, Lihong Zhang, Maohong Fan, Xiaoxing Wang, Mikel L.Walbridge, Qingyan Nong, Ying Wu, Leihong Zhao, Z-scheme SnO_{2-x}/g-C_3N_4 composite as an efficient photo-catalyst for dye degradation and Photocatalytic CO_2 reduction, Solar Energy Materials and solar cells, 137, 175-184 (2015).

A101. Qiaoying Li, Zhipeng Guan, Di Wu, Xiuge Zhao, Shenyuan Bao, Baozhu Tian and Jinlong Zhang, Z-Scheme BiOCl-Au-CdS Heterostructure with Enhanced Sunlight-Driven Photocatalytic Activity in Degrading Water Dyes and Antibiotics, *ACS Sustainable Chemistry Engineering, June (2017).* DOI: 10.1021/acssuschemeng.7b01157.

A102. Julie M.Pardiwala, Femina J.Patel and Sanjay S.Patel, Photo-catalytic degradation of RB21 dye by TiO_2 and ZnO under natural sunlight: Microwave Irradiation and UV reactor, International Journal of Advanced Research in Engineering and Technology,8(1), 8-16 (2017).

A103. Kirana Devarahosahalli Veeranna, Madhu Theeta Lakshamaiah, and Ramesh Thimmasandra Narayan, Photocatalytic Degradation of Indigo Carmine Dye Using Calcium Oxide, International Journal of Photochemistry, Volume 2014 (2014), Article ID 530570, 6 pages, **http://dx.doi.org/10.1155/2014/530570**.

A104. Yanan Liu , Ruixia Wang, Zhengkun Yang, Hong Du, Yifan Jiang , Congcong Shen, Kuang Liang , Anwu Xu, Enhanced visible-light photocatalytic activity of Z-scheme graphitic carbon nitride/oxygen vacancy-rich zinc oxide hybrid photocatalysts, Chinese Journal of Catalysis 36, 2135–2144 (2015).

A105. Yunjin Yao, Guodong Wu, Fang Lu, Shaobin Wang, Yi Hu, Jie Zhang, Wanzheng Huang, and Fengyu Wei, Enhanced photo-Fenton-like process over Z-scheme

$CoFe_2O_4$/g-C_3N_4 Heterostructures under natural indoor light, Environmental Science and Pollution Research, 23 (21), 21833–21845 (2016).

A106. Surender Kumar and Sahare, P.D, Photocatalytic acitivity of bismuth vanadate for the degradation of organic compounds, *NANO* **08**, 1350007, (2013), https://doi.org/10.1142/S1793292013500070.

A107. Shimin Xiong,, Tianhui Wu, Zihong Fan, Deqiang Zhao, Mao Du, and Xuan Xu, Preparation of a Leaf-Like BiVO4-Reduced Graphene Oxide Composite and Its Photocatalytic Activity, Journal of Nanomaterials, 2017, Article ID 3475248, 12 pages, https://doi.org/10.1155/2017/3475248.

A108. Peitao Liu, Yonggang Liu, Weichun Ye, Ji Ma and Daqiang Gao, Flower-like N-doped MoS_2 for photocatalytic degradation of RhB by visible light irradiation, Nanotechnology 27 (2016) 225403 (8pp).

A109. Shuijin Yang,Yongkui Huang,Yunzhi Wang,Yun Yang,Mingbo Xu, and Guohong Wang, Photocatalytic Degradation of Rhodamine B with H3PW12O40/SiO2 Sensitized by H2O2, International Journal of Photoenergy (2012). **DOI: 10.1155/2012/927132.**

A110. Luís F da Silva, Osmando F Lopes, Vagner R de Mendonça, Kele T G Carvalho, Elson Longo, Caue Ribeiro, Valmor R Mastelaro, An Understanding of the Photocatalytic Properties and Pollutant Degradation Mechanism of SrTiO3 Nanoparticles, *Photochemistry and Photobiology, 92 (3): 371-8(2016).*

A111. Md.Rakbuddin, Subrata Mandal, Rajkumar Ananthakrishnan, A novel ternary CuO decorated Ag_3AsO_4/GO hybrid as a z-scheme photocatalyst for enhanced degradation of phenol under visible light, New Journal of Chemistry41, 1380-1389(2017).

A112. Guangxin Zhang, Bin Wang, Zhiming Sun, Shuilin Zheng and Shushu Liu, A comparative study of different diatomite-supported TiO_2 composites and their photocatalytic performance for dye degradation, Journal of Desalination and Water Treatment, 57, (37) (2016).

A113. Yeoseon Choi, Min Seok Koo, Alok D. Bokare, Dong-hyo Kim, Detlef W. Bahnemann, and Wonyong Choi, Sequential Process Combination of Photocatalytic Oxidation and Dark Reduction for the Removal of Organic Pollutants and Cr(VI) using Ag/TiO2, Environmental Science Technology, 51, 3973-3981 (2017).

A114. Z. M. Abou-Gamra, M. A. Ahmed, and M. A. Hamza, Investigation of commercial PbCrO4/TiO2 for photodegradation of rhodamine B in aqueous solution by visible light**, Nanotechnology for Environmental Engineering,, 2017, 12, DOI: 10.1007/s41204-017-0024-9.**

A115. Ma X, Ma W, Jiang D, Li D, Meng S, Chen M, Construction of novel WO3/SnNb2O6 hybrid nanosheet heterojunctions as efficient Z-scheme photocatalysts for pollutant degradation, J Colloid Interface Sci. 2017 Jul 5;506:93-101. doi: 10.1016/j.jcis.2017.07.017.

A116. M. Shanthi and V. Kuzhalosai, Photocatalytic degradation of an azo dye acid Red 27 in aqueous solution using nano ZnO, Indian Journal of Chemistry, 51A, 428-434 (2012).

A117. Dasari Ayodhya, M. Venkatesham, A. Santoshi kumari, G. Bhagavanth Reddy, D. Ramakrishna and G. Veerabhadram, Photocatalytic degradation of dye pollutants under solar, visible and UV lights using green synthesized CuS nanoparticles, Journal of Experimental Nanoscience, 11 (6) 418-432, (2016).

A118. Omprakash Sharma and Mohan Kumar Sharma, Use Of Cobalt Hexacyanoferrate(II) Semiconductor In Photocatalytic Degradation Of Neutral Red Dye, International Journal of ChemTech Research, 5(4),1615-1622 (2013).

A119. **Priya Rathore, Rakshit Ameta and Sanyogita Sharma, Photocatalytic Degradation of Azure A Using N-Doped Zinc Oxide, Journal of Textile Science and Technology, 1, 118-126 (2015).**

A120. C. Karunakaran, P. Magesan, P. Gomathisankar, P. Vinayagamoorthy, "Photocatalytic Degradation of Dyes by Al_2O_3-TiO_2 and ZrO_2-TiO_2 Nanocomposites", Materials Science Forum, Vol. 734, pp. 325-333, 2013

CHAPTER 7

Nanostructures as applied for photo-electrochemical and photo-catalytic water splitting

Carbon free energy sources at the same price will be preferred option. This means that one has to attain nearly 43.5% efficiency in solar energy conversion. Even if one were to attain this level of efficiency in harnessing solar energy there are yet some more hurdles to surmount namely storage of the fuel produced and it distribution in places. The reaction of interest in this context is $H_2O \rightarrow \frac{1}{2} O_2 (g) + H_2 (g)$; $\Delta G = +237$ kJ mol^{-1}. There are essentially two configurations of photo-electrochemical cells normally proposed to be employed for water decomposition reactions. They are pictorially shown in Figure . They can be described as Schottky-type consisting of a photoanode and a cathode while the second tandem type which consists of a photoanode and a photocathode this can also termed as z type which are normally employed in photoelectrochemical water splitting.

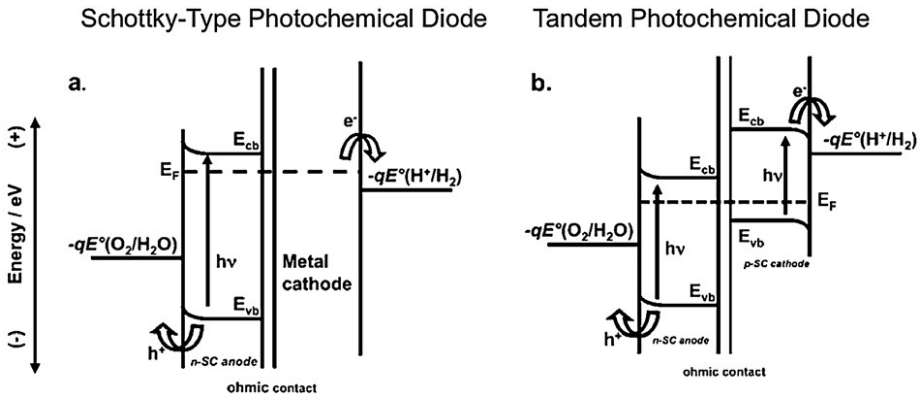

Figure The two normal configurations of photo-electrochemical cells for water decomposition reaction.

Tandem cells consist of a smaller band gap materials and these can be used to harness solar radiation effectively. The relative positions of the band edges in the two semiconductors favour facile transfer of charge across the interface. However, sustaining these two semiconductors is a major issue.

One way is to coat conventional photovoltaic cells with cocatalysts for water splitting or with protecting layers to inhibit photo-corrosion. This

has led to the champion water splitting devices. It also produced to the artificial leaf, a triple junction amorphous silicon cell, capable of photo-electrolysing water with a solar energy efficiency of up to 4.7%.

Another strategy involves the development of new metal oxide materials that combine suitable properties (visible bandgap, chemical stability, high carrier mobilities, long carrier lifetimes) for photoelectrochemical water splitting. Such materials can be made by directed synthesis, sometimes guided by theory, or they can be made by combinatorial approaches.

The third strategy is to exploit scaling laws and specific effects at the nanoscale to enhance the efficiency of existing semiconductors and metal oxides.

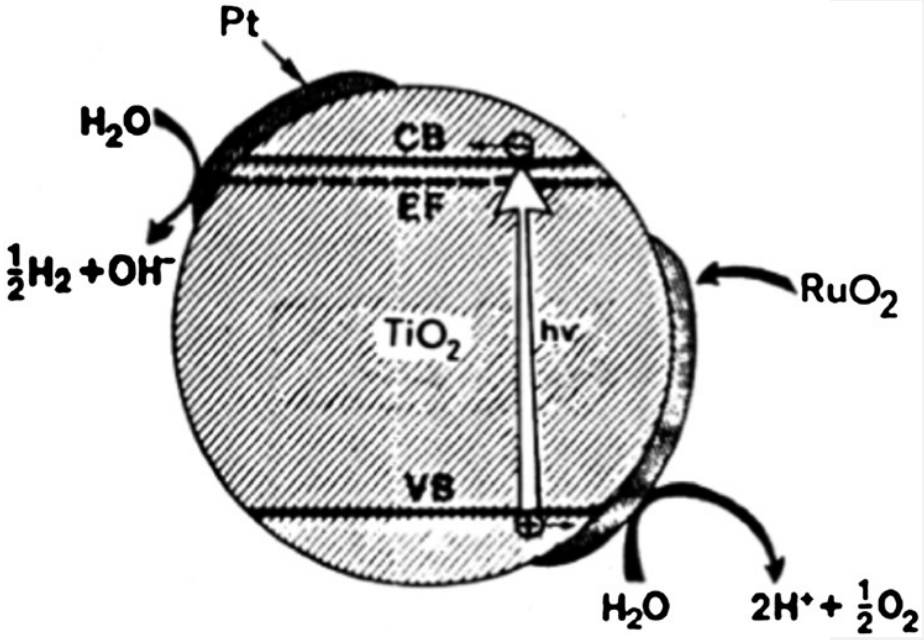

Figure A typical photo-electrochemical cell with hydrogen and oxygen evolving sites hooked on to the semiconductor to facilitate their evolution.

The parameter L depends on the carrier diffusion constant D and the carrier lifetime t (eqn (2)), and a dimensionality factor (q = 2,4,6 for one-, two-, or three-dimensional diffusion).

$$L^2 = qDt \quad (2)$$

For intrinsic semiconductors, usually Le > Lh because of the larger diffusion constant D of the electrons compared to holes. For example, Si has De = 49 cm ^{2} s $^{-1}$ and Dh = 13 cm ^{2} s $^{-1}$ (calculated from mobilities, mue = 1900 cm ^{2} V $^{-1}$ s $^{-1}$ and muh = 500 cm ^{2} V $^{-1}$ s -1 at 298 K using Einstein–Smoluchowski relation. Assuming te = th = 10 $^{-6}$ s, Le = 98 micro m and Lh = 51 microm for one dimensional diffusion (q = 2). Upon doping, the concentration of the majority carriers increases, and with it their t and L values. On the other hand, the lifetime and diffusion length of the minority carriers decrease. For optimum collection of both carrier types at the back contact, the semiconductor film thickness d has to be in the same range as Le and Lh .

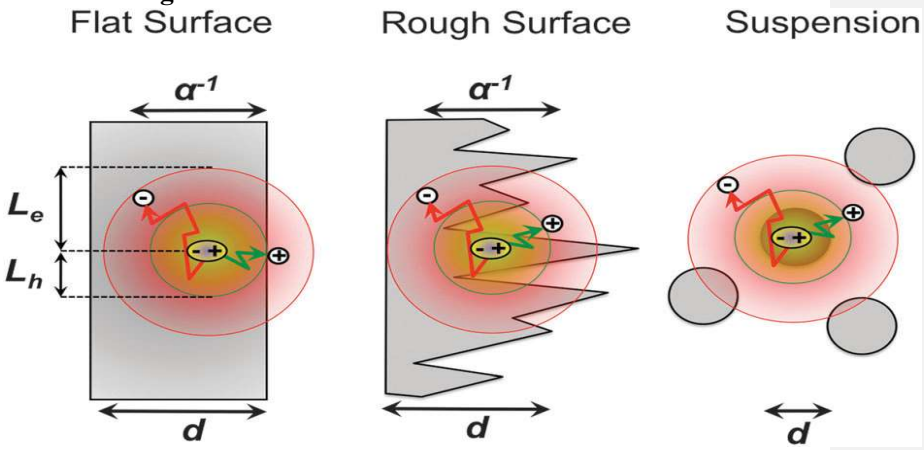

Charge Collection in flat and nanostructured films and in particle suspensions. d: film or particle thickness; Le: electron diffusion length; Lh: hole diffusion length. Suspended particles require both electrons and holes to be collected at the sc–electrolyte interface.

Improved light distribution.: The ability of a material to absorb light is determined by the Lambert Beer law and the wavelength-dependent absorption coefficient a. The light penetration depth α^{-1} refers to the distance after which the light intensity is reduced to 1/e of the original value. For example, for Fe2O3, α^{-1} = 118 nm at l = 550 nm, for CdTe, α^{-1} = 106 nm (550 nm),55 and for Si, α^{-1} = 680 nm (510 nm). To ensure >90% absorption of the incident light, the film thickness must be >2.3 times the value of α^{-1}. Surface-structuring on the micro- or nanoscale can increase the degree of horizontal light distribution via light scattering . This 'trapped' light would otherwise

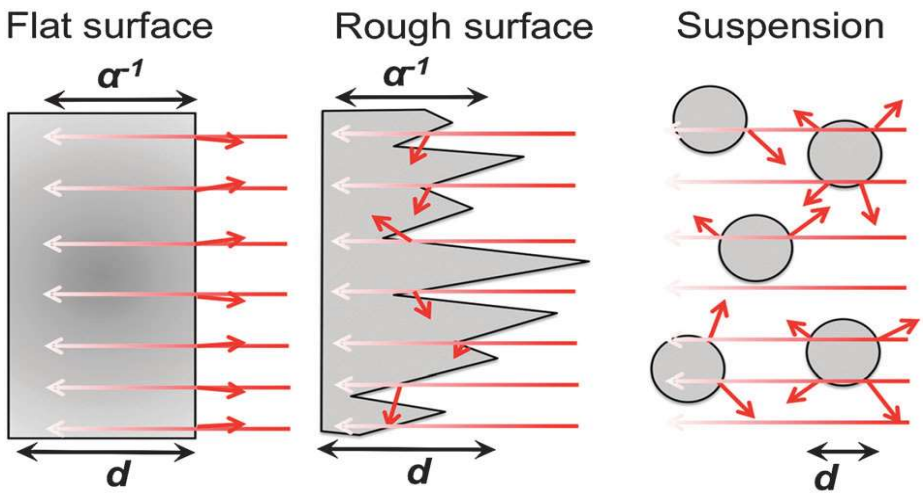

Light distribution in flat and nanostructured films, and in particle

suspensions. d: film or particle thickness; : α^{-1} optical penetration depth. Short

arrows signify scattered or reflected light

Quantum size confinement. The dependence of semiconductor energetics on particle size has been established in the mid 80's. The quantum size effect depends also on the material and the

nanocrystal shape. With increasing the band gap, the conduction band edge shifts to more reducing and the valence band to more oxidizing potentials. From Marcus–Gerischer theory it is expected that this increase in thermodynamic driving force increases the

rates for interfacial charge transfer and water electrolysis (Fig. 6).Indeed, this can be experimentally observed for charge transfer across solid–solid interfaces. A logarithmic

dependence of the photocatalytic proton reduction rate on the bandgap has also been verified with CdSe quantum dots. These effects will likely be used more often in advanced solar water splitting devices

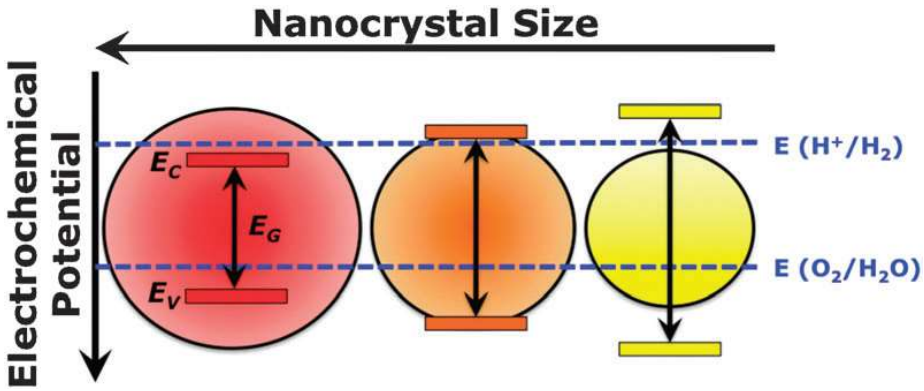

Quantum size effect in nanocrystals

Potential determining ions (PDI). The effect of potential determining ions on the interfacial energetics is well known. For example, the flatband potential of TiO2 is a linear function of the solution pH. Due to the small thickness of nanostructures, external electric fields can reach into the nanomaterial interior and modify the local energetic structure. Thus, the band edge potentials of nanomaterials, and resulting functions, incl. interfacial charge transfer can be controlled with PDIs (Fig.). Examples are the band shift caused by hydrosulfide on nano-Bi2S3 in TiO2 nanocrystal films, and the effect of pH on interfacial charge transfer.

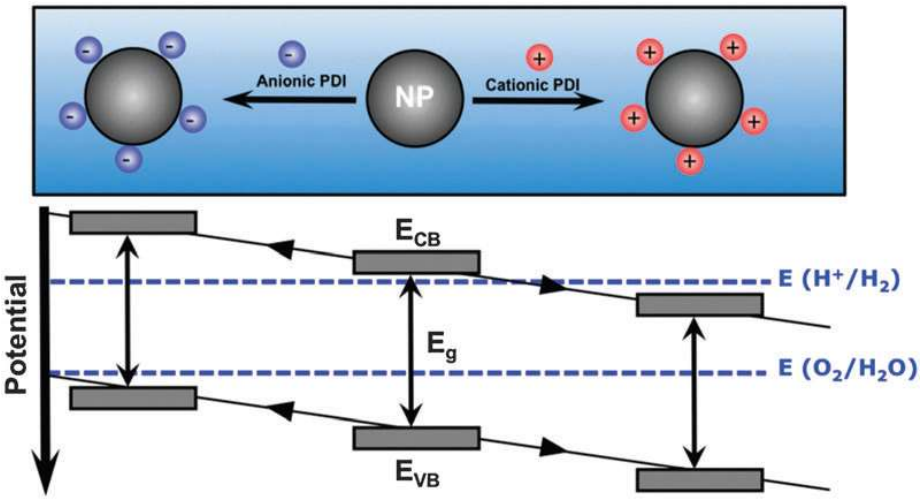

Effect of PDIs on nanocrystal energetics

surface area of nanomaterials promotes charge transfer across the material interfaces (solid–solid and solid–liquid), allowing

water redox reactions to occur at relatively low current densities and, correspondingly, low overpotentials. In other words, the increase of surface area allows to better match the photocurrents with the slow kinetics of the water redox reactions. In particular water oxidation is known to require milliseconds to seconds to proceed at Fe2O3 and TiO2, according to recent transient absorption measurements. Thus, increases of surface area reduce

the need for highly active, and often expensive cocatalysts, based on Ir, Rh or Pt.

Multiple exciton generation. The altered electronic structure of strongly size-confined nanocrystals gives rise to multiple exciton generation (MEG), i.e. the formation of several (n) electron–hole pairs after absorption of one photon with an energy n times of the band gap of the dot (Fig.). The MEG effect is responsible for the abnormally high efficiency of PbSe QD-sensitized TiO2 photoelectrochemical cells, and PbSe photovoltaic cells . The effect has not yet been applied to water photoelectrolysis. Future MEG-enhanced water splitting devices will likely be Tandem or multi-junction devices, because the individual quantum dots cannot produce a sufficient potential for overall water splitting.

This is because for efficient solar energy conversion, the band gaps of the relevant dots need to be a fraction of the energy of visible light photons (E = 1.55–3.1 eV).

While nanostructuring can improve the light harvesting, charge transport, kinetic, and energetic parameters of photoelectrosynthetic Cells. it also has significant disadvantages that can lead to reduced power conversion efficiency and lower durability of devices. Some disadvantages originate from the inherent properties of nanoparticles, e.g. decreased thermodynamic stability tied to increased surface energy. Others are specifically tied to photochemical energy conversion.

Increased surface recombination. Electron–hole recombination is the major loss mechanism in excitonic solar cells and in photocatalysts. Photogenerated charge carriers recombine through radiative or nonradiative processes in the bulk phase of the semiconductor, in the depletion region, or at defects at the surface (Fig.). These processes diminish the steady state concentrations of usable charge carriers and reduce the rates of water electrolysis and carrier extraction (thick black arrows in the figure). In nanostructured semiconductors, surface and interfacial recombination rates are enhanced due to their larger specific interfacial areas. It might be possible to control these losses by reducing surface defects through surface treatments. For example, for macroscopic silicon films, treatment with HF

can suppress surface recombination. Analogous treatments will have to be developed for nanomaterials.

Reduced space charge layer thickness. In nanomaterials,

carrier separation (thick arrows in Fig.) is more difficult than

in the bulk, because at average doping concentrations (n0 =

10^{17} cm^{-3}) space charge layers are not effective on the nanoscale. That is for spherical nanoparticles, the space charge layer thickness cannot exceed the radius of the particle (Fig.) , which restrains the possible barrier height at the interface. For example, for 16 nm TiO2 nanocrystals (ε = 160) with a charge carrier concentration of $n_0 = 10^{17}$ cm^{-3}, O'Regan calculated a barrier height of 0.3 meV under maximum depletion. This means that in the absence of a strong applied bias, the bands in a nanoparticle are essentially flat, as shown in Fig.

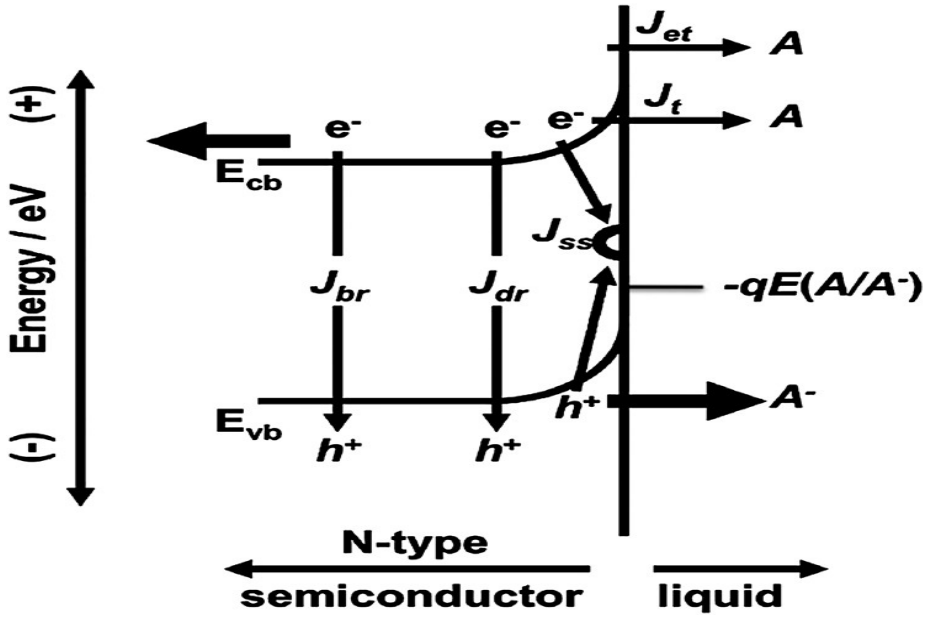

Recombination pathways for photoexcited carriers in a semiconductor PEC.The arrows signify bulk recombination (Jbr), depletion-region recombination (Jdr), and surface recombination (Jss). Additional loss mechanisms due to undesired charge transfer are also shown. Electron tunneling through and over the barrier produce the current densities (Jt) and (Jet). Electron collection by the back contact and hole collection by the redox couple (e.g., oxidation of water to

O2) are desired processes shown by thick black arrows.

Lower absorbed photon flux. A second consequence of the increased junction area in nanostructured photoelectrochemical cells is lower absorbed flux (if light scattering is neglected). This is shown in Fig. for a flat semiconductor liquid junction and for a

semiconductor wire array. The latter has a larger roughness, and thus receives a lower flux per unit area of exposed semiconductor. According to the Shockley diode equation , the open

circuit voltage of a solar cell is a logarithmic function of the absorbed flux J_{Phot} and of the reverse saturation current J_0 of the diode. Since $J_{Phot} >> J_0$, the voltage

decreases by 0.059 V for every decadic decrease of J_{Phot} (i.e. decadic increase of surface roughness). This reduces the thermodynamic driving force available for water electrolysis.

$V_{OC} = (kT/e) \ln \{Jphot / J0) +1\}$

J_0, reverse saturation current of diode; J_{Phot}, photocurrent =

photon flux times x irradiated area; V_{OC}, open circuit voltage.

Slow interparticle charge transport. In nanocrystalline films, charge carriers move by diffusion instead of drift. As a result, charge transport is much slower than in the bulk, increasing the chances for recombination and back reactions. If the nanoparticles are not fused together, additional barriers arise frominterparticle charge transport, which occurs by thermally activated hopping and by electron tunneling (Fig.). It depends on the interparticle distance and the electrostatic charging energy of the donor acceptor nanocrystal couple. Since nanostructured films can be several hundred nanometers thick, the resistance losses from charge transport are a significant factor.

Conclusion and outlook

The last decade has seen an increase in research activity on nanostructured photoelectrochemical and photocatalytic systems for solar water splitting. The nanoscaling approach has been shown to particularly improve the performance of metal oxide photoanode materials with low carrier mobility and with short excited state lifetimes. For electrocatalysts, nanoscaling has increased the electroactive surface area and allowed for more efficient materials use. For selected metal chalcogenides, the quantum size effect has been useful for controlling interfacial charge transport, and in promoting photocatalytic proton reduction. These examples clearly show the benefits of nanoscaling and highlight its potential for the development of improved photoelectrode materials.

At the same time it is apparent that the performance of a material is ultimately defined by the intrinsic materials parameters, i.e. by its chemical composition and structure. For

many metal oxides, low electrical conductivity, high defect concentrations, and short excited state lifetimes are important problems that cannot be solved through nanoscaling alone.

New materials with ternary and quaternary compositions are required here, to avoid these shortcomings. Even though inexpensive nanomaterials with low proton reduction overpotentials are now available (e.g. NiMo alloy), there is still a need for more active water oxidation catalysts, based on earth abundant elements. Nanostructuring can be a significant

asset in increasing the electroactive area, or in preventing back reactions, as in the case of Cr2O3-coated Rh nanoparticles. Also, due to the corrosive nature of water electrolysis, material

stability is a limiting issue that affects all non-oxide materials. Nanostructured coatings with inert materials have been shown to reduce corrosion, but not to eliminate it fully. Corrosion

must be considered as an important parameter in devising new photocatalysts for water splitting.

Some drawbacks of these materials, e.g. low electrical conductivity, may be circumvented with suspended photocatalysts, which are nanoscale in all three dimensions, and combine

photoanode and cathode materials in close proximity. Such integrated 'photochemical diodes' might have the additional advantage over photoelectrochemical cells, that they would be

easier to manufacture on a large scale, and be less costly in their operation.However, the key limitation of these systems is insufficient rectification. Since space charge layers are not

effective at the nanoscale, new ways of separating charge are needed. One possibility is charge-selective interfaces that could support 'kinetic rectification' – a concept that was

formulated by Helmut Tributsch in 2008, in analogy to natural photosynthesis . Alternatively, it might be feasible to increase the doping levels of nanocrystals, to improve the effectiveness of space charge layers on the nanoscale, although that again might come at the expense of

increased recombination. These highly integrated systems would also require higher precision in their synthesis/assembly, especially if several components are involved. This includes

better control of interfaces, so that the energy loss processes arising from the increased interfacial areas can be minimized. The development of surface treatment techniques, e.g. the use of chemical modifiers (Ga, Zn, Al ions), to reduce defects and improve carrier lifetimes will be essential for this purpose.

Based on the desired function, it is unlikely that an efficient solar energy driven photocatalytic water splitting system will exceed the complexity of a microprocessor. It is just that the

methods for making and integrating the microscale components at the necessary precision level are not available yet. To make them available in the near future should be one of the goals of scientists today. This will require not only more systematic efforts in materials preparation, but also in characterization and testing. For example, measurements of

the photoelectrochemical/photocatalytic performance should follow established standards. This challenge is particularly significant for nanomaterials, which show large property variations based on their morphology, surface termination, and surface charge. Such factors must be considered in the analysis.

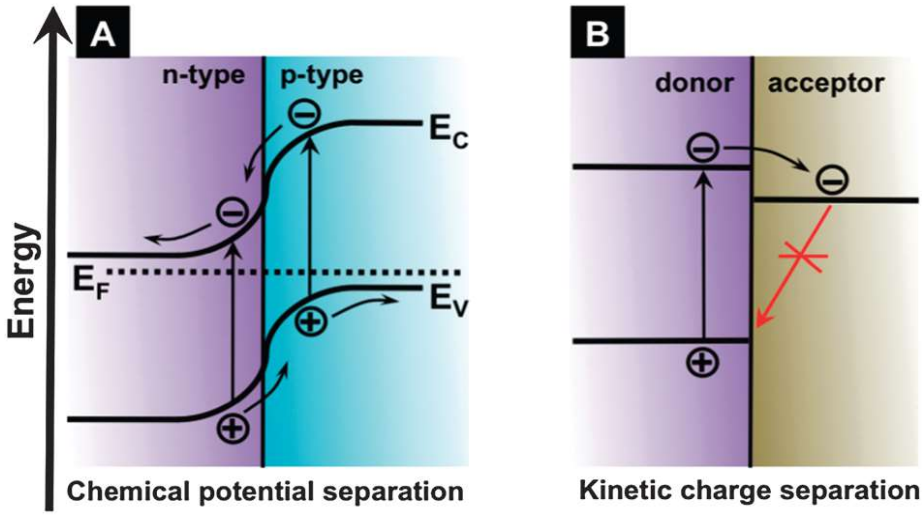

Chemical potential (A) versus kinetic (B) rectification

Coupled semiconductor- where is the Fermi Levels or do they have different redox properties

There has been anxiety to extend the light absorption to visible range, while employing mainly titanium dioxide based semiconductors. The motivation for this is to maximize the use of available solar radiation. Though various experimental strategies have been adopted to sensitize the semiconductor to visible range, the concept of "coupled semiconductors" has been receiving increasing attention these days. The principle of this concept is to couple another semiconductor which could absorb radiations in the visible range, but the energy levels, namely the top of valence band and the bottom of the conduction band are energetically at positions for easy transfer of both the electron and hole (exciton) or at least one of them namely the electron in a downhill fashion. The relative energetic positions of the coupled semiconductors are shown in Fig.1.

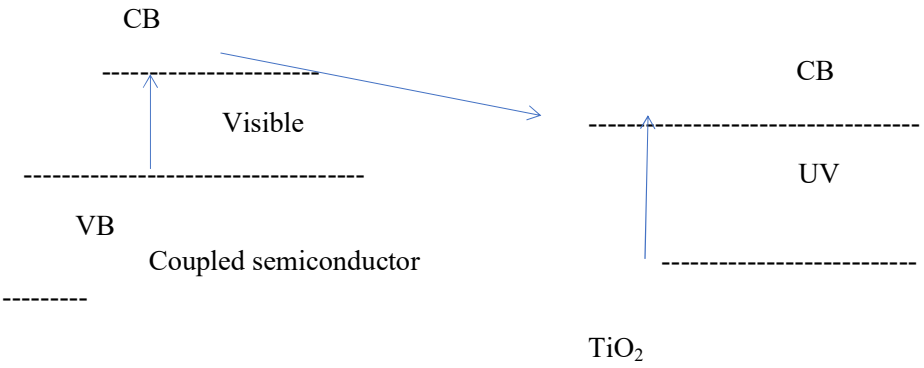

Fig.1. The relative energy positions of VB and CB for both the semiconductors

The excited electron in the conduction band of the semiconductor is energetically at less negative value and hence takes more stable allowable energy state in TiO_2 conduction band thus promoting the reduction reaction especially in hydrogen evolution reaction in water splitting.

This argument holds good only when the energetics of allowed states in semiconductors remain in tact when they are brought together. However, it is generally believed that when two conducting systems are brought together, the Fermi levels will be at the equal position. This postulate holds good for semiconductor/electrolyte interface or for two metallic systems. This may be true for systems where two semiconductors for a single solid solution. This is clear from the optical spectrum of these materials which normally show a single value for the absorption indicating a single valued band gap.

Based on this observation, one may presume that in the so called coupled semiconductors as well depending on the extent and strength of contact, there can be some kind of mixed phase at the interface and at least at this region the so called optical band gap can assume a unique and fixed value d in between the values of the two semiconductors involved. Under these circumstances, it is possible to promote the reduction reactions by the excited electrons and the hole can still promote the oxidation with different redox levels. The points that arise out of this argument are:

(i) How far it is true that the optical band gaps of the two coupled semiconductors remain intact as they were when the semiconductors are not coupled?

(ii) Do the Fermi levels in the two semiconductors remain as it was in the individual semiconductors?

(iii) The enhanced photo-catalytic activity normally observed with coupled semiconductors should be comparable to that observed on low band gap semiconductor.

It is possible that the arguments given in this short write up could be totally wrong and one should still consider as is done in most of the literature on this topic of coupled semiconductor operating in unison but still retain their individual character.

Definition of photocatalysis

- Photo-catalysis is a term that combines the basic notion of a catalyst as a material that enhances the rate as a reaction approaches equilibrium without being consumed with the notion that the reaction is accelerated by

photons, which of course are consumed. **Thus, it is a hybrid concept.** As with other areas of catalysis, it has its heterogeneous and its homogeneous dimensions with the former dominating the research literature.

CHAPTER

Semiconductors for water splitting: Material design principles

Sustainable energy through catalysis

The field of catalysis has important roles to play in many energy conversion processes like decomposition of water to generate hydrogen fuel, conversion of carbon dioxide to useful fuels and in the conversion of molecules into value added products. In this the selection of suitable and efficient materials has been one of the important tasks. Traditionally this exercise has been based on trial and error method of trying some materials and generating experimental data. These data have been subsequently used to formulate empirical rules for selection of materials for a particular application. For example, in the photo decomposition of water to generate hydrogen, one of the postulates is that the cation of the semiconductor should have d^0, d^5, and d^{10} configuration. Based on such empirical rules new formulations are proposed and tested but the success seems to be limited in these cases. These exercises have been manly to guide experimental efforts for screening candidate materials and also to build or promote the chosen material.

However, all materials proposed in this process are based on empirical basis. They have some experimental evidences as basis but their predictive capacity is not beyond doubt. When using them to make predictions, one can only say something new in regimes where the proposed model is not explicitly fitted to experimental observations. In these cases, the confidence level of the predictions is questionable. To use such empirical models as predictive tool one has to exercise caution and care.

In order to overcome this problem, most often theoretical methods are preferred but the time and accuracy of the methods are trade off. One such example is shown in the figure 1 for some quantum chemical methods that are commonly employed in these days.

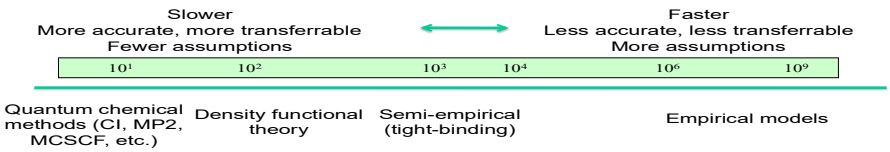

,Figure 1 the relationship between time and accuracy of the empical, semiempiral and quantum chemical methods

It is seen from figure 1 that more accurate results require fewer assumptions and also most often the results are transferable.

Now turning our attention to selection of material for photo-electrochemical decomposition of water, the material of choice should have some characteristics. These include that the material chosen should be stable under the experimental conditions employed, the band gap of the semiconductor material suitable for water decomposition, the band positions should be such that hydrogen and oxygen evolution reactions take place spontaneously and the charge carrier should have suitable mobility to react at the interface instead of undergoing recombination. In addition to all these, the sites on the semiconductor surface

should favour hydrogen and oxygen evolution reactions efficiently. In figure 2 the band positions of oxide semiconductors and the hydrogen and oxygen evolution potentials are shown and one can deduce from this figure which semiconductor is capable of evolving hydrogen and oxygen by the decomposition of water. A similar scheme is shown for sulphide semiconductors in Figure 3.

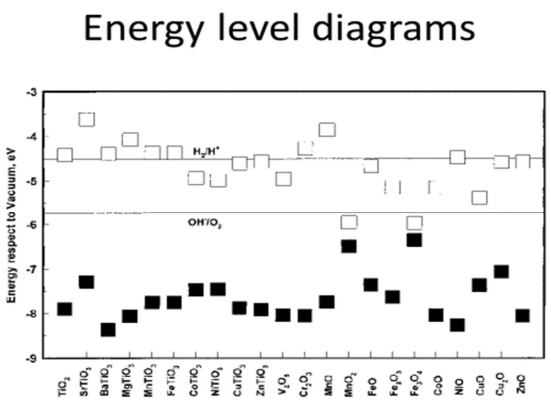

Figure 2 the position of the conduction band (open squares) and the position of the valence band (filled squares) for oxide semiconductors are shown> The hydrogen and oxygen evolution potentials are also shown.

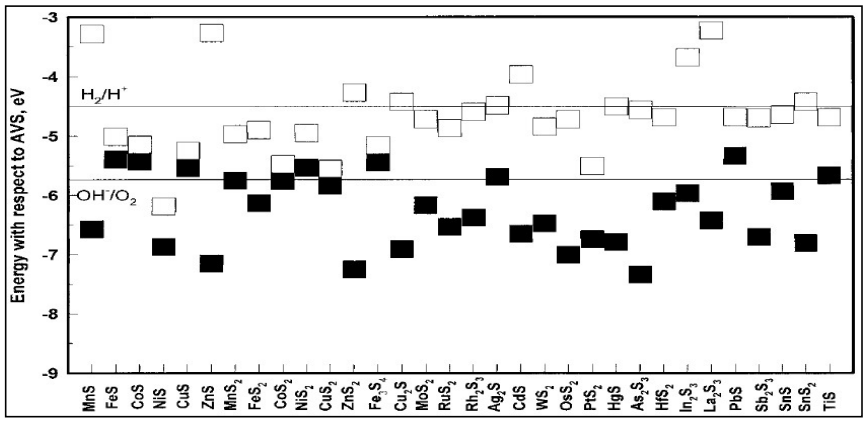

Figure 3. The position of the conduction band (open squares) and the position of the valence band (filled squares) for sulphide semiconductors are shown. The hydrogen and oxygen evolution potentials are also shown.

The positions of the conduction band minimum and valence band maximum can be deduced in a number of ways. These methods are based on the electronegativity values of the species concerned. The Mulliken electronegativity scale which is the average of the electron affinity and ionization energy has been used in these calculations. The Butler Ginley scheme makes use of d\following two equations namely

$E_{VB} = -X_{GM} - E_g/2$

$E_{CB} = X_{Gm} + E_g2$

Where X_{GM} is the geometric mean of the electronegativity values and E_g is the band gap value.

Let us illustrate these calculations with a typical example of TiO_2, ZnO and $SrTiO_3$.

The electronegativity values of Ti, O, Zn and Sr are 3.45, 7.43, 4.45 and 2.0 respectively. The band gaps of TiO_2, ZnO and $SrTiO_3$ are 3.2, 3.2 and 3.4 respectively. If one were to use these values one gets for the conduction band minimum and valence band maximum for these three semiconductors as follows

- TiO_2

  - VB -7.4 eV
  - CB -4.2 eV
- ZnO
  - VB -7.38
  - CB -4.18

$SrTiO_3$ is left out as an exercise.

Similarly, one can calculate for sulphide semiconductors and a compilation is given below.0

An alternate method of calculating the band edge positions is available in the following reference Gritsenko *et al.*, *Phys. Rev. A* **51**, 1944 (1995).

Table 1 Data of Band edges and band gaps of common sulphide semiconductors

Material	Electronegativity	Band gap (eV)	Conduction band	Valence band
Ag_2S	4.96	0.92	-4.50	-5.42
As_2S_3	5.83	2.50	-4.58	-7.08
CdS	5.18	2.40	-3.98	-6.38
$CuFeS_2$	5.15	0.35	-4.87	-5.32
FeS	5.02	0.10	-4.97	-5.07
FeS_2	5.39	0.95	-4.92	-5.87
In_2S_3	4.70	2.00	-3.70	5.70
MnS	4.81	3.00	-3.31	-6.31
MnS_2	5.24	0.50	-4.99	-5.49
MoS_2	5.32	1.17	-4.73	-5.90
NiS	5.23	0.40	-5.03	-5.43
NiS_2	5.54	0.30	-5.39	-5.69
PbS	4.92	0.37	-4.74	-5.11
$PbCuSbS_3$	5.22	1.23	-4.61	-6.11
PtS_2	6.00	0.95	-5.53	-6.48
Rh_2S_3	5.36	1.50	-4.61	-6.11

RuS_2	5.58	1.38	-4.89	-6.27
Sb_2S_3	5.63	1.72	-4.72	-6.44
SnS	5.17	1.01	-4.66	-5.67
SnS_2	5.49	2.10	-4.44	6.54
TiS_2	5.11	0.70	-4.76	-5.46
WS_2	5.54	1.35	-4.86	-6.21
ZnS	5.25	3.60	-3.46	-7.06
ZnS_2	5.56	2.70	-4.21	-6.91
$Zn_3In_2S_6$	5.00	2.81	-3.59	-6.40
ZrS_2	5.20	1.82	-4.29	6.11

The values are calculated using the two following equations:

$E_{CB} = -A = -X+0.5\ E_g$

$E_{VB} = -I = -X+ 0.5E_g$

X is the electronegativity, E_g is the value of the band gap, A is the electron affinity and I is the ionization potential

It is necessary to compare these computed band gap values with that experimental values and one such test is shown in Figure 3

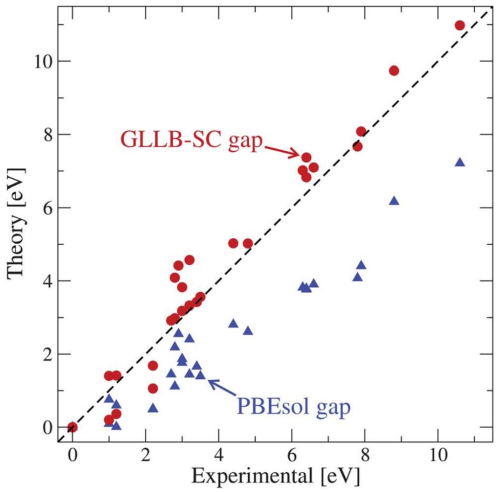

Fig. 3 DFT calculated bandgaps of selected oxides. Comparison between the theoretical and experimental bandgap of non-magnetic metal oxides in their most stable structure. The gaps are calculated using both the standard PBEsol (blue triangles) and the GLLB-SC functional (red circles). The dashed line represents the perfect matching between experiments and theory. (Details of the calculations with a list of the calculated oxides can be found in Table 1 of the ESI†). Plot of computed band gap values against the experimental values.[Reproduced from Ivano E. Castelli, Thomas Olsen, Soumendu Datta, David D. Landis, Søren Dahl, Kristian S. Thygesen and Karsten W. Jacobsen, Energy Environment Sci., 5,5814 (2012).]

One can assume the agreement is good enough and the values of band gap estimated by using these two equations can be used for all practical purposes

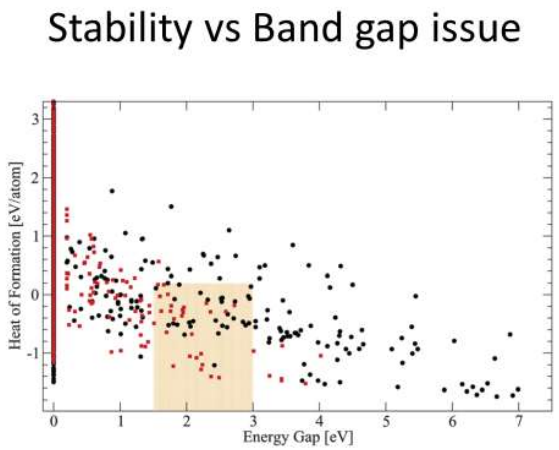

I.E. Castelli, T. Olsen, S. Datta, D.D. Landis, S. Dahl, K.S. Thygesen, and K.W. Jacobsen, Energ Environ Sci **5**, 5814 (2012).

Fig. 3 Correlation between the heat of formation per atom and the bandgap for the oxide (black circles) and oxynitride (red squares) compounds. The region for candidates for solar light harvesting corresponds to the orange area. [reproduced from I.E.Castelli et al., Energy Environment Sci., 5,5814 (2012).

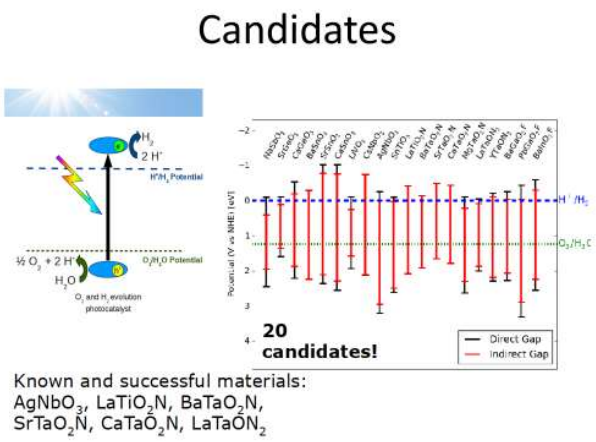

Fig. 4 The identified oxides and oxynitrides in the cubic perovskite structure with potential for splitting water in visible light. The figure shows the calculated band edges for both the direct (red) and indirect (black) gaps. The levels for hydrogen and oxygen evolution are also indicated

The essential steps involved in electrolytic water splitting reaction is listed below

$$H_2O(l0 + * \rightarrow OH* + H^+ + e$$

$$OH* \rightarrow O* + H^+ + e$$

$$O* + H_2O(l) \rightarrow OOH* + H^+ + e$$

$$OOH* \rightarrow * + O_2(g) + H^+ + e$$

Two simple concepts

For each elementary step:

$\Delta G(U) = \Delta G_0 - eU$

The limiting potential, U_0, where this step is exergonic:

$\Delta G(U_0)=0 <=> U_0=\Delta G_0/e$

The theoretical overpotential:

$\eta = U_0-1.23$ V

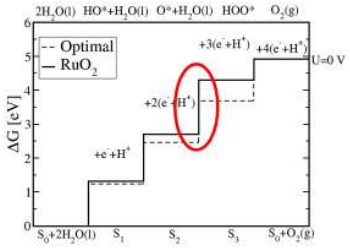

J.K. Nørskov, J. Rossmeisl, A. Logadottir, L. Lindqvist, J. Kitchin, T. Bligaard, and H. Jonsson, J. Phys. Chem. B **108**, 17886 (2004).

Hydrogen evolution

$$* + 2H^+ + 2e^- \leftrightarrow H^* + H^+ + e^-$$

$$H^* + H^+ + e^- \leftrightarrow * + H_2(g)$$

Free energy diagram

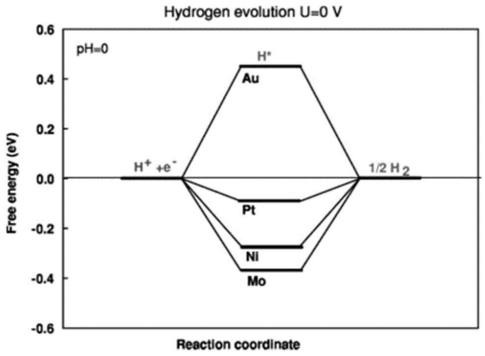

J.K. Nørskov, T. Bligaard, A. Logadottir, J.R. Kitchin, J. Chen, S. Pandelov, and U. Stimming, J. Electrochem. Soc. **152**, J23 (2005).

Hydrogen evolution volcano

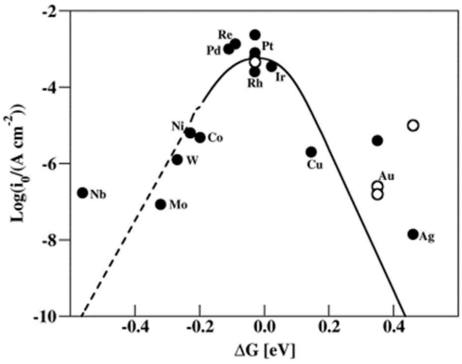

Tandem scheme

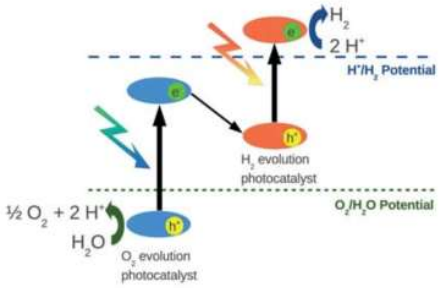

Conditions for tandem scheme

First semiconductor

- Valence band appropriate for oxygen evolution
- Conduction band appropriate for second semiconductor VB

Second semiconductor

- Conduction band appropriate for hydrogen evolution

Tandem cell

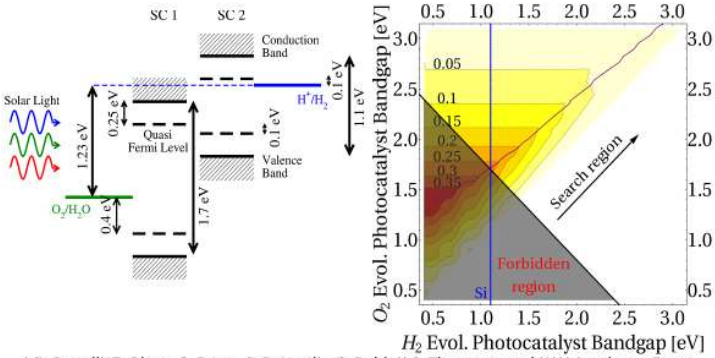

I.E. Castelli, T. Olsen, S. Datta, D.D. Landis, S. Dahl, K.S. Thygesen, and K.W. Jacobsen, Energ Environ Sci **5**, 5814 (2012).

Tandem cell

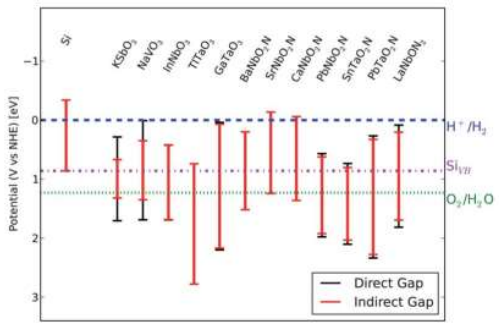

(b) Candidates for Tandem Cell WS

Transparent shield

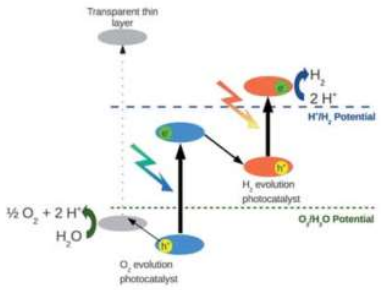

(a) Shield Scheme

Conditions for transparent shield

- Must be transparent
  - High band gap
- Valence band level between the edges of the photocatalyst and oxygen evolution for hole mobility

Candidates for transparent shield

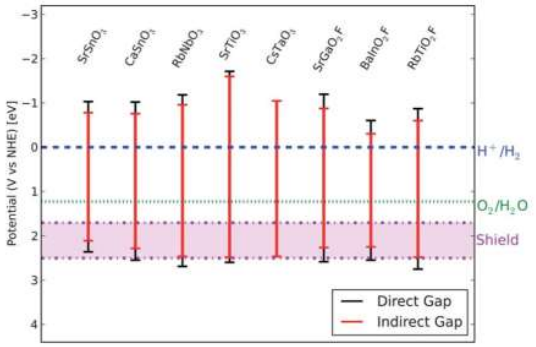

Database

Database: https://cmr.fysik.dtu.dk

CHAPTER

One approach for the design of semiconductor materials for photo-electrochemical applications

Today, it appears that the feasibility of photo-electro-chemical splitting of water is hampered by the correct choice of the semiconductor material that can be employed as photo-anode even though as many as 400 semiconductors have been examined with a variety of variations in each of them. This situation has arisen probably due to the fact that the system chosen has to perform both surface catalytic function for two important reactions namely hydrogen and oxygen evolution reaction and at same time should be capable of interacting with the photon field without undergoing degradation,yet possess the band edges so as to be thermodynamically capable of decomposing water yet possess reasonable value of the band gap (certainly greater than 1.23 eV (decomposition potential of water)preferably in the visible range(to be able to utilize most part of the solar radiation)yet possessing high absorption coefficient for photons. In addition, the system has to perform in a electrochemical cell mode, the electrode material should be able to withstand the inherent electrical field at the electrode/electrolyte interface and also may have to couple with both the photon and surface field necessary for the reaction. In the case of oxide semiconductors the valence band is mostly contributed by the 2p orbitals of oxygen and hence the top of the valence band in most of the oxide systems are more or less at the same level and that is between -7.5 and -8.0 eV from the vacuum level. This level may be favourable thermodynamically for the oxygen evolution reaction from the decomposition of water. However the substitution at the anionic sites will alter the position of the valence band and according to the nature of the substitution like Nitrogen, sulphur and other heteroatoms, the net free energy 1 for oxygen evolution reaction will be altered and possibly the oxygen evolution rate also. Similarly the substitution at the cationic position will have effect on the bottom of the conduction band and hence on the capacity to reduce H+ ions and evolve hydrogen. When these two states that is the top of valence band and bottom of the conduction band is shifted either way, the value of the band gap is automatically altered and this has been vigorously attempted and it is called the band gap engineering of materials. Since band edge positions have to be known, the empirical method adopted in Butler

Ginley scheme is usually employed and the values are compiled at various sources [2].Among the available semiconductors, the ones based on oxides and sulphides have been examined extensively and however none of them have yielded the desired efficiency for the water splitting. A recent screening study [3] considered nearly 19000 materials generated with 53 different elements, different anions like O, N, S, F, Cl and different crystal classes like perovskites, rutile and spinels. The essence of their results are given in Fig.1. It is seen from this figure that systems which have band gap value Figure 1: Stability of various semiconductors versus band gap value - Reproduced from I.E. Castelli, T. Olsen, S. Datta, D.D. Landis, S. Dahl, K.S. Thygesen, and K.W. Jacobsen, Energ Environ Sci 5, 5814 (2012). greater than 1.23 (thermodynamic reversible value for water splitting) and 3 eV are the systems of concern for water splitting application. Among the 20 candidates shown in Fig.2, the possible successful candidates are AgNbO3, LaTiO2N,BaTaO2N,SrTaO2N,CaTaO2N,LaTaON2 Another function of the photoelectrochemical material is the catalytic effect for both hydrogen and oxygen evolution. The essential steps in the oxygen evolution reaction can be written as follws:

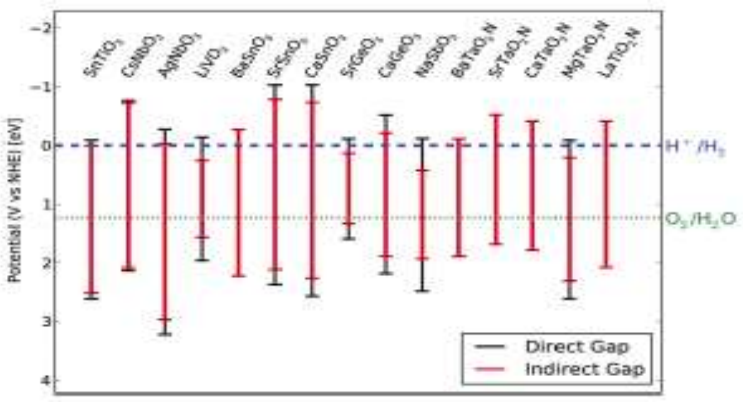

Figure 2: Some of the possible successful candidate materials; Black line direct band gap and red line indirect band gap the materials left to right are: NaSbO3, SrGeO3, CaGeO3, BaSnO3, SrSnO3, CaSnO3, LiVO3, CsNbO3, AgNbO3, SrTiO3, LaTaO2N, BaTaO2N, SrTaO2N, CaTaO2N, MgTaO2N, LaTaON2, YTaON2, BaGaO2F, PbGaO2F, BaInO2F

$H2O + * \rightarrow OH* + H+ + e$

$OH^* \rightarrow O^* + H^+ + e$

$O^* + H_2O \rightarrow {}^*OOH + H^+ + e$

$OOH \rightarrow * + O_2 + H^+ + e$

In this reaction sequence, the step three appears to have considerable overpotential and possibly limiting this reaction. This aspect has been discussed in the paper by Noreskov et al []. The reaction sequence for hydrogen evolution involves the following steps: +

$2H^+ + 2e \rightarrow H^* + H^{++} e$

$H^* + H^+ + e \rightarrow * + H_2 (g)$

The projection for suitable material for this reaction has also been considered in literature and have been published by Noreskov et al []. Another possibility considered in literature for selection of materials for Photo-electrochemical cells and the concept is pictorially represented in Fig.3. There have been predictions in literature for the search of materials for PEC applications. One such prediction is shown pictorially in Fig.4. There are some predictions on the possible candidates for tandem cells they are basically either perovskite oxides or oxynitrides. However there are some limitations on the choice of materials, these include, high band gap materials and the valence band level must lie in such position so that it promotes oxygen evolution and the holes formed must be mobile enough to effect this reaction. In this presentation we have restricted to some of the predictions in literature for obvious reasons. The interested readers can look to the original literature references given. 3

Figure 3: Pictorial representation of a tandem cell for photoelectrochemical applications

Figure 4: Pictorial representation for the selection of materials on the basis of H_2 and O_2 evolution 4 1

References

1.I.E. Castelli, T. Olsen, S. Datta, D.D. Landis, S. Dahl, K.S. Thygesen, and K.W. Jacobsen, Energ Environ Sci 5, 5814 (2012).

2. https://cmr.fysik.dtu.dk 3.J.K. Nrskov, T. Bligaard, A. Logadottir, J.R. Kitchin, J. Chen, S. Pandelov, and U. Stimming, J. Electrochem. Soc. 152, J23 (2005).(hydrogen evolution)

4.J.K. Nrskov, J. Rossmeisl, A. Logadottir, L. Lindqvist, J. Kitchin, T. Bligaard, and H. Jonsson, J. Phys. Chem. B 108, 17886 (2004).(oxygen evolution)

5.I.E. Castelli, T. Olsen, S. Datta, D.D. Landis, S. Dahl, K.S. Thygesen, and K.W. Jacobsen, Energ Environ Sci 5, 5814 (2012). band stability diagram)

6. B.Viswanathan and M Aulice Scibioh, Photoelectrochemistry – Principle

Abstract

The wide scope of photo-assisted catalytic processes especially for hydrogen evolving reactions are considered from the point of view of increasing the catalytic efficiency of the processes by suitable modification of the semiconductor catalyst. The understanding of the physical principles involved in the modification of the semiconductor materials are outlined. The utility of these photo-assisted catalytic processes in pollution control as well as in the conversion of biomass species to chemicals for storage of energy are evaluated.

1 Introduction

The present author has composed an article on this title in 1990s and it was considered that it may be worthwhile to revisit this topic in relation to the write up of the 1990s. Therefore. this write up is going to be a simple reproduction of the article written in 1990s and this will be followed by another article covering (possibly if not comprehensively) the literature in the subsequent years. The relevance of this reproduction will become obvious once one goes through the contents of this reproduced article. The reproduction suffers with alterations with respect language and hence this should not be considered as simple reproduction but with slight modifications to the language but not to the contents. The catalytic reactions assisted by the absorption and utilization of photons by the catalyst and not by the substrate are generally termed as photo-catalytic process. This broad definition was given in 1990s. The current definition will come up in the subsequent article. Bard [1,2] and Nozik [3] have proposed a classification of photo-chemical processes assisted by illumination of the solid catalyst. According to them, photo-catalytic processes are those in which the reactions are driven in the spontaneous direction (Δ G is less than 0) and the light energy is used only to surmount the activation barrier of the reaction. Photo-synthetic processes are those in which photos are used to drive the reaction in the non-spontaneous direction (—Δ G is greater than 0) so that the light energy is stored in the form of chemical energy. This differentiation seems to have been losing ground, since heterogeneous photo-chemical processes i.e. whether Δ G is less than 0 or greater than 0 are generally termed as photo-

catalytic processes. However, for puritans one can classify the second set of reactions as catalytic photosynthesis. The initial enthusiasm that was prevalent in the late 70s and 80s in exploiting these processes for solar energy conversion seems to slow down (this must be understood in the period of 90s), probably because of the frustrations and the unusual low quantum yields that are obtainable in these processes. Scientific groups active in this area throughout the world were awaiting some break-through in the materials that could be exploited, but they seem to realize now that their choice appears to be limited from various considerations like absorption of photons in the visible or near UV region, the long term stability of the material under photolysis conditions, the redox chemistry of the systems that could be successfully handled as well as the life times of the excitons produced by the absorption of photons. This presentation therefore aims at:

1. Deducing the rationale of the choice of typical photo-active semiconductors
2. Examining the ways and means of increasing the efficiency and selectivity of redox reactions

3. Understanding the ways and means of the effect of additives especially metal deposits and pre-treatment agents in the photo-catalytic properties of the semiconductors

4. Postulating active photo-catalysts for hydrogen evolving reactions using model substrates like alcohols and other organic substrates, polyols, (carbohydrates) carboxylic acids, esters (fats) and amino-acids) related to biomass species.

5.Evaluating photo-catalytic degradation processes for organic and inorganic pollutants.

It should also be kept in mind that no claim is made to the exhaustiveness and comprehensiveness of these points in this presentation as it is neither possible nor desirable in view of the various other presentations already available in literature [4]. This presentation is mainly aimed at examining critically the current state of knowledge on these five points. (remember this write up was made in 90s)

2 Rationale for the Choice of Photo-active Semiconductors

There is parallelism existing between photo-catalytic properties of semiconductors and photo-redox reactions taking place at the semiconductor/electrolyte interface. In both processes the electron-hole pair produced by the photon absorption is utilized for the oxidation reduction reaction in the substrate used. If the electrolyte present in the solution is a couple with redox potentials located within the band gap energy of the semiconductor, then the oxidation of the reduced species by the photo-holes at one of the electrodes will be compensated by the reduction of the oxidized species at the other electrode. In order to store the radiant energy as chemical energy the overall cell reaction has to be driven in the non-spontaneous direction (Δ G is greater than 0). This means that the cathodic redox couple must have more negative potential than the anodic redox couple. In this mode of operation, which is termed as photosynthetic cell, the energy stored corresponds to the energy difference between the two redox systems in the cell. However, when the cathodic redox couple has a less negative potential compared to the anodic couple, the reaction proceeds in the spontaneous direction and this mode of operation is called photo-electro-catalytic cell wherein the photon energy is used only to overcome the activation barrier of the redox reaction. These principles of photo-electrochemical cells can be extended to photo-catalytic properties of the semiconductor particles in various forms including colloids and nano state as well. Since in a given semiconductor particle, both anode and cathode (oxidation and reduction sites) are or can be present on the same particle, this can be considered as a short circuited photoelectrochemical cell. The absence of an external electrical circuit means that one can produce only chemicals in whatever mode of operation, namely in photo-synthesis or photo-catalytic mode of operation. However, it is clear that the effective use of the electrons and holes obtained by photon absorption can be achieved only when these charge carriers can be separated and utilized in the redox reaction within the life time of these charge carriers. Since recombination is one of the predominant routes by which the excitation energy will be dissipated, this pathway should be suppressed as far as possible in relation to induced chemical redox reaction. This is achieved in semiconductor photocatalysts by incorporating suitable electron and hole sinks like the deposition of metals or RuO_2 respectively. This aspect will be considered separately in the section on the modification of the semiconductors. The principles of parallelism between photo-electro-chemical cells (PEC) and photo-

catalytic micro-cells (PCM) are illustrated in Fig.1. From these postulates, it is clear that the relative positions of the conduction

Figure 1: Schematic representation of two photo-electrochemical cells with n-type semi-conductor as photo-anode (a) photoelectrosynthetic cell: (b) photo-catalytic cell; (c) Platinised semiconductor powder particle band and valence

band edges of the semiconductor and the redox potentials of the reduction and oxidation couples are deciding factors for selecting a particular semiconductor for a chosen photo-catalytic function. This is the basic criterion to be used for the selection of materials for photo-catalysis. However, the photo-catalytic efficiency will be governed by other competing processes like the recombination rate and the photo-corrosion processes. In Fig 2, the positions of band edges of a few semi-conductors exploited in PEC operation are given together with redox potentials of a few couples of interest to demonstrate how the choice of semiconductor is made with respect to the redox reaction on hand. The nature of wave functions of the energy states of valence and conduction bands also has an important implication in the selection of materials. In the case of oxides like ZnO and TiO_2 the holes generated in the valence band have mainly '2p' orbital character of oxygen anion sublattice, while reducible oxides like Fe_2O_3 and Co_3O_4, the excited state wave functions are mostly contributed by the 'd' states of the cations and the cation reduction pair because of variable valency and the energy states are mostly lying in the band gap of the semiconductor [5]. The symmetry of the wavefunctions and the absolute energy values of these states are responsible for their inactiveness or suppressed activity in promoting the desired redox reaction. Extending

Figure 2: Relative energy values of some common semiconductor electrode materials and redox systems in acid solution

this postulate, one can argue that the photo-activity of the systems will be inhibited by species which are capable of affecting the concentration of O^- species by one electron transfer acts at the surface. In some other systems like Fe_2 TiO_5, the recombination rate may be higher due to the decreased mobility of electrons .This type of reasoning leads to the conclusion that oxides which form valence band from pure '2p' states of oxygen ions with itinerant O^-- type electronic arrangement alone would be effective in PEC and PMC operations. This means that the choice of available for selection of materials appears to be grossly limited. These arguments could not hamper the enthusiasm for using chalgogenides [6] especially CdS, CdSe, CdTe and other hybrid systems as photo-electrochemical and photo-catalytic materials for the photo-splitting of substrates like water and hydrogen sulphide. The major difficulty encountered in these systems which have such lower band gaps than the corresponding oxides thus enabling harvesting of a larger fraction of the solar radiation, is the anodic dissolution process which necessitated the use of modified instead of the naked systems [7]. Another exotic material (at that time) that has been tried is the heteropoly compounds because they possess multiple reduction sites and could promote hydrogen generating reactions [8]. The interest in these compounds stems from the fact that many reducing equivalents could be stored at a single site and the redox behaviour

Table 1: Characteristics of Semiconductor Electrode Materials; EA Electron affinity; EC: conduction band energy relative to vacuum level;Eg: band gap;EV : valence band energy relative to vacuum level.

Material	Electron affinity E_A(eV)	Conduction band E_C(eV)	Band gap E_g (eV)	Valence Band E_V (eV)
ZnTe	3.50	-3.5	3.2	-5.8
Si		-4.0	1.1	-5.1
GaAs	4.07	-4.1	1.4	-5.5
ZnSe	4.09	-4.1	2,7	-6.8
ZnS	4.09	-4.1	3.6	-7.7
$SrTiO_3$		-4.3	3.2	-7.5
GaP	4.30	-4.3	2.3	-6.6
$KTiO_3$		-4.4	3.4	-7.8

InP	4.38	-4.4	1,3	-5.7
CdS	4.50	-4.5	2.4	-6.9
TiO_2		-4.6	3.2	-7.8
$MnTiO_3$		-4.7	3.1	-7.8
PbO		-4.9	2.8	-7.7
$FeTiO_3$		-4.9	2.8	-7.7
$BaTiO_3$		-4.9	3.3	-8.2
CdSe	4.95	-5.0	1.7	-6.7
WO_3		-5.0	2.7	-7.7
SnO_2		-5.0	3.5	-8.5
Fe_2O_3		-5.1	2.2	-7.3
Bi_2O_3		-5.1	2.8	-7.9
MoS_2		-4.53	1.75	-6.28
SiC		-3.04	3.0	-6.04

of these sites has already been probed by appropriate electro-chemical and esr techniques. It is regarded that the normal limitations that are present for the selection of materials for PEC applications may also hold good for catalytic photo-assisted processes, however a variety of materials can be examined for the later process though could not be effectively utilized in PEC applications. In Table 1 the characteristics of the conventional semiconducting materials used in PEC applications are given.

3. Ways and Means of Increasing the Efficiency and Selectivity of Redox Reactions in Photo-assisted Catalytic Processes on Semiconductors

3.1 Metallization It was seen in the previous section that most of the semiconducting materials show poor activity when used alone [9]. But the presence of a metal on a semiconductor increases its efficiency and hence semiconductor powders coated with metals are finding extensive application in the field of photo-assisted catalytic processes [10]. Schematically the electron-hole separation on an illuminated metallized semiconductor particle (M/SC) can be represented as shown in Fig.3. Irradiation of metallized semiconductor with light energy

Figure 3: Photon Induced electron-hole separation on a Metallized Semiconductor Particle (SC/M)

greater than the band gap (E > Eg) results in the formation of electrons and holes and the presence of metals with high electron affinity effectively traps the photo-excited electrons and uses it to perform the subsequent reduction reaction. The utilization of electron in the reduction reaction at the metal site implies that the hole can be made to perform the oxidation reaction unidirectionally thereby increasing the overall efficiency of the process. One can also use materials like RuO2 which can act as sinks for holes or employ both metals and hole sinks for achieving higher efficiencies. Even though, in

Table 2: Electron Affinities and Oxidation Potentials of various metal ion/metal redox couples of noble metals

Reactions	E^0 (V)	Electron affinity of the metal
$Pt \rightarrow Pt^{2+} + 2e$	-1.118	2.128
$Pd \rightarrow Pd^{2+} + 2e$	-0.951	0.557
$Rh \rightarrow Rh^{3+} + 3e$	-0.758	1.137
$Ru \rightarrow Ru^{3+} + 3e$	-0.455	1.05

principle one can have sinks for both electrons and holes, the effect of metallization of semiconductors which act as sinks for photoexcited electrons alone has been extensively studied. In this case, according to the photochemical diode model the oxidation should take place on the semiconductor surface for an n-type SC/M system.

3.2 Nature of the Metal Loaded

The choice of the metal is determined by the value of the electron affinity of the metal to be loaded. In addition to electron affinity being high, the metal should have low hydrogen overvoltage, if the reaction involves hydrogen evolution. The metal should have suitable work function to make a favourable contact and should show negligible tendency for oxidation. The electron affinity and oxidation potential of various couples of noble metals which are normally used are given in Table 2.

3.3 Method of Metal Deposition

Ever since Bard [11] demonstrated photo-deposition of Pt, Pd, Cu and Ag using reducing agents this method assumed importance, for the in situ preparation of metal loaded semiconductor [12]. In addition, conventional methods like impregnation [13], in situ reduction of metal salts [14], exchange impregnation and sputtering methods [15] have also been used to prepare metallized semiconductors.

3.3.1 Use of Sacrificial Agents Another approach used by Gratzel and his coworkers [16] is to use photoinduced reduction of a relay species (methyl viollogen, NN'dimethylpyridine dicaion MV2+ by a sensitizer [Ru(bipy)3] 2+ for the cleavage of water in presence of two redox catalysts on a colloidal semiconductor system. This scheme is shownin Fig.4. These studies have been favourably extended to niobium pentoxide substituted anatase (because of the favourable flat band potential, more cathodic to the extent of 300 mV than that of rutile) Pt-RuI_2 system for effecting visible light induced dissociation of water.

Figure 4: Scheme for photoredox process in presence of two redox catalysts

3.4 Pretreatments

Another method of increasing the photo-assisted catalytic activity of metal loaded semiconductors is to use various pretreatments. This procedure has been successfully employed for the photo-assisted catalytic dehydrogenation of methanol on metallized TiO_2 system [17]. Typical data generated given in Table 3 for Pd/TIO_2 and Ru/TiO_2 show that the activity is increased in the case of Pd/TiO_2 as also Pt/TiO_2 when it is subjected to oxygen followed by hydrogen treatment at 673 K while in the case of Ru/TiO_2 the favourable treatment is direct hydrogen treatment. Similar data have also been collected on Ru/TiO_2 system and they are given in Table 4. Table 5 shows the surface metal concentration data after various pretreatments and sputtering for the various metallized titania systems studied by XPS. Pt and Pd loaded systems showed an enrichment whereas Rh and Ru loaded systems exhibited an impoverishment of the metal on the surface after oxygen treatment compared to the untreated catalyst. This could be due to the migration of the metal species based on the surface energy values of the metal oxide and that of titania. These postulates agree well with the results

Table 3: Photocatalytic data on Pd/TiO2 system; 20 ml of methanol was irradiated in presence of 100 mg of the catalyst for 1 hour at 308 K (a) HCHO formed is given in brackets (b) oxygen/hydrogen treatment in oxygen followed in hydrogen at 873 K for 12 h, (c) Nitrogen/hydrogen treatment in nitrogen and then in hydrogen at 678 K for 12h and (d) hydrogen treatment at 678 K for 12 h

Wt % of Pd in Pd/TiO_2	Hydrogen (HCHO)[a] in micromoles per hour		
	OH[b]	NH[c]	H[d]
0.38	60(50)	39 (55)	8 (6)
1.50	79(64)	38 (37)	9 (9)
2.40	53 (45)	38 (37)	9 (9)

Table 4: Photocatalytic data on Ru/TiO2 system;; for other details see the previous table

Wt % of Ru in Ru/TiO_2	Hydrogen (HCHO)[a] in micromoles per hour		
	OH[b]	NH[c]	H[d]
0.04	15 (13)	49 (45)	53 (47)
0.08	15 (14)	60 (51)	62 (58)
0.22	15 (14)	56 (51)	56 (54)
0.38	19 (18)	49 (42)	53 (51)
0.69	19 (18)	45 (36)	53 (50)
1.46	19 (18)	45 (36)	51 (50)

Table 5: Surface metal amount after various pretreatments and sputtering for various M/TiO2 system determined by XPS: OO oxygen treatment followed by oxygen treatment in situ thus the underlined letters denote the treatment in the preparation chamber of the spectrometer

Metal (M)	nM/nTi Treated /untreated				nM/nT after/before sputtering	
	O<u>O</u>	O<u>OH</u>	OH<u>H</u>	H<u>H</u>	OH<u>H</u>	H<u>H</u>
Pt	1	82	34	18	68	38
Pd	141	97		6		65
Rh	72	66	74	12	30	60
Ru	14	16	6	56	120	40

of sputtering studies which indicate increased concentration of these metals in the bulk of the semiconductor.

4.Physics of Noble Metal - semiconductor Interface as well as before pretreatment

Pt supported titania is used for many catalytic processes because Pt is one of the catalysts for recombination and dissociation of H_2 and H_2O. Moreover, the electron affinity and hydrogen over voltage of Pt seem to be adequate for the catalytic effect. Depending on the nature of the metal and the surface characteristics of the semiconductor a metal-semiconductor contact may give rise to a Schottky barrier or an ohmic contact. The energy level scheme for these two types of contacts are given in Figs 6 and 7. As Schottky barrier will impede the flow of electrons to the metal and if metal deposits were to act as reduction centres the contact should be an Ohmic one. Aspnes and Heller [16] have measured the properties of electrical contacts between catalytically active metals with different work functions (Pt, Rh and Ru) and semiconductors like n-TiO_2, n-CdS, n-$SrTiO_3$ and P-InP. All air exposed contacts formed Schottky junctions with barrier heights ranging from 0.1 eV for N-TiO_2/Ru to 1.84 eV for CdS/Pt. But the exposure to a dry hydrogen atmosphere reversibly converted all the n-$SrTiO_3$ contacts to near Ohmic behaviour. The ambient gas induced barrier height changes observed by the authors are attributed to the formation of low resistance, ohmic junction by the dissolution of hydrogen in metal. Hope and Bard [19] have reported that thermal treatment of contact could lead to the inter diffusion of Pt and rutile. In the case of Pt/TiO2, the work function of Pt is 5.2 eV while the electron affinity of TiO_2 is 4 eV, thus favouring a schottky barrier which will prevent electron flow to metal centres which are to act as electron sinks. However, the inter

Table 6: Heats of formation of oxides, heats of sublimation and heats of vapourization of metals

Metal oxide	ΔH_f (kJ/mol)	ΔH^0_{sub} of oxide (kJ/mol)	ΔH^0_{vap} of metal (kJ/mol)
PdO	-42.8	91	376
PtO		565	512
Rh_2O_3	-47.9	556	497
RuO_2	-55.0		570

Diffusion could create an interfacial region in which there is a high density of surface states, thus the junction approaches an ohmic one. The interface region as deduced from AES depth profiling is approximately 10 nm with less defined boundaries, showing considerable intergrowth of the metal and the semiconductor. The pretreatments employed should create species which will facilitate this inter diffusion of the metal and semiconductor species thus leading to a true ohmic contact. This interdiffusion is facilitated by a number of factors, important among them being pretreatment. Pretreatment could give rise to species whose surface free energy values will be favourable for diffusion into the bulk of the semiconductor. This aspect has already been discussed in the previous section. The effect of pretreatment can also be explained based on the standard heats of formation or standard heats of vapourization of metals. These data for typical noble metals are given in Table 6. This was proposed by Wanke et al [20] for the changes in the dispersion of group VIII metals on alumina after high temperature treatments in various atmospheres. The order of surface metal concentration after OHH treatment (refer to data in Table 5) is Rh> Pt> Ru. This is because RuO_2 which has higher standard heat of formation compared to other oxides would sinter more and thereby stability is less because of the exothermicity of the reaction. Block et al [21] have reported that the oxides of Ru (RuO_2 and RuO_3) is mobile. However, after HH treatment (refer to table 5) the order of surface metal concentration is Ru >Pt> Rh> Pd which can be accounted for in terms of heats of sublimation or heats of vapourisation of the oxides. As the value of heat quantities increases the oxides will be stable and sintering will be less. The extent of sintering of metal particles in various atmospheres is also one of the causes of the difference in surface metal concentration after various pre-treatments. The exposed surface area from the metal is decreased when sintering is high and as a result surface metal concentration is also decreased.

Table 7: Rate of hydrogen evolution in micro moles/10h from neutral water and carbohydrates, amino acids, fatty acids, or various types of biomasses using TiO2-Pt catalyst (Data compiled from ref [22]

Reactants	Hydrogen evolution rate
Carbohydrates	

Glucose	1130
Sugar	920
Starch	240
Cellulose	40
Proteins (amino acids)	
Glycine	220
Glutamic acid	7126
Proline	10
Fatty acids	
Stearic acid	88
Pyruvic acid	323
Natural Products	
Ethanol	5080
Lignin	12
Food Materials	
Potato	39
Green algae and other sea weeds	
Chlorella	73
Seaweed	74

5. Active Catalysts for hydrogen evolving Reactions

The photo-catalytic reaction of importance for biomass conversion is the reaction of glucose, sugars, starch and cellulose with water to produce carbon dioxide and hydrogen. In combination with photo-synthetic reaction, the overall reaction will appear to be water splitting. The reaction sequence for glucose as substrate can be written as

$6CO_2 + 6H_2O \longrightarrow C_6H_{12}O_6 + 6O_2 \; \Delta G^0 = 2870$ KJ/mol

$C_6H_{12}O_6 \longrightarrow 6CO_2 + 12H_2 \; \Delta G^0 = -32$ KJ/mol

$12H_2O \longrightarrow 12H_2 + 6O_2 \; \Delta G^0 = 2838$ KJ/mol

The schematic representation of the photo-catalytic hydrogen evolution from various organic substrates is shown in Fig.8. In Table 7 typical data on the rate of hydrogen production from amino acids, proteins, fats and various biomasses in aqueous solution are given. Another reaction of interest is

Table 8: Brief summary of the data on the photo-catalytic reduction of nitrogen in presence of photo-electrolysis of water

Photocatalyst	Band gap (eV)	Yield of ammonia In micromoles	Weight of the catalyst
TiO_2	2.9-3.2	1.75	0.2
TiO_2/0.2 Fe_2O_3	2.9-3.2	6.0	0.2
Fe/TiO_2	2.9-3.2	6.4	0.2
Co/TiO_2	2.9-3.2	3.8	0.2
Mo/TiO_2	2.9-3.2	4.0	0.2
Pt/TuO_2		2.8	0.3
ZnO	3.2	2.1	0.3
Pt/ZnO	3.2	0.8	0.3
$SrTiO_3$	3.2	1.9	0.3
$Pt/SrTiO_3$		2.4	0.3
CdS	2.4	4.9	0.3
Pt/CdS	2.4	4.9	0.3
GaP		4.6	0.3
Pt/GaP		7.5	0.3
TiO_2-SiC		3.0	0.5
NiO-$SrTiO_3$	3.2	0.9	0.5
$RuO_2/SrTiO_3$	3.2	0.75	0.5
RuO_2-NiO-$SrTiO_3$	3.2	2.5	0.5
RuO_2-NiO-$BaTiO_3$		2.6	0.5
$CdS/Pt/RuO_2$	2.4	2.4	0.5

the photo-assisted catalytic reduction of dinitrogen in presence of photo-electrolysis of water. This is similar to the natural nitrogen fixation. Various attempts have been made to effect direct reduction of nitrogen in presence of photo-splitting of water. The available data are summarized in Table 8. The ammonia yields obtained were quite small since the energetics of the dinitrogen activation on the semiconductor used has not been properly elucidated so as to formulate a suitable modified photo-active catalyst system which can

simultaneously promote dinitrogen activation as well as the successive reduction of atomic nitrogen. Another reaction of interest in relation to the nature cycle is photo-methanation of carbon dioxide [24] this reaction has been found to be promoted selectively by dispersed Ru/TiO_2.

6.Catalysts for Photo-assisted degradation of Pollutants

6.1. Photo-assisted catalytic decomposition of hydrogen sulphide on metallised CdS

The photocatalytic hydrogen evolution from aqueous sulphide solution was measured under various experimental conditions and the initial rate data are presented in Table 9. The metal ions as metal chlorides did not show any activity. Among the metallized CdS the observed activity order is Rh> Ru > P>t Pd. XPS studies showed that the metallized CdS contain metal oxides formed by aerial oxidation. Though RuO_2 and Rh_2O_3 could function as hole trapping agents PtO and PdO are not useful as hole transferring agents and hence these two systems showed lower activity as compared to the other two metals. In the case of in situ metallisation the activity order is Rh > Pt >Pd >Ru=Ir >Co >Ni=Fe Even though the intrinsic activity of Pt for hydrogen evolution is more than those of the other metals, considering the combined effect of metal and metal oxide or metal and metal sulphide systems containing Rh is the most active one. In aqueous solutions, photocatalytic oxidation of many organic compounds are efficient. Typical photocatalytic oxidation of carboxylic acids, alcohols, aromatics and lactams have been reported in literature and typical reactions studied are given in Table 10. These studies show that there is potentiality for using heterogeneous photocatalysis as a means of decontaminating water and several studies have already been taken up in this direction [28]. It should therefore be of interest to extend these studies for some non-biodegradable pollutants. This is one direction in which photo-assisted catalytic process will be utilized in the near future.

Table 9. Initial rate data for the photo-catalytic hydrogen evolution from aqueous sulphide solution. Reactant 0.25 M sodium sulphide aqueous solution; weight of the catalyst 100 mg; light source 1000 W tungsten halogen lamp and noble metal content is 1.37 percent in each case as metal r metal ion

Photo-catalyst	Initial Hydrogen evolution rate in ml/h/g

CdS (naked)	0.31
Pt/CdS	2.08
CdS +Pt^{4+} as H_2PTCl_6	2.89
CdS + Ir^{3+} as $IrCl_3$	0.96
Ru/CdS	2.39
CdS + Ru^{3+} as $RuCl_3$	0.97
RuO_2 + CdS (thermal oxidation)	0.97
RuO_2 + CdS (Physical Mixture)	1.37
Ru/CdS + Chloride ions	2.38
Rh/CdS	2.53
Rh_2S_3 + CdS	2.83
CdS+Rh as $RhCl_3$	4.15
Pd/CdS	0.94
CdS + Pd^{2+} as $PdCl_2$	2.55
CdS + Ni^{2+} as $NiCl_2$	0.53
NiS/CdS	0.51
CdS + Co^{2+} as $CoCl_2$	0.58
CdS + Fe^{3+} as $FeCl_3$	0.52

Table 10 Examples of photo-catalytic reactions of organic molecules on TiO_2 powder

Reaction
Acetic acid →Methane + CO_2 + Hydrogen + ethane
Propionic acid →CO_2 + ethane +ethylene + hydrogen
n-butyric acid →CO_2 +Propane + hydrogen
n-valeric acid →CO_2 + isobutane + hydrogen +isobutylene
Toluene + oxygen →benzaldehyde + water
Methanol →formaldehyde + hydrogen
Ethanol →acetaldehyde + Hydrogen

7 Conclusion

Photo-assisted catalytic processes appear to have promising future especially in view of the prospects of solar energy conversion. Instead of aiming at evolving more efficient catalytic materials based on naked semiconductors, the research in the near future will be directed towards utilizing the available materials for new reactions which have relevance for energy conversion as well as pollution control.

The direction of activity in photo-assisted catalysis would begin the modification of the available semiconductors so as to increase

Table 9: Initial rate data for the photo-catalytic hydrogen evolution from aqueous sulphide solution. Reactant 0.25M sodium sulphide aqueous solution, weight of the catalyst is 100mg light source is 1000W tungsten halogen lamp and noble metal content is 1.37 percent in each case as metal or metal ion

the efficiency of processes especially in hydrogen evolving reactions and use of biomasses for chemical storage of energy.

8 REFERENCES

1. Bard, A.J., J.Photochem., 10,50 (1979).

2. Bard, A.J., Science, 207,139 (1980).

3. Nozik, A.J., Phil.Trans.R.Soc.London, Ser A, 295,453 (1980).

4. Gratzel, M., Energy resources through photo-chemistry and catalysis, Academic Press, New York, (1983). Schiavello,M., (Ed.) Photocheistry, Photocatalysis and photoreactors, Reidel Pub.Co.,(1985).

5. Cunningham, J., Hodnett,B.K., Ilyas,M., Leaby,E.M., and Tobin,J.P.

J.Chem.Soc., Faraday trans., 1,78,3297(1982)

6. Borgarellow,E., Serpone,N., Pelizzetti,E., and Barbeni,M., J.Photochem., 33,35 (1986) Enea,O., and Bard,A.J., J.Phys.Chem., 60,301 (1986). Makhmadmurodov,A., Gruzdkov, Yu.A., Savinov,E.N., and Parmon,V.N., Kinet.Catal., 27,121 (1986). Rufus,I.B., Ramakrishnan,V., Viswanathan,B., and Kuriacose, J.C., Int.Conf. on Photochemical conversion and storage of solar energy, Evanston, p.123 (1988)

7. Meissner,D., Memming,R., Kastening,B., andBahnemann,D., Chem.Phys.lett., 127,419 (1986). \

8. Yamase, T., Polyhedron, 5,79 (1986). Argities, P., Papa Constantinou,E., Inorg.Chem., 25,4386 (1986). Yamase, T., and Watanabe,R., J.Chem.Soc., Dalton Trans, 1669 (1988). Nomiya, K., Sigie, Y., Miyazaki,T., and Miwa, M.,

Polyhedron, 5,1267 (1988). Harriman,A., Photochemistry, Vol 19,The Royal Society of Chemistry, London, (1988) p.509.

9. Shrauzer G.N. and Guth, T.D., J.Am.Chem.Soc., 99,7189 (1977). Yoneyama,M., Koizumi,M., and Tamura,H. Bull Chem.Soc.Japan,52,3449 (1979). Yun,C., Anpo,M., Kodama,S., and Kubokawa, J.ChemSoc.Chem.Comm.,609 (1980). Damme,H., andHall W.K.,J.Am.Chem.Soc., 101,4373 (1979). Pichat,P., Herrman, J.-M.,Disdier,J., and Mozzanega,M,-N., J.Phys.Chem.,83,3122 (1979). Herriman,A., Thomas, J.M.,Zhou,W., and Jeffeson,D.A.,J.Solid State.Chem.,72,126 (1988). Kobayakawa,K., Sato,Y., Nakamura,J., and Fujishima, A., Bull.Chem.Soc.Jpn.,62,3433 01982) Sato,S., andKodowaki,T., J.Catal., 106,295 (1987) Harvey,P.R., and Rudham,R., J.ChemSoc.,Faraday Transs.,I 84,4181 (1988). Okamoto,K., Yamamoto,Y., Tanaka,H.,Tanaka,M., and Itaya,A., Bull.Chem.Soc.Jpn.,58,2015 (1985). Faust,B.C., Hoffman,M.R., and Bahnemann, J.Phys.Chem.,93,6371 (1989). Sato,S., J.Photochem. and Photobiology, A45,361 (1988). Shibata,K., Mimura,T., Matsui,M., Sugiura,T., and Minoura, H., J.Chem.Soc.,Chem.Commun.,1313 (1988) Hallmann,M., and Zuckermann,K., J.Chem.Soc., Chem.Commun.,455,(1986).

10. Furlong,D.N., Greiser,F., Hayes,D., Hayes,R., Sasse,W., and Wells, D., J.Phys.Chem.90,2388 (1986). Bahnmann,D.W., Monig,J., and Chapman,R., J.Phys.Chem.,91,3782 (1987). Sobczyski,A Bard A.J., Campion,A., Fox, M.A., Mallouk,T.E.,Webber,S.E., and White,J.M., J.Phys.Chem., 93,401 (1989). Escudero,J.C., Cervera-March,S., Gimenez,J., and Simaro,R., J.Catal.,123,319 (1990).

11. Kraeutler,B., and Bard,A.J., J.Am.Chem.Soc.,100,4317 (1978). Reiche,H., Dunn,W.M., and Bard,A.J., J.Phys.Chem.,83,2248 (1979).

12. Jacobs,J.W.M., Kampers, F.W.H., Rikken,J.M.G.,Bulle-Lieuwma,C.W.T. and Koningberger,D.C., J.Electrochem.Soc.,136,2914 (1989).

13. Ait-Ichou,I., Formenti,M., Pommier,B., and Teichner,S., J.Catal., 91,293 (1985).

14. Hoffmann, H.,Gratzel,M., and Kiwi,J., J.Mol.Catal., 43,183 (1987).

15. Albers,P., Seibold, K., McEvoy,A.J., andKiwi,J., J.Phys.Chem., 93,1510 (1989).

16. Kiwi,J., Borgarello,E., Pelizzetti,E.,Visca,M., and Gratzel,M., Angew.Chem.,Int.Ed.Eng.,19, (1980).

17. Mary U.D., Viswanathan,B., and Viswanath, R.P. ,Recent developments in Catalysis, Theory and Practice, Narosa publishing House, New Delhi (1991).

18. Apnes,L.A., and Heller, A., J.Phys.Chem.,87,4919 (1983).

19. Hope,G.A., andBard A.J., J.Phys.Chem.,87,1979 (1983).

20. Fiedorow R.M.J., Chahar,B.S., and Wanke,S.E., J.Catal., 51,193 (1978).

21. Chauh,G.K, Cocke,D.L.,Kruse,N,n., Abend,G., and Block,J.H.,J. Catal., 108,268 (1987).

22. Sakata,T and Kawai,T., in Energy Resources through photochemistry and catalysis, M.Gratzel,M., Academic Press, New York, (1983),pp.331.

23. Miyama,H., Fuji,N., andNagae,Y., Chem.Phys.Lett., 74,523 (1980). Li,Q., Domen,K.,Naito,S., Onishi,T., and Tamaru,K., Chem.Lett., 321 (1983) Taqui Khan M.M., Bhardwaj,R.C., and Bhardwaj,C., Indian J Chem., 25A,1 (1986) Scharuzer, G.N., and Guth,T.D., J.Am.Chem.Soc., 99,7189 (1977).

24. Thampi K.R., Kiwi,J., and Gratzel, M., Nature, 327,5066 (1980).

25. Bernard Rufus,I., Ph D thesis, Photoelectrochemical,photocatalytic and surface studies on metallized Cadmium chalcogenides, IIT Madras (1989).

26. Schiavello, M., (Ed.) Photocatalysis and Environment, Kluwer press

CHAPTER

On the selection Criteria of Semiconductors for Water Decomposition

1 Introduction

There have been persistent attempts to formulate and design solid matrices for use as either photo-catalysts or electrodes for photo-electro-chemical cells for

generation of hydrogen from the decomposition of water. Though a variety of guidelines have been evolved and applied, these methodologies have not yet yielded predictive power. There can be various reasons for this situation, possibly one of the reasons is the research has been mostly focused on band gap engineering with a view to utilize the major portion of solar spectrum. Band gap engineering has certainly provided a variety of methodologies for the formulation of modifying existing materials with a view to reduce the band gap but it has not yet fully provided means for the generation of new materials. In recent times, there have been consistent attempts to generate new visible light active systems by doping the conventional semiconductors like TiO2 or Titanium based other semiconductors with Nitrogen, Phosphorus, Sulphur, Carbon and Boron. It is generally believed that the top of the valence band of the semiconductor is altered towards negative values of electrochemical potential thus possibly reducing the band gap without altering the position of the bottom of the conduction band. However, there are alternate postulates to account for this expectation like creation of additional allowed energy states in the forbidden gap, altering the density of states of the valence band which can possibly explain the shift of the absorption wavelength to the visible region. It has also been postulated that the metal ion - anion bond character (extent of ionicity of the bond formulating more ionic character will give rise to higher band gap value)could be one of the possible ways of shifting the absorption to visible region and possibly this will also account for the life time of the exciton which is the main contributing factor for the observed photo-catalysis or Photo-electro-chemical decomposition of water. Even though sensitization of the semiconductor is one means of enhancing the activity of the system, inherently itself one has to look for opportunities to enhance the activity of the semiconductor.This may be possible only when one can formulate the governing principle for photoactivity of the system itself. Along these lines the first postulate that is predominant in literature is based on the electronic configuration of the cation of the semiconductor. Taking the example of TiO2 and ZnO, it is usually considered that the d0 and d10 configuration may be the suitable one. This postulate is possibly the reason the active metals shown in Fig 1 for photoactivity. This type of rationalization have some implications. Let us list them. (1) These semiconductors will be mostly ionic and hence the band gap will be high (nearly or more than 3 eV). (2) This rationalization can not be extended to ternary and other higher order type of semiconductors unless otherwise if one can visualize the multicomponent systems in terms of binary

system. (3) Even for binary systems, this governing principle does not provide the details for other (sulphide) semiconductors. When the percentage ionic character increases, the CB becomes more negative and VB becomes more positive, The more the percentage ionic character of the, the larger the band gap Let us revert back to the original postulate that d0 configuration of the cation of the semiconductor will be active systems. Two typical d0 systems considered are Cd2SnO4 and CdSnO3. Their band positions are shown in Fig.2. It has been shown that both these systems do not decompose water to generate hydrogen even though one of them does possess band positions suitable for the decomposition of water. Hence it may be postulated that the electronic configuration of the cation though determines the value of the band gap this parameter cannot be employed for deciding if a given semiconductor is capable of splitting water. The second attempt has been to make use of semiconductors which can utilize visible light since the component of visible light in solar radiation is around 45%. It is always a debate if we need to use such high percent of solar radiation since even harnessing the solar radiation for a day is sufficient to meet the energy needs of earth for many years. Leaving this aspect, there may be other aspects in harnessing UV light in solar radiation but the number of semiconductors with the band gap in UV region are small in number and their efficiency also is poor. These aspects have not been adequately addressed to in the literature since the focus has been mostly on band gap engineering. Another aspect that has received considerable attention in recent times is the so called Dye Sensitized Solar Cells (DSSC). There have been efforts put in to make it a viable energy conversion device. However, the promise and progress are not proportionate to each other or to the demand. There are a variety of aspects on which the success of this form of energy conversion device stand. The phenomenon of sensitization is well known to mankind. The semiconducting materials are often functioning by the sensitization of their charge carriers namely the electrons and holes. In the case of wide band gap semiconductors, the separation of the charge carriers requires considerable expansion of energy. The life on earth has always been sustained by solar power either directly or indirectly. It appears that mankind has resorted to the direct use of solar power for their energy needs and hence a variety of options are being examined including direct conversion of photons into electricity which is termed as photo-voltaics. Since the photons are used for the separation of electron hole pair, one has to resort to materials where the occupying state of the electron(valence band) should be different from the state (conduction band) from

which the electron is displaced in terms of energy and symmetry. Since the energy levels of both occupied and unoccupied states are continuous in conductors, the excited state of the electron will tend to recombine easily with the hole generated. Hence it is necessary that the states from which electrons are removed must be energetically different from the states at which the electrons are placed on excitation. This situation is obtainable in semiconductors or insulators where valence band (the state from which electron is excited) and conduction band (the state to which the electron is excited to) are separated both in terms of energy and the symmetry of the wave functions. However, the anxiety to utilize solar energy for excitation places a restriction on the use of semiconductors and that too only small band gap semiconductors since most of the solar radiation (in terms of energy) from the solar spectrum can be harnessed. However, not all small band semiconductors are stable under strong illumination conditions or amenable to be used as photo-anodes in the photo-voltaic devices. Among the available and exploited semiconductors (nearly 400 in number [1]), only a handful of them appear to be promising. For application in Dye Sensitized Solar Cells (DSSC) the most studied systems are TiO2, ZnO and tin oxide [2]. Unfortunately all these three systems are wide band gap semiconductors and absorb only UV radiation which is only about 5-8% of the total solar radiation. Secondly the conversion efficiency,(photon to electricity) is also governed by the process of recombination which is the predominant mode of decay when excitation is carried out in the semiconductor itself. It appears therefore, necessary that some kind of charge injection is resorted to. This may be possible if the excitation by photon is carried out in another system and the excited electron takes occupancy in the conduction band states of the wide band gap semiconductor so that the electron can be moved in the external circuit. The auxiliary system where photo-excitation is taking place is termed as the sensitizer. It is therefore clear that the sensitizer has to fulfill some specifications. The important ones are: i. The system chosen should be capable of absorbing light in visible and infra red region of the solar spectrum. ii. The energy state of the electron on excitation in the sensitizer should be on par or suitable with that of the conduction band of the semiconductor so that charge injection can be feasible iii. The sensitizer employed should be capable of being dispersed on the semiconductor so that the photon absorption can be maximized iv. The sensitizer should be stable under strong illumination conditions since electron excitation may ultimately after electron transfer lead to an oxidized form of the sensitizer and it should be capable of easily reduced by

the shuttled electron from the counter electrode v. The sensitizer should be stable on the semiconductor surface (good adhesion). It is therefore appropriate to note that the sensitizers may be any substance that can absorb low energy photons (visible and IR region) and also is capable of providing the electrons in the external circuit to draw the power. There are various motivations for including this dicussion. We list them as follows: (i) This technology is threatening to be a viable for the conversion of solar energy into electricity for nearly 20 years now. (ii) Efficiency of this type of solar cell has been consistently improving over the years either from the point of utilizing major portion of the solar radiation by appropriate choice of the dyes (the HOMO and LUMO levels of the dye could be altered to suit the available solar radiation) and/or their suitability with the semiconductor which is being sensitized. (iii) Various structural modifications of the dye are feasible and also tried. (iv) The cost of these solar cells has been considerably reduced with respect to time. (v) As of now, these devices appear to be environmentally acceptable and the available infrastructure may be able to sustain this technology (vi) These devices may be universally accepted, and (vii) Above all, market penetration is possible. In view of these reasons, in recent years there have been a number of perspective articles and reviews on this topic [only selected ones in 3-7]. It is a fact that vast literature is already available on this topic, as this topic is very contemporary and hence it is necessary to assess the scientific and technological developments at periodical intervals so that one does not miss out the important advances that are taking place in such an application area. The contents of this presentation therefore will be focusing on the various possible sensitizers that have been already examined for DSSC applications as well as other relevant aspects of this emerging technology. It may be appropriate at this stage to draw the comparison with the natural photosynthesis. Both DSSC and photo synthesis make use of photon absorption by a molecular dye (it is chlorophyll a and b in the case of photosynthesis). The excited electron is transferred effectively in the case of photosynthesis since it is an escalator type redox species and hence most of the excited electrons are effectively transferred and utilized in the reduction reaction. In photo synthesis the excited electron gets transferred to a variety of species so that effective and efficient electron transfer can take place to the species undergoing reduction. In essence, in photosynthesis after initial photo-excitation the electron takes appropriate energetic position in terms of reduction potential so as to be suitable for the species undergoing reduction. Such a situation is not realizable in the case of laboratory driven

reduction processes since one has only fixed value redox couples and hence effective transfer of electron and thus efficient reduction of carbon dioxide or water could not realized in the laboratory. However, in the case of DSSC, the excited electron has to be transported via the conduction band of the semiconductor and hence it is necessary to match the LUMO level of the molecular dye employed for sensitization and that of the bottom edge of the conduction band of the semiconductor. In addition, the electron mobility in the semiconductor has to be high enough so that fast electron transfer takes place without the concurrent recombination process. This similarity makes the DSSC to be considered as a form of bio-mimicry. However, it should be emphasized that the efficiency of DSSC cannot reach the levels of efficiency of photosynthesis.

3 Configuration of a Dye Sensitized Solar Cell

There are various forms of Photo-electrochemical cells (PEC). Some of these forms are considered, Among them, Dye Sensitized Solar Cells (various abbreviations are employed in the literature the prominent ones are DSSC, DSC or DYSC) are the prominent ones. These cells are simpler in construction compared to solid state solar cells. The first cell was constructed by Michael Gratzel and Brain ORegan in 1991 [8]. Dye sensitized solar cells (DSSC) have been claimed to be promising for energy conversion to electricity with the possibility of low fabrication cost, easy manufacturing feasibility and fairly high efficiency. In general, the conversion efficiency is less than that of the best thin film cells, but this could be compensated in terms of price/performance ratio which could be as much favourable as that of fossil fuel to electricity generation and hence these types of cells can be expected to be possible mode of energy converters in the near future. If one were to combine an electron rich semiconductor (n type) with an electron deficient semiconductor (p-type) then one can visualize the transfer of electrons from n to p due to the difference in the electro-chemical potential of the electrons in the two semiconductors. This shuttling of the electron (partly formed by photo-excitation in n type semiconductor) in the external circuit is made use of to derive energy so that the electron returns back to the n semiconductor in the valence band as it was in the original state before photo-excitation. Therefore, the harnessing of energy is related to the extent to which one can make use of the photons for increasing the electrochemical potential of the electrons. This manifests itself in the extent of

the available number of appropriate energy photons and also the absorption capacity of the semiconductor employed. The origin of the dye sensitized solar cells is in this direction meant to increase the extent of photon absorption (as dyes are good photon absorbers) and possibly also favours smooth transport of the electrons through the conventional semiconductor namely TiO2 in the external circuit. Configurationally, dye sensitized solar cells consist of conventional semiconductor (usually TiO2 which is the work horse semiconductor for photo-electrolysis) and a counter metallic (Pt) electrode usually in supported mode to reduce the extent of requirement of the noble metal. However, the oxide semiconductor has a surface coating of the dye (mostly mimicking chlorophyll in the leaves). This coating can be achieved in a variety of ways like dipping the semiconductor in a solution of the dye whereby the dye molecules are adsorbed on the semiconductor by probably covalent bonding. However other variations of the loading of the dye on the semiconductor can also be pursued. These include loading the dye with appropriate binder, preparing the electrode (in this case it functions as anode) materials from semiconductor oxide and the dye from a slurry. Improvements in the stability of DSSC have also been achieved in alternate use of the plasticized polymer electrolyte instead of the conventional I^-_3 /I^- system. For an elementary description of the dye sensitized solar cells, readers are referred to the site http://www.science20.com/mei/blog/dye sensitized solar cell-75581.

4 Sensitizers

It may be appropriate if one makes some comments on the sensitizers (not necessarily dyes alone) normally employed in DSSC since this is the central part of these cells. In a sense, they are the real converters of photon energy into electrons which are injected into the semiconductor to be passed on to the counter electrode for the reduction reaction. A variety of substances have been employed probably taking the clues from the natural photosynthesis process. The type of molecules that have been tried include a variety of ruthenium based complexes like cis Ru(L)2(NCS)2 where L is bipyrine carboxylic acid, or RuL(NCS)3 where L is a tripyridine carboxylic acid or RuL3, [9] or the corresponding analogs of Os [10] (These species give rise to intense (in the visible region) metal-to-ligand charge transfer (MLCT) bands with a favourable energetics for possible activation-less charge injection into the semiconductor. In essence, several organic [11] and inorganic compounds have been investigated for the

sensitization of the semiconductor which include chlorophyll derivatives [12], porphyrins [13], phtalocyanines [14,15], platinum complexes [16,17], fluorescent dyes [18], carboxylated derivatives of anthracene [19] , polymeric films [20], and coupled semiconductors [21,22] with lower-energy band-gaps, natural dyes like anthocyanin [23] from black rice, carotenoid [24] from erythinka and chlorophyll from variegata, rose ben8 gal, porphyrin complexes especially that of zinc [25],inorganic species like copper diselenium, [26], and iodide (doped in ZnO)[27], and organic dyes without the metal ions. A complete listing of 86 sensitizers that have been tried and their characteristics are given in a recent book [28]. In recent years a number of other possibilities are being examined. The relevant data on these systems are briefly given in Table in the appendix. Based on cost considerations, attempts have been made to use metal free dyes for DSSC applications. However, these systems exhibit lower efficiency as compared to the metal containing dyes. [3, 4, 29-31]. It may be useful to consider some general remarks on the dyes or essentially on the types of sensitizers conventionally employed in DSSC in terms of materials selection and logistics for consideration. (i) . The sensitizers conventionally provide the excited electrons to the semiconductor and hence they should be stable enough in the oxidized state such that it will return to the original state by electron injection from the cathode. This means that the dyes chosen should be capable of providing electrons of suitable energy so that the electrons can be injected into the conduction band of the semiconductor employed. This brings a condition that the energy of the excited electron in the dye must match at least with bottom of the conduction band of the semiconductor. (ii) Since the electrons are directly injected into the conduction band of the semiconductor from the excited state of the sensitizers, the holeelectron recombination within the semiconductor does not take place or at least less likely. (iii) The choice of the semiconductors are based on the spectral region where the absorption of photons can take place and it is usually preferred to extend the absorption region as lowenergy as possible namely to visible and IR region. Hence the molecular structures of the sensitizers are chosen such that they will have absorption in the spectral region of the choice. (iv) Since sensitizers (for this presentation it can be read as dyes) and the semiconductor are in electrical contact, there can be alterations of the electronic energy levels at the interface and it is preferable that the electron energy state in the sensitizers must be on par with that of the energy of the bottom of the conduction band of the semiconductor. This means that the energy band positions must be suitably

altered at the semiconductor/sensitizer interface. This brings us to a limitation that the sensitizers chosen should be such that their energy levels of the excited electrons should be capable of stabilizing the bottom of the conduction band edge. This is usually termed as moving the bottom of the conduction band edge downwards or negative conduction band shift due to favourbale dipolar field exerted by the sensitizer to the semiconductor. This may be at variance to conventional metal ion containing sensitizers like heteroleptic Ru(II)-dyes for which an opposite dipole effect has been reported thus increasing the value of the open circuit voltage V(OC) [32].

Figure 3: Schematic diagram of a dye sensitized solar cell. The photo-anode consists of semiconductor usually TiO2 and occasionally, ZnO or other semiconductors to which the dye is covalently attached and the photon absorption by the dye gives rise to electron injection into the semiconductor conduction band from where it is transported in the external circuit through the load to the cathode which is conventionally carbon supported metal system which injects the electrons to carry out the reduction reaction in the tri-iodide/iodide couple I− 3 / I−. Other couples or electron shuttles can be employed to facilitate the electron reinjection into the dye. A variety of electrolytes have been employed.

(iv) In a recent publication, [33] there has been an attempt to use an inverse sensitized photocathode in combination with the conventional sensitized photo-anodes (where electron injection was conceived to take place) so as to increase photon to electron yield several times as compared to the conventional n-DSCs. This type of tandem pn-DSCs may be one of the possible alternatives however, it should be remarked that the available dyes for p-DSC are till now poor performers and hence there is a need to develop new systems which can function in this mode. It has been claimed that the donor-acceptor dyes, studied as photo-cathodic sensitizers, comprise a variable-length oligothiophene bridge, which provides control over the spatial separation of the photo-generated charge carriers. (vi) It is appropriate that some comments are also available in the nature and structure of the sensitizers that have been tried for DSSC. The logic for the selection of sensitizers must be (i) the required excitation energy must fall in the IR or visible region so

that most part of the solar spectrum can be used. It means one has to have a fair idea of the available solar spectrum which is shown in Fig.2. (ii) The chosen sensitizer should be capable of covalently bonded to the semiconductor employed. (i) As mentioned elsewhere, there must be appropriate energetic position of the conduction band of the semiconductor which must be overlapping with the excited state energy of the electron in the sensitizer. (ii) The hole electron recombination within the sensitizer should be minimum, this can be achieved to an extent from smaller size (length in case of polyene dyes) of sensitizers or in other words the electron path in the dye system should be as short as possible so that the electron is injected into the semiconductor before recombination takes place. (iii) The sensitizers in the excited state should not prefer the de-excitation route through intermolecular interaction with the acceptor species in the electrolyte. (iv) The dyes in general used in DSSCs tend to degrade over time, thus leading to decreased efficiency and also the life time of the dyes are also limited and hence needs replacement of costly dyes. Attempts are being made to enhance the life time of the dyes in DSSCs in a variety of ways [34, 35] and it is hoped that the stability problems may eventually be overcome in the near future. (v) Even though it is generally claimed that the DSSCs are affordable in terms of cost, it is to remarked that most of the contemporary DSSCs use complexes of the relatively rare metals like ruthenium or osmium and other noble metals as sensitizing species which may not be amenable for large scale applications. Research efforts are made for designing alternate dyes including metal-free organic and natural dyes [36-38]. However, it should be remembered that metal free and natural dyes are generally show lower efficiencies as compared to the metal containing dyes [6, 38, 39-42]. (vi) The reported efficiencies of dyes sensitized solar cells are in the range of 5-11%. This is lower than most other solar cells like solid state photovoltaics. DSSCs with metal free sensitizers show lower efficiencies in the range of 5%. The reason for this may be that metal free dyes may show high molar extinction coefficients (50,000-20,000 $M^{-1} cm^{-1}$) but narrow range of absorption ($\Delta\lambda \approx 250$ nm) while metal containing dyes may show low molar absorption coefficient (5000-20,000 $M^{-1} cm^{-1}$) but fairly broad absorption spectra ($\Delta\lambda \approx 350$

nm)[43]. The overall conversion efficiency of the dye sensitized cell is normally estimated form the measured values of photo-current measured at short circuit current,ISC, the open circuit photo-voltage,Voc , the fill factor of the cell (ff) and the intensity of the incident light (IS) and is given as =[IP h.Voc.(ff)]/IS. The search for the type of dyes employed for sensitization has centred around the following points: The dyes normally employed in DSSCs have good capacity to convert a photon into an electron almost around 80% efficiency. However efforts are on for improving (in terms of the structure of the dye and also increasing the range of wavelength of absorption to visible and IR region this is essentially attempted by bringing in conjugation in the side chain) it to almost perfect conversion in the new dyes that are introduced, an overall efficiency of 90% has been achieved with the ”lost” 10% being largely accounted for by optical losses. This limitation can indicate that the DSSC based arrays may have to be sufficiently larger than solid state photovoltaic arrays to produce the same amount of power. However this disadvantage is offset by the lower cost and greater construction flexibility of DSSCs. Any improvement in efficiency will make DSSCs to be competitive to other types of energy conversion devices. Since DSSCs employ a liquid electrolyte, its operation at lower temperatures will be of still lower efficiency and also will lead to other problems due to freezing of the electrolyte.[44] Even though alternatives that would prevent the freezing problem are being considered, it is unlikely that DSSCs will probably be suitable for cold climates in the near future. The net conversion efficiency of the DSSC depends on the dynamics of the various processes that take place in the cell. Unfortunately all the possible processes in a DSSC are not of the same time scale and hence some processes proceed faster than others and hence the net conversion efficiency does not reach high and desirable levels. Secondly the electron has to be transported from the excited state of the dye to the conduction band of the semiconductor and there-from it is transported in the external (load) circuit to the cathode where it reduces the charge carriers which regenerate the dye from its oxidized state. Generally the diffusion length of the electron generally controls this process and the diffusion length is given by the equation, Ln = (DnX n)1/2 where Dn is

the diffusion coefficient of the electron, n is the life time of the electron. It is therefore necessary that we know the time scales of the various processes that take place in a DSSC. Some estimates of these times are given in terms of the values of rate constants in Table 1. The second important parameter of concern is the life time of the dye and various governing criteria have been evolved either in terms of number of cycles (a figure 50 million cycles is claimed) or in terms of time of continuous exposure (this is of the order of 1000s hours) before the dye degradation sets in. (iii)There is always a concern on the nature of the dye with respect to the electrolyte medium employed. If the electrolyte medium is aqueous then the dyes chosen should have hydrophobic character so that they will be fairly well anchored on the semiconductor electrode. (iv) For improving the stability of the DSSC (either with respect to temperature or chemicals) solid state gel or polymer gel electrolyte or melt of multiple salts have been employed. These studies showed some improvements in terms of efficiency, however, improving the efficiency alone cannot be considered as a sole criterion for designing DSSCs. (v) Designing of appropriate dyes for DSSCs (either with or without metal linkages) has been made by a variety of ways. The main factors considered in these studies include the HOMO-LUMO energy gap in the dye (usually estimated through semi-empirical quantum mechani14 cal calculations like DFT or variations thereon [45], the estimation of the life time or properties (dipole moment) of the excited states of the dye and other relevant spectroscopic properties. (vi)In order to increase the light harvesting in DSSCs electron relay dyes have been employed where in the excitation takes place in energy relay dye from which the transfer takes place by Foster energy transfer process to the sensitizing dye. This architecture permits broader spectral absorption, increase in the amount of the dye loading and gives rise to flexible design features for the DSSCs. An increase of nearly 25% in power conversion efficiency has been already achieved.[43]. (vii)The degradation of the dye and the long term durability of the DSSCs are other factors of concern and it has been briefly mentioned above. Conventional photon induced de-carboxylation or decomposition may take place and it is possible that one can device methods to restrict this kind of degradation. However, it

should be remembered that the dye molecules are in the presence of relay species which can be I−/I3− (alternatively Br− /Br3−) or other amine in the electrolyte and these can also induce (or at least promote) the degradation of the dye. Since the DSSCs cannot be operated without these kinds of electrolyte media, more attention is needed on the dye degradation process[[46]. 4 The semiconductor Electrode The commonly used anode material is based on TiO2 (ZnO is also employed and a variety of other materials are also employed [47-58]) for the following reasons. (i) The energetics of the conduction band of TiO2 is well established and hence the appropriate dye could be employed so that the electron transfer from the excited state of the dye can be facilitated. This transfer probably restricts the recombination of the electron with the hole generated. (ii) Since this transfer has to take place between the dye and the semiconductor, the dye should be capable being adsorbed on the semiconductor and also the coverage (θ) by the dye on the semiconductor should be almost near to 1, since otherwise, the photon will be absorbed or scattered (loss) by the semiconductor. (iii) The semiconductor employed must be amenable for surface modification so that the dye molecule can be easily anchored on the surface and also the excitation energy (the difference between HOMO and LUMO levels of the dye) can be suitably modulated so that the absorption range can be extended to visible and even to IR region of the solar spectrum.[59] 15 5 Electrolyte The electrolyte and the medium to be used in DSSC generally control the potential of the positive electrode. In any form of electrochemical cells, the electrolyte has a significant role in the electron transfer since the medium permits the diffusion of the redox species forth and back to the counter electrode. Generally,high conversion efficiencies are reported in DSSCs in which electrolyte is an acetonitrile solution of iodine ions (I−/I− 3). The physical properties of the organic medium in this case acetonitrile (like melting/boiling point and the decomposition potential) control the concentration (due to evaporation at higher temperatures or decomposition due to potential) and hence causes drop of conversion efficiency at higher temperatures or with long-term use. Alternate methodologies have also been tried like sealing the electrolyte (that controls the evaporation loss) solidification of the electrolyte or

employing solid electrolytes like CuI or CUSCN, Conductive polymers like polypyrrole , low molecular weight materials like triphenyldiamine or amorphous organic compounds. At this moment, the selection of electrolyte does not seem to attract much attention though there are sporadic reports on the use of alternate electrolyte medium. 6 Counter electrode The counter electrode acts as the conduit for the return of the electron to the dye. Since the electrolyte can be corrosive, it is essential that the material of the counter electrode is fairly corrosion resistant, and is also capable of reducing tri-iodide to iodide ion. The appropriate material can be conductive glass electrode having a dispersion of Pt. However carbon electrodes and conductive polymers can also be the alternate choices. However, these materials cannot come up to Pt in terms of the reduction rate. 7 Packaging of the DSSCs It is known that this technology is threatening to be commercially viable for a number of years in recent times. This means a neat packaging of this technology must be in place if this technology were to be adopted for energy conversion process. Since packaging may lead to efficiency loss, it is necessary to encapsulate DSSC appropriately like in optical nanofibers [60,61] Various single cell configurations for long term stability and also for grid connection possibilities are being examined with plastic substrate [62,63] 16 8 Possible Routes for Electron Transfer in DSSC The values of rate constants of for electron transport in DSSC have already been considered in an earlier section. It is essential that one considers the dynamics of this transport both from the points of view of electron transport feasibility and also the flexibility. This section addresses these aspects in some detail. A pictorial representation of the various possible processes for the electron excitation, de-excitation, electron injection, transport, recombination, and utilization in regeneration is given in Fig.3. The photon is absorbed by the dye and the electron is excited from the HOMO level of the dye to the LUMO level of the dye. The excited electron from the LUMO level of the dye is injected into the conduction band of the semiconductor. This injection rate constant is assumed to be of the order of $5 \times 1013s^{-1}$ for perylene derivatives [64] and it is of the order of $4 \times 1014s^{-1}$ for Ru complexes. It is also assumed that the injection rate of the electrons from the sensitizer to the semiconductor is of the same order of magnitude in

both electrolyte and solid state solar cells. However it should be remarked that the transfer rate may depend on the density of states in the conduction band of the semiconductor and also the symmetry of the wave functions that constitute the electronic states in the conduction band of the semiconductor. The excitation in the dye takes place in femto-second time scale while the charge injection from the excited state dye D∗ to the conduction band of the semiconductor (typically in TiO2 (CB) takes place in sub-pico second time scale. This statement of the time scales is based on the assumption that the excited state dye does not undergo intra-molecular relaxation which not only can alter the time scale of electron injection but also may complicate the injection process itself. The electrons in the semiconductor can be thermalized by lattice collisions and phonon emissions in the time scale of femto-seconds. If the relaxation of the excited state dye takes place in the time scale of nanoseconds, then the efficiency of electron injection process in the semiconductor can become nearly unity. In this case, the excited state dye has to be regenerated by the iodide ions from the mediator. This process will be in the domain of microsecond. This regeneration may prevent the recombination of the electron from conduction band of the semiconductor with the HOMO level of the dye which could be in the range of mill-second time scale. This favourable time scales facilitate the electron percolation and the capture of the electron by the oxidized relay namely I−/I3 − which takes place in millisecond or higher time scales. The processes that take place in a DSSC are given in the form of equations below: D/T iO2 + hν → D ∗ /T iO2(Excitation of the Dye) (1) D ∗ /T iO2 → D +/T iO2 + e(CB T iO2)(Charge injection into SC) (2) D ∗ /T iO2 → D/T iO2 + hν + Δ(Relaxation) (3) D +/T iO2 + 2I − → D/T iO2 + I2(Regeneration of the dye) (4) D +/T iO2 + 3 2 I − → ‘D/T iO2 + 1 2 I − 3 (5) D + /T iO2 + e(CB) → D/T iO2(Recombination) (6) 1 2 I − 3 + e − → ‘ 3 2 I −; I − 3 + 2e → 3I −Cathode reactions (7) It may be appropriate if some general remarks are made on the statements made in this section (i) The electron transfer routes outlined in equations (1-6) are only indicative of the various possibilities. It should not be considered exhaustive since the possibilities like the trapping of the electrons in defect or surface states of the semiconductor, and other possible electron transfers with impurities and

other species present in the system are not considered and they can also contribute for the loss of efficiency

(v) (ii) The life times that are given are indicative and they may not be exact. In addition the life times given are for pure species namely the time indicated for the excitation in the dye is when the dye is in the isolated state while in the experiments the dye will be in the adsorbed on the semiconductor and hence the time required for excitation can be different. This could be due to the fact that in the adsorbed state, the molecular structure of the dye molecule might have changed depending on how and with what functionalities the dye molecule is adsorbed on the semiconductor. Similar arguments may hold good for the mediator species as well. (iii) Even though the reactions are shown in a sequence, the process can take place in a competitive and also concurrent manner thus accounting for the loss in efficiency. (iv) The other parameters on which the rate of electron injection depends include the length of the spacer between the electron donor and acceptor, the density of acceptor states in the semiconductor, the interaction between the dye and the semiconductor (already mentioned).The total electron transfer rate is related to the density of states (DOS) at the appropriate energy relative to the bottom of the conduction band edge of the semiconductor, the reorganization energy and the temperature T. The electron injection in the semiconductor depends on the magnitude of DOS in the semiconductor in the conduction band. When the dye is adsorbed on the semiconductor (most probably through functional groups (like carboxyl groups in the dye) the electron transfer essentially takes place between the * orbital of the sensitizer dye and the conduction band energy levels (which is essentially the unoccupied d states of the transition metal in the semiconductor for example Ti d states). Since the density of states in the conduction band of the semiconductor can be large (of the order of Avogadro number) the electron injection into the semiconductor takes place at a higher rate compared to the relaxation from the excited state to the ground state (that is relaxation through emission). It may be realized that this electron injection is the key for the higher efficiency and hence the choice of the semiconductor and the dye should be such that the energetic positions of the conduction band of the semiconductor and the energy of the excited state are appropriately matched. (v) The

injected electron is transported through the semiconductor to the back contact and this could be slower in the nano-crystalline semiconductor as compared to single crystal dye sensitized semiconductor

(vi) (vi) The recombination of the electron with the excited state of the dye can occur over a time period of picoseconds to millisecond. This wide time scale arises due to the charge trapping possibilities by the localized surface states in the semiconductor. In addition the photon field may alter the energy states of the semiconductor (thus altering the position of the quasi Fermi level) and thus may favour the occupancy of the trap states. (vii) The electron transport can also be controlled by the composition of the electrolyte employed and also the applied potential. (viii) The recombination is also dependent on the nature and structure of the dye employed. In the operation of DSSC, the regeneration of the dye is an important step. The life time of the cationic form of the dye can be of the order of milliseconds in the presence of pure solvents and can be altered by the nature of the electrolyte. The most widely employed redox system is I^-/I_3^- . The regeneration of the dye depends on the concentration of iodide ions. The relative energetic positions of the mediator and dye decide the open circuit potential achievable. Till now I^-/I_3^- redox system is the best electrolyte for DSSC. Efficiency of more than 11% with acetonitrile based electrolyte and 8% and long term stability with other low volatile electrolyte have been reported.[65-68].Other ionic liquids with fairly ionic conductivity have also been examined like pure imidazolium I^-/I_3^- [69 -73]. Quasi solid electrolytes by gelation with aliphatic gels, polymer and even nano particles have also been examined for DSSC application.[74-78]. Other redox couple that has also been tried is Br^-/Br_3^- [79]. In addition hole conductors like CuSCN, CuI, organic hole conductors like triarylamines, polymer hole conductors like poly(3-alkyl thiophene, polyaniline) have also been tried in DSSC.[80-88]. 9 Current Voltage Characteristics of DSSC The standard illumination on a DSSC is usually referred as AM 1.5 with an intensity of 1000 W/m2 also referred to as 1 sun. This spectrum corresponds to sunlight that passes through the atmosphere 1.5 times longer than when the sun is directly overhead. The current voltage characteristics of DSSCs are monitored under standard illumination conditions by varying the external load from zero

value (short circuit condition) to infinite load (open n circuit condition). A parameter called fill factor is defined as follows: F F = Jpowermax × Vpowermax/JSC × VOC (8)

(vii) The solar cell efficiency is given by the ratio of the power generated and power of the incident light η = Pout/Pin = (JSC × VOC × (F F)/Pin (9) Another parameter of relevance is the Incident Photon to Current Conversion Efficiency (IPCE) which denotes how efficiently the light of a particular wavelength is converted into current and is given by the expression IP CE = h × c/λ×JSCmA/cm2 /q)/PinmW/cm2 = 1240JSCmA/cm2 /λnm.PinmW/cm2 (10) The parameter Absorbed Photon to current conversion efficiency (APCE) denotes how efficiently the absorbed photons are converted into current, the IPCE and APCE are related to each other through light harvesting efficiency (LHE), Transmittance (T) and Absorbance (A) according to the following equation AP CE(%) = [IP CE(%)/LHE(%)] × 100LHE = 1 − T andT = 1 − 10−A (11) IPCE itself can be expressed as IP CE(%) = LHE × Φinj × ηreg × ηcc (12) Where (Φinj),(ηreg), and(ηcc) denote the quantum yield of charge injection,

(viii) dye regeneration and charge collection efficiency respectively. The efficiency of a DSSC can also be examined from another point of view. Essentially the efficiency of DSSC depends on how many photons are converted and collected in the external circuit in the form of electrical power. This conversion efficiency (IPCE)(λ)(incident photon to current efficiency) depends on three factors namely, the light harvesting efficiency (LHE) which denotes the number of photons absorbed by the dye, the electron injection efficiency (Φinj) which is a measure of how many absorbed photons result in injection of electrons into the semiconductor, (this probably accounts for the return of the excited of the dye to the ground state) and charge collection efficiency η(c) (probably accounts for the loss in the semiconductor itself without transfer to the external circuit). IP CE(λ) = LHE(λ) × Φinj × ηc (13) All of three processes in the DSSC are kinetic in nature and hence their efficiency is determined by how fast they occur relative to competing processes like de-excitation of the dye, electron loss in the semiconductor and processes internal to the system. One has to therefore consider the essential characteristics of the dye since the

photon to electron conversion critically depends how best the dye absorbs the photon.

(ix) 10 Dye Characteristics In this section, the important characteristics of the dye will be considered in addition to what has already been discussed in the section on sensitizers. The light harvesting dye is clearly the crucial and central component of the DSSC design. These dyes need to fulfill several functions: adsorption onto metal or semiconductor surface, its absorption spectrum must overlap effectively with the solar spectrum, the dyes should be capable of injecting electrons efficiently into metal oxide and must be stable for many cycles. These aspects have been already outlined. Adsorption of the dye onto the metal oxide surface is normally facilitated by inclusion of a functional substituent that will adsorb readily. In the case of metal complexes like ruthenium species, ligands which have capacity to bind to the metal ions, are preferred, the well studied ligands are those containing carboxyl-substituted ligands. The possibility of adsorbing the ruthenium complex on TiO2 surface is shown pictorially in Fig 5. It is given as an example for the process of adsorption and one can visualize alternate modes of adsorption of the dye on the semiconductor surface. In the table given in the appendix to this chapter the typical listing of some of the sensitizing species so far employed and their structures are given. It may be conceived that these species will be adsorbed on the semiconductor surface (TiO2, or ZnO or any other semiconductors) through the functional groups contained in them. The spectral absorption of the dye or adsorbed sensitizer should be such that it overlaps with the solar spectrum so that as much of the suns energy as possible is utilized in exciting the sensitizer. Most of the dyes or sensitizers normally employed in DSSCs absorb in the visible and near infrared region (in the region 400 to 700 nm), capturing about half the available power and a third of the available photons from the solar radi23 ation. The ruthenium complexes which are currently employed as sensitizers have a limitation in that their extinction coefficients (approxmately $2\times104\ M^{-1}\ cm^{-1}$) are comparatively low. This means that one must have sufficient number of sensitizers adsorbed on the semiconductor surface thus necessitating the metal oxide semiconductors have to be prepared with very high surface areas. It is

expected that normally efficiencies of greater than 15% is preferable, the designed DSSCs will have to absorb about 80% of light between 350 to 900 nm. In order to extend the spectral region, complexes of osmium has been examined in place of ruthenium, which extended the absorption further into the low energy red region and enhanced the response of the cell to light relative to the ruthenium analogues. The charge transfer transitions in osmium are more intense than in ruthenium complexes. Organic dyes have also been used successfully as seen from the data given in the table in the appendix. For facile electron transfer from the excited state of the dye to the semiconductor, it is necessary that the energy of the excited state of the dye is suitable with respect to the bottom of the conduction band of the semiconductor so that energetically the electron transfer process will be a downhill process in addition the electron injection process into the semiconductor must be faster than the relaxation process in the excited state of the dye by luminescence or non-radiative decay. It has been pointed out elsewhere in this presentation the relative time scale of each of these processes. In the case of ruthenium species, the injection takes place in the time scale of femto second while the decay process is taking place leisurely in the sub-picosecond time scale. However as pointed out earlier, it is necessary to assess if these time scales determined in the molecular scale will be applicable to the adsorbed state.[89] .Nevertheless, the very fact that fairly efficient DSSCs are available supports these contentions , it is necessary that caution is required in ensuring that efficiency of the DSSCs is not reduced by other design factors of the cell. One way of ensuring that the dye or sensitizer absorbs sufficiently in the red region, one has to lower the LUMO level of the dye or sensitizer, but this option has to be carefully considered since this lowering cannot be done in such way that the LUMO is lower than the conduction band of the semiconductor and also the position of LUMO level should be such that facile electron injection will take place without considerable activation barrier. In a recent publication, the group from Stanford has coupled luminescent choromophores which absorb high energy photons and pass their energy to the sensitizing dyes. These options possibly can show some improvement in the net efficiency. [43].

11 Semiconductor Material After the successful injection of the electron into the semiconductor, the electron should be transported in the external circuit through the load to the working electrode. Semiconductors like TiO2 or ZnO are the common material employed in DSSCs. The normal criterion for the choice of the type of semiconducting material is that they must be relatively inert, cheap, and must be amenable for flexible and scalable synthesis with high surface area. The factors that contribute to the choice of anatase form of TiO2 as the choice of the semiconductor are: (i) Anatase has a higher band gap (3.2 eV) as compared to rutile (3.0 eV). Hence the anatase phase absorbs limited range of the solar spectrum and the remaining region is available for absorption by the sensitizer. (ii) The recombination of the electron with the hole in the valence band is slower than it has been observed with Rutile form. It must be remarked that the multilayer semiconductors with varying nm sized particles have been advocated as best materials from the point of view increasing the exposed surface area which could sustain considerable layers of the sensitizer molecules so that improved photon absorption condition could be ensured. The time taken for the electron to percolate through the external circuit to the transparent conducing electrode is of the order of 100s of microseconds. Even though this time scale is longer, it is lower than the conduction band dye recombination or other conduction band decay process within the semi conductor. In order to effectively transfer the electron in the external circuit it will be advantageous to employ one dimensional nano tubes or nano rods rather than bulk materials. These configurations can be expected to facilitate vectorial transfer of charge [90]. . This aspect may be addressed in the future [90] 12 Electrolyte and Regeneration The electrolyte contains the redox couple, which regenerates the oxidized dye D+ which was formed by the injection of electron from the dye to the semiconductor layer. The redox couple should be efficient enough at reducing the dye cation (D+) back to the original state for another cycle, but should not intercept or capture the electrons being injected. The most commonly employed redox couple for this electron transfer is tri-iodide/iodide (I^-_3 /I^-) system for the transfer of electron from the conduction band of the semiconductor to the oxidized form of the dye or sensitizer. Even though the time scales

of this electron transfer process in the tri-iodide/iodide couple may be favourable for the DSSC application, the redox chemistry of tri-iodide/iodide 25 couple is not very well understood even now. This places some restrictions in the selection of appropriate dyes as sensitizers. One of the alternate possibilities may be to use solid state redox couples. This may allow the use of higher concentrations of the redox couple and possibly can extend the applicability of the device. 13 Summary Dye-sensitized solar cells is receiving considerable attention in recent times and threatening to be one of the possibilities for alternative renewable energy provider. The principle of operation is to harvest light efficiently by a sensitizer and pass on the energy to a semiconductor surface, which connects to an external circuit generating current. The light harvesting dye is regenerated by mean of a suitable redox couple. It appears that each of the process steps in DSSC like the electron excitation, electron injection into the semiconductor, electron transport in the external circuit, the redox species that facilitates the back transfer of the electron to the sensitizer, and the times scales for each of these processes can offer a wide variety of options and examining them and making an appropriate combination appears to be the job on hand in this exciting area.section

14 References

1.Frank E. Osterloh, Chem. Mater., 2008, 20 (1), 35-54.

2. http://en.wikipedia.org/wiki/Dye-sensitized solar cell

3. Michael Grtzel, ”Photoelectrochemical Cells”, Nature, Vol 414, 15 November 2001.

4.Michael Grtzel, ”Solar Energy Conversion By Dye-Sensitized Photovoltaic Cells”, Inorganic Chemistry, 2005, vol 44, issue 20 6841-6851.

5. Jiu Kawakita, Trends of research and development of Dye-sensitized solar cells, Science and technology Trends, original Japanese version was published in 2009 see also http://www.nistep.go.jp/achiev/ftx/eng/stfc/stt035e/qr35pdf/STTqr3505.pdf

6. N.Sekar and Visal Y Gehlot, Metqal complex dyes for dye sensitized solar cells: Recent Developments, Resonance, 819-831 (2010).

7. Gratzel, M (2003). ”Dye-sensitized solar cells”, Journal of Photochemistry and Photobiology C: Photochemistry Reviews 4: 145. doi:10.1016/S1389-5567(03)00026-1. http://photochemistry. epfl.ch /EDEY/DSC review.pdf.
8. Brian O’Regan, Michael Grtzel (24 October 1991). ”A low-cost, highefficiency solar cell based on dye-sensitized colloidal TiO2 films”. Nature 353 (6346): 737740. doi:10.1038/353737a0
9. 9. M. K. Nazeeruddin, A. Kay, I. Rodicio, et al., Conversion of light to electricity by cis-Xbis(2,2-bipyridyl-4,4-dicarboxylate)ruthenium(II) chargetransfer sensitizers (X=Cl, Br, I, CN, and SCN) on nanocrystalline TiO2 electrodes, Journal of the American Chemical Society, vol. 115, no. 14, pp. 63826390, 1993.
10. G. Sauv, M. E. Cass, G. Coia, et al., Dye sensitization of nanocrystalline titanium dioxide with osmium and ruthenium polypyridyl complexes, Journal of Physical Chemistry B, vol. 104, no. 29, pp. 68216836, 2000.
11. Tamotsu Horiuchi, Hidetoshi Miura and Satoshi Uchida, Highly efficient metal-free organic dyes for dye-sensitized solar cells, Journal of Photochemistry and Photobiology A: Chemistry, 164,29, (2004).
12. A. Kay and M. Graetzel, Artificial photosynthesis. 1. Photosensitization of TiO2 solar cells with chlorophyll derivatives and related natural porphyrins, The Journal of Physical Chemistry, vol. 97, no. 23, pp. 62726277, 1993.
13. F. Odobel, E. Blart, M. Lagre, et al., Porphyrin dyes for TiO2 sensitization, Journal of Materials Chemistry, vol. 13, no. 3, pp. 502510, 2003.
14. M. K. Nazeeruddin, R. Humphry-Baker, M. Grtzel, et al., Efficient near IR sensitization of nanocrystalline TiO2 films by zinc and aluminum phthalocyanines, Journal of Porphyrins and Phthalocyanines, vol. 3, no. 3, pp. 230237, 1999. \
15. J. He, A. Hagfeldt, S. E. Lindquist, et al., Phthalocyanine-sensitized nanostructured TiO2 electrodes prepared by a novel anchoring method, Langmuir, vol. 17, no. 9, pp. 27432747, 2001.
16. W. Paw, S. D. Cummings, M. A. Mansour, W. B. Connick, D. K. Geiger, and R. Eisenberg, Luminescent platinum complexes: tuning and

using the excited state, Coordination Chemistry Reviews, vol. 171, no. 1, pp. 125150, 1998.
17. A. Islam, H. Sugihara, K. Hara, et al., Dye sensitization of nanocrystalline titanium dioxide with square planar platinum(II) diimine dithiolate complexes, Inorganic Chemistry, vol. 40, no. 21, pp. 53715380, 2001.
18. .J. M. Rehm, G. L. McLendon, Y. Nagasawa, K. Yoshihara, J. Moser, and M. Grtzel, Femtosecond electron-transfer dynamics at a sensitizing dyesemiconductor (TiO2) interface, Journal of Physical Chemistry, vol. 100, no. 23, pp. 95779578, 1996.
19. .P. V. Kamat and W. E. Ford, Photochemistry on surfaces: triplet-triplet energy transfer on colloidal TiO2 particles, Chemical Physics Letters, vol. 135, no. 4-5, pp. 421426, 1987. 30
20. S. Das, C. S. Rajesh, C. H. Suresh, et al., Photophysical and photoelectrochemical behavior of poly[styrene-co-3-(acrylamido)-6-aminoacridine], Macromolecules, vol. 28, no. 12, pp. 42494254, 1995.
21. .D. Liu and P. V. Kamat, Photo-electrochemical behavior of thin CdSe and coupled TiO2/CdSe semiconductor films, Journal of Physical Chemistry, vol. 97, no. 41, pp. 1076910773, 1993.
22. .K.T. Ranjit and B.Viswanathan, Photocatalysis, Principles and some selected results,in Selected Studies in Heterogeneous Catalysis, Editor: B. Viswanathan, Department of Chemistry, Indian Institute of Technology, Madras (Chennai), India, pp 150-178, May, 1996.
23. Cherepy, Nerine J.; Smestad, Greg P.; Grtzel, Michael; Zhang, Jin Z. (1997). ”Ultrafast Electron Injection: Implications for a Photoelectrochemical Cell Utilizing an Anthocyanin Dye-Sensitized TiO2 Nanocrystalline Electrode”. The Journal of Physical Chemistry B 101 (45): 934251. doi:10.1021/jp972197w. http://solideas.com/papers/JPhysChem B.pdf.
24. .Sancun Hao, Jihuai Wu, , Yunfang Huang and Jianming Lin, Natural dyes as photosensitizers for dye-sensitized solar cell, Solar energy, 80, 209, (2006) ; M.S. Roy, P. Balraju, Manish Kumar and G.D. Sharma, Dye-sensitized solar cell based on Rose Bengal dye and nanocrystalline TiO2, Solar Energy Materials and Solar Cells 92, 909 (2008)

25. .PORPHYRIN-BASED PHOTOSENSITIZER DYES FOR DYE-SENSITIZED SOLAR CELLS, United States Patent Application 20100125136
26..http://en.wikipedia.org/wiki/Dye-sensitized solar cell
27. Y-Z Zheng, X.Tao, Q.Hou, D T Wang, W L Zhou and J F Chen, Iodine doped Zno nanocrystalline aggregates for improved dye-sensitized solar cells, Chem.Mater., 23, 3 (2011)
28.
29. Tamotsu HoriuchiJun-ichi FujisawaSatoshi UchidaMichael Gratzel, Data book on Dye-sensitized Solar Cells, CMC Publishing CO.,LTD (2008).
30. Patrocnio, A., Mizoguchi, S., Paterno, L., Garcia, C., and Iha, N. (2009). Efficient and low cost devices for solar energy conversion: Efficiency and stability of some natural-dye-sensitized solar cells. Synthetic Metals, 159(21/22), 2342-2344. doi:10.1016/j.synthmet.2009.08.027
31. .http://www.elp.uji.es/juan home/research/solar cells.htm 32.Horiuchi, T., Miura, H.,and Uchida, S. (2004). Highly efficient metal-free organic dyes for dye-sensitized solar cells. Journal of Photochemistry and Photobiology A: Chemistry, 164(1-3), 29-32.
32.
33. Chen P, Yum JH, De Angelis F, Mosconi E, Fantacci S, Moon S J, Baker RH, Ko J, Nazeeruddin M , Grtzel M. Nano let., 2009 Jun;9(6):2487-92.
34. A. Nattestad, A. J. Mozer, M. K. R. Fischer, Y.-B. Cheng, A. Mishra, P. Buerle and U. Bach, Nature Materials, 9, 31 (2010)
35. Sommeling, P., Spth, M., Smit, H., Bakker, N., and Kroon, J. (2004). 31 Long-term stability testing of dye-sensitized solar cells. Journal of Photochemistry and Photobiology A: Chemistry, 164(1-3), 137-144. doi:10.1016/j.jphotochem.2003.12.017
36. Nogueira, V., Longo, C., Nogueira, A., Soto-Oviedo, M., and Paoli, M. (2006). Solid-state dye-sensitized solar cell: Improved performance and stability using a plasticized polymer electrolyte. Journal of Photochemistry and Photobiology A: Chemistry, 181(2/3), 226-232. doi:10.1016/j.jphotochem.2005.11.028

37. T.Horiuchi, H.Miura, and S.Uchida, Highly efficient metal free organic dyes for dye-sensitized solar cells, Journal of photochemistry and photobiology, A Chemistry, 164, (2004) 29-32.
38. T.Horiuchi, H.Miura, K.Sumioka and S.Uchida, High eficency of dye sensitized solar cells on metal-free indoline dyes J.Am.Chem.Soc., 126 (2004) 12218.
39. C.Teng, X.Yang, C.Yuan, C.Li, R.Chen, H.Tian, S.Li, A.Hagfeldt and L.Sun, Two novel carbazole dyes for dye-sensitized solar cells with open circuit voltagtes upto to 1 V based on Br-/Br3- electrolytes, Organic Letters, 11 (2009),5542. 40. F.O. Lenzmann and J.M.Kroon, Recent advances in Dye sensitized solar cells, Advances in optoelectronics, (2007) Article ID 65073 DOI:1155/2007/76507
40.
41. Tannia Marinado, Ph D Thesis, Photoelectrochemical studies of dyesensitized solar cells using organic dyes, School of chemical Science and Engineering, Kungliga Tekniska Hogskolar, Stockholm, (2009)
42. M.Sokolsky and J Cirak, Dye-Sensitized solar cells: Materials and processes, Acta Electrochimca et informatica 10, (2010)78.
43. K.Hara, T.Sato, R.Katoh, A.Furube, T.Yoshihara, M.Murai, M.Kurashige, S.Ito, A.Shinpo, S.Suga and H.Arakawa, Novel conjugated organic dyes for efficient Dye-sensitized solar cells, Advanced functional Materials,15 (2005) 246 and references cited therein.
44. B.E.Hardin, E.T.Hoke, P.B.Armstrong, J-Hyum, P.Comte, T.Torres, J.M.J.Frechet, M.K.Nazeeruddin, M.Gratzel and M D McGehee, Increased light harvesting in dye-sensitized solar cells with energy relay dyes, Nature Photoniccs 3, (2009)406.
45. Nogueira, V., Longo, C., Nogueira, A., Soto-Oviedo, M., and Paoli, M. (2006). Solid-state dye-sensitized solar cell: Improved performance and stability using a plasticized polymer electrolyte. Journal of Photochemistry and Photobiology A: Chemistry, 181(2/3), 226-232. doi: 10.1016/j.jphotochem.2005.11.028
46. B.N.Wong and J G Cordaro, Coumarin dyes for Dye-sensitized solar cells A long range corrected density functional study.

47. H Tananka et al,, Solar energy Materials and Solar cells, 93, 1143 (2009)
48. He, J. J., Lindstrom, H., Hagfeldt, A. and Lindquist, S. E. Dye-sensitized nano-structured p-type nickel oxide film as a photocathode for a solar cell J. Phys. Chem. B 103, 8940-8943 (1999).
49. Borgstrom, M. et al. Sensitized hole injection of phosphorus porphyrin into NiO: Toward new photovoltaic devices. J. Phys. Chem. B 109, 22928- 22934 (2005).
50. He, J. J., Lindstrom, H., Hagfeldt, A. and Lindquist, S. E. Dye-sensitized nanostructured tandem cell-first demonstrated cell with a dye-sensitized photocathode. Sol. Energy Mater. Sol. Cells 62, 265-273 (2000).
51. Mizoguchi, Y.and Fujihara, S. Fabrication and dye-sensitized solar cell performance of nanostructured NiO/Coumarin 343 photocathodes. Electrochem. Solid State Lett. 11, K78-K80 (2008).
52. Morandeira, A., Boschloo, G., Hagfeldt, A. and Hammarstrom, L. Photoinduced ultrafast dynamics of coumarin 343 sensitized p-type-nanostructured NiO films. J. Phys. Chem. B 109, 19403-19410 (2005).
53. Morandeira, A. et al. Improved photon-to-current conversion efficiency with a nanoporous p-type NiO electrode by the use of a sensitizer-acceptor dyad. J. Phys. Chem. C 112, 1721-1728 (2008).
54. Mori, S. et al. Charge-transfer processes in dye-sensitized NiO solar cells. J. Phys. Chem. C 112, 16134-16139 (2008).
55. Qin, P. et al. Design of an organic chromophore for p-type dye-sensitized solar cells. J. Am. Chem. Soc. 130, 8570-8572 (2008).
56. Vera, F. et al. Preparation and characterization of Eosin B- and Erythrosin J-sensitized nanostructured NiO thin film photocathodes. Thin Solid Films 490, 182-188 (2005).
57. Zhu, H., Hagfeldt, A. and Boschloo, G. Photoelectrochemistry of mesoporous NiO electrodes in iodide/triiodide electrolytes. J. Phys. Chem. C 111, 17455-17458 (2007).
58. Nattestad, A., Ferguson, M., Kerr, R., Cheng, Y.-B. and Bach, U. Dyesensitized nickel(II) oxide photocathodes for tandem solar cell applications. Nanotechnology 19, 295304-295313 (2008).
59. Nakasa, A. et al. A high voltage dye-sensitized solar cell using a nanoporous NiO photocathode. Chem. Lett. 34, 500-501 (2005).

60. H. Burcksummer et al, Organic letters, 12, 3666(2010)
61. Bourzac, Katherine (2009-10-30). ”Wrapping Solar Cells around an Optical Fiber”. Technology Review. http://www.technologyreview.com/energy/23829/. Retrieved 2009-10-31.
62. Benjamin Weintraub, Yaguang Wei, Zhong Lin Wang (2009-10-22). ”Optical Fiber Nanowire Hybrid Structures for Efficient Three-Dimensional DyeSensitized Solar Cells”. Angewandte Chemie International Edition 48 (47): NA. doi:10.1002/anie.200904492. PMID 19852015
63. http://innovation.nikkeibp.co.jp/etb/20080228-00.html; and also large scale module for direct outdoor se[http://www.fujikura.co.jp/rd/field/mt.html.
64. Chrubin, Noumissing Sao, Dye-sensitized solar cells based on perylene 33 derivatives, Dissertation, for the Degree Doctor of Natural Sciences, Universitt Kassel (2009).
65..P. Wang, C. Klein, R. Humphry-Baker, S. M. Zakeeruddin, M. Grtzel, J. Am. Chem. Soc. 2005, 127, 808
66. M. Grtzel, J. Photochem. Photobiol. A 2004, 164, 3.
67. P. Wang, C. Klein, R. Humphry-Baker, S. M. Zakeeruddin, M. Grtzel, Appl. Phys. Letts. 2005, 86, 123508
68. D. Kuang, C. Klein, S. Ito, J. E. Moser, R. Humphry-Baker, S. M. Zakeeruddin, M. Grtzel, Adv. Func. Mater. 2007, 17, 154.
69. P. Wasserscheid, T. Welton, Ionic Liquids in Synthesis; Wiley: Weinheim, Germany, 2002.
70. R. D. Dogers, K. R. Seddon, Science 2003, 302, 792.
71. J. Dupont, R. F. de Souza, P. A. Z. Suarez, Chem. Rev. 2002, 102, 3667.
72. W. Xu, C. A. Angell, Science 2003, 302, 422.
73. D. B. Kuang, P. Wang, S. Ito, S. M. Zakeeruddin, M. Grtzel, J. Am. Chem. Soc. 2006, 128, 7732.
74. W. Kubo, K. Murakoshi, T. Kitamura, Y. Wada, K. Hanabusa, H. Shirai, S. Yanagida, Chem. Lett. 1998, 27, 1241.
75. W. Kubo, S. Kambe, S. Nakade, Kitamura, T. K. Hanabusa, Y. Wada, S. Yanagida J.Phys. Chem. B 2003, 107, 4374.

76. P. Wang, S. M. Zakeeruddin, I. Exnar, M. Grtzel, Chem. Commun. 2002, 2972.
77. F. Cao, G. Oskam, P. C. Searson, J. Phys. Chem. 1995, 99, 17071.
78. P. Wang, S. M. Zakeeruddin, P. Comte, I. Exnar, M. Grtzel, J. Am. Chem. Soc. 2003, 125, 1166.
79. J. Desilvestro, M. Grtzel, L. Kaven, J. Moser, J. Am. Chem. Soc. 1985, 107, 2988.
80. B. ORegan, F. Lenzmann, J. Phys. Phys. Chem. B 2004, 108, 4342.
81. B. ORegan, F. Lenzmann, R. Muis, J. Wienke, Chem. Mater. 2002, 14, 5023.
82. B. ORegan, D. T. Schwartz, S. M. Zakeeruddin, M. Grtzel, Adv. Mater. 2000, 12, 1263.
83. T. Taguchi, X. T. Zhang, I. Sutanto, K. Tokuhiro, T. N. Rao, H. Watanabe, T. Nakamori, M. Uragami, A. Fujishima, Chem. Comm. 2003, 2480.
84. A. Konno, T. Kitagawa, H. Kida, G. R. A. Kumara, K. Tennakone, Curr. Appl. Phys. 2005, 5, 149.
85. G. R. A. Kumara, A. Konno, K. Shiratsuchi, J. Tsukahara, K. Tennakone, Chem. Mater. 2002, 14, 954.
86. H. Snaith, S. M. Zakeeruddin, Q. Wang, P. Pechy, M. Grtzel, Nano Lett. 2006, 6, 2000.
87. D. Gebeyehu, C. J. Brabec, N. S. Sariciftci, Thin Solid Film 2002, 403-34 404, 271.
88. S. Tan, J. Zhai, M. Wan, Q. Meng, Y. Li, L. Jiang, D. Zhu, J. Phys. Chem. B 2004, 14. 108, 18693.
89. ChunHung Law, Shehan C. Pathirana, Xaioe Li, Assaf Y. Anderson, Piers R. F. Barnes, Andrea Listorti, Tarek H. Ghaddar, Brian C. ORegan , Water-Based Electrolytes for Dye-Sensitized Solar Cells, Advanced Materials, 22, (2010), pages 45054509; Koops SE, O'Regan BC, Barnes PR, Durrant JR., Parameters influencing the efficiency of electron injection in dye-sensitized solar cells., J. Am. Chem. Soc., 2009, 131, 4808).
90. Pagliaro, http://photochemistry.wordpress.com/2009/08/17/dye-sensitisedsolar-cells-dssc/ ; Nanochemistry aspects of titania in dye-sensitized solar cells, Pagliaro, M., Palmisano, G., Ciriminna, R. and Loddo, V., Energy Environ. Sci., 2009, 2, 838 844. Advancing beyond

current generation dye-sensitized solar cells, Hamann, T.W., Jensen, R. A., Martinson, A. B. F., Van Ryswyk, H and Hupp, J. T., Energy Environ. Sci., 2008, 1, 66-78.

CHAPTER
PLASMONIC PHOTOCATALYSIS

introduction

Plasmonic photocatalysis is one of the recent additions to the field of photocatalysis. This field has been shown to be giving rise to efficient and new catalytic materials for the photo-decomposition of water, pollutants removal and photoreduction of CO2 into valuable fuels [1]. The formation of Localized Surface Plasmon Resonance (LSPR), energy transfer, and surface reaction are the significant steps in this process. LSPR plays an essential role in the performance of plasmonic photocatalysts as it promotes excellent, light absorption over a broad wavelength range while simultaneously facilitating an efficient energy transfer to semiconductors. The LSPR transfers energy to a

semiconductor through various mechanisms, which have both advantages and disadvantages. The four critical features for plasmonic photocatalyst design, are the nature of the plasmonic materials, size, shape of plasmonic nanoparticles (PNPs), and the contact between PNPs and semiconductor.

Plasmonic photocatalysis has come into focus as a very promising technology for high-performance photocatalysis. Many reviews have already appeared and some of them are given in references2-11. [2-11]. It involves dispersal of noble metal nanoparticles (mostly Au and Ag, in the sizes of tens to hundreds of nanometers) into semiconductor photocatalysts and obtain enhancement of photo-reactivity under the irradiation of UV and of visible light. The use of noble metal nanoparticles in contact with semiconductors brings many benefits to photocatalysis, the important ones are shown in Figure 1. Compared to the common semiconductor photocatalysis, plasmonic photocatalysis possesses mainly two distinct features—a Schottky junction and Localized s\Surface Plasmon Resonance (LSPR) and both of them cause benefits in photocatalysis differently. For instance, the Schottky junction results from the contact of the noble metal and the semiconductor. It builds up an internal electric field in a region (the space-charge region) inside the photocatalyst part but close to the metal/semiconductor interface. This would force the electrons and holes to move in different directions once they are created inside or near the Schottky junction. In addition, the metal part provides a fast lane for charge transfer and its surface acts as a charge-trap center to host more active sites for photoreactions. The Schottky junction and the fast-lane charge transfer work together to suppress the electron–hole recombination.

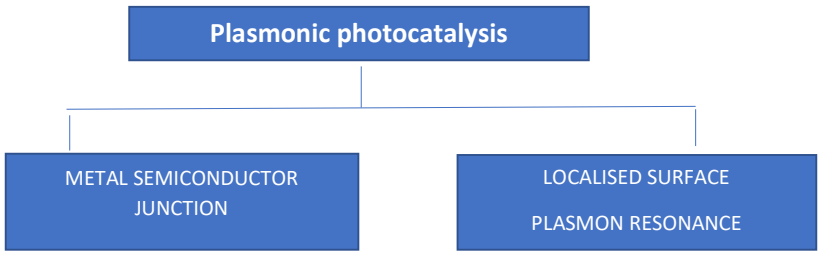

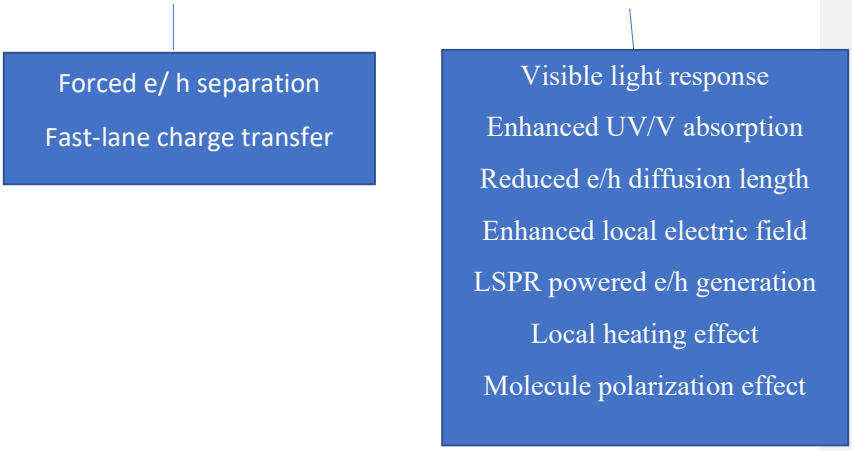

Figure 1 Some of the beneficial effects of Plasmonic Photocatalysis

Among the many novel photocatalytic systems developed in recent times, plasmonic photocatalytic composites possess great potential for use in applications and are one of the most intensively investigated photocatalytic systems owing to their high solar energy utilization efficiency. In these composites, the plasmonic nanoparticles (PNPs) efficiently absorb solar light through Localized Surface Plasmon Resonance (LSPR) and convert it into energetic electrons and holes in the nearby semiconductor. This energy transfer from PNPs to semiconductors plays a role in the overall photocatalytic performance. The enhancement in activity due to plasmonic photocatalysis arises due to reduced recombination rates of the generated electron-hole pairs. Some of the benefits arising due to plasmonic photocatalysis are given in Table 1

Table 1 some of the benefits of Plasmonic Photocatalysis

Schottky Junction type	Localized Surface Plasmon Resonance
Fast charge transfer Internal electric field	Enhanced solar light absorption Enhanced local electric field

	Heating effect

Data on plasmonic resonances for various types and shapes of nano particles are assembled in Table 2.

Table 2. Values of wavelength and energy range for plasmon resonances for nano-shapes (values are approximate and have only indicative)

Particle	Wavelength range in nm	Energy in eV
Silver nanoparticles	`400-520	3.2-2.4
Gold nanoparticles	`580-750	2.1-1.65
Nanosheets, Nanoeggs	~580-1050	2.1-1.2
Nano rods	~480-1050	2.6-1.2
Triangles	~580-1150	2.1-1.1
Cubes	~600-950	2.0-1.3
Nanorice	~550-1100	2.25-1.1

Noble metal/semiconductor systems for plasmonic photocatalysis

In majority of plasmonic photocatalysts, the noble metal nanoparticles serve as sensitizers mainly enabling the absorption of visible light by capitalizing on LSPR. Greater utilization of the solar spectrum is one of the advantages of plasmonic photocatalysts, which results in improved photocatalytic performance. It is now well known that the optical properties of plasmonic photocatalysts are altered by modulating the size, geometry and surrounding environment of noble metals nanoparticles. Some other effects that mediate photoactivity can also thought of but they are not considered.

Size Effect

The collective charge oscillations are limited by the size of noble metal nanostructures due to surface confinement [12]. Surface plasmons can be understood as coherent (in phase) oscillations of delocalized electrons in a metal particle which are excited by the electromagnetic

field of incident light at a metal-dielectric interface. In surface plasmon resonances (SPRs), metal nanostructures serve as antennas to convert light to localized electrical fields or as waveguides to direct light to desired locations with nanometer precision. Noble metals, especially Au and Ag, are intimately associated with plasmonic resonance as their strongly enhanced SPRs lie in or near the visible range of the spectrum. SPR can be divided into two modes based on the geometry of the metallic structure that facilitates them. The two modes are surface plasmon polaritons (SPPs) and localized surface plasmon resonances (LSPRs). If one dimension of a continuous metal nanostructure, such as nanowire is larger than the wavelength of incident light, SPPs can be excited on it by employing prism couplers or gratings. These plasmons usually propagate tens to hundreds of micrometers along the metal surface. LSPRs are created when the metal nanostructure is smaller than the electron mean free path as well as the wavelength of incoming light. The electron clouds in the conduction band of the metal oscillate collectively when driven by electric fields induced by incident light. If the oscillation is in resonance with the incoming light of a certain frequency, a strong oscillation of electrons will be observed. The frequency at which LSPR occurs is called the plasmon resonance frequency. This kind of non-propagating plasmon can be excited on metal nanoparticles and around nanoholes or nanowells in thin metal films. By modulating and designing the composition and geometry of plasmonic nanoparticles, LSPRs can be produced by incident light over the solar spectrum.

As the size of the nanostructure increases, charge separation is promoted. Thus, a lower frequency is required for the collective electron oscillation, which can be seen by the red-shift of the plasmonic peaks in the spectrally resolved absorption. By tailoring the size of the noble metal particles, the light response triggered by plasmon resonance can be varied from the visible to near-infrared region. After combining with a semiconductor, photocatalysts show a similar response.

For example, through modulating the size of Au nanostructures deposited onto TiO_2 nanowire arrays, the absorption of the

photocatalysts in the entire UV–Visible region from 300 to 800 nm can be effectively enhanced, resulting in an increased incident photon to-electron conversion efficiency (IPCE)

Geometry Effect

In addition to size, the geometry of plasmonic metal nanostructures exerts a non-trivial influence on plasmonic photocatalysts. During coherent electron oscillation, nanostructures with sharp corners facilitate charge separation more easily than rounded structures. This reduces the restoring force for the electron oscillation, leading to a longer resonance wavelength. Additionally, the low-symmetry nanostructures favor enhanced resonances as the asymmetry enables the electrons to be polarized in more than one way. Ag@c-Si core@shell nanocones have been designed for the enhancement of broad band solar absorption.. The metallic core assures strong near field enhancement, providing the increased absorption efficiency. The special nanocone-like structure contributes to a linear gradient through the radius of the c-Si shell. This leads to the production of multiple plasmon resonances and, consequently, enhances the light absorption.

Influence of Dielectric Environment

When LSPRs are produced, the incident photons are coupled into surface plasmons, which can be observed as peaks in the absorption spectrum. For plasmonic photocatalysts, one of the most interesting characteristics is the absorption wavelength caused by LSPR effect. The plasmon resonance frequency ω is inversely related to the square root of the dielectric constant of the surrounding medium. It is therefore to be remarked that the dielectric constant of the surrounding medium influences the LSPR wavelength.

It has been reported that Au nanoparticles (D = 50 nm) exhibit an LSPR peak at 543 nm. After combining Au with TiO_2 to yield Janus and core-shell nanoparticles, these heterojunction nanostructures demonstrated a red-shift in plasmonic peaks because the presence of a

high refractive index TiO_2 layer which leads to an increase in dielectric constant of the medium and thus a decrease in ω. The Au nanoparticle in the core@ shell structure was encapsulated by the TiO_2 shell, while half of the Au nanoparticle in the Janus structure was exposed to solution (i.e., isopropyl alcohol) and the other half to TiO_2. As TiO_2 possesses higher refractive index than the solution, the LSPR peak of core@shell nanoparticles occurred at a longer wavelength. For the metal@semiconductor core@shell nanostructure or thin semiconductor layer-deposited noble metals, the thickness of semiconductor should be carefully tuned as it greatly affects the LSPR properties of photocatalysts. Since the electromagnetic field will extend into the surrounding environment, the overall dielectric constant is dictated by both the semiconductor and the liquid or gas around the plasmonic photocatalyst if the semiconductor shell or layer is within the electromagnetic field.

Other Effects

Noble metal nanostructures (e.g., Au nanoparticles, $Ag@Ag_3(PO_4)_{1-x}$ core@shell nanoparticles,) were coupled to the surface of semiconductors (e.g., TiO_2 photonic crystals, ZnO nanorod arrays, dendritic TiO_2 nanorod arrays). The amount of deposited noble metal needs to be well controlled. A high coverage of noble metal on the semiconductor will reduce the light exposure of the semiconductor as well as hinder the reactant access of semiconductor. While low coverage will lead to poor light utilization efficiency during photocatalysis. Thus, an optimum coverage exists between these two degrees of coverage. The composition of plasmonic metals greatly affects the properties of photocatalysts as well. Lin et al. deposited $Ag@Ag_3(PO_4)_{1-x}$ core@shell nanoparticles on ZnO nanorod arrays to capitalize on visible light absorption introduced by Ag due to its plasmonic properties as well as $Ag_3(PO_4)_{1-x}$ due to its narrow band gap. This system ultimately achieved oxygen evolution in a nonsacrificial electrolyte. Ag is easily oxidized during the photocatalytic process and cannot be sustained for long periods. Therefore, Au is more commonly utilized. Semiconductor nanostructures can also affect the performance

of plasmonic photocatalysts. For better utilization of the LSPR property, photonic crystal structures can be employed. A photonic crystal is a periodic structure that possesses a photonic band gap, in which light will not pass through but instead be trapped. Au nanoparticles incorporated onto a bi-layer TiO_2 structure composed of a photonic crystal and nanorods. When the plasmon resonance frequency of the noble metal matches the photonic band gap of the semiconductor, the LSPR effect is markedly promoted. This leads to higher photoconversion (i.e., light-to-chemical energy) efficiency relative to other photocatalyst systems. In addition, some studies focused on raising the surface area of semiconductors to enhance the adsorption capability of photocatalysts. Three-dimensional hierarchical dendritic Au@TiO_2 nanorod arrays were synthesized with larger surface area. Compared to pure TiO_2 branched nanorod arrays, they exhibited improved charge separation and charge transfer effi ciency. In addition, the properties of semiconductors should also be considered. Some semiconductors have small band gaps, but suffer from short charge carrier diffusion lengths, which make them unsuitable for use as photocatalysts on their own. For example, hematite $Fe_2 O_3$ has a small band gap of 1.9 to 2.2 eV, depending on the fabrication method and crystalline status, which is desirable for the visible light absorption. [However, the short exciton diffusion length (several nanometers without bias and tens of nanometers with bias) leads to severe recombination of photo-induced electron-hole pairs in the bulk of hematite . Several strategies for solving this problem have been developed. First, other types of semiconductor with high carrier mobility can be intimately combined with Fe_2O_3 to improve the carrier transfer rate due to the strong internal electric field. The further incorporation of plasmonic metal nanostructures increases the generation of charge carriers close to the Au/Fe_2O_3 interface and shortens the charge carrier diffusion distance to the electrolyte thus enabling a higher photoactivity. The second strategy is to incorporate Fe_2O_3 nanorod arrays into patterned Au nanohole arrays or craft a thin

Fe_2O_3 layer onto Au nanopillars to utilize the SPP effect and further boost photocatalytic efficiency.

Perspectives

1. The visible and UV component of Solar radiation is `~ 52% while the infra -red component accounts for ~43%. It is always the desire to make maximum use of these radiations. In order to do this , the energy transfer process must be coupled with materials suitable for up-conversion. One approach to improve the up-conversion emission efficiency is to combine different host matrices with rare-earth atoms. Some other alternative efforts have been made to enhance the up-conversion emission through the hetero-integration of rare earth-element-doped up-conversion materials with metallic Au or Ag nano particles. In photocatalysis, commonly used up-conversion materials are lanthanide-doped materials sensitized by Yb^{3+} and other rare earth (eg. Er and Tm) ions. When up-conversion nanoparticles (UCNPs) are combined with metals, the spectroscopic properties of UCNPs are changed as a result of the local electrical field generated by SPR. However, simultaneously non-radiative relaxation as well as quenching by non-radiative energy transfer from the up-conversion materials to metal surface occurs. The competition between these processes governs the final degree of enhancement of up-conversion emission.
2. The surface Plasmon Coupled Emission (SPCE) is possible by frequency matching between localized plasmon resonance and the emission band of the up-conversion material. It is known that the nnno-material shape, size, dielectric constant of the influence the plasmon resonance frequency. Alterations of the local electric filed can also influence the plasmon resonance frequency and these can be achieved by suitable fabrication of the nanoparticle.
3. It is interesting to note that recently rare-earth-element doped upconversion materials have been utilized in photocatalysis. However, plasmon-mediated upconversion materials have rarely garnered attention from photocatalytic researchers. In this context, the main aim is to make use of the maximum amount of solar radiation.

4. Many multifunctional materials composed of noble metals and semiconductors can be crafted for plasmonic photocatalysis. First, a mixture of plasmonic photocatalysts containing complex plasmonic structures (i.e., plasmonic nanoparticles, nanorods and nanowires) can be rationally designed and synthesized. For the dimension of noble metal particles that is larger than the quasistatic limit, the red-shift of plasmonic peaks will occur due to the retardation effect when the particles become larger. Such plasmonic photocatalysts containing a mixture of noble metals is highly desirable as they enable broader light absorption by extending into the near-infrared region.
5. Plasmonic metal nanostructures with sharp geometries possess lower restoring force for the charge oscillation, the corresponding plasmonic peak shifts towards the longer wavelength. Therefore, photocatalytic materials with sharp geometry are favorable in photocatalysis.
6. Advances in alloyed noble metals have garnered attention due to their improved stability, chemical properties and tunable plasmonic resonances. The combination of semiconductors and alloyed plasmonic metals may provide a promising opportunity to create stable plasmon-mediated photo catalysts for long-term use.
7. The control over shape and size of the nanomaterials will open up another avenue for plasmon mediated catalysis. This could be achieved in many synthetic strategies.
8. The field of plamonic photocatalysis is still in its infancy stage and dedicated effort to the development of plasmonic photocatalysis can be expected in the near future.
9. The rapid advances in synthetic techniques, a greater diversity of materials with good size and shape control will become available.
10. It is notable that such synthetic techniques are useful for not only novel materials but also the rational and deliberate combination of existing well-characterized materials. Needless to state that rational design and fabrication of nano materials is necessary in this field. It can be hoped that the development of methodology for designing and synthesizing established materials are essential for the development of

the research field of plasmonic photocatalysis with improved performance.

References

[1] Nhu-Nang Vu, Serge Kaliaguine, and Trong-On Do, ChemSusChem 2020, 13, 1 – 26.
[2] S. N. Habisreutinger, L. Schmidt-Mende, J. K. Stolarczyk, Angew. Chem. Int. Ed. 2013, 52, 7372
[3] M. Wang, M. Ye, J. Iocozzia, C. Lin, Z. Lin, Adv. Sci. 2016, 3, 1600024; [4] X. Zhang, Y. L. Chen, R.-S. Liu, D. P. Tsai, Rep. Prog. Phys. 2013, 76, 046401
[5] S. Linic, P. Christopher, D. B. Ingram, Nat. Mater. 2011, 10, 911
[6] N. Serpone, A. V. Emeline, J. Phys. Chem. Lett. 2012, 3, 673 – 677.
[7] H. Cheng, K. Fuku, Y. Kuwahara, K. Mori, H. Yamashita, J. Mater. Chem. A 2015, 3, 5244 – 5258.
[8[N. L. Reddy, V. N. Rao, M. Vijayakumar, R. Santhosh, S. Anandan, M. Karthik, M. V. Shankar, K. R. Reddy, N. P. Shetti, M. N. Nadagouda, T. M. Aminabhavi, Int. J. Hydrogen Energy 2019, 44, 10453 – 10472.
[9] X. Zhou, G. Liu, J. Yu, W. Fan, J. Mater. Chem. 2012, 22, 21337 – 21354.
[10] V. Kumar, S. C. O'Donnell, D. L. Sang, P. A. Maggard, G. Wang, Front. Chem. 2019, 7, 299.
[11] R. Kavitha, S. G. Kumar, Mater. Sci. Semicond. Process. 2019, 93, 59 – 91
[12] W. Knoll, Annu. Rev. Phys. Chem. 1998, 49, 569

CHAPTER

PHOTOCATALYTIC DECOMPOSITION OF WATER USING SUNLIGHT ON SUSPENDED NANOPARTICLES

The decomposition of water using sunlight on semiconductor partlcles has been pursued for several decades now [1-4]. Even though many materials have been employed and variety of concepts have been proposed, there appears to be still lingering questions on the photocatalytic nature of this decomposition reaction. The reaction under consideration is as follows:

$$H_2O \rightarrow H_2 + \tfrac{1}{2} O_2 \quad \Delta G = +237 \text{ kJ/mol};=+2.46.\text{eV}=+1.23 \text{ eV per electron}$$

The simple requirement for this reaction to be truly photo-catalytic, it should give H_2 to O_2 molar ratio has to be 2 and the turn over number (TON) has to be grater than one. Both these conditions have not been established in most of the studies reported.

Recently in a perspective article, Hicham Idriss [5] has raised a number of points which shows that the photocatalytic decomposition on particulate systems appears to be elusive. The main argument in favour of his hypothesis is that the only reproducible results reported in water decomposition reactions are carried out in the presence of electron donors or acceptors and the reaction is driven by the organic or inorganic redox potential. In order to understand that the reaction is truly photo-catalytic means (1) the evolution of hydrogen and oxygen should be in the molar ratio of two (2) the observed turn over number (TON) should be greater than one (if the reaction were to be truly catalytic) and (3) the experiments must involve direct measurement of hydrogen and oxygen evolved instead of the measurement of current [5].

In spite of all these, the search for photo-catalysts for overall water splitting goes on as revealed by the review [6]. Two different configurations have been proposed for overall water decomposition using sunlight usually termed as either one step or two step photoexcitation routes.. Although, originally, it was difficult to generate even small amounts of hydrogen and oxygen under ultraviolet irradiation, it is now appears possible to demonstrate highly efficient Overall water splitting (OWS) processes with Apparent Quantum yield (AQY >50%) using wide-gap oxide photocatalysts. Various new types of semiconductors capable of harnessing visible light have been developed over the past two decades

Although considerable advances have been made, important scientific challenges must be overcome to allow the practical use of large-scale solar water splitting. The Solar to hydrogen (STH) conversion efficiency for a one-step photo-excitation should reach at least 10% for hydrogen production so as to meet the cost of other conventional industrial processes.

The semiconductor materials which will respond to UV and visible radiation mostly exhibit not sufficient thermal stability and photostability. These drawbacks can be mitigated to an extent by the deposition of effective co-catalysts. Surface Plasmon Resonance is yet another way of enhancing photocatalytic activity but this subject is not dealt with in this chapter. This technology can in the future become a new branch of research in solar energy conversion systems.

With regard to the development of co-catalysts for efficient conversion, one can learn and adopt from the natural photosynthesis. This will facilitate the understanding and mimicking photosynthetic reaction centres and based on these concepts efficient electrocatalysts have been fabricated., In spite of all efforts, there appears to be difficulty in formulating efficient co-catalyst formulations. This difficulty is mainly due to the fact that one has to deal with three interfaces simultaneously, namely co-catalyst/semiconductor, co-catalyst/ solution and semiconductor/solution interfaces and appropriately engineer them so that the forward charge transfer takes place preferentially.

Furthermore, much more effort should be directed towards understanding the fundamental photocatalytic processes and also increasing the efficiency of the system from about 1% now realized to above 10% require extensive studies using advanced characterization techniques. Another important challenge is to use earth abundant and to eliminate the use of rare and expensive elements. The particulate photocatalyst systems would be advantageous because of their greater scalability and operability.

One-step photoexcitation is the simplest model for overall water decomposition on a single semiconductor photocatalyst (FIG. 1). In this system, photogenerated electrons and holes diffuse to the surface of photocatalyst particles and subsequently participate in the HER and OER, respectively. A thermodynamic prerequisite for the semiconductor is to have band-edge positions straddling the H^+/H_2 reduction potential and O_2/H_2O oxidation potentials. Two-step photoexcitation based on combining two types of photocatalysts that separately

evolve Hydrogen and Oxygen has also become a popular approach to OWS. This technique is inspired by natural photosynthesis and is termed Z-scheme water splitting. In this case, photogenerated electrons reduce H^+ to Hydrogen, whereas holes in an another photocatalyst oxidize H_2O to O_2 (FIG. 1b and c).. The photoexcited electrons and holes remain in the respective photocatalysts, respectively, and their recombination via an aqueous redox mediator (FIG. 1b) or a solid-state electron mediator (FIG. 1c) completes the photocatalytic cycle. These aspects have been described in another chapter.

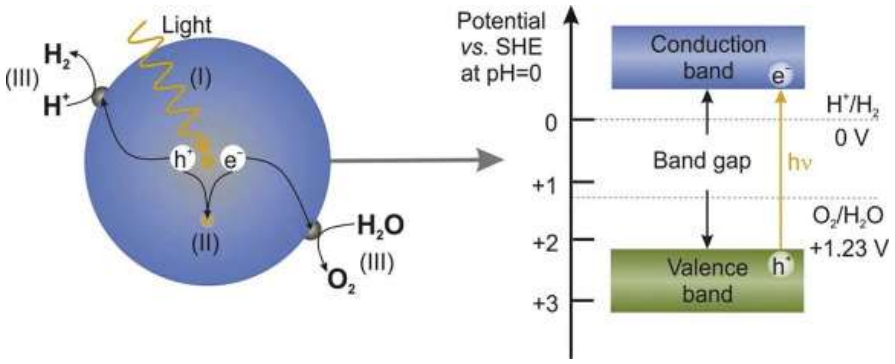

Figure 1. The main processes and the principle of photocatalytic water splitting in semiconductor photocatalysts. Simplified picture of one step process.

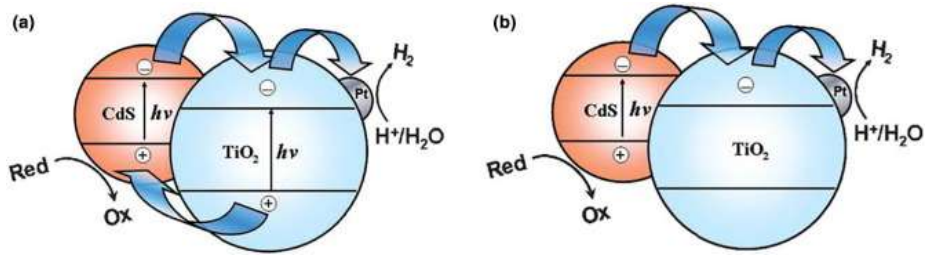

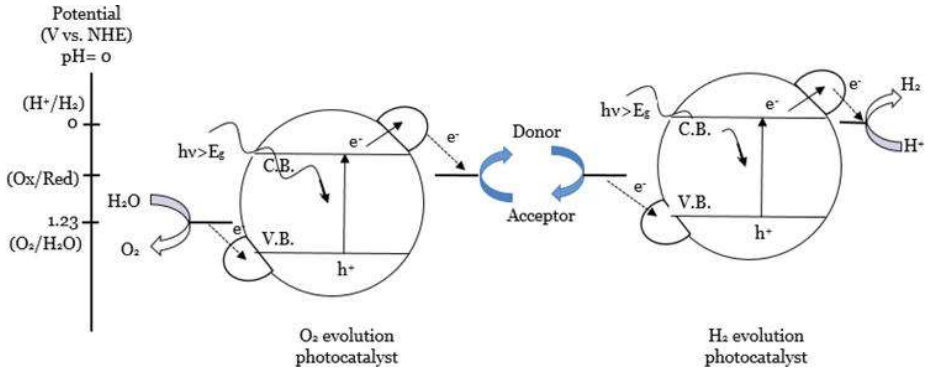

Figure 1, Transfer of photogenerated electron/hole pairs in CdS-sensitized TiO_2 under UV (A) and visible light (B) irradiation

There are still a number of challenging aspects of this process for which solutions have to be evolved. First and fore most the reaction is thermodynamically unfavourable reaction

$H_2O \rightarrow H_2 + ½\ O_2 \quad {}_{\Delta G}{}^{0} = 237$ kJ/mol

These processes include (1) excitation of the semiconductor photocatalyst with photons having energy equal to or higher than the band gap of the material (2) transfer of the photo-generated electrons and holes to the reaction sites (3)Utilization of these charge carriers in the oxidation and reduction reactions and (4) desorption of the products from the surface of the photocatalyst to the liquid or gas medium.

As the time scale of these steps varies, recombination of the electron and hole in the bulk or on the surface takes place more often than the rate of chemical oxidation/reduction reactions. This is therefore considered to be one of the main reasons limiting the realizable photocatalytic activity. Another factor is the back-oxidation reaction which takes place on metal sites and other mass transfer limitations which cumulatively account for low efficiency normally observed in this reaction. However, natural photosynthesis probably yields higher rate of oxygen evolution as compared to the artificial water splitting due to improved charge carrier and mass transfer possibilities. It is therefore clear that the design of photo-catalyst has not yet reached the perfection required as compared to the natures splendid design.

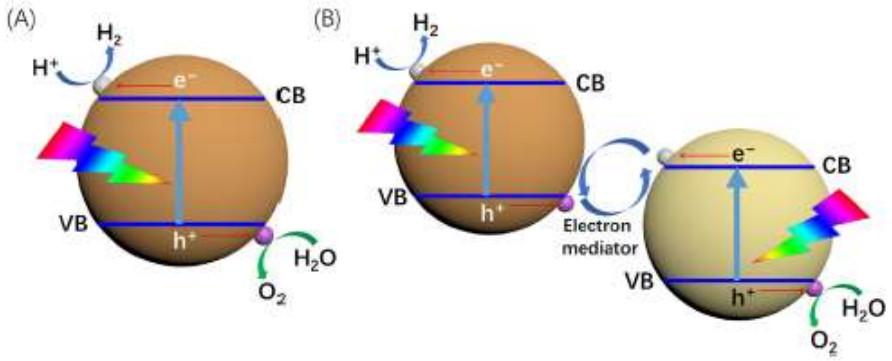

Figure 2. Schematic energy diagram for different types of photocatalytic overall water-splitting systems. A: One-step photoexcitation B: Two step photoexcitation [Reproduced from ref.11]

On the whole, many types of systems have been exploited as $^{-1}$photocatalysts for the decomposition of water. Among them the following four types of catalysts, namely (1) perovskite compounds, (2) metal oxides (sulfides and nitrides), (3) Bi and In-based materials, and (4) multicomponent catalysts The essential data generated on these four types of systems are given Table 1. In these several strategies have been employed to enhance photocatalytic activities: (a) tuning particle sizes and shapes, (b) creating defects, (c) loading dual cocatalysts, (d) constructing core/shell structures, (e) fabricating isotropic facets, (f) forming solid solutions, (g) embedding carbon nanodots in a semiconductor matrix, (h) generating synergistic effects of multi-components, and (i) combining thermal and photon activation.

Table 1 Photocatalytic results of some typical systems collected from literature [data extracted from ref 7]

Photocatalyst Type	Catalysts	Light source	Yield (μ mol $g^{-1}h^{-1}$)\

TiO_2 based	Au-NiO_x/TiO_2	300 W Xe	18.3 (H_2)
	Cl^-Pt/TiO_2	300 W Xe	300 (H_2)
	Pt-Mg loaded TiO_2	300 W Xe	850 (H_2)
Perovskites	$Rh_{2-y}Cr_yO_3$ loadedAl-dopedSrTiO_3	300 W Xe	5500 (H_2)
	NiO-$SrTiO_3$	300 W Xe	240 (H_2)
	Pt-$Co_3O_4/SrTiO_3$	300 W Xe	4089 (H_2)
	$CaTaO_2N$	300 W Xe	6.5 (H_2)
	NiO loaded$Cd_2Ta_2O_3$	300 W Xe	567.7 (H_2)
	Nio/$NaTaO_3$:La	400 W Xe	5900(H_2)
	Ni/$Sr_2Nb_2O_7$	450 W Xe	6.7 (H_2)
	NiO/Ba-$La_2Ta_2O_7$	450 W Xe	5000(H_2)
	Pt/H-$SrBi_2Ta_2O_9$	250 W Xe	4910 (H_2)
	NiO_x-$BaLa_4Ta_4O_{15}$	300 W Xe	4600(H_2)
	Pt/$KCa_2Nb_3O_{10}$	300 W Xe	260 (H_2)
Metal oxides and sulphides	Cu_2O	300 W Xe	3.6 (H_2)
	Ni/Zn-Ga_2O_3	450 W Xe	4100 (H_2)
	Nanocrystalline CoO	AM1.5G	
	C Dot/CoO	300 W Xe	33.4(H_2)
	Pt/CdS@Al_2O_3	300 W Xe	62.1(H_2)
Nitride based	RuO_2loaded β-Ge_3N_4	450 W Xe	93.3 (H2)
	Mg Doped GaN	300 W Xe	4.0(H_2)
	Mg^{2+} doped InGaN/GaN	300 W Xe	3.46(H_2)
	RuO_2 loaded GaN:ZnO	450 W Xe	3200 (H_2)
	$Rh_{2-x}Cr_xO_3$ loaded GaN:ZnO	450 W Xe	3090 (H_2)
	C Dots-C_3N_4	300 W Xe	105(H_2)
	Pt/g-C_3N_4	300 W Xe	61(H_2)
	CoP-Pt/g-C_3N_4	300 W Xe	26.25 (H_2)
Bi and In Based	RuO_2 loaded Bi YWO6	500 W Xe	13.7 (H_2)
	$ZnRh_2O_4/Ag/Bi_4V_2O_{11}$	700nm	0.25 (H_2)

	Pt loaded $Bi_xY_{1-x}VO_4$ RuO_xloaded	300W Xe	357.5 (H_2)
	$Bi_2Ga_{3.6}Fe_{0.4}O_9$	300 W Xe	41.5 (H_2)
	$NiO_y/In_{1.x}Ni_xTaO_4$	300 W Xe	33.2 (H_2)
	In-Ni-Ta-O-N	300 W Xe	62.4 (H_2)
	$Ba_2In_2O_5/In_2O_3$	400 W Xe	58.6 (H_2)
Multi-components	$CoO/g\text{-}C_3N_4$	300 w Xe	50.2 (H_2)
	$GaFeO_3$	300 W Xe	9.0 (H_2)
	$Na_2ZrTi_5O_{13}$-CuO	UV (254)	2909 (H_2)
	Cu_2O@ZnCr LDH	300 W Xe	45 (H_2)
	$BiVO_4$-Ru/$SrTiO_3$;Rh	300 W Xe	40.1 (H_2)

In a recent publication the importance of 2D materials have been specifically mentioned [1] but it must be remarked the use of layered compounds has been initiated from early stages of investigations on this topic.

Water source is another variable and in that sea water splitting assumes importance due to the complex nature of the source. The recent progress in this field is reviewed in reference [9]. Therefore, the development of efficient photocatalysts for water reduction and oxidation in a suspension system appears to be the cornerstone for the development of solar energy conversion. The new materials development covering inorganic materials especially oxides, nitrides and sulfides and other semiconducting compound photo-catalysts are extensively considered in reference [10]. This is an important reference source for this field.

Charge recombination

Due to the presence of the multiple processes, the overall photocatalytic reactions are complicated. In order to obtain an efficient photocatalytic performance, the photo-generated charges must be transferred to the surface reaction sites as rapidly as possible while preventing recombination

or trapping of these charge carriers. It is reported that approximately 60% of the trapped electron–hole pairs recombine with a timescale of about 25 ns while releasing heat of 154 kJ/mol. As the defects such as vacancies and dislocations are considered as recombination sites, higher crystallinity of the photocatalysts is often aimed to decrease the recombination rates. From diffusion point of view, the shorter distances for the charge carriers to the surface reaction centers are also aimed to prevent the recombination. Shorter pathways are achieved via smaller crystal/particle sizes of the photocatalysts. Another method for reducing the charge recombination is to make use of phase junctions. Loading the photocatalysts with co-catalysts such as noble metals or transition metal oxides to accelerate the reduction/oxidation reactions is a commonly employed method. These co-catalysts are known to enhance the charge migration from the semiconductor depending on the alignment of the potentials of the semiconductor and the co-catalyst. As these co-catalysts accelerate the desired H_2 evolution and O_2 evolution reactions, they can also increase the rates of undesired secondary reactions such as hydrogen oxidation or oxygen reduction to water reactions namely the back reaction.

Back oxidation reaction

It is known the catalyst systems employed for water decomposition reaction can also promote the back-oxidation reaction on the same sites on which the decomposition takes place. These systems also promote the recombination of the charge carriers that are generated by photon absorption. In the absence of fast removal of products, the reverse reaction is highly probable. This can be considered one of the reasons for the observed low efficiency. This will be true on metal (like Pt) loaded semiconductor systems under the same experimental conditions used for decomposition reaction. It has been shown that Pt is active for the dark recombination reaction even at room temperature. Modification of the surface-active Pt sites can be blocked by F modification. Another way to block the active sites is molecular adsorption of CO.

Coupled (Z scheme) semiconductors

This is yet another particulate system which gives improved efficiency in the decomposition of water. The logic in designing such systems is the relative positions of the valence band maximum and conduction band

minimum in the choice of the semiconductor combinations. This is to facilitate the charge carrier transfer between the chosen semiconductors. In addition, the photon absorption can be shifted to visible range by selecting a low band gap semiconductor as one of the components. In figure x, a pictorial representation of one such system is shown and note the relative band edge positions relative to each other.

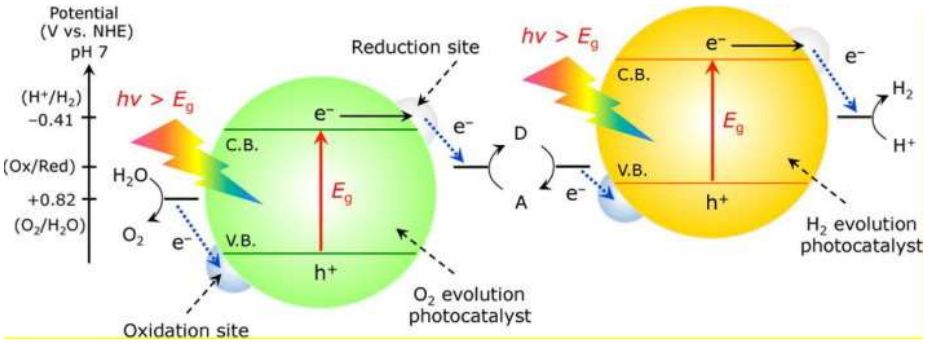

Figure 3. Schematic energy diagram of photocatalytic water splitting by a two-step photoexcitation system. C.B., conduction band; V.B., valence band; Eg, bandgap. D and A indicate electron donating and accepting species, respectively.

It has been already stated that the particulate systems chosen must mimic the natures photosynthesis path way. Photosynthesis pathway is essentially separating the reduction and oxidation sites and also utilizing the photon absorption appropriately. The corresponding particulate system is shown in Figure using g-C_3N_4 as the hydrogen evolution photocatalyst and $BiVO_4$ surface as oxygen evolving photocatalyst.

re

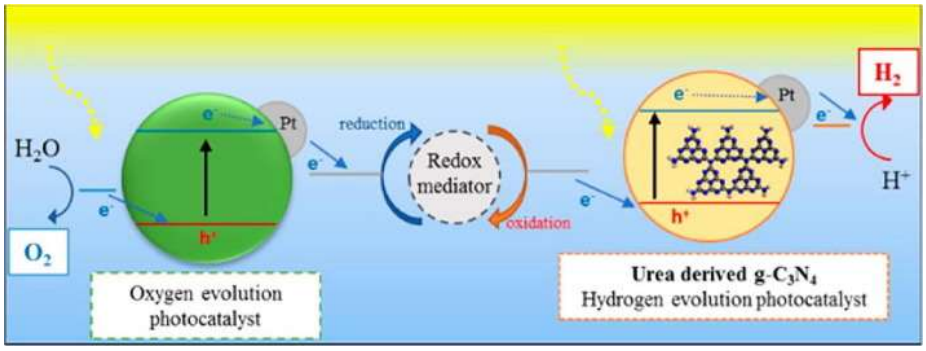

Figure 4. Schematic diagram of photogenerated electron transfer in a nature-inspired water splitting system. Urea derived g- C_3N_4 worked as the hydrogen evolution and two different metal oxides, $BiVO_4$ and WO_3, served as the O_2 evolution photocatalyst under UV/visible light irradiation

This brings to a situation that one should a prori know the relative positions of the Conduction Band Minimum (CBM) and Valence Band Maximum (VBM) so that the water decomposition potential can saddle between them. These values have been tabulated elsewhere. These data are shown pictorially in Figure 5.

In spite of all these efforts, the author in reference 5 brings forth a number of doubts and questions which we shall try to list them as follows:

[1] The rate of production of hydrogen more importantly no molecular oxygen decreases with time. This means that the catalytic reaction is not sustainable. The supporting evidence is the increase in the amount of water as function of time. This objection can be and has been answered by measuring sustainable hydrogen production for a number of hours.

[2] The hydrogen evolved could have come from the hydrocarbon contaminants present on the catalyst system and reaction medium. This has been proved to be not true by experiments wherein special care has been taken to avoid hydrocarbon contamination.

{3] The added electron donors in the system could be the cause of hydrogen evolution. In addition, the added hole scavengers, the reaction is driven by the redox potential of the redox potential of the inorganic compound and is not related to water splitting reaction. This could be proved by suitable choice of the reaction conditions.
[4] The photon fluxes normally employed is too small in the reported experiments. This can be established by using more intense photon flux.
[5] The electron transfer can take place by suitable orbital overlap and the character of the bands in the semiconductors employed is not suitable. This can be accounted for by suitable choice of the semiconductor material.
[6] Suspended particles at present do not offer a possible way forward for hydrogen production. This appears to be an opinion.
[7] The hydrogen production is measured in terms of the current and not the measurement of hydrogen and oxygen evolved. This objection can be answered by measuring and monitoring the gases evolved.

All these points only emphasize the care and accuracy necessary for measurements and experiments involving photocatalytic water decomposition. These are remarks to be taken care off by experimentalists in the future design and development of systems for this reaction.

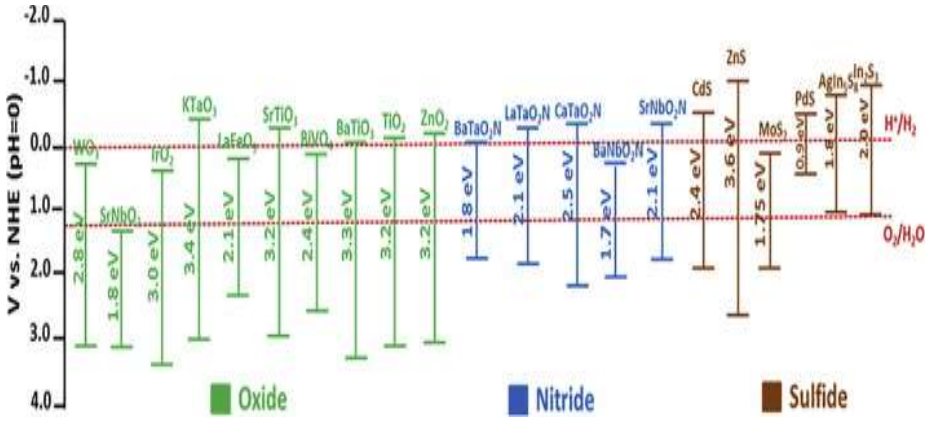

Figure 5. Bandgaps and band-edge positions of representative oxide (green), nitride (blue) and sulfide (brown) semiconductors in relation to the redox potentials for water splitting at pH = 0. The CB potential of a semiconductor material in aqueous solution usually exhibits a pH dependence described according to $E_{CB} = E^{0}_{CB\ (pH\ 0)} - 0.059\ pH$. The redox potentials of water also have the same linear pH dependence with a slope of 0.059 V per pH.

References

[1] Muhammad Rafque, Rikza Mubashar, ·Muneeb Irshad, · S. S. A. Gillani · M. Bilal Tahir · N. R. Khalid · Aqsa Yasmin · M. Aamir Shehzad, A Comprehensive Study on Methods and Materials for Photocatalytic Water Splitting and Hydrogen Production as a Renewable Energy Resource, Journal of Inorganic and Organometallic Polymers and Materials, https://doi.org/10.1007/s10904-020-01611-9.

[2] 1 A. Miseki and Y. Kudo, Heterogeneous photocatalyst materials for water splitting, Chem. Soc. Rev., 2009, 38, 253–278.

[3] F. E. Osterloh, Photocatalysis versus Photosynthesis: A Sensitivity Analysis of Devices for Solar Energy Conversion and Chemical Transformations, ACS Energy Lett., 2017, 2, 445–453.

[4] J. W. Ager, M. R. Shaner, K. A. Walczak, I. D. Sharp and S. Ardo, Experimental Demonstrations of Spontaneous, SolarDriven Photoelectrochemical Water Splitting, Energy Environ. Sci., 2015, 8,2811-2824

[5] Hicham Idriss, The elusive photocatalytic water splitting reaction using sunlight on suspended nanoparticles: is there a way forward?, Cat.Sci.Technol.,2020, 10,304.

[6] Shanshan Chen, Tsuyoshi Takata and Kuzunari Domen, Particulate photocatalysts for overall water splitting, Nature Reviews [Materials]2017.2.1-17.

[7] Siyuan Fang and Yun Hang Hu, Recent progress in photocatalysts for overall water splitting, Int.J.Energy Res.,2018,1-17.

[8] Mazuhiko Maeda and Kazumari Domen, Photocatalytic water splitting:Recent Progress and Future Challenges, I. Phys.Chem.Lett;, 2010,1,2655-2661.

[9] Jining Zhang,, Wenping Hu , Shuang Cao and Lingyu Piao Recent progress for hydrogen production by photocatalytic natural or simulated seawater splitting, Nano Reserch, https://doi.org/10.1007/s12274-020-2880-z.

[10] Dan Kong , Yun Zheng , Marcin Kobielusz, Yiou Wang Zhiming Bai Wojciech Macyk, Xinchen Wang and Junwang Tang, Recent advances in visible light-driven water oxidation and reduction in suspension systems, Materials Today, 2018,21,897-924.

[11] Lihua Lin, Takashi Hisatomi, Shanshan Chen, Tsuyoshi Takata, and Kazunari Domen, Visible-Light-Driven Photocatalytic Water Splitting: Recent Progress and Challenges. Trends in Chemistry, Month 2020, July 13, https://doi.org/10.1016/j.trechm.2020.06.006

Chapter

Energy Scene

Total available Energy and its easy access are essential for the well-being of humanity. Energy provides the means for comfort living and thus possibly account for poverty alleviation. Ensuring everyone gets sufficient access is an pressing challenge for the development of the world. However the use of energy results in environmental damages. Current energy systems are mostly dependent on fossil fuels that has climatic effect in the form of greenhouse gases. This means the world needs a significant change in the energy sources.

To overcome the challenges of developing new energy sources. Keeping in mind the environmental issues and at the same satisfy the energy needs of all people finding an appropriate energy source appears to be difficult proposition. In this context, hydrogen generation from abundantly available source like water appears to be an attractive option even though, there can be many questions to be answered before transforming to hydrogen based economy. This transformation is attractive from another point of view namely we will go to a regime of low carbon sources.

In order to understand the magnitude of the problem, we must look into the presently available energy sources and the extent of contribution from each of these sources. The data pertaining to the year 2018 are collected in Table 1.

Table 1 Various energy sources that were available in the year 2018

Source	Amount (figures for the year 2018)	% (approximate)
Other renewables	625.8 TWh	0.4
Solar	584.6 TWh	0.37
Wind	1270 TWh	0.80
Nuclear	2701.5 TWh	1.72
Hydropower	4193.1 TWh	2.67

Natural Gas	35488.6 TWh	22.6
Crude oil	54219.6 TWh	34.5
Coal	43869.5 TWh	27.9
Traditional Biofuels	11111.1 TWh	7.1

- [**This chapter is mainly based/ reproduced/abstracted/adopted from the publication by Francesco Parrino , Vittorio Loddo , Vincenzo Augugliaro , Giovanni CameraRoda , Giovanni Palmisano , Leonardo Palmisano , and Sedat Yurdaka, Heterogeneous photocatalysis: guidelines on experimental setup, catalyst characterization, interpretation, and assessment of reactivity, *Catalysis Reviews*, 2019, 61,163-213; https://doi.org/10.1080/01614940.2018.1546445**]

The work of Fujishima and Honda [1] on TiO2 photo-induced water decomposition, the field of heterogeneous photocatalysis has almost started [2–6]. This field is treated as a "green" and possibly sustainable technology for the degradation of toxic and nonbiodegradable species both in gaseous and liquid phases. The limitation of this "advanced oxidation process" is the low photonic conversion efficiency (ξ), that is, the ratio of the rate of the photoreaction measured for a specified time interval to the rate of incident photons within a wavelength range .[7] In fact, each absorbed photon is able to generate an electron/hole pair which can be efficiently utilized only if spatially separated and transferred to substrate species with appropriate redox potential. The alternate route namely the recombination of the charge carriers results in energy loss.[8]

Various techniques have been used to overcome this problem like the application of a small bias voltage [9] or by adding external electron acceptors, efficient than oxygen, such as hydrogen peroxide, peroxydisulfate ions, or ozone.[3,4,8,10] The charge recombination can also be reduced by surface modification of the semiconductor or by grafting suitable species. It has been reported that 0.05Pt and 1% Mg^{2+} doped TiO_2 appeared to be most efficient photocatalyst to give 0.26% efficiency in light conversion.[11] \

In recent times, photocatalysis has attracted great interest as an alternative method to traditional synthetic methods of fine chemicals.[12,13] The possibility of producing high value added products in small scale and with good selectivity has been often reported in literature,[14] although in most cases the products have been only detected by means of chromatographic methods. However, unlike

traditional synthetic methods performed in harmful solvents, making use of stoichiometric amounts of strong oxidants in severe conditions of temperature and pressure, photocatalysis perfectly shows the features of a green process. In fact, photocatalysis may operate at atmospheric pressure and room temperature by using water, alcohols or dimethyl carbonate as cheap and non-toxic solvents and it allows the potential exploitation of solar light and the use of safe powdered or supported, composite and doped photocatalysts. The possibility of using a membrane in photoreactor can bring additional advantages of easy separation, the purification of the product, and easy control of the process. Another strategy to improve the yield of partial oxidation reactions is the combination of heterogeneous photocatalysis with electrocatalysis. The resulting process is called photo-electrocatalysis. The number of papers published on photocatalysis from 1992 to 2017 shows an almost linear growth. Many books or reviews on the fundamentals[2–4,15,16] and on specific applications of photocatalysis for environmental remediation,[17] selective oxidations,[12,13,18] novel photocatalysts,[19,20] photocatalytic hydrogen generation,[21,22] and photocatalytic CO2 reduction[23,24] have been reported. Moreover, the importance of reactions activated by light is confirmed by IUPAC, which published the "Glossary of terms used in photocatalysis. Also few publications on misconceptions in photocatalysis [25-27] can be found. In particular, reviews by Herrmann [27] and Emeline et al.[25] report on the mechanistic aspects of photocatalytic reactions, whereas Ohtani [26] mainly approaches some issues encountered when writing articles on photocatalysis. The purpose of this chapter is to give some guidelines to perform future photocatalytic experiments so the results can be compared to each other.

The chosen photocatalyst should be photoactive, stable against photo-corrosion and electrolytes, harmless, cheap and chemically inert. Moreover it should be active in UV and visible region. These systems can be used with sunlight as a sustainable source of energy and its wavelength ranges from 280 to 4000 nm, with the UV photons which account for just a small percentage of the total energy (3–5%).[28]

The assessment of the performance of a catalyst is important, and it should be evaluated precisely. The catalyst crystal phase, specific

surface area, particle size, surface morphology, crystallinity, and number of active sites and its distribution are essential important parameters.[3] The photocatalyst crystalline phase strongly influences the photoactivity like the anatase phase of TiO_2 is more active than the Rutile Phase . Generally, combination of different semiconductors [29] or different phases [30] present photoactivity higher than the pure components due to heterojunctions able to efficiently spatial separating the photogenerated charges. An example of this synergistic effect is represented by the most active commercial TiO_2 Degussa P25 (Evonik), which is a mixture of anatase (ca. 75%) and rutile (ca. 25%). Since the relevant steps of a photocatalytic reaction mainly occur onto the photocatalyst surface or in its immediate proximity, the specific surface area is one of the main parameters to be considered. Reducing particle size often results in increased surface area and photoactivity. On the other hand, when the particle size becomes comparable with the distance between the photogenerated charges, their recombination is very likely so that a detrimental effect on the photoactivity is often observed.[31] Moreover, reduction of the particle size on a quantum scale causes dramatic changes in the optical features of the photocatalysts. Generally, highly ordered crystalline semiconductors show higher photoactivity than the correspondent partially amorphous materials.[32] However, thermal treatments normally applied in order to endow the catalysts with higher crystallinity, reduce the specific surface area due to sintering of particles with a consequent reduction of the photoactivity. On the other hand, partially amorphous catalysts have been successfully applied for synthetic purposes.

Characterization techniques of the photocatalysts

X-ray diffraction (XRD) is a characterization technique which is run always on inorganic semiconductors, providing quantitative information on their crystallinity as a function of different parameters such as annealing temperature, treatment time, pH of precursors solution. The Scherrer's equation allows to determine the main particle size of the photocatalyst. Moreover, by comparing specific patterns with those of reference materials, it is possible to get information on the extent of crystallinity of the material and on the percentage of possible amorphous phases. XRD allows also to assess the geometry of crystals

and the percentage of certain exposed facets. Further information can be obtained by means of Raman spectroscopy. This technique is surface sensitive and very useful when the crystallinity of films rather than powders needs to be assessed. The information given by Raman is not only related to semiconductor crystal structures, but also to defects in the crystals. For instance, in the TiO anatase phase a positive shift in Eg wavenumber, signal produced by O-Ti-O symmetric stretching vibrations, can be correlated to the abundancy of oxygen vacancies. In turn, these defects can drastically affect the reactivity and the hydrophilic properties of the material. However, the intensity of the Raman peaks is influenced by the background fluorescence and the surface density of the analyzed material. Accordingly, Raman spectra cannot provide quantitative information on crystal phases or degree of crystallinity, which are instead provided by XRD.

X-ray photoelectron spectroscopy (XPS) is a powerful technique affording information on the type and oxidation state of the species constituting the semiconductor by investigating their binding energy. Quantitative and qualitative information as the intensity of the signals may be related to the amount of the species of interest and their oxidation state. Moreover, by varying the sputtering intensity it is possible to know the composition of the surface or of the bulk. Notably, also the optical absorption edge of a semiconductor may be retrieved by means of XPS. XPS is also used to analyze trace dopants in semiconductors., However, sometimes XPS sensitivity is not enough to discriminate between different oxidation states, and one needs to perform X-Ray Absorption Spectroscopy (XAS) measurements at a synchrotron facility, especially if the catalyst is supported as a film on a substrate giving a strong background signal, The surface morphology, which can have significant effects on reactivity and some textural properties may be directly observed by means of different microscopy techniques such as scanning electron microscopy (SEM), transmission electron microscopy (TEM), and atomic force microscopy (AFM). The specific surface area (SSA) of a catalyst is one of the main parameters to be considered when photoactivity results are presented. In many publications the authors compare different photocatalysts by keeping constant their surface area. Although this approach expresses the relevance of SSA in photocatalysis by analogy with heterogeneous thermal catalysis, it neglects the essential role played by the optical

features. Furthermore, the photoactivity results may be easily normalized per unit specific surface area thus eliminating the SSA dependence.

Thermogravimetric characterization allows to quantify the amount of hydroxyl groups on the surface of the oxide photocatalysts. Particular attention must be paid to distinguish between physically adsorbed water molecules and OH groups. To do so, a multistep heating must be performed allowing the needed time to desorb physisorbed water from the surface, taking place at temperatures below 120 ºC. Hydroxyl groups are typically recognized as active sites where photogenerated electrons or holes can be trapped. However, it was recently shown that the amount of reactive species formed during photocatalysis, is not directly related to the density of hydroxyl surface groups but also to structural parameters of the samples. Therefore, it has been proposed that not all of the surface hydroxyl groups play an active role in determining the photoactivity. This finding has been obtained by means of electron paramagnetic resonance (EPR) spectroscopy which should be mentioned among the important characterization techniques allowing qualitative and quantitative information on the reactive paramagnetic species generated upon irradiation.

Acidity is another essential feature of the surface, affecting the interaction with substrates and the intermediates. It is well known that some of the hydroxyl surface groups behave as Lewis acids or bases, differently interacting with the molecules present in the reacting medium. Titration procedures, also coupled with other techniques such as thermogravimetry, allow to get information on the acidity of the surface.

It is worth to mention that Fourier transformed infrared spectroscopy (FTIR) and solid state nuclear magnetic resonance (NMR) are classical but powerful tools to investigate the interactions and the dynamics of compounds on the surface of semiconductors. However, the most discussed and intriguing feature of the surface is the presence of morphological and structural defects which are of importance to determine the activity of a semiconductor. The “virtue of defects” consists in creating on the surface highly reactive sites due to impurities, geometric dislocations and/or local stoichiometric variations, capable to confer unexpected properties. Morphological characterization, especially transmission electron microscopy (TEM) is able to evidence some types of defects. However, a special class of point defects, known as oxygen

vacancies may be considered as the “invisible agents” on the surface of oxidic materials. Indirect evidences of oxygen vacancies may be obtained by taking into account their influence on the optical properties of the material or, inter alia, by considerations drawn from photoluminescence spectroscopy (PL), solid state NMR, XPS, and EPR results. Direct observation of oxygen defects may be achieved by means of atomically resolved scanning tunneling microscopy (STM) which also allows observation of their dynamics and their interactions with molecular oxygen. However, the great importance of the oxygen defects consists in their influence on the electronic structure of the material.

Optical and electronic characterization

Optical and electronic characterization techniques take into account the modifications occurring in the material upon light excitation. Inorganic photocatalysts are generally semiconductor materials in which energetically similar full or partially filled molecular orbitals create the so-called valence band (VB), while empty orbitals energetically close to each other form the conduction band (CB). The energetic gap between VB and CB is a fundamental parameter to be considered in order to decide the wavelength range in which the material can absorb the impinging radiation. Diffuse reflectance spectroscopy (DRS) is the most used and simple technique to get information, and it allows to distinguish between direct and indirect band gap, and sometimes also to detect multiple band gaps occurring especially in composite photocatalysts. The most used method to determine the band gap of a photocatalyst is to consider the absorption coefficient of the powder proportional to the Kubelka Munk function, $F(R'_\infty)$, which in turn can be obtained from reflectance (R'_∞) dara by means of Equation

$$F(R'_\infty) = [(1-R_\infty)/2R_\infty] = \alpha/s$$

where α and s are the absorption and scattering coefficient, respectively. A plot of $(F(R'_\infty)\, h\nu)^n$, where n is a coefficient related to the type of the electronic transition, versus the incident photon energy (hν), and a subsequent extrapolation of the linear part of the plot to the x axis, defines the band gap energy. By considering some reports recently published, it is useful here to point out that the intercept must be taken with the x axis which is described by the equation y = 0 (i.e. $(F(R'_\infty)\, h\nu)^n = 0$ in the Tauc

plot). Furthermore, this routine procedure can be used only under defined conditions such as monochromatic irradiation, infinitely thick sample (normally about 5 mm), low sample concentration, uniform distribution, and absence of fluorescence. The situation is even complicated by the presence of intermediate energy states, generally due to defectivity, whose energetic position cannot be safely evaluated with this method. Notably, a detailed "electronic map" of the energy states of a semiconductor, along with their relative electronic density can be retrieved by means of photoacustic spectroscopy or a spectro-electrochemical approach which have been proposed.

However, the knowledge of the band gap of a semiconductor is not sufficient for the knowledge of the absolute potential of the conduction and valence bands. In order to determine the potential of the photogenerated electrons many characterization techniques can be used. Photoelectrochemical methods such as capacitance, photocurrent onset, and open circuit photovoltage measurements have been proposed. Other methods such as a combined spectro-electrochemical approach or potentiometric titrations have been also reported. By coupling the knowledge of the band gap and the absolute position of the conduction band edge, it is possible to estimate the potential of the valence band edge, thus obtaining a rough electronic map of the material.

Qualitative information on the recombination of the photogenerated charges can be obtained by means of photoluminescence (PL) spectroscopy. In fact, recombination often results in releasing radiative energy which can be measured upon excitation of the sample at a suitable wavelength, so that higher values of the photoluminescence intensity correspond to higher recombination. However, the relationship between photoluminescence and photoactivity is not straightforward, as samples showing high photoluminescence response may be highly photoactive too. This may account for the hypothesized energy transfer-based reaction mechanisms, only rarely approached up to now, occurring under experimental conditions favoring recombination.

Steady state photoluminescence is not conclusive to assess electron-hole recombination, since a decrease of the PL signal switching from one catalyst to another, can be due either to a decrease of crystal defects and

surface trap states, or to an increase of the charges lifetime. The only way to discriminate between the two components is to perform time resolved photoluminescence measurements, which are able to provide information on lifetimes.

Very detailed information on the electronic transitions and position of the bands can be obtained by using Resonant X-Ray Emission Spectroscopy (RXES): by exciting the semiconductor with a finely tuned X-Ray energy corresponding to the absorption edge of the semiconductor under study. This technique allows to simultaneously map the highest occupied electronic states (upon monitoring the valence to core transition), and the valence band by measuring the core to core transition.

Transient spectroscopy or photoelectromotive force measurements have been used to evidence the life time and the dynamics of the photogenerated charges, which are also important parameters to be considered.

Photoreactors

Several types of photoreactors with different geometry, for gas phase or liquid phase reactions to be operated in continuous or in batch regime are available. The geometry is one of the key parameters to consider when designing a reactor. Indeed, it strongly influences the radiant field distribution and the mass transfer dynamics. It is worth mentioning that the comparison of photocatalytic results obtained in different researches is almost meaningless if the mass transfer is the rate limiting step. Similarly, if the geometry (or the amount of the photocatalyst) does not ensure homogeneous illumination and light distribution, the active photoreactor volume may be smaller than the nominal one, because the part of the reactor which is poorly irradiated gives a negligible contribution to the reaction. Figures 1 and 2 show some examples of different configurations of photoreactors with slurry and immobilized photocatalyst, respectively. Generally, the walls of the photoreactors are made by Pyrex glass although quartz glass sometimes is used, to allow total transmittance of visible and near UV radiation. The choice of the type of photoreactor depends on the aim of the research study. Generally, for laboratory tests focused on organic and/or inorganic pollutants degradation in liquid suspensions, batch photoreactors are preferred both mixed or in total recirculation mode because this configuration allows easy setting and control of the operating parameters. As far as the gas phase is concerned, it is convenient, whenever possible, to use continuous systems directly connected to the analysis instruments by means of automatic sampler valves. Similar

considerations can be done in the case of photocatalytic syntheses, even if in these cases further optimization studies should be carried out in order to maximize selectivity and conversion. To this aim, microreactors have been recently proposed with promising results. For kinetics studies the system must be in kinetic regimen, thus mass transport phenomena must be avoided.

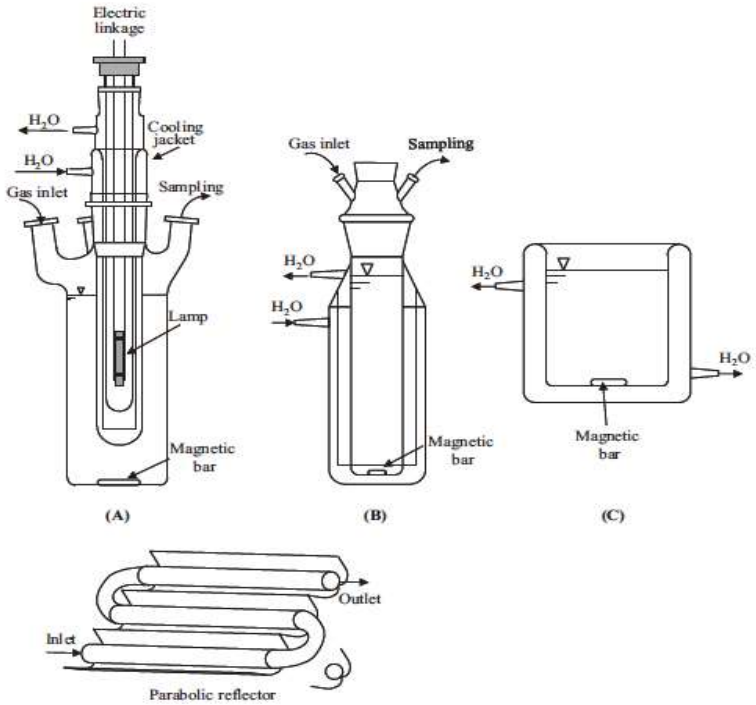

Fig.1. Schemes of slurry Photoreactors: (A) Annular batch photoreactor with immersed lamp axially positioned and cooling jackt (B) externally irradiated cylindrical bath photoreactor with cooling jacket (C) cylindrical batch photoreactor with cooling jacket irradiated from top; (D) Plug flow photoreactor (batch or continuous0 externally irradiated artificially with solar light [Reproduced from ref.33]

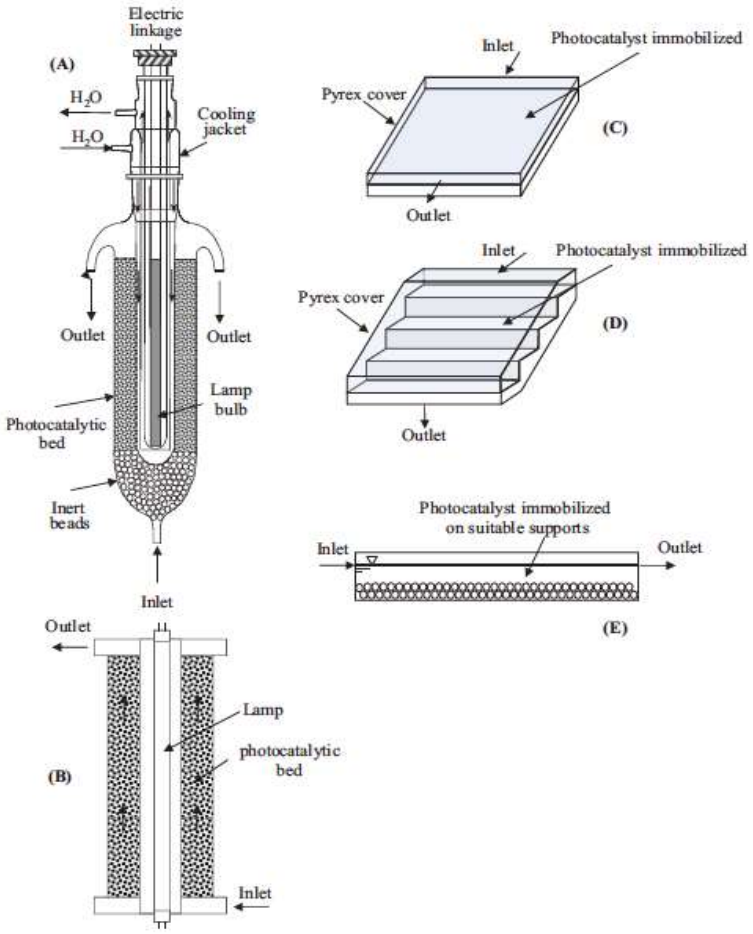

Figure 2. Some schemes of photoreactors with immobilized photocatalyst: (A) annular photoreactor (batch or continuous) with cooling jacket, irradiated internally and/or externally; (B) cylindrical photoreactor without cooling jacket, with the lamp axially positioned; (C) flat photoreactor with immobilized photocatalyst irradiated artificially or with solar light from the top; (D) step photoreactor with immobilized photocatalyst irradiated artificially or with solar

light from the top; (E) flat photoreactor with supported photocatalyst irradiated artificially or with solar light.[reproduced from ref.33]

Microreactors

The use of photocatalytic microreactors not only produces logistic advantages, such as the reduction of plant spaces and the possibility of mobile systems, but intrinsically affects conversion and selectivity of the considered reaction. In fact, with respect to conventional photoreactors it is possible to easily obtain laminar flow conditions, short molecular diffusion distances, large surface-to-volume ratios, high spatial illumination homogeneity, and good light penetration. However, the most appealing feature of microreactors consists in the possibility to scale-up the process by simply increasing their number, each considered as a unit cell. The combination of several devices in parallel would definitely avoid the difficulties and the high capital costs of scaling from laboratory to production plant, while avoiding demanding pilot plant experiments and allowing faster transfer of results from research to production.

Solvents

The choice of a solvent, should be based on its capability to dissolve reagents and products, increase the reaction activity and selectivity (as it strongly affects the reaction mechanism and mass and heat transfers), facilitate product separation and catalyst recovery and recycling. Moreover, the solvent should allow the direct contact between reagents and stabilize (for selective oxidations) or destabilize (for degradation or mineralization reactions) intermediates to hinder or promote their further conversion. Finally, it should not compete with reactants to the catalytic sites and should be non toxic, nonvolatile and possibly cheap. The best solvent fulfilling these characteristics is water, widely used to conduct photocatalytic degradation of pollutants at low concentration levels. However, due to the low solubility of many organic compounds in water and the generation of strongly oxidizing radicals from this solvent, water has a limited utilization in selective organic conversions.

The majority of the photocatalytic syntheses have been performed in organic solvents such as acetonitrile, water has been successfully used as the solvent for oxidation reactions and a variety of other organic reactions.

Mixed solvents are used to overcome the solubility limitation. Dimethyl carbonate and supercritical carbon dioxide have also been used as solvents. Ionic

liquids are another option despite the cost but their production is hazardous and costly. Glycerol is another option but its high polarity and viscosity limits its use.

Irradiation Sources

The radiation source is an important factor to be considered in a photocatalytic system. Many different types of lamps with different emission spectra and powers are commercially available.

There are five main types of radiation sources: (a) arc lamps; (b) fluorescent lamps; (c) incandescent lamps; (d) LEDs; (e) lasers.

In particular, for mercury lamps a classification based on the pressure of Hg can be as follows:

1. Low-pressure Hg lamps: The pressure of Hg vapor is about 0.1 Pa at 25 °C and the lamp emits mainly at 253.7 and 184.9 nm.

2. Medium-pressure Hg lamps: The radiation source contains Hg vapor at pressures ranging between 100 and several hundreds of kPa. This type of lamp emits mostly from 200 to 1000 nm with most intense bands at 313, 366, 436, 576, and 578 nm.

3. High-pressure Hg lamps: The radiation source contains Hg vapor at a pressure higher than 10 MPa with emission in a continuous back ground and broad lines from 200 to 1000 nm,

4. Xenon and Hg-Xenon lamps: Xenon lamps are used to simulate the solar radiation and the addition of Hg vapor increases the intensity of radiation in the ultraviolet region (both Xe and Hg vapors are at high pressure).

In the fluorescent lamps an emitting fluorescent substance deposited in the inner side of a glass cylinder emits at suitable wavelength when it is properly excited by the plasma generated with an electric discharge in the gas filling the lamp. Actinic lamps have emission in the near-UV region with a typical emission peak at ca. 365 nm.

Sometimes also incandescent lamps are used in photocatalysis. Indeed, halogen lamps have a tungsten filament sealed in a transparent case filled with an inert gas with small amounts of a halogen as iodine or bromine. This type of lamp is used to simulate sunlight (emits also in the near-UV region) and needs a cooling system.

LEDs are special diodes formed by a thin layer of p-n junction doped semiconductor material which emits photons through the recombination of electron-hole pairs. For instance GaN based LEDs are used to generate UV light at ca. 350–370 nm.

LEDs are the most used radiation sources due to their low price, flexibility and wide range of intensity and emission spectra. However, despite the advantages of LEDs, these can result in irradiation systems less effective than the traditional lamps, since light distribution can hardly be optimized, with highly heterogeneous irradiation intensities in reacting systems. Accordingly, the reactor design must take into consideration the use of LEDs to provide homogeneous light distribution, thus minimizing detrimental effects on reactivity. In fact, if the reactor is not uniformly illuminated, as it generally occurs by using LEDs, a 3D simulation with a suitable number of spatial points and directions of propagation of light is required for a rigorous kinetic analysis. However, the local values of the kinetic parameters may be satisfactorily approximated by the average values experimentally accessible for sufficiently low values of optical thickness. Some lamps supposed to emit visible light, such as halogen lamps and metal halide lamps, present small shoulders in the UV region which may considerably affect the photoactivity results. In this case it is important to use solid cut off filters or solutions (as $NaNO_2$) able to cut off the UV radiation. Notably, sunlight simulators, ensuring reproducibility and repeatability of experiments, are commercially available.

Sunlight irradiation

Experiments under real sunlight have to be carefully carried out. Indeed, many factors influence the irradiation as location and time at which the experiments are performed and weather conditions. In order to ensure reproducibility, photoactivity results under solar irradiation must be plotted versus the cumulative photonic energy incident on the reactor, E_{hv}, rather than versus irradiation time which is in practice the dose of the radiant energy received by the reactor. However, in view of the fact that the quantum yield is a function of the radiation intensity, this procedure is not fully correct. In fact, if the time evolution of the sunlight intensity changes, the same photocatalytic conversion may be achieved with different values of the cumulative photonic energy or the same cumulative photonic energy may give different conversions.

Anyway, this quantity can be evaluated as:

$$E_{hv} = \int I(t)\, dt$$

where I(t) is the photon flow [Einstein/s] at time t and t the irradiation time. The values of I may be obtained from the measured irradiance (UV_G , W·m−2) through Equation :

$$I = UV_G \; S$$

where S is the geometrical irradiated surface and UV_G can be easily expressed in Einstein·s^{-1} ·m^{-2} by using the Planck's equation ($E = hc/\lambda$) when the radiation spectrum is known.

Photocatalysts: in suspension or as immobilized films?

Reactors with suspended photocatalyst particles have a uniform catalyst distribution and a relatively high photocatalytic surface-to-volume ratio. As a consequence, the typical slurry systems applied in laboratory show greater efficiencies than immobilized systems. This configuration presents some drawbacks.

(1) The first one is the separation of the solid particles from the solution in order to be reused. This task is not easy as in some cases to completely remove the solid is not possible, and moreover it is an expensive and time-consuming process. \

(2) The second drawback is the penetration depth of UV light which rapidly decreases due to the strong absorbing properties of the photocatalyst particles and other organic molecules and to scattering and reflection phenomena.

Fixed bed photoreactors are a better and more practical option for photocatalytic reactions. The main drawbacks of immobilized photocatalyst are the limited amount of exposed active surface area, and the possibility of mass transfer limitations.

In many cases, some commercial applications of photocatalytic technology have encountered problems due to the lower photonic efficiencies and reactor performance of the scaled-up systems with respect to the preliminary laboratory experiments. Notably, reactor performance refers to the capability of the set-up to afford the reaction rate, selectivity and conversion as similar as possible to the maximum values theoretically obtainable. Key phenomena in this regard are light penetration, mass transfer limitations, and photocatalyst loading. They influence the irradiation efficiency, that is, the amount of activated photocatalyst (i.e. effectively irradiated) with respect to its total amount in the system.

Moreover, for industrial purposes, slurry systems still require large installation areas for an effective utilization of the captured radiant energy.

In any case, the irradiation efficiency, can be optimized more easily in systems with immobilized photocatalyst, given that the penetration depth of UV light in a slurry is limited, while absorption of thin photoactive layers is smoothly achieved.

On the other hand, photocatalytic thin layers present problems related to the transport of the reactants toward the photocatalyst surface, so that the overall process may be controlled by mass transfer steps. Notably, the optimization of the thickness of the photocatalytic bed is not straightforward because the radiation propagation through the bed is not a linear phenomenon, and the support used in the photocatalytic bed must be transparent to the applied radiation. Finally, it is worth to mention that most of the commercially available photocatalytic applications are related to air purification based on gas solid photodegradation reactions on supported photocatalytic materials. Even if of higher technical importance, gas/solid applications have been less investigated with respect to the liquid/ solid systems in the relevant scientific literature. However, this attitude is rapidly changing by considering the growing interest on photocatalytic microreactors.

Standardization issues

Standardized protocols have been developed to assess the performances of supported films for industrial applications, allowing a comparison of different photocatalysts. In particular, in the field of air purification, ISO standards are available for testing abatement of various pollutants. Apriori setting of the experimental conditions, although necessary for standardization purposes, may give rise to some issues. For instance, a critical point concerns reactor type and configuration used in the standardized experiments, and the conditions to be met in order to obtain reliable results. Generally, the central problem for standardization of the photocatalytic efficiency is the reaction rate evaluation. In gas/solid experiments, different reactors, such as batch or flow-through (both continuous stirred-tank reactor, CSTR, or plug flow reactor, PFR) have been used. However, the ISO 22197 norms describe test methods carried out in a PFR. It is evident that only in a continuous reactor system it is possible to unambiguously observe, for example, catalyst poisoning or improvements of the reaction rate, whilst in batch regimen these effects will be hidden due to the interference of the products which can in turn degrade according to their kinetic law. However, as the section of flow is fixed (50 × 5 mm), the PFR configuration is problematic for real supported samples with a surface curvature, or for which a perfect cutting is not possible. On the other hand, a reactor allowing to place samples of arbitrary volume and surface, like CSTR, presents relevant advantages

with respect to PFR. Even if a PFR is more efficient than a CSTR having the same volume, in a CSTR all the catalyst surface is exposed to the same (output) concentration. The resulting perfect mixing condition implies that different samples can be fit in the reactor thus overcoming the limitations. Furthermore, a CSTR configuration presents a lot of advantages for practical uses. In fact, mass transfer limitations can be reduced by using forced ventilation and consequently volume, shape of supported catalyst and gas flow can be changed without relevant constraints. Furthermore, while the values obtained in PFR may be seen as mean values, the CSTR configuration affords an evaluation of the photocatalytic rate closer to the intrinsic ones.

Some researchers focused the problem of identifying a reference photocatalyst which could be considered an indicator for high activity. Commercial TiO_2 Degussa P25 (Evonik) is the most used photocatalyst for comparison purposes. In fact, it has been thoroughly investigated and it presents a very high photoactivity. However, its high activity could not be guaranteed for all of the reactions, and in some cases it is useful to compare photocatalysts in the same polymorphic form because P25 consists of a mixture of anatase and rutile. Commercial TiO_2 powders are available in the form of anatase (Merck), rutile (Sigma-Aldrich) or brookite (Sigma-Aldrich) and these samples can be also used as standards when the crystal phase is a relevant parameter.

Assessment of catalyst amount

In many publications, fixed masses of different photocatalysts are used and the results are compared without performing any optimization procedure. Generally, very high amounts of photocatalysts are used. It is important to consider that the optimum catalyst amount depends mainly on the optical features of the photocatalyst suspension, the photoreactor geometry, and the properties of the used light source. This problem is not barely an experimental issue, as it dramatically influences the possibility of comparing scientific results. Rate constants are often reported in the literature to compare the activity of various photocatalysts, as usually done in thermal Chemistry. However, this approach is not justified for all of the reactions induced by light in which light absorption mainly influences the reaction. Therefore, most of previously reported comparisons have to be taken with care. In fact, the reaction rate depends on the absorbed light intensity, which is difficult to be estimated, especially in heterogeneous systems where scattering and reflection phenomena cannot be disregarded. This problem can be faced by solving the radiant transport equation locally describing the radiant field, or by introducing simplifications which allow

a semiquantitative comparison, at least within one research group where, generally, one reactor type is used. For instance, it has been proposed to measure the reaction rate as a function of the increasing catalyst amount. The reaction rate first increases linearly and then reaches a plateau. In irradiated slurries the photoreaction rate depends on the rate of photon absorption, which in turn depends on the concentration of the species which can absorb light. At high catalyst amounts per unit volume the observed reaction rate generally reaches a plateau because the increase of reaction rate due to the increased exposed area is balanced by the reduced penetration depth of photons. Indeed, for amounts of catalysts higher than an optimum value which depends on the system under investigation, only the dispersion layers closer to the light source are effectively irradiated, whilst the farthest layers are shadowed by the nearest ones, thus reducing the active reaction volume of the reactor. For these reasons, in order to compare the photoactivity of different photocatalysts it is important to select their amount close to the onset of the plateau region, where most of the incident photons are absorbed by the reacting suspension. Some authors select the catalyst amount by means of photon flux measurements, as the one which ensures that not more than 10% of the incident radiation exits the reacting suspension.

Model compounds for photocatalytic tests

As a matter of fact, dyes are the most used model compounds for photocatalytic tests. This is mainly due to the very simple analytical techniques, generally UV-Vis spectroscopy, used for their quantification in liquid solutions even at low concentrations. However, the utilization of dyes as model pollutants should be limited as their use undermines the generality required when testing novel photocatalysts, particularly under visible irradiation. Indeed, the primary light induced step in the presence of dyes may be their light absorption in the visible region and the consequent injection of electrons from their excited state to the conduction band of the semiconductor. In this case an “indirect” photocatalytic mechanism can take place, and no information on the activity of the photocatalyst as the primary light absorbing species could be obtained. For these reasons, it is strange that methylene blue (MB) has become one of the most commonly used model compounds in photocatalysis, and it is not rare to find reports where the visible light photocatalytic activity of some powders is claimed on the basis of MB decolorization tests. Notably, ISO standard 10678:2010 restricts the use of MB only to tests performed under UVA irradiation. In addition to the above mentioned issues common to all dyes, MB presents highly peculiar photochemical properties which make its use in photocatalysis even more odd. In

particular, two electrons reduction of MB yields leuco-methylene blue (colorless), while one electron reduction produces the corresponding pale yellow anion radical. Furthermore, it has been recently pointed out that MB degradation on $InVO_4$ /$BiVO_4$ composites is induced by singlet oxygen generated from triplet oxygen through the well-known visible light induced MB sensitization. Given this highly specific photochemistry of MB, its use as a model pollutant should be discouraged.

Other molecules, absorbing in the UV region, once adsorbed on the semiconductor may form charge transfer (CT) complexes who behave as the light absorbing species, initiating an indirect photocatalytic mechanism. Indeed, this mechanism could allow visible light activation of a system in which neither the photocatalyst nor the adsorbate themselves absorb visible light. Even if the adsorbate is colorless, it could form a colored charge transfer complex chemically interacting with the surface of TiO_2. Therefore, these types of substrates must be avoided when testing novel photocatalysts. In this case a simple diffuse reflectance spectrum of the photocatalyst impregnated with the substrate, may evidence formation of novel CT bands, thus indicating if the molecule is a suitable model compound or not.

Mechanistic Aspects

As pointed out if the semiconductor absorbs the impinging light, the resulting photocatalytic process is called “direct”. On the other hand, when the light absorbing species is the substrate or its charge transfer (CT) complex with the semiconductor, the process is called “indirect.” The two mechanisms can be experimentally distinguished. If the action spectrum, that is, a plot expressing the wavelength dependence of the reaction rate, is similar to the UV-Vis absorption spectrum of the photocatalyst, the mechanism is direct, while if it is similar to the absorption spectrum of the substrate or of the CT complex the mechanism is indirect. Generally, the photogenerated charges reduce and oxidize an electron acceptor (A) and an electron donor (D), respectively. In most of the photocatalytic reactions, the primary redox products $A^{-\cdot}$ and $D^{+\cdot}$ evolve into the final products according to a mechanism which has been classified as type A photocatalysis. Some rare examples of additions of two or three components have been also reported and can be classified as type B photocatalysis.

Recently, it has been observed that the photo-catalytically produced stable compounds further react in the bulk of the solution or catalytically on the surface of the semiconductor thus producing the target species. Worth of note are the

cases where the activity of mixed semiconductors is under consideration. In those cases the optical and electronic properties of the single components and the deriving interactions should be considered to propose a mechanistic hypothesis. Generally, if the bands edges position allows spatial charge separation, the activity of the composites is generally higher than that of the single components. Notably, in some cases, when the components present strong electronic interactions, the resulting electronic structure of the composite is altered compared to the single components so that the energetic values retrieved in literature may not be safely used for mechanistic considerations. This occurs for instance in vanadium, chromium, iron or nickel doped TiO_2 prepared by ion implantation, for GaN–ZnO solid solutions and for some ZnO-Fe_2O_3 systems. The strong interactions between two electronic systems may be unveiled by simple UV-Vis spectroscopy which generally evidences band gap shifts rather than novel adsorption shoulders. Degradation experiments of emerging contaminants are often carried out by measuring the reduction of the pollutant concentration during irradiation time. However, the toxicity of degradation intermediates and by-products may be even higher than that of the starting contaminant. Therefore, it is necessary to investigate the degradation path of the considered substrate in order to determine the highest possible number of generated intermediates along with their toxicity. The total mass balance must be verified by means of total organic carbon (TOC) analysis which gives information on the percentage of mineralization, i.e. the total oxidation of the organics to small molecules where they appear in their highest oxidation state (e.g. CO_2 and H_2O when the substrate contains only C, H, and O). Obviously, the percentage of the initial substrate totally mineralized should be maximized. Notably, TOC analysis is a powerful tool also when photocatalysis is used for synthetic purposes. Indeed, by measuring variation of TOC in the reacting medium, it is possible to determine the amount of CO_2 (inorganic carbon) generated by the total oxidation of the reactant.

Modeling photocatalytic reactions

Photo-adsorption

The dark adsorption properties of many semiconductors with respect to specific substrates cannot be neglected. As generally the substrate concentration is measured in solution, the adsorbed amount under dark should be taken into consideration. Therefore, it is advisable before illumination of the photocatalytic system, to wait until adsorption-desorption equilibrium is obtained. This may be easily done by measuring the substrate concentration prior to irradiation until a

constant value is reached. Analogously, dissolved oxygen concentration must reach its saturation limit at the given experimental conditions before irradiation. Despite the important role played by dark adsorption in photocatalysis, as above mentioned, a thorough discussion on this topic is out of the aims of the present work. In fact, unlike the thermally activated catalytic reactions, where dark adsorption is of fundamental importance as testified by the endless related literature, light induced processes must also take into account the interaction of molecules with an irradiated surface. Indeed, the surface of the photocatalyst dramatically changes under irradiation, thus causing photo-adsorption and/or photo-desorption phenomena, depending on many factors such as crystal phase and crystallinity, surface properties of catalyst, features of adsorbed molecules, radiation spectra and its intensity in the measured region, pH, and solvent features. Unfortunately, dark adsorption tests are often straightforwardly related with the photoactivity. Even if, generally, strongly adsorbed substrates (in the dark) may be degraded faster than weakly adsorbed ones, the interaction molecule-surface may dramatically change under irradiation. For this reason, photo-adsorption and photo-desorption phenomena must be taken into account, although they are difficult to be estimated due to the fact that during irradiation the substrate not only photoadsorbs or photodesorbs, but it is also chemically consumed. Moreover, the formed intermediates may compete with the substrate so that several parameters are involved making the problem challenging.

It has been proposed a method to evaluate the photo-adsorption phenomena in liquid-solid systems. This study allows to evaluate the photo-reaction mechanism and kinetics on the catalyst surface in real operative reaction conditions and to correctly compare the performance of different photocatalytic systems.

The Langmuir-Hinshelwood (LH) model can be used satisfactorily for the description of the observed kinetics of a catalytic reaction. This model assumes that the rate determining step is the reaction between reactants adsorbed in monolayer onto the catalytic surface and that the adsorption/ desorption steps are rapid equilibrium processes. Moreover, both reaction rate and adsorption isotherm have the same analytical form (i.e. saturation function of Langmuir isotherm form). However, in the case of photo-induced processes some precautions should be taken. For instance, the dark adsorption equilibrium constant is not the same as the equilibrium photo-adsorption constant which depends also on the light absorption. The obtained equation by using LH model for photo0adsorption determination is shown

$$\frac{V}{WS_S}\cdot\frac{1}{kK_L^*}\ln\frac{C_{L,0}}{C_L}+\frac{V}{WS_S}\cdot\frac{1}{k}\left(C_{L,0}-C_L\right)+\frac{1}{S_S}\cdot\frac{N_S^*}{k}\ln\left(\frac{1+K_L^*C_L}{1+K_L^*C_{L,0}}\frac{C_{L,0}}{C_L}\right)=t$$

[equation x]

in which, C_L is the concentration in the liquid phase [M] at time t, $C_{L,0}$ the substrate initial concentration [M] after photo-adsorption equilibrium is established, k the pseudo-first-order rate constant [mol m^{-2} h^{-1}], K^*_L the Langmuir equilibrium photo-adsorption constant [M^{-1}], N^*_S the maximum capacity of photo-adsorbed moles of substrate [mol g^{-1}], $N^*_{S\ ox}$, the maximum capacity of photo-adsorbed moles of oxygen [mol g^{-1}], S_S the catalyst specific surface area [m^2 g^{-1}], t the time [h], V the volume of the liquid phase [dm^3], W the mass of catalyst [g].

The value of $C_{L,0}$ is unknown but it could be determined by the regression analysis carried out with the experimental data obtained after starting irradiation.

Equation x contains four unknown parameters, K^*_L, N^*_S, k, and $C_{L,0}$, whose determination may be carried out by a best fitting procedure. Indeed, k and $C_{L,0}$ may be determined considering the two asymptotic situation of the Langmuir isotherm at very low and very high substrate concentrations. At very high substrate concentration ($K^*_L C_L \gg 1$) the fractional sites coverage by the substrate can be written as:

$$\theta_{Sub}=\frac{n_S}{WN_S^*}=\frac{K_L^*C_L}{1+K_L^*C_L}\approx 1$$

which leads to the following equation:

$$C_L=C_{L,0}-\frac{WS_S}{V}k\cdot t$$

representing a linear relationship between the substrate concentration in the solution and the irradiation time. The intercept and slope allow to determine the $C_{L,0}$ and k values.

At very low concentrations the inequality $K^*_L\ C_L \ll 1$ is assumed to hold and the fractional sites coverage by the substrate becomes:

$$\theta_{Sub} = \frac{n_S}{WN^*_S} = \frac{K^*_L C_L}{1 + K^*_L C_L} \approx K^*_L C_L$$

leading to the following equation:

$$\frac{C_{L,0}}{C_{T,0} - C_{L,0}} = \frac{V}{WN^*_S K^*_L} + \frac{V}{WN^*_S} C_{L,0}$$

in which $C_{T,0}$ is the total initial concentration of the substrate (adsorbed onto the catalyst and dissolved in solution). Also this Equation represents a straight line in which $C_{L,0}$ /($C_{T,0} - C_{L,0}$) is the dependent variable, $C_{L,0}$ is the independent variable, V/($WN^*_S\ K^*_L$) is the linear coefficient, and V/(WN^*_S) is the slope of the straight line. Thus, by plotting $C_{L,0}$ /($C_{T,0} - C_{L,0}$) versus $C_{L,0}$, one can determine the maximum adsorption capacity, N^*_S, and the equilibrium photo-adsorption constant, K^*_L, respectively.

Determination of K^*_L allows checking the inequalities expressed by $K^*_L\ C_L \gg 1$ and $K^*_L\ C_L \ll 1$. For the runs for which the previous inequalities do not hold, Equation x must be used for determining the only unknown parameter contained in it, that is, the $C_{L,0}$ value.

It could be interesting to present, as an example, the determination of the photo-adsorption of benzyl alcohol on a mainly amorphous home-prepared TiO_2 photocatalyst. Figure reports the photoactivity results obtained from representative runs carried out at different initial benzyl alcohol concentrations under UV irradiation by using the same amount of HP0.5 (0.4 g/L). The concentration values reported for zero time correspond to those of the starting solution, that is, without catalyst and irradiation. It must be noticed that at the end of a dark period, lasting 30 minutes, the benzyl alcohol concentration in the suspension is only a little smaller than that of the starting solution. Calculations of photoadsorbed amount, however, have been performed by hypothesizing that all the molecules present on the catalyst surface participate to the photo-process

and therefore the concentration of the starting solution has been taken into account.

On this basis the Langmuir isotherm satisfactorily describes the photo-adsorption phenomenon. The validity of Langmuir model to describe photo-adsorption has been confirmed by using its linear form. Indeed, Figure reports the values of the $C_{L,0}/(C_{T,0} - C_{L,0})$ group (obtained with the same mass of catalyst and the same lamp power) versus the equilibrium concentration of benzyl alcohol ($C_{L,0}$). Straight lines represent Equation applicability and a very good fitting ($R2 > 0.99$) with the experimental data (symbols) can be noted.

N^*_S and K^*_L can be retrieved from the slope and the linear coefficient of the straight lines shown in Figure. The obtained values are very similar to those determined by using Equation (standard deviation ca. 4 %). Figure also shows the adsorption results under dark conditions. The LH equilibrium constant (K_L = 350 M^{-1}) and the maximum adsorption under dark conditions ($N_S = 4.57 \cdot 10^{-6}$ $mol \cdot g^{-1}$) values were determined by a least square fitting procedure. It can be noticed that the photon flow absorbed per unit mass of photocatalyst is the parameter which mainly affects the photo-adsorption phenomenon. Indeed, results reported in Figure show that K^*_L N^*_S, and k values increase by increasing the specific photonic absorption. The positive influence of light intensity on the photoadsorption is shown in Figure 9 which reports also results of dark experiments.

The values of K^*_L and N^*_S are one and two orders of magnitude, respectively, higher than those obtained in the absence of irradiation.

Radiant field

The main difference between a photo-process and a classical one is the need of photons which act as reagents for the generation of electron-hole pairs. The photons participating to a reaction can be considered as immaterial reactants, which cannot be mechanically “mixed”, differently from the “conventional” ones.

Then, in order to obtain an optimal and efficient light distribution, the properties of the system (i.e. geometry of the reactor and of the irradiation source) are of fundamental importance.

The radiant field in the reaction environment depends on: (i) light absorbing species; (ii) type of reactor and its geometry; (iii) radiation source; and (iv) type of photocatalyst. The radiant field modeling requires the application of mass balances related with fluid-dynamics aspects, and with the kinetics law. Moreover, it is necessary to know the rate of photon absorption, which cannot be measured locally and may vary much in different points inside a photocatalytic reactor.

The scattering albedo (ω) which considers the optical properties of the photocatalyst (the fraction of dispersed energy) and the optical thickness (τ) which characterizes the degree of opacity of the reacting dispersion are the most important dimensionless parameters to be considered:

$$\omega = \sigma^* / (\sigma^* + k^*)$$

$$\tau = (\sigma^* + k^*) C_{cat.\backslash}. \delta.$$

where C_{Cat} is the photocatalyst mass concentration, δ the thickness of the reaction volume and κ* and σ* the specific absorption and scattering coefficients, respectively. These are average values calculated over the spectrum of the incident radiation. Depending on the particle size, the scattering phenomena involved can be described by using different laws. Rayleigh scattering (elastic scattering) occurs in the presence of particles of very small size ($dp < 0.5$ μm for near-UV radiation). Even if the most rigorous approach to the problem consists in solving the radiation transfer equation, some simplifications may be assumed under certain conditions. One of the most used approximations is that the radiation field intensity within the suspension may be described by means of expressions similar to the Lambert–Beer law (LBL). This approximation is based on the following assumptions: (i) the incident radiation impinges vertically on the suspension which is assumed consisting of parallel rectangular shaped layers, (ii) each layer is subjected to diffuse radiation, (iii) both absorption and scattering coefficients are intrinsic properties of the irradiated layer, (iv) the cosine–Lambert law is valid (hypothesis of isotropic distribution of scattering, neglecting the regular reflection) and in this case the phase function is equal to one, (v) the particles with size smaller than the thickness of the layer are randomly distributed and, (vi) the size parameter z satisfies the following relation:

$Z = [\pi\, d_p\ n\, \lambda / \lambda\ ] > 5$

Experimental methods have been developed to determine the optical parameters under specific conditions. Both scattering and absorption coefficients of aqueous TiO_2 suspensions irradiated by a monochromatic radiation by means of transmitted photon flow measurements were determined. Actinometric analyses, as a function of the mass of photocatalyst allowed to estimate the transmitted light (T) and an asymptotic form of the Kubelka–Munk solution of the radiative transfer equation has been used to determine the scattering and absorption coefficients. The solution of the radiative transfer equation, in its hyperbolic form, may be expressed by Equation

$$T = \frac{\sqrt{\left(1+\frac{\kappa^*}{\sigma^*}\right)^2 - 1}}{\left(1+\frac{\kappa^*}{\sigma^*}\right)\sinh\left[2\sigma^* x\sqrt{\left(1+\frac{\kappa^*}{\sigma^*}\right)^2 - 1}\right] + \sqrt{\left(1+\frac{\kappa^*}{\sigma^*}\right)^2 - 1}\cosh\left[2\sigma^* x\sqrt{\left(1+\frac{\kappa^*}{\sigma^*}\right)^2 - 1}\right]}$$

in which x represents the thickness of the participating medium and the two parameters κ* and σ* are the absorption and scattering coefficients, respectively.

The influence of the optical thickness (i.e. photocatalyst load) on the reaction rate depends on type of solid, particle size and optical parameters previously described. Generally, the dependence between the observed reaction rate and the concentration of the photocatalyst is linear by increasing the amount of photocatalyst. Consequently, a plateau is reached in condition of light saturation, and finally a decrease of the observed reaction rate is observed for high τ, due mainly to the reduced penetration depth of light.

Reaction rate and quantum yield

The intrinsic rate of a photocatalytic reaction depends on the quantum yield and

on the absorbed radiation.

The rate, r̂, per unit mass of photocatalyst is the product of the specific rate of photon absorption, φ^ (SRPA) and the quantum yield η:

$$\hat{r} = \eta \cdot \hat{\varphi}$$

φ^ expresses the moles of photons absorbed per unit mass of photocatalyst and per unit time i.e., the ratio between the volumetric rate of photon absorption, φλ, and the photocatalyst concentration :

$$\hat{\varphi}_\lambda = \frac{\varphi_\lambda}{C_{Cat}}$$

The primary quantum yield can be defined, in general, as the ratio between the moles of molecules reacted in the primary processes (i.e. the initial interfacial electron transfer) and the moles of absorbed photons at wavelength λ:

$$\eta_\lambda = \frac{\text{moles of molecules}_{prim}}{\text{moles of photons at } \lambda \text{ absorb.}}$$

ηλ = moles of molecules$_{prim}$/ moles of photons at λ absorb:

It is possible to find a different definition of quantum yield, the "overall quantum yield", used for practical applications. This parameter is not an intrinsic kinetic parameter, but it depends on the process. It is defined as the ratio between the moles of molecules of the reactant reacted and the moles of absorbed photons at the wavelength λ:

$$\eta_{overall,\lambda} = \frac{\text{moles of molecules reacted}}{\text{moles of photons at } \lambda \text{ absorb.}}$$

For its determination not only the primary events but also all of the other secondary reactions are taken into account.

This has caused many researchers to report a so-called "quantum yield" estimated on the basis of the incident light rather than the light actually absorbed by the heterogeneous system. Indeed, the determination of the absorbed photons implies also the knowledge of the fractions of transmitted, reflected and scattered light in dispersed photocatalytic systems. In some cases, for peculiar experimental set-ups, it is possible to simplify this problem.

It has been proposed to apply the concept of a black body like reactor to measure the quantum yield of photochemical reactions in liquid-solid heterogeneous systems. Due to the reactor geometry and the sufficiently high loadings of photocatalyst, both reflectance and transmittance of light, can be neglected, so that the experimental determination of the quantum yield required only measurements of reaction rates and irradiance of the actinic light.

Studies proposed the application of an integrating sphere to determine the absorbed light and developed a standard protocol using the photodegradation of phenol over TiO_2 (Degussa P25) as the standard photoreaction. Another experimental method which used a macroscopic balance of energy by actinometric measures of transmitted photons.

As far as the photoreactions in gas-solid regimen are concerned, it has been obtained the amount of photons absorbed by a supported photocatalyst by means of a portable radiometer, an optical fiber and a suitable home-made accessory, during the oxidation of isopropyl alcohol, as the test reaction. However, the most rigorous and general approach to determine the quantum yield and to correctly model the kinetics of photocatalytic reactions is to solve the radiation transfer equation (RTE) which considers the effects of absorption and scattering. The solution of RTE has been carried out by using numerical methods based on Monte Carlo simulations and also by means of the discrete ordinate method (DOM), analogously to the case of radiative heat transfer. However, these methods require to perform two independent measurements to obtain separate values of the absorption and scattering coefficients, and moreover they do not provide analytical solutions.

Are average values enough to describe intrinsic kinetics?

Generally, the radiation inside the reactor volume is not homogeneously distributed. Then, in any kinetic experiment, it is necessary to differentiate the local values of the different quantities (quantum yield, SRPA, reaction rate) from their average values, which may be measured by an external observer. The local values (impossible to be experimentally measured) represent the theoretical values that should be known for the evaluation of the “intrinsic kinetics”, i.e. the rate which considers only events occurring at a molecular level. Therefore, by definition the intrinsic kinetics does not depend on phenomena such as radiant energy and mass transport occurring on a macroscopic scale in a real reactor. It is possible to determine experimentally both the quantum yield and the quantum efficiency for geometrically simple systems. In general, their correct evaluation requires the demanding solution of the radiant transport equation. On the other hand, the local values are similar to the average ones for a photo-differential reactor, that is, when the difference between the light entering the system and that transmitted is low (theoretically infinitesimal). This occurs when the catalysts mass concentration is very low. However, in these conditions the reaction time would be very long thus causing experimental disadvantages. Recently, it has been demonstrated that at sufficiently low values of the optical thickness, τ, the

reactor approaches the “photo-differential” behavior and it is possible to use the average values of the reaction rate in the kinetic equation instead of the local values with negligible error. The possibility of operating at this value of the optical thickness is positive because it allows to use the experimentally accessible average values for the kinetic analysis, and at the same time to absorb enough radiant energy with a significant reduction of the reaction time. The maximum acceptable value of the optical thickness depends on the extent and the type of scattering and on the reactor geometry. As an example, for Evonik P25 TiO_2 under UV light irradiation, the optical thickness which makes the reactor similar to a photo-differential one is about 2.5. Moreover, these conditions allow to obtain high values of the average SRPA even at low irradiation conditions. On the contrary, at higher optical thickness values, it is not possible to correctly determine the intrinsic kinetics because the average values significantly differ from the local ones.

Anyway, the local values of the reaction rate and of the SRPA can be obtained by the solution of the radiant energy transfer equation, the flow field and the substrate mass balance. By using these values, the kinetic analysis is rigorous and does not need specific simplifications. To this aim the system needs to be quite strictly modeled. For instance, if the reactor is not well illuminated, a 3D simulation with a suitable number of spatial points and of directions of propagation of the light is required.

Physical meaning of kinetic parameters and different kinetic models

Kinetic analysis is employed to obtain the rate equation and to estimate the related parameters. The Langmuir–Hinshelwood (LH) model is used very often to describe the observed kinetics of most of the photocatalytic reactions in liquid-phase. By assuming LH kinetics for a general photocatalytic degradation process of a species A, the expression for the reaction rate, r_A, can be written as:

$$r_A = k_{LH}\ \theta_A\ \theta_{Ox}$$

where θ_A and θ_{Ox} are the fractional sites coverages by A and O2 and k_{LH} is the second order surface rate constant (which depends mainly upon the radiation flux, I):

$$\theta A = K_A C_A / (1+ K_A C_A$$

$$\theta_{Ox} = K_{Ox} C_{Ox} / (1+ K_{Ox} C_{Ox})$$

K_A and K_{Ox} are the equilibrium adsorption constants, and C_A and C_{Ox} the concentrations of A and oxygen, respectively. It is well known that the adsorption isotherm and the reaction rate may be described by the same analytic form, i.e. the saturation function of the Langmuir adsorption isotherm is formally similar to the Langmuir-Hinshelwood kinetic rate form. On the contrary, the dark adsorption equilibrium constant (K_A) is not the same as the apparent adsorption constant under irradiation. This was experimentally evidenced which observed, for the photocatalytic degradation of imazapyr, that the apparent adsorption constant obtained under irradiation was significantly larger than the adsorption constant obtained in the dark. These findings highlight the purely empirical nature of the Langmuir approach which, even if useful for predictive and design purposes, can be hardly substantiated mechanistically for light induced reactions. In fact, under irradiation of suitable energy, the surface of the solid undergoes a change in its physico-chemical properties and the Langmuir Hinshelwood type kinetic expression for semiconductor photocatalysis can be written as:

$$r_A = k'_{LH} \cdot \frac{K'_A C_A}{1 + K'_A C_A}$$

$k'_{LH} = k \cdot I^{\alpha}$ is a proportionality constant (I is the incident irradiance) which depends on the system. The term α, is equal to 1 at low values of I and to 0.5 at high values of I. K'_A is the Langmuir apparent adsorption constant which can be experimentally determined together with k'_{LH}, by plotting the reciprocal of the initial reaction rate as a function of the reciprocal of C_A, that generally yields a straight line.

The physical meaning of the Langmuir adsorption coefficient K'_A is depending on the mechanism hypothesized. However, by considering the same photocatalytic reaction, the values of k'_{LH} and K'_A differently depend on the light intensity. In fact, increasing the light intensity results in decreasing K'_A and increasing k'_{LH}. On the other hand, K_A does not depend on light intensity, as it is the ratio between the adsorption and the desorption rate constants under dark, which individually have the same dependence on light intensity.

The light intensity dependence of K'_A is apparent by considering the following mechanism. Excitation of the light absorbing species S produces an activated state (S*) which in turn can undergo radiative or nonradiative quenching or react with a reactant A to give the product :

$$S + h\nu \rightarrow S^*$$

$$S^* \rightarrow h\nu + S$$

$$S^* \rightarrow heat + S$$

$$S^* + A \rightarrow Product$$

In the presence of photogenerated charges the following Equations should be also considered:

$$S + e^-(h^+) \rightarrow S^-(S^+)$$

$$S^-(S^+) + h^+(e^-) \rightarrow S$$

On the basis of this mechanism, the kinetics can be described according to the Langmuir-Hinshelwood or the Eley-Rideal approach if the species A reacts after adsorption or directly from the liquid or gas phase:

$$r_A = \frac{k_1 k_2 I^{\alpha} C_A}{1 + k_2 C_A}$$

where k_1, k_2 and α are fitting constants.

However, under irradiation adsorption/desorption equilibria of reactants are generally not established due to the fast reactivity of the photogenerated charges or radicals. Therefore a pseudo steady state approach should be used not only for the intermediates (as in the original LH model where steady state adsorption/desorption of reactants was inferred) but also for reactants.

For this reason, the simple LH model (which can be straightforwardly applied to thermally activated reactions is simply a manifestation of saturation-type kinetics and cannot universally describe light induced processes in heterogeneous systems. As a consequence, the kinetic parameters can be hardly mechanistically substantiated and their physical meaning is rather questionable.

Modifications of the LH model have been proposed to take into account these problems as, for instance, the disrupted adsorption model or others based on the direct and/or indirect transfer mechanism:

$$r_A = kI^{\alpha}C_A = \frac{k_1 I^{\alpha} C_{A,sol}}{1 + k_2 I^{\alpha} + k_3 C_{A,sol}}$$

Many of these models present various adjustable parameters which decrease their degree of generality. It has been adopted an original model expressed by an equation containing only one kinetic parameter (k) and some relevant variables such as the rate of photon absorption (φ), concentration of substrate (C_A), oxygen (C_{Ox}) and catalyst (C_{Cat}):

$$r_A = k\left(\sqrt{1 + 2\frac{\varphi/C_{Cat}}{kC_{Ox}C_A}} - 1\right) \cdot C_{Ox}C_{Cat}C_A$$

The catalyst concentration can be eliminated by considering the values of reaction rate (^rA) and rate of photon absorption (φ^) per unit mass of photocatalyst:

$$\hat{r}_A = \eta \cdot \hat{\varphi} = k \cdot C_{Ox}C_A\left(\sqrt{1 + \hat{\varphi} \cdot \frac{2}{k \cdot C_{Ox}C_A}} - 1\right)$$

where η is the quantum yield.

Kinetic parameters determination

The rate law is characterized by kinetic parameters whose number should be minimized in order to avoid overfitting. At the same time the number of parameters should be enough to afford a model with good descriptive capability.

As mentioned ,the knowledge of the rate of photon absorption is of paramount importance to carry out a correct kinetic analysis. However, its local value cannot be experimentally obtained in a real photocatalytic reactor. For this reason, the intrinsic rate of reaction is not experimentally accessible and may greatly differ from the average rate of reaction which, on the contrary, may be directly determined. It has been shown that the differential and/or the integral methods of kinetic analysis may be used if a suitable mathematical model satisfactorily describes the essential features of the reaction. Both the methods have been applied in photocatalysis often neglecting problems related to the specific task of irradiating a slurry system. Some of them are listed below:[

1. Most of the proposed laws are similarly consistent with the experimental results. This confirms the difficulty to mechanistically substantiate a kinetic model. Furthermore, for engineering purposes, it implies the need of choosing a congruent number of data to minimize experimental errors and correctly evaluate the best fit.

2. Soon after the beginning of a photocatalytic reaction, intermediate products are formed and agglomeration of particles may occur. A correct kinetic analysis must explicitly consider the effects of these phenomena as for instance. Alternatively, experimental data must be retrieved at sufficiently short reaction times, when these phenomena are surely negligible.

3. The non-linearity of the kinetic equations in C_S and φ^ imposes the use of non-linear regressions. Although linearization would simplify the problem from a numerical point of view, it would afford an inaccurate kinetic analysis.

4. The local values of the quantities of interest (SRPA, reaction rate, quantum yield) may greatly differ from their average values. While the average values could in theory be measured by an external observer, the local values cannot be experimentally retrieved. Therefore, if the radiant field distribution is unknown, the "intrinsic kinetics" cannot be determined, unless the reactor behavior is photo-differential, that is, when SRPA does not significantly change inside the reactor.
5. The distribution of the SRPA may be obtained by solving the radiant transport equation (RTE). While analytical solutions of RTE are possible only in few cases (simple geometries and boundary conditions) numerical methods such as Monte Carlo, discrete ordinate and finite volume methods. and recently some CFD (Computational Fluid Dynamics) software (ANSYS Fluent, 2015. User's guide, version 6.3. COMSOL Multiphysics, 2015. Heat transfer module, User's guide

version 5.2) accurately describe the radiation field when the spatial and directional discretization is sufficiently fine.

When the reaction is performed in the presence of photocatalysts immobilized on specific supports the post process separation of the powder required in slurry systems can be avoided, but the influence of mass transfer phenomena (inside and/or outside the film) cannot be disregarded.

The effectiveness factor η_F is a good indicator of the extent of the influence of mass and photons transport limitation for a supported photocatalytic film:

$$\eta_F = \frac{\text{observed reaction rate}}{\text{reaction rate at } C_S = C_{S0} \text{ and } I = I_0}$$

in which the reaction rate is calculated at the initial concentration of the substrate (C_{SO}) and at the light intensity impinging on the film.

The trend of the observed rate of reaction as a function of the film thickness is different when the film is irradiated from the top or from the rear side. In the first case the rate increases up to a plateau, while it reaches a maximum and then decreases in the second case. It has been highlighted the influence of the porosity of the film by introducing, along with the internal diffusion, also the dependence of the reaction rate on external mass transport.

References

[1] Fujishima, A.; Honda, K. Electrochemical Photolysis of Water at a Semiconductor Electrode. Nature. 1972, 238, 37–38. DOI: 10.1038/238037a0.

[2] Schiavello, M., Ed. Photoelectrochemistry, Photocatalysis, and Photoreactors. Fundamentals and Developments; Reidel: Dordrecht, Holland, 1985. ISBN: 9027719462-9789027719461.

[3] Schiavello, M., Eds. Heterogeneous Photocatalysis; Wiley: Chichester, UK, 1997.

[4] Serpone, N.; Pelizzetti, E., Eds. Photocatalysis: Fundamentals and Applications; Wiley: New York, 1989. ISBN: 9780471967545-20160527.

[5] Hashimoto, K.; Irie, H.; Fujishima, A. TiO2 Photocatalysis: A Historical Overview and Future Prospects. Jpn. J. Appl. Phys. 2005, 44, 8269–8285. DOI: 10.1143/JJAP.44.8269.

[6] Fujishima, A.; Zhang, X.; Tryk, D. A. TiO2 Photocatalysis and Related Surface Phenomena. Surf. Sci. Rep. 2008, 63, 515–582. DOI: 10.1016/j.surfrep.2008.10.001.

[7] Braslavsky, S. E.; Braun, A. M.; Cassano, A. E.; Emeline, A. V.; Litter, M. I.; Palmisano, L.; Parmon, V. N.; Serpone, N. Glossary of Terms Used in Photocatalysis and Radiation Catalysis (IUPAC Recommendations 2011). Pure Appl. Chem. 2011, 83, 931–1014. DOI: 10.1351/pac200779030293.

[8] Dionysiou, D. D.; Suidan, M. T.; Baudin, I.; Laîné, J.-M. Effect of Hydrogen Peroxide on the Destruction of Organic Contaminants-Synergism and Inhibition in a Continuous-Mode Photocatalytic Reactor. Appl. Catal. B. 2004, 50, 259–269. DOI: 10.1016/S0926-3373(04)00087-6.

[9] Özcan, L.; Yurdakal, S.; Augugliaro, V.; Loddo, V.; Palmas, S.; Palmisano, G.; Palmisano, L. Photoelectrocatalytic Selective Oxidation of 4-Methoxybenzyl Alcohol in Water by TiO2 Supported on Titanium Anodes. Appl. Catal. B. 2013, 132–133, 535–542. DOI: 10.1016/j.apcatb.2012.12.030.

[10] Wang, C.; Zhang, X.; Liu, Y. Promotion of Multi-Electron Transfer for Enhanced Photocatalysis: A Review Focused on Oxygen Reduction Reaction. Appl. Surf. Sci. 2015, 358, 28–45. DOI: 10.1016/j.apsusc.2015.08.055.

[11] Kiwi, J.; Grätzel, M. Heterogeneous Photocatalysis: Enhanced H2 Production in TiO2 Dispersions under Irradiation. The Effect of Mg Promoter at the Semiconductor Interface. J. Phys. Chem. 1986, 90, 637–640. DOI: 10.1021/j100276a031.

[12] Parrino, F.; Palmisano, L. Reactions in the Presence of Irradiated Semiconductors: Are They Simply Photocatalytic? Mini-Rev. Org. Chem. 2018, 15, 157–164. DOI: 10.2174/ 1570193X14666171117151718.

[13] Augugliaro, V.; Camera Roda, G.; Loddo, V.; Palmisano, G.; Palmisano, L.; Soria, J.; Yurdakal, S. Heterogeneous Photocatalysis and Photoelectrocatalysis: From Unselective Abatement of Noxious Species to Selective Production of

High-Value Chemicals. J. Phys. Chem. Lett. 2015, 6, 1968–1981. DOI: 10.1021/acs.jpclett.5b00294.

[14] Hetterich, W.; Kisch, H. Heterogeneous Photocatalysis. V. Cadmium-Zinc Sulphides as Catalysts for the Photodehydrodimerization of 2,5 Dihydrofuran. Chem. Ber. 1988, 121, 15–20. DOI: 10.1002/cber.19881210104.

[15] Fujishima, A.; Rao, T. N.; Tryk, D. A. Titanium Dioxide Photocatalysis. J. Photochem. Photobiol. C. 2000, 1, 1–21. DOI: 10.1016/S1389-5567(00)00002-2.

[16] Fox, M. A.; Dulay, M. T., Heterogeneous Photocatalysis. Chem Rev. 1993, 93, 341–357. DOI: 10.1021/cr00017a016.

[17] Hoffmann, M. R.; Martin, S. T.; Choi, W.; Bahnemann, D. W. Environmental Applications of Semiconductor Photocatalysis. Chem Rev. 1995, 95, 69–96. DOI: 10.1021/cr00033a004.

[18] Kou, J.; Lu, C.; Wang, J.; Chen, Y.; Xu, Z.; Varma, R. Selectivity Enhancement in Heterogeneous Photocatalytic Transformations. Chem Rev. 2017, 117, 1445–1514. DOI: 10.1021/acs.chemrev.6b00396.

[19] Dozzi, M. V.; Selli, E. Doping TiO2 with p-Block Elements: Effects on Photocatalytic Activity. J. Photochem. Photobiol. C. 2013, 14, 13–28. DOI: 10.1016/j.jphotochemrev.2012.09.002.

[20] Ong, W.-J.; Tan, L.-L.; Ng, Y. H.; Yong, S.-T.; Chai, S.-P. Graphitic Carbon Nitride (gC3N4)-Based Photocatalysts for Artificial Photosynthesis and Environmental Remediation: Are We a Step Closer to Achieving Sustainability? Chem Rev. 2016, 116, 7159–7329. DOI: 10.1021/acs.chemrev.6b00075.

[21] Maeda, K. Photocatalytic Water Splitting Using Semiconductor Particles: History and Recent Developments. J. Photochem. Photobiol. C. 2011, 12, 237–268. DOI: 10.1016/j. jphotochemrev.2011.07.001.

[22] Hisatomi, T.; Kubota, J.; Domen, K. Recent Advances in Semiconductors for Photocatalytic and Photoelectrochemical Water Splitting. Chem. Soc. Rev. 2014, 43, 7520–7535. DOI: 10.1039/C7CC01190C.

[23] Oh, Y.; Hu, X. Organic Molecules as Mediators and Catalysts for Photocatalytic and Electrocatalytic CO2 Reduction. Chem. Soc. Rev. 2013, 42, 2253–2261. DOI: 10.1039/ C2CS35276A.

[24] Yamazaki, Y.; Takeda, H.; Ishitani, O. Photocatalytic Reduction of CO2 Using Metal Complexes. J. Photochem. Photobiol. C. 2015, 25, 106–137. DOI: 10.1016/j. jphotochemrev.2015.09.001.

[25] Emeline, A. V.; Ryabchuk, V. K.; Serpone, N. Dogmas and Misconceptions in Heterogeneous Photocatalysis. Some Enlightened Reflections. J. Phys. Chem. B. 2005, 109, 18515–18521. DOI: 10.1021/jp0523367.

[26] Ohtani, B. Preparing Articles on Photocatalysis - beyond the Illusions, Misconceptions, and Speculation. Chem. Lett. 2008, 37, 217–229. DOI: 10.1246/cl.2008.216.

[27] Herrmann, J. M. Photocatalysis Fundamentals Revisited to Avoid Several Misconceptions. Appl. Catal. B. 2010, 99, 461–468. DOI: 10.1016/j.apcatb.2010.05.012.

[28] Ohtani, B. Photocatalysis A to Z: What we Know and what we do not Know in a Scientific Sense. J. Photochem. Photobiol. C. 2010, 11, 157–178. DOI: 10.1016/j. jphotochemrev.2011.02.001.

[29] Di Paola, A.; Bellardita, M.; Megna, B.; Parrino, F.; Palmisano, L. Photocatalytic Oxidation of Trans-Ferulic Acid to Vanillin on TiO2 and WO3-Loaded TiO2 Catalysts. Catal. Today. 2015, 252, 195–200. DOI: 10.1016/j.cattod.2014.09.012.

[30] Sun, X.; Dai, W.; Wu, G.; Li, L.; Guana, N.; Hunger, M. Evidence of Rutile-to-Anatase Photo-Induced Electron Transfer in Mixed-Phase TiO2 by Solid-State NMR Spectroscopy. Chem Commun. 2015, 51, 13779–13782. DOI: 10.1039/C5CC04971G.

[31] Monticone, S. Tufeu, R.; Kanaev, A. V.; Scolan, E.; Sanchez, C., Quantum Size Effect in TiO2 Nanoparticles: Does It Exist? Appl. Surf. Sci. 2000, 162–163, 565–570. DOI: 10.1016/S0169-4332(00)00251-8.

[32] Yurdakal, S.; Palmisano, G.; Loddo, V.; Augugliaro, V.; Palmisano, L. Nanostructured Rutile TiO2 for Selective Photocatalytic Oxidation of Aromatic Alcohols to Aldehydes in Water. J. Am. Chem. Soc. 2008, 130, 1568–1569. DOI: 10.1021/ja709989e.

[33] Francesco Parrino , Vittorio Loddo , Vincenzo Augugliaro , Giovanni CameraRoda , Giovanni Palmisano , Leonardo Palmisano , and Sedat Yurdaka, Heterogeneous photocatalysis: guidelines on

experimental setup, catalyst characterization, interpretation, and assessment of reactivity, *Catalysis Reviews*, 2019, 61,163-213; https:// doi.org/ 10.1080/01614940.2018.1546445]

The Current Status of Hydrogen Economy

Hydrogen Economy has been vigorously pursued for the past five decades. There are various analyses accounting for the delay in the introduction of this economy. In this article, some of the other intrinsic elements are being examined and how these elements are still not allowing the economy to come into force.

1. Introduction

Hydrogen Economy [1] and Methanol Economy [2] are the two prominent terms among others that are used for the past few decades for energy starved world. The realization that hydrogen will be the fuel of the future is revealed in the words of Jules Verne [3] in as early as 1874 namely "**Water will one day be employed as fuel, that hydrogen and oxygen which constitute it, used singly or together, will furnish an inexhaustible source of heat and light, of an intensity of which coal is not capable… When the deposits of coal are exhausted we shall heat and warm ourselves with water. Water will be the coal of the future**." Unfortunately electrochemical conversion of water into its constituents, is not as easy as conceived by Jules Verne, but possibly relies on advanced electro-catalysts. Despite the technology being the subject of on-going statement that "Fuel cell technology is always 10 years", perhaps the future Jules Verne is referring to is now. Hydrogen can be used as fuel cell for electricity generation, though the efficiency of this conversion has been claimed to be higher than direct combustion [4]. There are various versions of fuel cells and a simplified schematic version is shown in **Fig.1. E**ven though there are a variety of options in the choice and design of fuel cells, the cost of converting fuel into electricity has not reached the level that is competitive to other modes of electricity production. In addition, the economically viable design and fabrication have

been eluding the scientific community for several decades. There are various reasons for this situation notably the use of the costly noble metal electrodes and also the formulation of cost effective membrane as substitute to Nafion ®[5] as at present the nafion® membranes alone appear to be suited.

There are various other debates on the feasibility and possibility of hydrogen economy coming into force. The transition to "Hydrogen Economy" is a sea change in the energy infrastructure and is not to be taken lightly. As an energy carrier, hydrogen is to be compared to electricity, the only wide spread and viable alternative. When hydrogen is employed to transmit renewable electricity, only 50% can reach the end user due to losses in electrolysis, hydrogen compression and the fuel cell. The rush into a

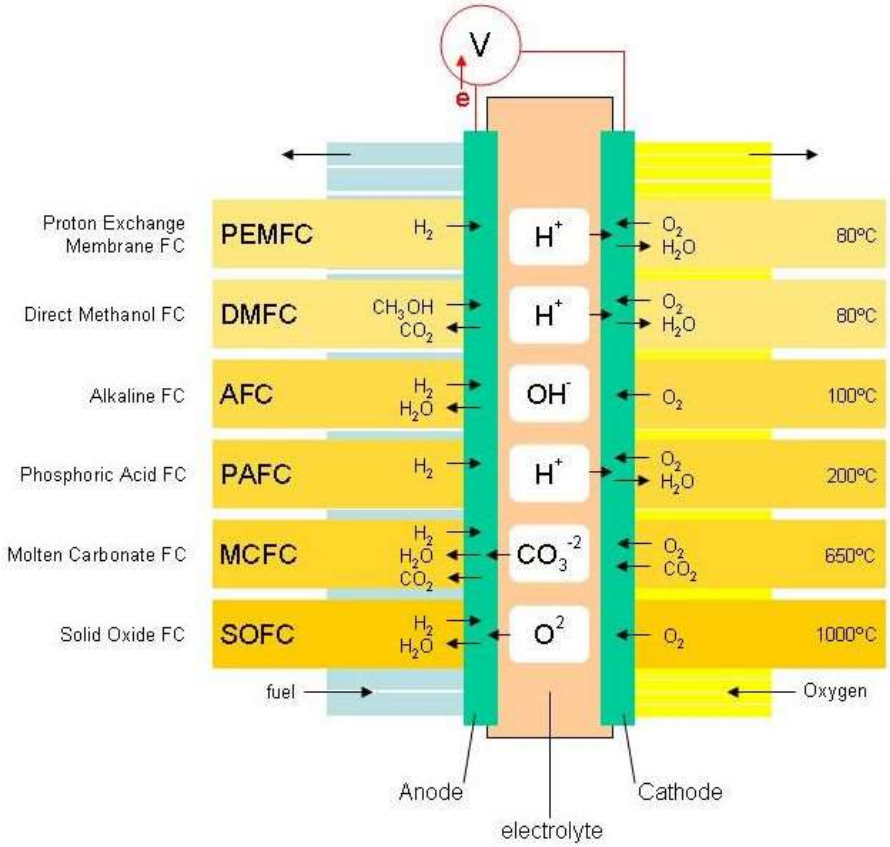

Fig.1. Different types of fuel cells based on temperature of operation and electrolytes.

Hydrogen economy is neither supported by energy efficiency arguments nor justified with respect to economy or ecology. In fact, it appears that hydrogen will not play an important role in a sustainable energy economy because the synthetic energy carrier cannot be more efficient than the energy from which it is made. Renewable electricity is distributed well by electrons than by hydrogen. Because of the wastefulness of a hydrogen economy, the promotion of hydrogen may counteract all reasonable measures of energy conservation. Even worse, the

forced transition to a hydrogen economy may prevent the establishment of a sustainable energy economy based on an intelligent use of precious renewable resources [6]. These views of these authors can be considered in the present context are very pessimistic. There are various components of hydrogen Economy and a simplified version of these components is schematically shown in **Fig.2**. The essential commercial components of this economy are the production from various sources and since hydrogen under normal conditions is in gaseous state its safe and economic storage (solid state storage among the various possibilities is preferred for various reasons) is another important component.

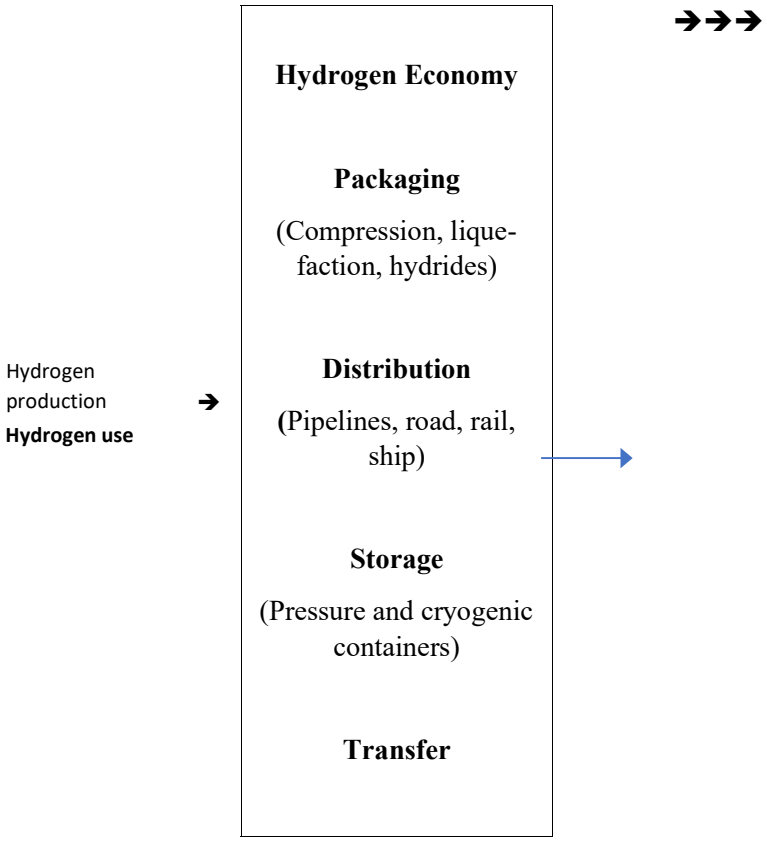

Fig.2. Schematic representation of key components of hydrogen Economy [Adopted from ref.7]

2. Hydrogen Production

Hydrogen can be produced from various sources like fossil fuels, water and other organic compounds (refer to **Fig.3.**). In this section, the prospects of hydrogen production from water alone can be considered in some detail.

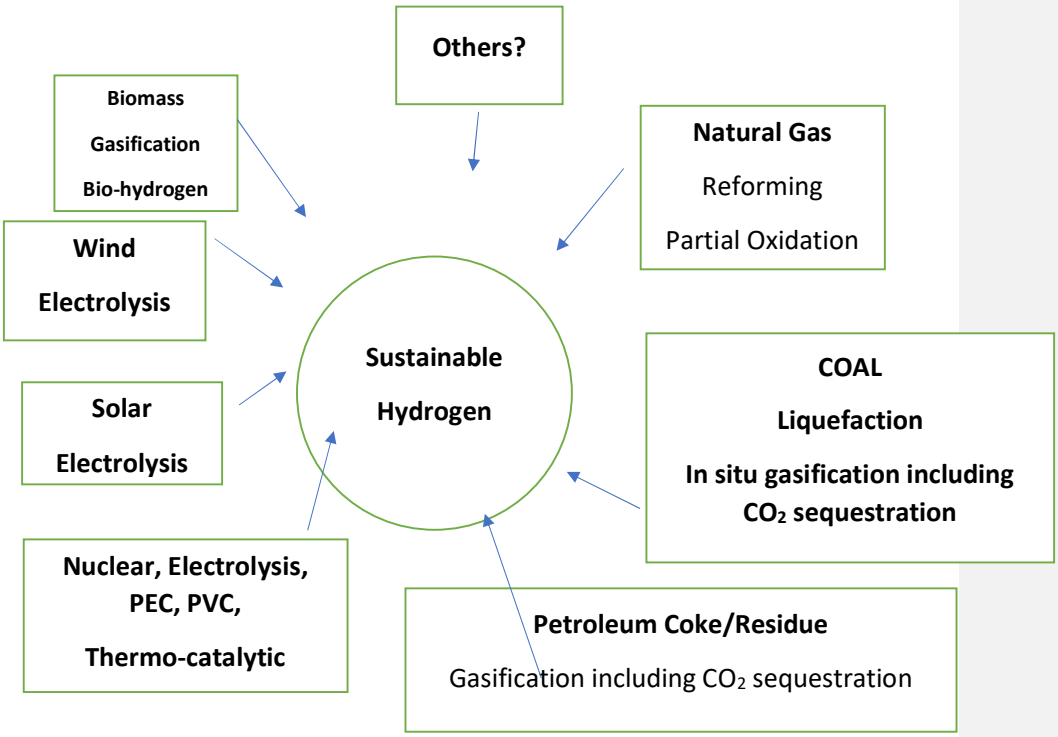

Fig.3. Possible Hydrogen Production Sources

Even though there are many options for the production of hydrogen, electrolysis based methods are probably preferred due to the level purity of hydrogen produced. The harnessing hydrogen by electrolysis cannot be carried out at the thermodynamic reversible potential (1.229V) due to various conventional over-potential restrictions, which are a loss from commercial point of view. There are various estimates of the cost of hydrogen in comparison to other conventional fuels and the inference that comes out of these analyses is that at a commercial level introduction of hydrogen will require some more time.

The Hydrogen Council states the international hydrogen market may be worth around US$2.5 trillion by 2050, possibly accounting to 18-30 percent of global energy demand and reducing carbon dioxide emissions by 6 gigatonnes per year [8].

Though there are various examinations on the prospects of hydrogen Economy coming into force [9]. These projections predict that hydrogen Economy will be in force in the near future at least in fifteen of the countries. These predictions are based on statistical analyses. However, the real stumbling block in achieving this goal depends on research and development in certain vital components of Hydrogen Economy. In this presentation, some aspects of these efforts are briefly reviewed.

The first component of hydrogen economy is hydrogen production. Apart from reforming of hydrocarbons, the only other option doe hydrogen production is based on electrolysis. General electrolysis as stated is governed by over potential restrictions and also the design and fabrication of electrolysis cells and the electrode fabrication with correct geometry and required textural characteristics. These components of electrolysis make this process not economically viable.

Photo-electrochemical decomposition of water has been evolving as one of the processes that will evolve as a commercially viable processes [10] Various attempts like band gap engineering and modifying or sensitizing the semiconductor have been attempted in the last 50 years but still no single semiconductor material has been identified which will promote this reaction in a

economically viable. A simple complication of these attempts is given in **Tables.1 and 2**.

Table 1: Photo-electrochemical splitting of water on various catalysts

Photo-catalyst	Wight (g)	Reaction system	Light source	Rate of evolution (µmol/h)	
			[[a] Hg lamp [b] others	H_2	O_2
Pt/TiO_2	0.3	2.17 M Na_2CO_3	400 W {a}	568	287
ZrO_2	1.0	Distilled water	400 W{a}	72	36
Pt/ZrO_2	1.0	).94M $NaHCO_3$	400W{a}	120	61
Ru_2O/ZrO_2	1.0	Distilled water	400W{a}	11	5
Cu/ZrO_2	1.0	Distilled water	400W{a}	14	6
$NiO/Sr_2Nb_2O_7$	1.0	Distilled water	400W{a}	110	36
$NiO/Sr_2Ta_2O_7$	1.0	Distilled water	400 W{a}	1000	480
Ortho-$BaTa_2O_6$	1.0	Distilled water	400 W{a}	33	15
$NiO/BaTa_2O_6$	1.0	Distilled water	400 W{a}	629	303
$Ni/Rb_4Nb_6O_{17}$	1.0	Distilled water	400 W[a]	036	451
Pt/TaON	0.2	5mM NaI	300 W[b]	24	12
$K_4Nb_6O_{17}$	1.0	Water	450 W[a]	8	1
NiO/ $K_4Nb_6O_{17}$	1.0	Water	450 W[a}	77	37
$Pt/SrTiO_3/RhWO_3$	0.3	2mM $FeCl_2/FeCl_3$	500 W[b]	1.6	0.8

Commented [v1]:

Table 2. Photo-electrochemical water splitting reaction on various Electrodes

Photo-electrode	Area (Cm^2)	Electrolyte	Light source	Efficiency /H_2 yield	Applied Bias (V)
TiO_2	1	Fe^{3+} solution	500 W Xe	QE = 10%	NA
$SrTiO_3$	0.25	0.5 M NaOH	Argon Laser	QE = 11%	NA
$SrTiO_3$	154	1M NaOH	150 W Halogen lamp	QE – 3.5%	0.5
TiO_2	2	0.5 M H_2SO_4/ 1M NaOH	UV 25 mW/cm^2	60 micromol in 8hr	NA
$Vis\text{-}WO_3/Vis\text{-}TiO_2$	2	0.025MH_2SO_4/0.05 M NaOH	UV 2.5mWcm^2	39 micromol in 8 h	NA
$Vis\text{-}WO_3/Vis\text{-}TiO_2$	2	0.025MH_2SO_4/0.05 M NaOH	A.M. 1.6	6 micromol in 8 h	NA

Pillar TiO_2	2	0.5M H_2SO_4/1M NaOH	UV,25 mW/cm^2	37 micromol in 8 h	NA
WSe_2	0.0125	1M KI + 0.05 MI_2	60 mW tungsten lamp	ABPE = 17.1%	NA
p-GaAs/n-GaAs/p-$GaInP_2$	0.2	3M H_2SO_4	150 W , W-halogen lamp	ABPE-12.4%	0.3
$GaInP_2$/GaAs	0.5	2MKOH	75W Xe lamp	ABPE = 16.5%	NA
Si	0.3	2M KOH	75W Xe lamp	ABPE = 7.5%	NA
ALGaAs/si	0.22	1M $HCLO_3$	50W W-halogen lamp	ABPE = 18.3%	NA
n-TiO_2	0.2	5M KOH	150 W Xe	ABPE = 8.3%	0.3
n-TiO_2	0.2	5MKOH	150 W Xe	ABPE=1.08%	0.6

It is seen from the data shown in Tables 1 and 2, several semiconductor materials and photo-catalytic systems have been tried for water splitting of water under irradiation. It has been observed that photo-induced charge separation, preventing back reaction, effective utilization of charge carriers generated, are the essential components for achieving high photo-conversion efficiency. The hole that is created on photon absorption has to be scavenged by suitable sacrificial agents in order to increase the efficiency of the processes, which will also reduce recombination. Another aspect of the present studies is the design of suitable reactor configuration so that both hydrogen and oxygen are separately harnessed in safe manner.

Various synthetic methodologies have been proposed and new configurations (Z-scheme or dye sensitization) have been attempted to increase the efficiencies of the process.

At this stage the photo-electrochemical decomposition of water is in cross roads and the solution does not appear to depend on the capability of the scientists and technologists, requires a break through in the concept which will be taken up subsequently [11].

It is probably clear that the appropriate material has not been identified in spite of so many semiconducting materials have been evaluated. Various sensitization methods like doping, band gap engineering, coupling the semiconductors and others have been tried with limited success. There are many theoretical postulates

on this phenomenon but none of them could lead to success. The static positions of the conduction band minimum (oxidizing power) and valence band maximum (oxidizing power) have been used to test the utility of a chosen semiconductor for water decomposition. These band positions under the reaction conditions in the electrolyte and the double layer at the interface may have caused alterations and this situation might be one of the reasons for the observed activity. However, it is necessary to understand the positions of the band edges under the reactions medium and this aspect may require careful examination. The band gap engineering has to be associated modulated with the extent ionicity of the cation and anion bond. This postulate needs careful consideration. Until the photo-electrochemical decomposition of water, this process cannot become economically viable technology for hydrogen production.

Electrolysis in various forms is the only available method for the generation of pure hydrogen though it is not economically equivalent due to over potential and other associated losses. It appears that the development of cost effective electrodes is one of the steps for cost reduction in addition to other cost effective design of the electrolytic cell for commercial production of hydrogen.

Even if the process of hydrogen production becomes economically viable, the other components of hydrogen economy face major hurdles. But Hydrogen is normally in the gaseous state; its storage and transport will be preferred in the solid state. Even if one assumes that hydrogen is occluded in the solid-state matrix, the most probable situation would be one species per one metallic species and thus maximum storage capacity depends on the atomic weight of the metallic species. This postulate is only for hydrogen storage and not for hydride formation. It is originally estimated by DOE that the solid-state storage has to be at least 6.5 weight percent and it should be reversible at ambient conditions to be useful as a fuel. Though there are many attempts to introduce materials like metals, intermetallics, porous carbons, Metal organic frameworks (MOF) or (COF), this limit of storage of hydrogen could not be demonstrated. Until this level of hydrogen storage under reversible conditions could be reached, then there is little scope for hydrogen economy comes into force.

Thus, the first two components of Hydrogen economy, namely production and storage have not yet reached the stage of economically usable stage. The third component namely safe distribution infrastructure will require time and effort

from many of the countries in different continents. The search for hydrogen storage materials has always been centred around the materials listed and it might be possible an unusual materials have to be identified and their characteristics have to clearly demarked and justified. The choice of material for hydrogen storage may be directed towards materials with large void volume to accommodate hydrogen in the molecular form, which will be beneficial for the reversibility. The search has to be based on the atomic or species radius and the crystal structure that the system will adopt in the final phase formation.

It may be possible the other components of hydrogen economy may have some hurdles but they are governed by logistics and do not require any innovative implementation.

Hydrogen Economy has been analyzed in many attempts on the basis of cost reduction of the components and how to economize the organization of the existing structure but rarely focused on the innovative material introduction in improving these components. The introduction of Hydrogen Economy may not be wholly dependent on economic considerations but innovative research efforts have to evolve at making the components economically viable and also sustainable.

There is considerable hope on the introduction of hydrogen economy in the place of fossil fuel based economy, which is not equitably distributed and polarize the countries economically. There are other attempts and among them, the methanol economy introduced and advocated by Professor Olah, is prominent but still hydrogen economy is pursued and is expected to be introduced in the fuel market of the countries. Hydrogen economy today is at cross roads and solely dependent on research innovation.

At this stage, there are a few issues on which some comments are in order. There have been many projections on the penetration of hydrogen economy in the last five decades. None of these expectations have been realized till date. There can be many reasons for this situation, like the effective conversion of hydrogen into other forms of energy like electricity (due to failure in developing efficient conversion devices like fuel cells) [12]. In an optimistic estimate, if 20-25% of the energy needs of the universe were to be met by hydrogen in 2050, then it will mark the advent of Hydrogen Economy. This is only an expectation. It can take any other course in the mean time.

In India, many initiatives including Government (DST and MNRE) and private industry-based, especially in transport sector have been made from early1970s. The spread of these initiatives has not penetrated as expected due to various hurdles like transport and distribution of hydrogen in addition to the production of hydrogen from easily available raw material sources. There have been some intensive task forces like the one headed by Dr Kasthuri Rangan at that time a member of Parliament, Ex-Chairman ISRO and many others to look into the introduction of hydrogen Economy. Many attempts have reached the stage of demonstration units being built. One such effort has been by CFCT (Centre for Fuel Cell Technology, in Chennai). There were many other initiatives in this period. The development of lightweight cylinders is one of the major hurdles in addition to the established distribution system with good and regularized practice. The standards and controls with stipulated proper regulations have to be evolved before the introduction of Hydrogen Economy. There have been attempts in this direction by government agencies and it has to be taken to completion and implementation. Various R and D efforts in both research centres and industries have been initiated but coordinated and sustained efforts like the major auto-industry around the globe has to be initiated and monitored. In India such efforts may be successful if Industry and academic institutions understand each other and cooperate in the last 20% of the development of transforming development efforts of academic and other institutions into a viable technology then it will lead to a solution to the energy issues in this country. Concerted efforts are still awaiting.

Conclusion

There are several important barriers to the development of hydrogen as a fuel, fuel cells, and hydrogen economy. These barriers include technical feasibility, economic cost, consumer acceptance, and safety. These issues will have to be addressed over a long-term time frame. This will evolve as research and technology expands options for hydrogen and fuel cell use. Understanding of the long-term potentials and limitations of hydrogen economy is critical for assessing introduction of Hydrogen Economy.

Some standards have to be evolved and some regulations have to be introduced and practiced.

.

Acknowledgment: The support of department of Science and Technology (DST) and MNRE of the Government of India to National Centre for Catalysis Research (NCCR) IIT Madras is gratefully acknowledged.

References

[1] Transitioning to hydrogen: Assessing the engineering risks and uncertainties". *theiet.org*. (Retrieved on 8th May, 2020).

[2] George A. Olah, Alain Goeppert and G.K.Surya Prakash, Beyond oil and Gas: The Methanol Economy, Wiley VCH Verlag (20□□□□

[3] Verne, J., The mysterious Island, (1874), Airmont Publishing Company, USA

[4] M. Aulice Scibioh and B. Viswanathan, Fuel Cells, Principles and Applications, The University Press, 2007.

[5] B.Viswanathan and M. Helen, Is Nafion the only choice? Bull of the Catalysis Society of India (2007).

[6] M.Aulice Scibioh and B.Viswanathan, Hydrogen future Facts and Fallacies, Bull. Of the Catalysis Society of India,3,72 (2004)

[7] Ulf Bossel and Baldur Eliasson, Energy and the Hydrogen Economy, https://afdc.energy.gov/files/pdfs/hyd_economy_bossel_eliasson.pdf.

[8] Michael Joyce and Kelvin Mahal, The Emerging Hydrogen Economy, https://www.akingump.com/en/experience/industries/energy/speaking-energy/the-emerging-hydrogen-economy.html.

[9]F HYDROGEN: A RENEWABLE ENERGY PERSPECTIVE, Report prepared for the 2nd Hydrogen Energy Ministerial Meeting in Tokyo, Japan (2019), https://irena.org//media/Files/IRENA/Agency/Publication/2019/Sep/IRENA_Hydrogen_2019.pdf and many other documents in the web.

[10] Fujishima, Akira; Honda, Kenichi (7 July 1972). "Electrochemical Photolysis of Water at a Semiconductor Electrode" *Nature* **238** , 37–38. doi:10.1038/238037a0. PMID 12635268.

[11] Chi-Hung Liao, Chao-Wei Huang and Jeffrey C. S. Wu, Hydrogen Production from Semiconductor-based Photo-catalysis via Water Splitting, Catalsts, 2,490 (2012).

[12] N. P. Brandon and Z.Kurban, Clean energy and the hydrogen economy, Phil. Trans. R. Soc. A 375: 20160400 (2017). http://dx.doi.org/10.1098/rsta.2016.0400

The Relevance of Photocatalysis for Energy Conversion and Storage

Photocatalysis is an emerging area of research in energy conversion and storage. In this sense, the production of fuels by the photocatalytic water splitting and reduction of carbon dioxide and dinitrogen assumes importance. The prospects of these three reactions in this context are evaluated. The prospects of storage of hydrogen and carbon dioxide in solid-state materials are also considered.

Introduction

The Science of catalysis has seen many facets and changes in the last century. The two important factors for sustaining the living beings on this earth are energy conversion and environment. Though the science of catalysis, in general, contributes to both these issues, a new and recent domain called 'Photocatalysis' a misnomer or not, plays a vital role in fulfilling these two functions. Photon assisted process has taken new dimensions in many ways like photoelectrochemical decomposition of water for fuel hydrogen production [1] and the conversion of one of the most inert (stable) molecules namely carbon dioxide into value-added chemicals [2] in addition to decomposition of dyes [3] and chemicals in water treatment. In reality, the photons are activating the solid catalyst by altering the potential of charge and the catalytic reaction takes place only on the surface sites of the photoactive materials. It must be admitted that there are still views that many of these challenging processes of energy conversion have reached the time window where these could have happened have now come to an end [1]. Despite this pessimism, there is still scientific curiosity on these processes and still there are persistent attempts to make these processes commercially feasible. This situation is generally assumed to have started from the initial publication of Fujishima and Honda [4], though there were attempts in this direction before this period [5]. In the near future, the energy conversion process will center around four simple molecules, namely water, dinitrogen, carbon monoxide and carbon dioxide [6]. Though the activation of these small molecules was known for a long time, (positively systematically from the 1950s) the transformation of these molecules for energy conversion has not still reached the stage of economic and commercial feasibility sometimes even led to frustration among the proponents. It appears that it is time one analyzes this situation to propose the direction in which these

processes will become economically feasible. The purpose of this presentation is an attempt in this direction to bring out the reasons for this situation and also to seek remedies for the same, though one cannot assume getting appropriate answers and success in this difficult task.

Photocatalysis

Some Basis One of the reasons for this obsession on this topic is the available nature of solar energy even some of the shortcomings like the diurnal and intermittent nature and non-uniform distribution of this form of energy [7]. Photocatalytic materials are mostly centered around semiconducting solids since available and exploitable photon sources (natural or artificial) can provide energy range (1-3.5 eV) for changing the potential energy of the active species (electrons or holes). The realized catalysis action is due to these activated species (excitons) and not the photons and in this sense the term photocatalysis appears to be a misnomer. However, these excitons may recombine within the lifetime of these species and thus not utilized in promoting the surface catalyzed reaction. This may be one of the reasons for the inconsistency often reported in the results [8]. Compared to conventional approaches, photocatalysis has the advantage of using sunlight to activate and drive the degradation and decomposition processes, thus making it more energetically sustainable and eco-compatible. The possible applications of photocatalysis is pictorially shown in Fig.1.

Fig.1. Main envisioned applications of photocatalysis [reproduced from ref. 9].

Typical processes taking place on semiconducting solids in photocatalysis can be summarized by the following steps:

(1) Photon absorption (governed by the photon absorption coefficient usually termed as molar extinction coefficient) to generate electron-hole with sufficient potential to promote the desired redox reaction.
(2) Recombination of the charge carriers within the semiconducting solids.
(3) The separated charges have to migrate to surface reaction sites.
(4) The redox reactions with charge transfer taking place on the generated surface sites.

There are still some challenges in photocatalysis. These aspects including the kinetics and the energy of the photon source have been discussed frequently in literature [10]. The enthusiasm that this field evoked in the early days slowly wanes these days for various reasons like the efficiency of this technology in the energy conversion process especially hydrogen production from the photocatalytic splitting of water and converting carbon dioxide to chemicals and fuels. In the following, the prospects of photocatalysis for fuel production from the most of the four molecules are considered.

Photocatalytic splitting of water

The essential energy requirements for the decomposition of water is that hydrogen evolution potential has to be less negative with respect to the bottom of the conduction band edge while oxygen evolution reaction potential should be less positive as compared to the valence band top edge. This situation is pictorially represented in Fig 2 (though in this figure other reactions also are shown).

The selection of the semiconductor for hydrogen and oxygen evolution reactions in water decomposition is based on the energy portions of these two edges.

The conduction band bottom and valence band top positions and the values of band gaps shown in the figure as static positions but they may alter depending on the interface depending on the nature of the interface. This situation if it were to exist, then the observed results have to be analyzed differently. Though the efficiency of the photocatalytic

decomposition of water splitting has not yet reached the levels in order this process can be exploited commercially, there are persistent efforts to increase this parameter by sensitizing the semiconductor in the form of coupled semiconductors or doping the semiconductor or dye sensitization and others. These attempts are mainly to alter and match the energy requirements for the process probably because the process is not only dependent on energy matching but also other factors like geometric and site symmetry may be responsible. 'Bandgap engineering' is one of the concepts probably over-emphasized in photocatalysis. It may be possible that even harnessing with vide band semiconductors may provide energy conversion necessary for all the living beings.

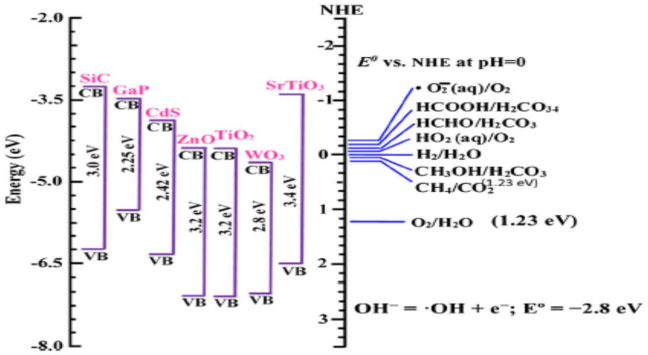

Fig.2. The positions of conduction band bottom and top of the valence band of typical semiconductors. The selection of the semiconductor for hydrogen and oxygen evolution reactions in water decomposition is based on the energy positions these two edges.

Typical selected results on the hydrogen production rate on semiconducting solids by photo-splitting of water are assembled in Table 1. It is seen from the results given in Table 1, that the hydrogen production rate has not yet reached the stage of commercial exploitation. It appears that identifying the appropriate photocatalyst for water splitting has not yet reached the desired stage.

Table 1. Typical results (in the units of micromoles per hour per gram on photo-splitting of water [abstracted from 11]

Typical Photocatalysts	Hydrogen production rates in micromoles per hour per gram
Ta doped TiO_2	11.7
Pt/C-TiO_2	5713.6
Pt/TiO_2	932
CuS/ZnCdS	7735
CdS/ZnS	239,000
Ni/CdS/g-C_3N_4	1258
CdS/WS/graphene	1842
Au/TiO_2	647,000
MoS_2/CuZnS	202

Photocatalytic Reduction of Carbon dioxide

The listing of simple reactions in relation to the reduction of carbon dioxide are given below:

$CO_2 + 2H^+ + 2e \rightarrow CO + 2H_2O \quad E^0 = -0.53$ V

$CO_2 + 2H^+ + 2e \rightarrow HCOOH \quad E^0 = -0.61$ V

$CO_2 + 4H^+ + 4e \rightarrow HCHO + H_2O \quad E^o = -0.48$V

$CO_2 + 6H^+ + 6e \rightarrow CH_3OH + H_2O \quad E^o = -0.38$ V

$CO_2 + 8H^+ + 8e \rightarrow CH_4 + 2H_2O \quad E^o = -0.24$V

$CO_2 + e \rightarrow CO_2^- \quad E^o = -1.90$V

Essentially, these reactions are dependent on the activation of the inert carbon dioxide molecule.

Even though the molecule of carbon dioxide can be associated with oxygen, carbon or mixed coordination as shown in Fig.3, the conversion of this molecule into a fuel or chemical depends on the proper activation of the molecule at the appropriately formulated active site (typically a stepped surface sites) on the catalyst surface. The inertness of carbon dioxide is reflected in the values of Gibbs free energy as seen from the data shown in Fig.4. The capture and utilization of carbon dioxide have become an important component of today's research efforts as revealed in the statements of Prof. Olah (one of the Nobel Prize winners) namely "Carbon dioxide. ... can be chemically transformed from a detrimental greenhouse gas causing global warming into a valuable, renewable and inexhaustible carbon source of the future allowing environmentally neutral use of carbon fuels and derived hydrocarbon products".

The prospects of the utilization of carbon dioxide in combination with hydrogen (like water) will be a source of fuel production in the future is reflected in the cycle presented in Fig.5. The main process in the conversion of carbon dioxide is the production of synthesis gas by tri-reforming reaction one of the typical reaction is:

CH4 + CO2 4 2CO + 2H2 247/3 kJ.mol-1.

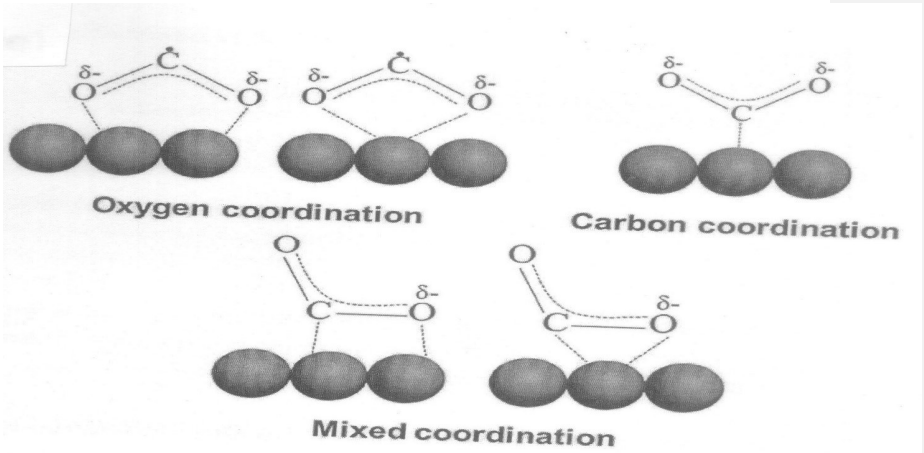

Fig.3. Possible modes of activation of carbon dioxide on solid surfaces through the coordination nature.

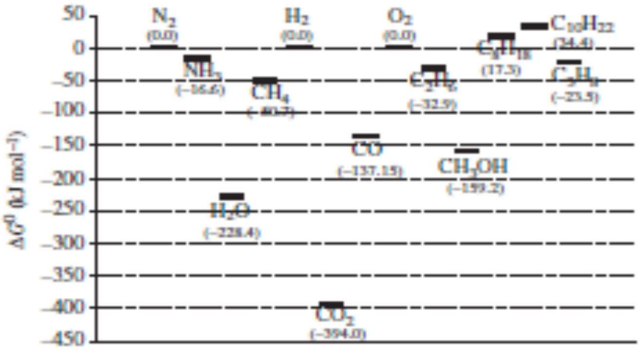

Fig.4. Values of Gibbs free energy of formation for selected (typical) chemicals [data base from http://webbook.nist.gov/chemistry/name-ser.html];

This may become one of the important steps in the reforming reaction as well in the utilization of carbon dioxide shortly.

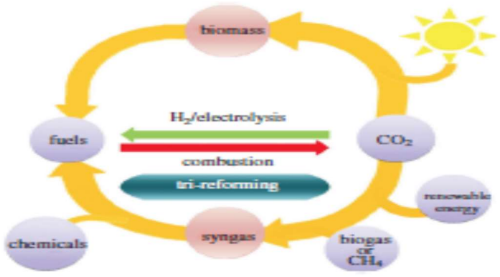

Fig.5. The possible cycle for fuel and chemical production from carbon dioxide [ref.12]

The Reduction of Dinitrogen

One of the current exploited processes in the reduction of dinitrogen is the ammonia synthesis which goes under the name of the Haber Process at high temperatures (623-823 K) and pressures (150-350) atmospheres. However today the ammonia production alone requires nearly 1% of the total energy by this universe. There have been attempts in the past to formulate a catalytic process for reducing dinitrogen at low temperatures and 1 atm. However, reduction of dinitrogen, probably the most stable diatomic molecule known, by protons and electrons or by dihydrogen to ammonia under these conditions appears to be more difficult than it was conceived. It appears to be possible to reduce dinitrogen catalytically at a single molybdenum center due to intellectual advance in the minds inorganic, bioinorganic and biological scientists. There are many issues in this reduction reaction. Are there many ways and processes to reduce dinitrogen to ammonia under mild conditions? Is molybdenum as believed the most efficient metal for dinitrogen reduction?

There is yet another domain for this reduction reaction. The problem for Nitrogen Reduction Reaction (NRR) is the lack of effective electrocatalyst for effecting this reaction under ambient conditions. This situation may be due to high overpotential for dinitrogen reaction and/or

the low Faradaic efficiencies for ammonia formation. This situation is due to the fact that electrochemical reduction of dinitrogen takes place at negative potentials and in this sense, the dominant reaction is the competing hydrogen evolution reaction thus reducing the selectivity. This situation for NRR has multiple dimensions in the sense that formulating intrinsically reactive and selective electrocatalyst, interface engineering controlling the proton/electron transfer rate and also to decouple the nitrogen fixation and ammonia formation steps [13].

Storage

Energy storage can be achieved in various ways. Gas storage is one of them especially for hydrogen and carbon dioxide in solid-state materials [14]. Let us first consider the storage of hydrogen since it is known for a long time. Metals can take up hydrogen as metal hydrides, the familiar one is palladium hydride. The orig- 33 Fig.4. Values of Gibbs free energy of formation for selected (typical) chemicals [data base from http://webbook.nist.gov/chemistry/nameser.html] Fig.5. The possible cycle for fuel and chemical production from carbon dioxide [ref.12] The original DOE (Department of Energy) recommendation is that at least a solid should take up at least 6.5 weight percent so that the cost of energy will be comparable to the present-day economy, even though there can be other issues concerned with solid-state hydrogen storage.

So far, no metallic or intermetallic systems have been identified which can store hydrogen to this extent. This situation has to be carefully analyzed and as most of the structures of solid-state materials (metals and intermetallics) normally consists of a polyhedron and only one hydrogen atom can be contained in each of the polyhedra and hence in these systems the storage cannot exceed 2 to 3.5 weight percent if the metal is from the transition group. Low atomic weight metals like magnesium and others may be able to store a higher percentage (>6.5 weight %) but they have other issues to be addressed. In this connection, layered structures (like carbon) can be considered as alternative materials but still the desired levels of storage have not been achieved in these materials as well.

A similar situation exists in the case of carbon dioxide capture and storage. Even the introduction of the Metal-organic framework (MOF) or the corresponding COF structured materials, though initially showed promise, have not reached the expected levels of storage. It appears that

more innovative thinking and execution are required in this direction.

Summary

Today. energy conversion processes depend on the generation of hydrogen by splitting of water, in the conversion of carbon dioxide into value-added fuels and reduction of dinitrogen under ambient conditions. In this article the prospects of these three processes becoming economically viable are examined. Also, the storage of hydrogen and carbon dioxide in solid-state materials is briefly considered.

References

1. T. Jesper Jacobsson, Photoelectrochemical water splitting: an idea heading towards obsolescence? Energy Environ. Sci.,11,1977 (2018).
2. M. Aulice Scibioh and B. Viswanathan, Carbon dioxide to chemicals and fuels, Elsevier (2018).
3. B. Viswanathan, Photocatalytic Degradation of Dyes: An Overview, Current Catalysis 7 (2), 99-121 (2018) DOI: 10.2174 /2211544707666171219161846.
4. A. Fujishima and K. Honda, Electrochemical photolysis of water at a semiconductor electrode, Nature, 238,37-38 (1972).
5. K. Hashimoto, Hiroshi Irie and A. Funishima, TiO2 Photocatalysis: A historical overview and Future prospects, Japanese Journal of applied Physics, 44,8269 (2005).
6. Jens K. Norskov (Ed) Research needs towards sustainable production of fuels and chemicals, The EU-funded ENERGY-X project (Horizon 2020 Grant Agreement No 820444) (2019).
7. Sgasga Zhu and Dunwei Wang, Photocatalysis: Basic Principles, Diverse Forms of Implementations and Emerging Scientific Opportunities, Adv. Energy Mater. 2017, 7, 1700841.
8. Pavel Moroz, Anthony Boddy and Mikhair Zamkov, Challenges and Prospects of Photocatalytic Applications Utilizing Semiconductor Nanocrystals, Front. Chem., 15 August 2018 | https://doi.org/10.3389/fchem.2018.00353.
9. Henry Agbe, Emmanuel Nyankson, Nadeem Raza, David Dodoo-Arhin, Aditya Chauhan, Gabriel Osei, Vasant Kumar and Ki-hyun Kim, Recent advances in photoinduced catalysis for water splitting and environmental applications, Journal of Industrial and Engineering Chemistry, 72,31-49 (2019).

10. Seunghyun Weon, Fei He and Wonyong Choi, Status and challenges in photocatalytic nanotechnology for cleaning air polluted with volatile organic compounds: visible light utilization and catalyst deactivation, Environ. Sci.: Nano, 6,3185 (2019).
11. Tahereh Jafari, Ehsan Moharreri, Alireza Shirazi Amin, Ran Miao, Wenqiao Song and Steven L. Suib, Photocatalytic Water Splitting—The Untamed Dream: A Review of Recent Advances, Molecules 2016, 21, 900; doi:10.3390/molecules21070900
12. Z. Jiang, T.Xiao, V.L. Kuznetsov and P.P.Edwards, Turning carbon dioxide into fuel, Phil. Trans. R. Soc. A (2010) 368, 3343–3364 doi:10.1098/rsta.2010.0119.
13. Xiaoyang Cui, Cheng Tang, and Qiang Zhang, A Review of Electrocatalytic Reduction of Dinitrogen to Ammonia under Ambient Conditions, Adv. Energy Mater. 2018, 8, 1800369
14. Renju Zacharia and Sami Ullah Rather, Review of Solid State Hydrogen Storage Methods Adopting Different Kinds of Novel Materials, Journal of Nanomaterials, Volume 2015 |Article ID 914845; https://doi.org/10.1155/2015/914845.

CHAPTER

Dye-sensitized solar cells (DSSCs) have been considered as an alternate to the conventional p-n junction photovoltaic cells. In the 1960s, it was reported that electricity is generated by illuminating organic dyes in electrochemical cells. First chlorophyll-sensitized zinc oxide (ZnO) electrode was synthesized in 1972. For the first time, through electron injection of excited dye molecules into a wide band gap of semiconductor, photons were converted into electricity [1]. A lot of research has been done on ZnO-single crystals [2], but the efficiency of these dye-sensitized solar cells was poor, as the monolayer of dye molecules was able to absorb incident light only up to 1%. At this stage, it was felt that the semiconductor electrode should be porous in nature. As a result, nano-porous titanium dioxide (TiO_2) electrodes with a roughness factor of 1000 were introduced. This study showed 7% efficiency in DSSC mode [3]. These cells were invented in 1988 by Brian O'Regan and Michael Grätzel. This invention was developed by them at Ecole Polytechnique Fédèrale de Lausanne (EPFL). Brian O'Regan and Michael Grätzel fabricated a device based on a 10-μm-thick, high surface area and optically transparent film of TiO_2 nanoparticles, coated with a monolayer of a charge transfer dye with ideal spectral characteristics to sensitize the film for light harvesting. The device harvested a high proportion of the incident solar energy flux of 46% and showed exceptionally high efficiencies, even more than 80% efficiencies for the conversion of incident photons to electrical current. The overall incident photon to current conversion efficiency (IPCE) yield was 7.1–7.9% in simulated solar light and 12% in diffuse daylight. A large short circuit current density J_{SC} (greater than 12 $mA.cm^{-2}$) and exceptional stability (sustaining at least five million turnovers without decomposition) and low cost made the practical application feasible [3]. In 1993, Grätzel et al. reported 9.6% efficiency of cells, and then in 1997, they achieved 10% at the National Renewable Energy Laboratory (NREL). The sensitizers are usually designed to have functional groups such as –COOH, $–PO_3H_2$, and $–B(OH)_2$ for stable adsorption onto the semiconductor substrate [4, 5]. Recently in 2018, an efficiency of 8.75% was reported for hybrid dye-titania nanoparticle-based DSSC for superior low temperature by Costa et al. [6]. In a traditional solar cell, Si provides two functions: acts as source of photoelectrons and provides electric field to separate the charges and create a current. But, in DSSCs, the bulk of semiconductor is only used as a charge transporter and the photoelectrons are

provided by photosensitive dyes. The theoretically predicted power conversion efficiency (PCE) of DSSCs was approximately 20% [7, 8]; thus, an extensive research has been made over the years on DSSCs to improve the efficiency and to augment its commercialization. However, in the last few decades, a lot of experiments were carried out to improve the performance of DSSCs.

Anandan reviewed the improvements and arising challenges in dye-sensitized solar cells till 2007 [9]. the maximum IPCE of 7% was stated in the review paper for naphthyridine coordinated Ru complex [10] which was good till 2007. The review paper published by Bose et al. [11] deals with the current state and developments in the field of photoelectrode, photosensitizer, and electrolyte for the period till 2015.

Shalini et al. [12] emphasized on sensitizers, including ruthenium complexes, metal-free organic dyes, quantum-dot sensitizer, perovskite-based sensitizer, mordant dyes, and natural dyes. However, this article provides a great knowledge about the different types of sensitizers, but lacks the information regarding other important components of the DSSCs. Again, apart from discussing all different components of DSSCs, the review article by Jihuai Wu et al. [13] was concentrated over the counter electrode part. They have discussed the study of different types of counter electrodes based on transparency and flexibility, metals and alloys, carbon materials, conductive polymers, transition metal compounds, and hybrids. A highest efficiency of 14.3% was discussed for the DSSC fabricated with Au/GNP as a counter electrode, $Co^{3+/2+}$ as a redox couple, and LEG4 + ADEKA-1 as a sensitizer [14] and was shown in the review article. Similarly, Yeoh et al. and Fan et al. [15, 16] have given a brief review over the photoanode of DSSC. They have classified modification of photoanode into three categories, namely interfacial modification through the introduction of blocking and scattering layer, compositing, doping with non-metallic anions and metallic cations, interfacial engineering, and replacing the conventional mesoporous semiconducting metal oxide films like with 1-D or 2-D nanostructures.

Construction of DSSCs

DSSC is an assembly of working electrode soaked with a sensitizer or a dye and sealed to the counter electrode soaked with a thin layer of electrolyte with the

help of a hot melt tape to prevent the leakage of the electrolyte (as shown in Fig. 1). The components as well as the construction and working of DSSCs are shown in Fig.1.

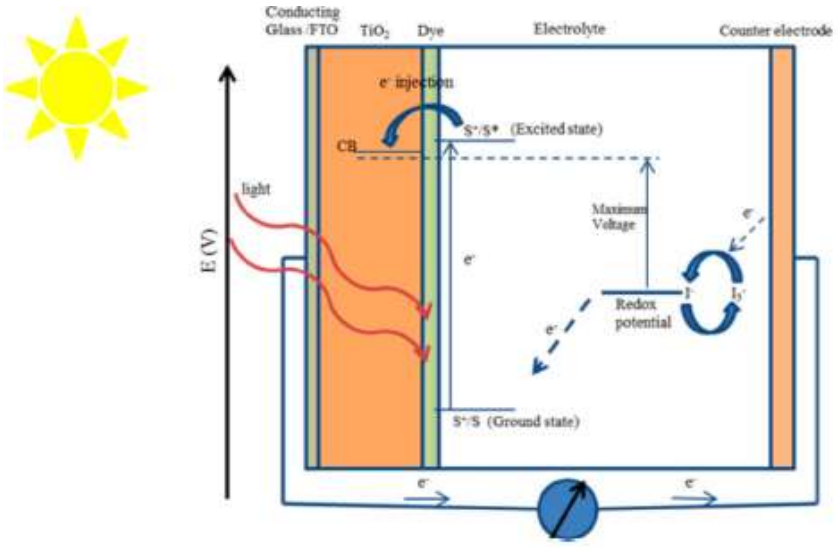

Fig.1. Construction and working principle of the dye-sensitized solar cells

Transparent and Conductive Substrate

DSSCs are typically constructed with two sheets of conductive transparent materials, which help a substrate for the deposition of the semiconductor and catalyst, acting also as current collectors [17, 18] There are two main characteristics of a substrate being used in a DSSC: Firstly, more than 80% of transparency is required by the substrate to permit the passage of optimum sunlight to the effective area of the cell. Secondly, for the efficient charge transfer and reduced energy loss in DSSCs, it should have a high electrical conductivity. The fluorine-doped tin oxide (FTO, SnO_2: F) and indium-doped tin oxide (ITO, In_2O_3: Sn) are usually applied as a conductive substrate in DSSCs. These substrates consist of soda lime glass coated with the layers of indium-doped tin

oxide and fluorine-doped tin oxide. The ITO films have a transmittance > 80% and 18 Ω/cm^2 of sheet resistance, while FTO films show a lower transmittance of ~ 75% in the visible region and sheet resistance of 8.5 Ω/cm^2 .

Working Electrode (WE)

The working electrodes (WE) are prepared by depositing a thin layer of oxide semiconducting materials such as TiO_2, Nb_2O_5, ZnO, SnO_2 (n-type), and NiO (p-type) on a transparent conducting glass plate made of FTO or ITO. These oxides have a wide energy band gap of 3–3.2 eV. The application of an anatase allotropic form of TiO_2 is more commendable in DSSCs as compared to a rutile form due to its higher energy band gap of 3.2 eV whereas the rutile form has a band gap of about 3 eV, although alternative wide band gap oxides such as ZnO and Nb_2O_5 have also given promising results. Due to being non-toxic and less expensive and its easy availability, TiO_2 is mostly used as a semiconducting layer. However, these semiconducting layers absorb only a small fraction of light in the UV region; hence, these working electrodes are then immersed in a mixture of a photosensitive molecular sensitizer and a solvent. After soaking the film within the dye solution, the dye gets covalently bonded to the TiO_2 surface. Due to the highly porous structure and the large surface area of the electrode, a high number of dye molecules get attached on the nanocrystalline TiO_2 surface, and thus, light absorption at the semiconductor surface increases.

Photosensitizer (Dye)

Dye is the component of DSSC responsible for the maximum absorption of the incident light. Any material being dye should have the following photo-physical and electrochemical properties: (1) The dye should be luminescent. (2) The absorption spectra of the dye should cover ultraviolet-visible (UV-vis) and near-infrared region (NIR) regions. (3) The energy of the highest occupied molecular orbital (HOMO) should be located far from the surface of the conduction band of TiO_2 and the energy of the lowest unoccupied molecular orbital (LUMO) should be placed as close to the surface of the TiO_2, and subsequently should be higher with respect to the TiO_2 conduction band potential. (4) HOMO should lie lower than that of redox electrolytes.

(5) The periphery of the dye should be hydrophobic to enhance the long-term stability of cells, as it results in minimized direct contact between electrolyte and anode; otherwise, water-induced distortion of the dye from the TiO_2 surface can appear which may reduce the stability of cells. (6) To avoid the aggregation of the dye over the TiO_2 surface, co-absorbents like chenodeoxycholic acid (CDCA) and anchoring groups like alkoxy-silyl, phosphoric acid, and carboxylic acid group were inserted between the dye and TiO_2. This results in the prevention of dye aggregation and thus limits the recombination reaction between redox electrolyte and electrons in the TiO_2 nanolayer as well as results in the formation of stable linkage.

Electrolyte

An electrolyte (such as I^-/I^-_3, Br^-/Br^-_2, SCN^-/SCN_2, and Co(II)/Co(III) [has five main components, i.e., redox couple, solvent, additives, ionic liquids, and cations. The following properties should be present in an electrolyte: (1) Redox couple should be able to regenerate the oxidized dye efficiently. (2) Should have long-term chemical, thermal, and electrochemical stability.(3) Should be non-corrosive with DSSC components.(4) Should be able to permit fast diffusion of charge carriers, enhance conductivity, and create effective contact between the working and counter electrodes. (5) Absorption spectra of an electrolyte should not overlap with the absorption spectrum of the dye.

I^-/I^-_3 has been demonstrated as a highly efficient electrolyte, but there are certain limitations associated with its application in DSSCs. I^-/I^-_3 electrolyte corrodes glass/TiO_2/Pt; it is highly volatile and responsible for photodegradation and dye desorption and has poor long-term stability. Acetonitrile (ACN), *N*-methylpyrrolidine (NMP), and solvent mixtures, such as ACN/valeronitrile, have been used as a solvent having high dielectric constants. 4-Tert-butylpyridine (TBP) is mostly used as an additive to shift the conduction band of TiO_2 upwards, which results in an increase in the value of open circuit voltage

(V_{OC}), reduced cell photocurrent (J_{SC}), and less injection driving force. It is believed that TBP on a TiO_2 surface reduces recombination through back transfer to an electrolyte. However, the biggest drawback allied with the ionic liquid is their leakage factor. Thus, solid-state electrolytes are developed to avoid the drawbacks associated with ionic liquid (IL) electrolytes. Also, to test the failure of the redox electrolyte or the sealing under long-term illumination, long-term light soaking tests on sealed cells have also progressed significantly over the years.

Counter Electrode (CE)

CE in DSSCs are mostly prepared by using platinum (Pt) or carbon (C). Both working and counter electrodes are sealed together, and subsequently, an electrolyte is filled with a help of a syringe. Counter electrode catalyzes the reduction of I^-/I^-_3 liquid electrolyte and collects holes from the hole transport materials (HTMs). Pt is used mostly as a counter electrode as it demonstrates higher efficiencies, but the replacement of Pt was much needed due to its higher cost and less abundance. Thus, several alternatives have developed to replace Pt in DSSCs, such as carbon, carbonylsulfide (CoS), Au/GNP, alloy

CEs like FeSe and $CoNi_{0.25}$, although the different types of the CEs are also discussed by Jihuai Wu et al. [13].

Working Principle

The working principle of DSSC involves four basic steps: light absorption, electron injection, transportation of carrier, and collection of current. The following steps are involved in the conversion of photons into current.

1. The incident light (photon) is absorbed by a photosensitizer, and thus, due to the photon absorption, electrons get promoted from the ground state (S^+/S) to the excited state (S^+/S^*) of the dye, where the absorption for most of the dye is in the range of 700 nm which corresponds to the photon energy almost about 1.72 eV.

2. The excited electrons with a lifetime of nanosecond range are injected into the conduction band of nano-porous TiO_2 electrode which lies below the excited state of the dye, where the TiO_2 absorbs a small fraction of the solar photons from the UV region. As a result, the dye gets oxidized.

3. These injected electrons are transported between TiO_2 nanoparticles and diffuse towards the back contact (transparent conducting oxide [TCO]). Through the external circuit, electrons reach at the counter electrode.

4. The electrons at the counter electrode reduce I^-_3 to I− ; thus, dye regeneration or the regeneration of the ground state of the dye takes place due to the acceptance of electrons from I− ion redox mediator, and I− gets oxidized to I^-_3 (oxidized state).

5. Again, the oxidized mediator (I^-_3) diffuses towards the counter electrode and reduces to I ion

Evaluation of Dye-Sensitized Solar Cell Performance

The performance of a dye-sensitized solar cell can be evaluated by using incident photon to current conversion efficiency (IPCE, %), short circuit current (JSC, mAcm− 2), open circuit voltage (VOC, V), maximum power output [Pmax], overall efficiency [η, %], and fill factor [FF] (as shown in Fig. 3) at a constant light level exposure as shown in Eq. 1.

The current produces when negative and positive electrodes of the cell are short circuited at a zero mV voltage. VOC (V) is the voltage across negative and positive electrodes under open circuit condition at zero milliampere (mA) current or simply, the potential difference between the conduction band energy of semiconducting material and the redox potential of electrolyte. Pmax is the maximum efficiency of the DSSC to convert sunlight into electricity. The ratio of maximum power output (Jmp × Vm) to the product (VOC × JSC) gives FF.

FF = (J mp x V_m)/ (VOCXISC) See the figure 2

Also, the overall efficiency (%) is the percentage of the solar energy (shining on a photovoltaic [PV] device) converting into electrical energy, where η

increases with the decrease in the value of JSC and increase in the values of VOC, FF, and molar coefficient of dye, respectively.

$$\eta\ (\%) = (J_{SC} \text{ X } V_{oc} \text{ X FF }).Pim\backslash$$

External quantum efficiency (also known as IPCE) is the ratio of number of electrons flowing through the external circuit to the number of photons incident on the cells surface at any wavelength λ. It is given as follows:

$$IPCE\ (\%)(\lambda) = 1240 \text{ X}(J_{Sc} / P_{im})$$

IPCE values are also related to LHE, φE1, and ηEC.

$$IPCE\ (\lambda\ nm) = LHE, \varphi E1\ \eta EC$$

where LHE is the light harvesting efficiency, φE1 is electron injection quantum efficiency, and ηEC is the efficiency of collecting electrons in the external circuit.

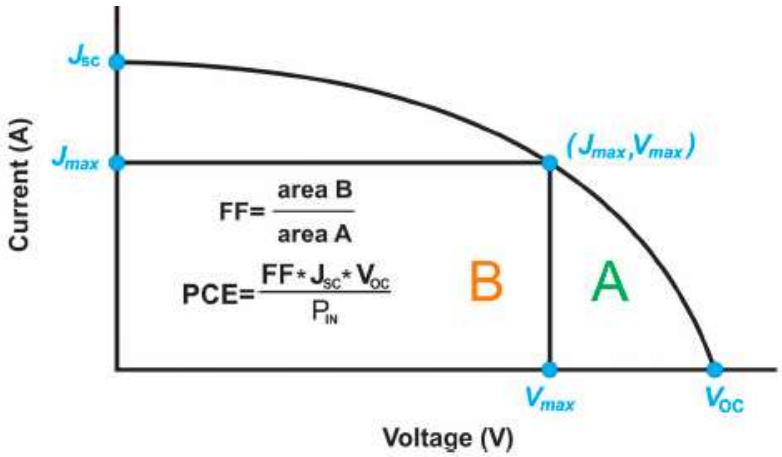

Fig.2. I–V curve to evaluate the cells performance

Limitations of the Devices

In the recent years, comparable efficiencies have been demonstrated for the DSSCs, but still they need a further modification due to some of the limitations associated with these cells. In terms of limitations, stability failure can be characterized in two different classes: (i) limitation towards extrinsic stability and (ii) limitation towards intrinsic stability. Also, a huge amount of loss in energy of oxidized dye takes place during the process of regeneration, due to the energy mismatch between the oxidized dye and an electrolyte. Thus, in the queue to enhance the efficacy of these cells, different electrolytes have been developed. Grätzel et al. showed over 900-mV open circuit voltages and short circuit currents ISC up to 5.1 mA by blending the hole conductor matrix with a combination of TBP and $Li[CF_3SO_2]_2N$, yielding an overall efficiency of 2.6% at air mass 1.5 (AM 1.5) illuminations. Also, the sheet resistance of FTO glass sheet is about 10 Ω/sq.; thus, this makes scaling of the device difficult and acts as a limiting factor for an active cell area > 1 cm^2. Therefore, to increase the sheet resistance as well as to maintain spacing between working and counter electrode, the short circuiting of the solar cell is required or either the spacing should be increased by 25 to 50 μm in small modules (where these modules consist of small stripes of an active cell area (1 cm^2) with adjacent silver lines). As a consequence, a drop in the IPCE value from 10.4 to 6.3% for a 1-cm^2 cell was observed for a submodule of 26.5 cm^2.

To upscale the cell performance, silver fingers can be used to collect the current and using a sealant material like hotmelt tape, for the protection from the leakage of the electrolytes. Although due to the chemically aggressive nature of the electrolyte, the use of silver fingers is less feasible. And due to the small modules, the chances of leakage increase which results in reduced active cell area by 32%. Another factor is the conductivity of the glass sheet that affects the performance of the DSSCs. Therefore, the conductivity of the transparent conducting oxide (TCO) can be improved by combining the indium-doped tin oxide (ITO, highly conductive but less chemically stable) and fluorine-doped tin oxide (FTO, highly chemically stable but less conductive) together. This results in the reduction of the sheet resistance of TCO glass to 1.3 Ω/sq.

Limitation Towards the Stability of the Devices

The DSSCs need to be stable extrinsically as well as intrinsically as to be comparable to that of Si-solar cells, so that they can fulfill market needs, and thus, their commercialization can be increased. The limitations towards the stability are as follows:

Limitation Towards Extrinsic Stability (Stability of Sealant Material)

Sealant materials like Surlyn® and Bynel® hotmelt foils are used in DSSCs to seal the cells. Their sealing capability decreases when the pressure builds up inside the cell and also if exposed within a cyclic or regular temperature variation. But due to their low cost and easy processing, their utilization cannot be neglected. Thus, it is required to increase their adhesion with glass by pretreatment of the glass with metal oxide particles. As an alternative, sealants based on low melting glass frits were also developed which offer more stability than the hotmelt foils, but these sealants are not suitable for the large area module production.

Limitation Towards Intrinsic Stability

To examine the intrinsic stability of the cell, accelerated aging experiments were performed. These accelerated aging experiments lasts for 1000 h to show the thermal stability of the dye, electrolyte, and Pt-counter electrode at 80 °C of temperature. Through these experiments, it was found that small test cells can maintain 90% of the initial efficiency under elevated temperatures and the observed initial efficiencies were 7.65% and 8% , respectively. Also, under AM 1.5 and 55–60 °C moderate temperatures, the device was stable for 1000 h. But when both the stress factors, i.e., temperature about 80 °C and light soaking, were combined, a rapid degradation in the performance of the cell was observed]. Therefore, improvement in the intrinsic stability of the cell is required as 80 °C temperature can be easily attained during sunny days.

Different Ways to Augment the Efficiency of DSSCs

To enhance the efficiency as well as the stability of the DSSCs, researchers have to focus on fundamental fabrication methods and materials, as well working of these cells. Different ways to improve the efficiency of these solar cells (SCs) are discussed:

1. To increase the efficiency of DSSCs, the oxidized dye must be firmly reduced to its original ground state after electron injection. In other words, the regeneration process (which occurs in the nanosecond range) should be fast as compared to the process of oxidation of dye [the process of recombination (0.1 to 30 μs)]. As the redox mediator potential (I^- ion) strongly effects the maximum photovoltage, thus the potential of the redox couple should be close to the ground state of the dye. To carry out this viable repeated process, about 210 mV driving force is required (or ca. 0.6 V).

2. By increasing the porosity of the TiO_2 nanoparticles, the maximum dye absorption takes place at WE.

3. Reducing or prohibiting the formation of the dark current by depositing a uniform thin layer or under layer of the TiO_2 nanoparticles over the conduction glass plate. Thus, the electrolyte does not have a direct contact with the FTO or back contact and hence not reduced by the collector electrons, which restricts the formation of the dark current.

4. Preventing the trapping of nanoporous TiO_2 nanoparticles by TBP molecules or by an electrolyte solvent. Thus, uniform sensitization of the WE by a sensitizer is required. If the entire surface of the nanoporous TiO_2 electrode is not uniformly covered by the sensitizer, then the naked spots of nanoporous TiO_2 can be captured by TBP molecules or by an electrolyte solvent.

5. Co-sensitization is another way to optimize the performance of DSSC. In co-sensitization, two or more sensitizing dyes with different absorption spectrum ranges are mixed together. to broaden the spectrum response range .

6. By promoting the use of different materials in the manufacture of electrodes like nanotubes, nanowires of carbon, graphene; using varied electrolytes instead of a liquid one like gel electrolyte and quasi-solid electrolytes; providing different pre-post treatments to the working electrode like anodization pre-treatment and TiCl4 treatment; using different types of CEs and by developing hydrophobic sensitizers, the performance as well as the efficiency of these cells can be tremendously improved.

7. By inserting phosphorescence or luminescent chromophores, such as applying rare-earth doped oxides into the DSSC, coating a luminescent layer on the glass of the photoanode, i.e., using plasmonic phenomenon and adding energy relay dyes (ERDs) to the electrolyte.

. Previous and Further Improvements in DSSCs

To fabricate low cost, more flexible, and stable DSSCs with higher efficiencies, new materials that are light weight, thin, low cost, and easy to synthesize are required. Thus, previous as well as further improvement in the field of DSSCs is included in this section. This section gives a brief account on the work done by the different researchers in the last 10–12 years and the results they observed for respective cells.

Working and Counter Electrodes Grätzel and co-workers showed drastic improvements in the performance of DSSCs. They demonstrated efficiency of 7–10% under AM 1.5 irradiation using nanocrystalline (nc) TiO_2 thin-film electrode with nano-porous structure and large surface area, and used a novel Ru bipyridyl complex as a sensitizer and an ionic redox electrolyte at EPFL. The conduction band level of TiO_2 electrode and the redox potential of I^-/I^-_3 as − 0.7 V versus saturated calomel electrode (SCE) and 0.2 V versus SCE has been evaluated. A binary oxide photoelectrode with coffee as a natural dye was demonstrated, in 2014 . SnO_2 (x)–ZnO (1 − x) binary system with two different SnO_2 composition (x = 3, 5 mol%) were prepared by solid-state reaction at high temperature and employed as a photoanode. An improved efficiency was demonstrated for the larger SnO_2 composition and an overall power conversion efficiency (PCE) observed for SnO_2: ZnO device was increased from 0.18% (3:97 mol%) to 0.26% for a device with SnO_2 :ZnO (5:95 mol%) photoanode. Hu et al. observed that the performance of the DSSCs with graphite-P25 composites as photoanodes has been significantly enhanced by 30% improvement of conversion efficiency compared with P25 alone. They found an enhancement in the value of JSC from 9.03 to 12.59 mA/cm^2 under the condition of 0.01 wt% graphite amount and attained the conversion efficiency of 5.76%. Apart from TiO_2 , carbon and its different allotropes are also widely applied in DSSCs to fulfill future demand and arisen as a perfect surrogate material for DSSCs. Some reports have shown that incorporating carbon nanotube (CNT) in TiO_2 by hydrothermal or sol–gel methods greatly improved the cell's performance. Also, by improving the interconnectivity between the TiO_2 and CNT, an increase in the IPCE can be

found. Sun et al. reported that the DSSCs incorporating graphene in TiO_2 photoanode showed a PCE of 4.28%, which was 59% higher than that without graphene. Sharma et al. has shown the improvement in the PCE value from 7.35 to 8.15% of the co-sensitized solar cell using modified TiO_2 (G-TiO_2) photoanode, instead of pure TiO_2 photoanode. In 2014, it was shown that the electronically and catalytically functional carbon cloth works as a permeable and flexible counter electrode for DSSC. The researchers have found that the TiN nanotube arrays and TiN nanoparticles supported on carbon nanotubes showed high electrocatalytic activity for the reduction of triiodide ions in DSSCs . Single-crystal $CoSe_2$ nanorods were applied as an efficient electrocatalyst for DSSCs by Sun et al. in 2014. They prepared single-crystal $CoSe_2$ nanorods with a facile one step hydrothermal method. By drop-casting the $CoSe_2$ nanorod suspension onto conductive substrates followed by simple drying without sintering, they fabricated the thin $CoSe_2$ films and used as a highly efficient electrocatalyst for the reduction of I^-_3. They showed a power conversion efficiency of 10.20% under AM1.5G one-sun illumination for DSSCs with the standard N719 dye. Park et al. prepared a mesoporous TiO_2 Bragg stack templated by graft copolymer for dye-sensitized solar cells. To enhance dye loading, electron transport, light harvesting and electrolyte pore-infiltration in DSSCs, they prepared organized mesoporous TiO_2 Bragg stacks (om-TiO_2 BS) consisting of alternating high and low refractive index organized mesoporous TiO_2 (om-TiO_2) films. They synthesized om-TiO_2 films through sol-gel reaction using amphiphilic graft copolymers consisting of poly(vinyl chloride) backbones and poly(oxyethylene methacrylate) side chains, i.e., PVC-g-POEM as templates. They showed that a polymerized ionic liquid (PIL)-based DSSC fabricated with a 1.2-μm-thick om-TiO2 BS-based photoanode exhibited an efficiency of 4.3%, which was much higher than that of conventional DSSCs with a nanocrystalline TiO2 layer (nc-TiO_2 layer) with an efficiency of 1.7%. An excellent efficiency of 7.5% was demonstrated for a polymerized ionic liquid (PIL)-- based DSSC with a hetero-structured photoanode consisting of 400-nm-thick organized mesoporous TiO_2 interfacial (om-TiO_2 IF) layer, 7-μm-thick nc-TiO2, and 1.2-μm-thick om-TiO_2 BS as the bottom, middle, and top layers, respectively, which was again higher than that of nanocrystalline TiO_2 photoanode with an efficiency of 3.5%. Lee et al. reported platinum-free, low-cost, and flexible DSSCs using graphene film coated with a conducting polymer as a counter electrode. In 2014, Banerjee et al. demonstrated nickel cobalt sulfide nanoneedle-array as an effective alternative to Pt as a counter electrode in dye-sensitized solar cells. Calogero et al. invented a transparent and low-cost counter electrode based on platinum nanoparticles prepared by a

bottom-up synthetic approach. They demonstrated that with such a type of cathode, the observed solar energy conversion efficiency was the same as that obtained for a platinum-sputtered counter electrode and even was more than 50% obtained with a standard electrode, i.e., one prepared by chlorine platinum acid thermal decomposition, in similar working condition. By using a special back-reflecting layer of silver, they improved upon the performance of a counter electrode based on platinum sputtering and achieved an overall η of 4.75% under 100 $mWcm^{-2}$(AM 1.5) of simulated sunlight. They showed that, for the optical transmittance at different wavelengths of platinum-based films, i.e., Pt nanoparticles, Pt thermal decomposition, and Pt sputtered deposited onto FTO glass, the platinum nanoparticle-based cathode electrode (CE) prepared by Pt sputtering deposition method appeared more transparent than the platinum CE prepared using the Pt acid thermal decomposition method. Meanwhile, when Pt nanoparticle deposition method was employed, the transmittance was very poor . Anothumakkool et al. showed a highly conducting 1-D aligned polyethylenedioxythiophene (PEDOT) along the inner and outer surfaces of a hollow carbon nanofiber (CNF), as a counter electrode in a DSSC to enhance the electrocatalytic activity of the cell. They showed that the hybrid material (CP-25) displayed a conversion efficiency of 7.16% compared to 7.30% for the standard Pt counter electrode, 4.48% for bulk PEDOT and 5.56% for CNF, respectively. The enhanced conversion efficiency of CP-25 was accredited to the accomplishment of high conductivity and surface area of PEDOT through the 1-D alignment compared to its bulk counterpart. Further, through a long-term stability test involving efficiency profiling for 20 days, it was observed that CP-25 exhibited extraordinary durability compared to the bulk PEDOT. Recently, Huang et al. improved the performance of the device by inserting a $H_3PW_{12}O_{40}$ layer between the transparent conductive oxide layer and the compact TiO_2 layer. They observed the reduction in the recombination of the electrons upon the addition of $H_3PW_{12}O_{40}$ layer, resulting in longer electron lifetime and obtained a η = 9.3%, respectively. Li et al. reported that the transition metal nitrides MoN, WN, and Fe_2N show Pt-like electrocatalytic activity for dye-sensitized solar cells, where MoN showed superior electrocatalytic activity and a higher PV performance. Characteristic J–V curves of DSSCs using different metal nitrides and Pt counter electrodes showed that the cell fabricated with the MoN counter electrode achieved a FF = 0.66, which was higher than that of the Pt electrode . However, JSC = 11.55 $mAcm^{-2}$ was relatively high and the VOC of 0.735 V was almost same to the VOC = 0.740 V offered by Pt electrode. In the case of WN, VOC and JSC were relatively low, indicating a low efficiency of 3.67%.

DSSC with the Fe2N electrode attained lower values of VOC and FF, i.e., 0.535 V of VOC and 0.41 of FF, resulting in a poor η = 2.65%. Thus, above data shows superior performance of MoN-based DSSC among all other metal nitrides as CE material. Gokhale et al. showed a laser-synthesized super-hydrophobic conducting carbon with broccoli-type morphology as a CE for dye-sensitized solar cells in 2012. In 2014, plasmonic light harvesting of dye-sensitized solar cells by Au nanoparticle-loaded TiO_2 nanofibers was demonstrated by Naphade et al. because the surface morphology of a WE and a CE play a key role in the performance of DSSC. Usually, mesoporous TiO_2 nanoparticle films are used in WE fabrication because they provide large surface area for efficient dye adsorption. However, there are certain limitations associated with them as short electron diffusion length (10– 35 μm) and random electrical pathway induced by the substantial trapping and detrapping phenomena that take place within excessive surface states, defects, and grain boundaries of nanoparticles and disorganized stacking of TiO_2 films which limits the electron transport. Thus, doping of metallic cations and non-metallic anions in TiO_2, treating FTOs, applying 1-D nanostructures like nanowires, nanorods, nanosheets, nanoplates, and hollow spheres are approaches to modify the WE. However due to the low surface area, these 1-D nanostructures show poor dye loading. In 2015, Zhao et al. studied the influence of the incorporation of CNT-G-TiO_2 NPs into TiO_2 NT arrays and attained an efficiency of 6.17% for the DSSC based on CNT-G-TiO_2 nanoparticles TiO_2 nanotube double-layer structure photoanode . An efficiency of 8.30% was demonstrated by Qiu et al. for the DSSC based on double-layered anatase TiO_2 nano-spindle photoanodes. Apart from NTs, bilayer TiO_2 hollow spheres/TiO_2 nanotube array-based DSSC also showed an effective efficiency of 6.90%. Efficiency can also be improved by incorporating SnO_2 as a shell material on a photoanode. The integration of SnO_2 as a shell material on ZnO nanoneedle arrays results in a larger surface area and reduced recombination rate, thus increasing the dye adsorption which plays a crucial role in the performance of a cell. Huang and co-workers synthesized mesoporous TiO_2 spheres of high crystallinity and large surface area and applied it as a WE in the device. An excellent efficiency of 10.3% was achieved for the DSSC-employed TiO_2 spheres with long-term stability due to the terrific dye-loading and light-scattering abilities as well as attenuated charge recombination. Further, the efficiency was improved by performing the $TiCl_4$ treatment. Maheswari et al. reported various DSSCs employing zirconia-doped TiO_2 nanoparticle and nanowire composite photoanode film. They demonstrated highest η = 9.93% for Zirconia/TNPW photoanode with a hafnium oxide (HfO_2) blocking layer and observed that the

combination of zirconia-doped photoanode with blocking layer possibly restrains the recombination process and increases the PCE of the DSSCs effectively. However, many ideas do not achieve a great efficiency initially but at least embed different ideas and aspects for the synthesis of new materials. For instance, by using carbon-coated stainless steel as a CE for DSSC, Shejale et al. demonstrated a $\eta = 1.98\%$, respectively. Recently in 2018, a study was carried out to determine the effect of microwave exposure on photoanode and found an enhancement in the efficiency of the cell upon exposure. For the preparation of the DSSC, a LiI electrolyte, Pt cathode, TiO_2 photoanode, and Alizarin red as a natural sensitizer were used. An efficiency of 0.144% was found for the cell, where 10 min of microwave exposure was carried upon the photoanode.

Similarly, varied materials as mentioned earlier are synthesized as CE for efficient DSSCs. Last year, Guo et al. synthesized an In2.77S4@conductive carbon (In2.77S4@CC) hybrid CE via a two-step method and achieved $\eta = 8.71\%$ for the DSSC with superior electrocatalytic activity for the reduction of triiodide and, also, comparable to the commercial Pt-based DSSC that showed PCE of 8.75%, respectively. The doping of an organic acid, 1S-(+)-camphorsulfonic acid, with the conductive polymer poly(o-methoxyaniline) to form a hybrid (CSA/POMA) and its application in DSSCs as CE has been examined by Tsai et al. This CE showed increased surface roughness, decreased impedance, and increased crystallinity. In 2017, Liu et al. fabricated DSSCs employing $Co(bpy)_3^{3+/2+}$ as the redox couple and carbon black (CB) as the CE. The observation revealed superior electrocatalytic activity of a well-prepared CB film compared to that of conventional sputtered Pt. Due to the flexible nature of Cu foil substrates, Cu_2O has also been employed as a CE in DSSC. The fabrication of different samples by varying the sintering temperature of the CEs and obtaining the maximum efficiency of 3.62% at 600 °C of temperature has been reported . In 2013, by replacing the FTO with Mo as the conductor for the counter electrode, an increase in the value of FF as well as η was found . The EIS Nyquist plots showed the difference in R_s between the devices employed FTO (15.11 Ωcm^2) and Mo (7.25 Ωcm^2) due to the dissimilarity of the sheet resistance between FTO (8.2 Ω/sq) and Mo (0.16 Ω/sq). Also, by replacing FTO with Mo, a decrease in the R_{ctl} value from 6.87 to 3.14 Ωcm^2 was induced by the higher redox reactivity of Pt on Mo than that on FTO. In the queue of developing new materials, Maiaugree et al. fabricated DSSCs employing carbonized mangosteen peel (MPC) as a natural counter electrode with a mangosteen peel dye as a sensitizer. They observed a typical mesoporous honeycomb-like carbon structure

with a rough nanoscale surface in carbonized mangosteen peels and achieved the highest value of $\eta = 2.63\%$. By analyzing the Raman spectra , they found a broad D-peak (130.6 cm^{-1} of FWHM) located at 1350 cm^{-1} indicating the high disorder of sp3 carbon and a narrower G peak (68.8 cm^{-1} of FWHM) at 1595 cm^{-1} which correlated with a graphite oxide phase observed in 2008 . Thus, it was concluded the graphite oxide from MPC was a highly ordered sp2 hexagonal carbon oxide network. Furthermore, *I–V* characteristics of DSSCs employing different WE and CE are summarized in Table 1.

Electrolyte

To improve and study the performance of DSSCs, different electrolytes like gel electrolytes, quasi-solid-state electrolytes, ionic liquid electrolytes etc. have been applied as mediators so far. However, a different trend to optimize the performance of the DSSCs has been initiated by adding the energy relay dyes to the electrolyte.

Liquid Electrolyte

The cells efficiency through liquid electrolyte can be augmented by introducing iodide/triiodide redox couple and high dielectric constant organic solvents like ACN, 3-methoxypropionitrile (MePN), propylene carbonate (PC), γ-butyrolactone (GBL), *N*-methyl-2-pyrrolidone (NMP), ethylene carbonate (EC), and counter ions of iodides, where solvents are the key component of a liquid electrolyte. On the basis of their stability, organic solvents can be sequenced as imidazolium < picolinium < alkylpyridinium. Among various characteristics of solvents like donor number, dielectric constants, and viscosity, the donor number shows manifest influence on the V_{OC} and J_{SC} of DSSCs. Adding the small amounts of electric additives like *N*-methylbenzimidazole (NMBI), guanidinium thiocyanate (GuSCN), and TBP hugely improves the cell performance. Just like solvents, a co-absorbent also plays a key role in the functioning and performance of an electrolyte. The addition of co=absorbents in an electrolyte trims down the charge recombination of photoelectrons in the semiconductor with the redox shuttle of the electrolyte. Secondly, a co=absorbent may alter the band edge position of the TiO_2-conduction band, thus resulting in an augmentation in the value of V_{OC} of the cell. This suppresses the dye aggregation over the TiO_2 surface and results in long-term stability of the cell as well as increase in V_{OC}. Although the best regeneration of the oxidized dye is observed for iodide/triiodide as a redox couple for a liquid electrolyte, its characteristic of

severe corrosion for many sealing materials results in a poor long-term stability of the DSSC. Thus SCN^-/SCN_2, Br^-/Br_2, and $SeCN^-/SeCN_2$bipyridine cobalt (III/II) complexes are some of the other redox couples applied in DSSCs. The ionic liquids (IL) or room temperature ionic liquids (RTIL) are stand-in material for organic solvents in a liquid electrolyte. Despite the many advantages, i.e., negligible vapor pressure, low flammability, high electrical conductivity at room temperature (RT), and wide electrochemical window, they are less applicable in DSSCs. Because of their higher viscosity, restoration of oxidized dye restricts due to the lower transport speed of iodide/tri-iodide in solvent-free IL electrolytes. Thus, the performance of the dye-sensitized solar cells can also be enhanced by modifying the TiO_2 dye interface, i.e., by reducing vapor pressure of the electrolyte's solvent. In 2017, Puspitasari et al. investigated the effect of mixing dyes and solvent in electrolyte and thus fabricated various devices. They have used two types of gel electrolyte based on PEG that mixed with liquid electrolyte for analyzing the lifetime of DSSC. They also changed solvents as distilled water (type I) and ACN (type II) with the addition of concentration of KI and iodine, and achieved better efficiency for the electrolyte type II.

As low-viscous solution can cause leakage in the cell, thus, application of solidified electrolytes obtained by in situ polymerization of precursor solution containing monomer or oligomer and the iodide/iodine redox couple results in a completely filled quasi-solid-state electrolyte within the TiO_2 network with negligible vapor pressure. Komiya et al. obtained initial efficiency of 8.1% by applying the aforementioned approach. But still a question arises whether the polymer matrix will degrade under prolonged UV radiations or not. The effect on the addition of SiO_2 nanoparticles to solidify the solvent was also studied as to increase the cell efficiency, where only inorganic materials were applied in this technique. However, there are certain limitations associated with the addition of organic solvents within a liquid electrolyte, i.e., this leads hermetic sealing of the cell and the evaporation of solvents at higher temperature, and thus the cells do not uphold long-term stability. Therefore, more research was carried over the developments and implementation of gel, polymer, and solid-state electrolytes in the DSSCs with various approaches, such as the usages of the electrolytes containing p-type inorganic semiconductors, organic hole transporting materials (HTMs), and polymer gelator (PG). Chen et al. fabricated a solid-state DSSC using PVB-SPE (polyvinyl butyral-quasi-solid polymeric electrolyte) as an electrolyte. They measured the efficiency approximately 5.46%, which was approximately 94% compared to that of corresponding liquid-state devices, and

the lifetime observed for the devices was over 3000 h. Recently, a study explained the stability of the current characteristics of DSSCs in the second quadrant of the *I–V* characteristics. The study explains the continuous flow of the forward current and the operating voltage point that gradually shift towards more negative voltages in the second quadrant of the *I–V* characteristics. The increase in the ratio of iodide to tri-iodide in the electrolyte rather than to the decomposition or the coupling reactions of the constituent materials was considered to be the reason behind it. According to the studies, these changes were also considered as reversible reactions that can be detected based on the changes in the color of the electrolyte or the *I–V* measurements.

However, ILs with lower viscosity and higher iodine concentration are needed as to increase J_{SC} by increasing iodine mass transport. Laser transient measurements have been attempted and revealed that the high iodide concentration present in the pure ILs leads to a reductive quenching of the excited dye molecule. Due to the low cost, thermal stability, and good conductivity of the conductive polymers based on polytiophenes and polypyrroles, they can be widely applied in DSSCs despite using ILs. For the application point of view, the IL should have a high number of delocalized negative charge and counterions with a high chemical stability. Also, the derivatives of imidazolium salts are one of the best applicable in DSSCs. When 1-ethyl-3-methylimidazolium dicyanamide [EMIM] [DCA] with a viscosity of only 21 mPa s was combined with 1-propyl-3-methylimidayolium iodide (PMII, volume ratio 1:1), an efficiency of 7.4% was observed and, after prolonged illumination, some degradation was also found. A cell with a binary IL of 1-ethyl-3-methylimidazolium tetracyanoborate in combination with PMII showed a stable efficiency of 7% that retained at least 90% of its initial efficiency after 1000 h at 80 °C in darkness and 1000 h at 60 °C, at AM 1.5. Moudam et al. studied the effect of water-based electrolytes in DSSC and demonstrated a highly efficient glass and printable flexible dye-sensitized solar cells upon application. They used high concentrations of alkylamidazoliums to overcome the deleterious effect of water. The DSSCs employed pure water-based electrolyte and were tested under a simulated air mass 1.5 solar spectrum illumination at 100 $mWcm^{-2}$ and found the highest recorded efficiency of 3.45% and 6% for flexible and glass cells, respectively. An increase in the value of V_{OC} from 0.38 to 0.72 V on the addition of TBP to the electrolyte has been observed. Thus, to improve the efficiencies of DSSC, new materials were synthesized and applied in DSSCs. L-cysteine/L-cystine redox couple was employed in DSSC by Chen et al. which showed a comparable efficiency of

7.70%, as compared to the cell using I^-/I_3^- redox couple (8.10%). In 2016, Huang et al. studied the effect of liquid crystals (LCs) on the PCE of dye-sensitized solar cells. They observed that the addition of minute amounts of LC decreases the J_{SC} because it reduces the electrochemical reaction rate between the counter electrode and an electrolyte. Also, it delays the degradation rates of the cell because of the interaction between cyano groups of the doped LCs and organic solvent in the liquid electrolyte. Main components of different kinds of electrolytes are discussed:

Pyridine Derivatives (Like 4-Tert-Butylpyridine [TBP], 2-Propylpyridine, *N*-Methylbenzimidazole [NMBI])

The improved efficiency for a DSSC can be achieved by adding about 0.5 M of pyridine derivative within the electrolyte, due to which an increase in the value of V_{OC} occurs. This improved V_{OC} can be attributed to the positive band edge movement and slightly affected charge recombination rate on the basis of intensity-modulated photovoltage spectroscopy (IMVS). The study showed that after the adsorption of pyridine ring on TiO_2 surface, the pyridine ring induced electron density into the TiO_2 creating a surface dipole. But, the band edge movement results in the slight decrease in J_{SC} as compared to the untreated cell, due to the diminution in the driving force for electron injection. Further, application of NMBI over TBP was studied in 2003, due to its long-term stability under elevated temperature.

Alkyl Phosphonic/Carboxylic Acids (Like Decylphosphonic Acid [DPA], Hexadecylmalonic Acid [HDMA])

An improved V_{OC} with slight decrease in the J_{SC} have been observed when DPA and HDMA were combined. This was due to the presence of self-assembled long alkyl chain on the surface of TiO_2, which is responsible for the formation of densely packed hydrophobic monolayer and reduction in recombination rate too, as these long alkyl chains repel iodide from TiO_2 surface.

Guanidinium Derivatives (GuSCN)

The addition of guanidium thiocyanate as a co-absorbent in an electrolyte results in enhanced V_{OC} by ca. 120 mV with a downward shift in the conduction band by ca. 100 mV at the same time due to the suppression in the recombination rate by a factor of 20 and a difference of 20 mV gained for V_{OC}. By limiting the

downward shift in the conduction band, an improvement in the overall efficacy can be attained.

Solid-State Electrolyte (SSE)

The SSE falls in two subcategories: (1) where hole transport materials are used as a transport medium and (2) SSE containing iodide/triiodide redox couple as a transport medium. Both kinds of SSEs are discussed:

Hole Transport Materials (HTMs)

HTMs fall in the category of solid-state electrolytes, where HTMs are used a medium. These materials have set a great milestone in DSSCs and effectively applicable in cells because iodine/iodide electrolytes are highly chemically aggressive by nature and corrodes other materials easily, mostly metals. Most of the HTMs are chemically less-aggressive inorganic solids, organic polymers, or p-conducting molecules, although the results are still unmatched with the one obtained for iodine/iodide redox electrolytes because of the following reasons: 1. Due to their solid form, an incomplete penetration of solid HTMs within nano-porous TiO_2-layer leads to poor electronic contact between HTMs and the dye. Thus, incomplete dye regeneration takes place. 2. The high frequencies of charge recombination from TiO_2 to HTMs. 3. Due to the presence of organic hole conducting molecules, the series resistance of the cell increases due to the low hole mobility in the organic HTMs as compared to IL electrolytes. 4. HTM results in a drop in V_{OC}, as the recombination rate of electrons of CB with HTM becomes higher as compared to iodine/iodide redox electrolytes. 5.Low intrinsic conductivities of HTMs.

Thus, researchers need to synthesize and focus on HTMs whose VB energy should be slightly above the energy of the oxidized dye, should not absorb light, and must be photochemically stable, so that they can keep a healthy contact with the dye. Among a number of HTMs, some of the HTMs are considered:

Inorganic CuI Salt

CuI halogens and pseudo-halogens are two classes of inorganic CuI salts that can be applied as HTMs in a DSSC. Copper bromide (CuBr), copper iodide (CuI), and copper thiocyanate (CuSCN) are some copper-based compounds which work as a hole conductor and are more effective due to their good conductivity.

Although CuSCN is one of the best pseudo-halogen HTMs and despite its high hole mobility, its application results in high series resistance and does not support high current and also shows poor electronic contact between CuSCN and the dye, and poor pore filling due to their fast crystallization rates, which resulted in low η of < 4% for the corresponding solid-state DSSCs. Thus, to reduce the high recombination rate of electrons, additional blocking layers of insulating materials like SiO_2 or Al_2O_3 can be applied or coated around the TiO_2 particles which enhance the V_{OC} due to the suppressed recombination rate. With respect to halogens, CuBr showed an efficiency of 1.53% with thioether as an additive and demonstrated high stability under prolonged irradiation of about 200 h at RT and the application of nickel oxide (NiO) showed moderate PCEs of 3%. But, due to the poor solubility as well as crystallization of these materials, their application became a challenge and, thus, pseudo-halogens have proven to be more stable and efficient in DSSCs. But the devices were found to be highly unstable and the reproducibility became dubious.

Hole-Conducting Molecules

spiro-OMeTAD {2,2′,7,7′-tetrakis(N,N′-di-p methoxyphenylamine)-9,9′-spirobifluorene} is one of the most suitable candidate in the prospect of hole conducting molecules and thus also widely applicable in integrated devices. It was first introduced in 1998 with a high glass transition temperature of ca. 120 °C. The researchers observed the formation of amorphous layers that are necessary for the complete pore filling and showed an IPCE of 33%, yielding overall efficiency to about 0.74%, and finally 4% of efficiency with an ambiphillic dye Z907 was demonstrated. Some other triphenylamine detrivatives also demonstrated sufficient efficiencies in DSSCs. Again, spiro-OMeTAD has certain limitations as it has low charge carrier mobility, ca. 104 cm^2/Vs, that limits the thickness of the TiO_2 layer up to 2 μm and thus leads to incomplete light harvesting efficiency (LHE) of dye. Also, a high recombination rate between TiO_2 and FTO leads to low efficiencies in DSSCs.

Triphenylamine (TPA)

Phenylamines demonstrate a remarkable charge transporting property which makes them great hole transporting materials in organic electroluminescent devices. However, despite a huge range of non-conjugated polymers of di- and triphenylamine which are synthesized and used efficiently as HTMs in organic electroluminescent devices, their conjugated polymers are still rare. Polyaniline

(PANI) is the only well-recognized conjugated diphenylamine polymer due to its highly electrical conductive property and is environmentally stable in the doped state. In 1991, triphenylamine (TPA)-conjugated polymers were synthesized by Ni-catalyzed coupling polymerization. Okada et al. reported dimer (TPD 9), trimer (TPTR 10), tetramer (TPTE 11), and pentamer (TPPE 12) of TPA with the aid of Ullmann coupling reaction between the corresponding primary or secondary arylamines and aryl iodides.

SSE Containing Iodide/Triiodide Redox Couple

These SSEs have larger applications than those of HTMs, because interfacial contact properties of these solid-state electrolytes are better than those of HTMs. Fabrication of a DSSC based on solid-state electrolyte was reported by adding TiO_2 nanoparticle into poly(ethylene oxide) (PEO) and the overall light-to-electricity conversion efficiency of 4.2% for the cell was obtained under irradiation of AM 1.5100 $mWcm^{-2}$.

Quasi-Solid-State Electrolyte (QSSE)

QSSE has a hybrid network structure, because it consists of a polymer host network swollen with liquid electrolytes, thus showing the property of both solid (cohesive property) and liquid (diffusive transport property), simultaneously. Thus, to overcome the volatilization and leakage problems of liquid electrolytes, ILs like 1-propargyl-3- methylimidazolium iodide, bis(imidazolium) iodides and 1-ethyl-1-methylpyrrolidinium and polymer gel-like PEO, and poly(vinylidinefluoride) and polyvinyl acetate containing redox couples are commonly used as QSSEs. In 2015, Sun et al. fabricated a DSSC employing wet-laid polyethylene terephthalate (PET) membrane electrolyte, where PET is a commonly used textile fiber used in the form of a wet-laid non-woven fabric as a matrix for an electrolyte. According to their observations, this membrane can better absorb electrolyte turning into a quasi-solid, providing excellent interfacial contact between both electrodes of the DSSC and preventing a short circuit. The quasi-solid-state DSSC assembled with an optimized membrane exhibited a PCE = 10.248% at 100 $mWcm^{-2}$. To improve the absorbance, they plasma-treated the membrane separately with argon and oxygen, which resulted in the retention of the electrolyte, avoiding its evaporation, and a 15% longer lifetime of the DSSC compared to liquid electrolyte.

Hole-Conducting Polymers

IPCE of 3.5% by the application of C60/polythiphene derivative in DSSCs has been achieved for pure organic solar cells. However, this field is developing slowly, as its deposition by standard methods (like CBD) is difficult, because solid polymer does not penetrate the TiO_2-nanoporous layer. Hence, there are only few groups applied as conducting polymers in DSSCs. Ravirajan et al. demonstrated a monochromatic efficiency of 1.4% at 440 nm by applying fluorene-thiophene copolymer. Researchers are working hard so long to develop new efficient materials for electrolytes. Jeon et al. reported that the addition of alkylpyridinium iodide salts in electrolytes enhanced the performance of the dye-sensitized solar cells. They observed better *J–V* characteristics, 7.92% efficiency with $V_{OC} = 0.696$ V, $J_{SC} = 17.74$ mA/cm^2, and FF = 0.641 for the cell applying EC6PI (pyridinium salts) as compared to EC3ImI (imidazolium salts), whose $\eta = 7.46\%$ with $V_{OC} = 0.686$ V, $J_{SC} = 16.99$ mA/cm^2, and FF = 0.64. For a comparison, they added UV spectra for C6ImI and observed that the higher quantum efficiencies from the cell with EC6PI were obtained within the wide range from 460 to 800 nm. The quantum efficiencies were almost the same in the range of shorter wavelengths, may be due to the ability of C6PI to absorb more incident light than C3ImI at shorter wavelengths. Even so, the absorption coefficients for C6PI were higher than those for C6ImI over all the range, but the cell efficiencies are quite comparable. Lee et al. developed and utilized the conjugated polymer electrolytes (CPEs) like MPF-E, MPCZ-E, MPCF-E, and MPCT-E containing quaternized ammonium iodide groups in polymer solution and gel electrolytes for DSSCs. They observed, as the polymer content in the electrolyte solution increased, the electrochemical impedance also increased for the cells based on CPE containing polymer solution electrolytes, whereas the PV performances showed the reverse trend. Table 2 shows the FF and efficiencies for the DSSCs employing various dyes and mediators.

Table 2 Efficiencies for different dyes and electrolytes

Developments in Dye Synthesis

As dyes play a key role in DSSCs, numerous inorganic and organic/metal-free dyes/natural dyes, like N3, N719 , N749 (black dye) , K19 , CYC-B11, C101, K8, D102, SQ, Y123, Z907, Mangosteen , and many more have been utilized as sensitizers in DSSCs.

Metal (Ru) Complexes

Metal complex dyes produced from the heavy transition metals such as the complexes of ruthenium (Ru), Osmium (Os), and Iridium (Ir) have widely been used as inorganic dyes in DSSCs because of their long excited lifetime, highly efficient metal-to-ligand charge transfer spectra, and high redox properties. ML2(X)2 is the general structure of the sensitizer preferred as a dye, where M represents a metal, L is a ligand like 2,2′-bipyridyl-4,4′-dicarboxylic acid and X presents a halide, cyanide, thiocyanate, acetyl acetonate, and thiocarbamate or water substituent group. Due to the thermal and chemical stability and wide absorption range from visible to NIR, the ruthenium polypyridyl complexes show best efficiencies and, thus, have been under extensive use so far.

Ru Complexes

In 1991, O'Regan and Grätzel reported the efficiency of 7.12% for the very first DSSC based on the ruthenium dye (black dye) [3]. Later, an efficiency of about 10% was reported by them using Ru-based dye (N749) which has given this topic a new sight. Most of the Ru complexes consist of Ru(II) atoms coordinated by polypyridyl ligands and thiocyanate moieties in octahedral geometery, and because of the metal to ligand charge transfer (MLCT) transitions, they exhibit moderate absorption coefficient, i.e., < 18,000 M^{-1} cm^{-1}. Ru (II) complexes lead the inter crossing of excited electron to the long-lived triplet state and augmentation in the electron injection. Further, to improve the absorption and emission as well as electrochemical properties of Ru complexes, bipyridyl moieties can be replaced by the carboxylate polypyridine Ru dyes, phosphate Ru dyes, and poly nuclear bipyridyl Ru dyes. Table 3 show the photoelectric performance for DSSCs based on different metal complex [polypyridyl (RuII)] dyes.

Table 3 Absorption spectra and photoelectric performance for DSSCs based on different metal complex [polypyridyl (RuII)] dyes

N3/N719/N712 Dyes

In 1993, Nazeeruddin et al. reported DSSC based on Ru-complex dye known as N3 dye {cis-di(thiocyanato)bis(2,2-bipyridine-4,4-dicarboxylate)ruthenium}, which contained one Ru center and two thiocyanate ligands (LL') with additional carboxylate groups as anchoring sites and absorbed up to 800 nm radiations. They obtained 10.3% efficiency for a system containing N3 dye and treated the dye

covered film with TBP. At 518 and 380 nm wavelength, this dye attained maximum absorption spectra with respective extinction coefficients as $1.3 \times 10^4\ M^{-1}\ cm^{-1}$ and $1.33 \times 10^4\ M^{-1}\ cm^{-1}$, respectively. The dye has showed the 60 ns of excited state lifetime and sustained for more than 10^7 turnovers without the significant decomposition since the beginning of the illumination. Further, the absorption of the dye can be extended into the red and NIR by substituting the ligands such as thiocyanate ligands and halogen ligands. For example, a device containing acetylacetonate showed $\eta = 6.0\%$, followed by a pteridinedione complex with 3.8% efficiency and a diimine dithiolate complex with 3.7% efficiency.

It has been investigated that during esterification, the dye gets bounded to the TiO_2 chemically which results in the partial transformation of protons of the anchoring group to the surface of the TiO_2. Thus, it was concluded that the photovoltaic (PV) performance of the cell gets influenced by the presence of the number of protons on the N3 photosensitizer or, in other words, the modification in protonation level of N3 (N712, N719) affects the performance of the device, in two major aspects. Firstly, the increase in the concentration of the protons results in the positively charged TiO_2 surface and the downward shift in the Fermi level of TiO_2. Hence, a drop in the V_{OC} takes place due to the positive shift of the conduction band edge induced by the surface protonation. Secondly, the electric field associated with the surface dipole enhances the absorption of the anionic Ru(II) complexes and, thus, insists the electron injection from the excited state of the dye to the conduction band of the TiO_2. In 2001, Nazeeruddin et al. reported a 10.4% of efficiency for the DSSCs using a ruthenium dye, i.e., “black dye”, where its wide absorption band covers the entire visible range of wavelengths. Grätzel and group demonstrated the PCE of 9.3% for the monoprotonated sensitizer N3 $[TBA]_3$ closely followed by a diprotonated sensitizer N3$[TBA]_2$ or N719 with a conversion efficiency of 8.4%. Later, Wang et al. and Chiba et al. reported a $\eta = 10.5\%$ and $\eta = 11.1\%$, for the devices that used black dye as a sensitizer in DSSCs.

A new dye “N719” was reported by Nazeeruddin et al. by replacing four H^+ counterions of N3 dye by three TBA^+ and one H^+ counterions and achieved $\eta = 11.2\%$ for the respective device. Despite having almost the same structure to the N3 dye, the higher value of η for N719 was accredited to the change in the counterions, as they altered the speed of adsorption onto the porous TiO_2 electrode, i.e., N3 is fast (3 h) whereas N719 is slow (24 h). The dye-

sensitized solar cell database (DSSCDB) yields around 329 results assembled from over 250 articles when queried as "N719," where the reported efficiencies range between 2 and 11%.

Recently, Shazly et al. fabricated the solid-state dye-sensitized solar cells based on $Zn_{1-x}Sn_xO$ nanocomposite photoanodes sensitized with N719 and insinuated with spiro-OMeTAD as a solid hole transport layer and achieved highest efficiency of 4.3% with $J_{SC} = 12.45$ mA.cm^{-2}, $V_{OC} = 0.740$ V, and FF = 46.70. Similarly, by applying different techniques, like post treatment of photoanode, optimizing the thickness of the nc-TiO_2 layer, and the antireflective filming, Grätzel group reported $\eta = 11.3\%$ for the device containing the dyes C101 and $\eta = 12.3\%$ for Z991 dye-based DSSCs. Again, if a sensitizer does not carry even a single proton, the value expected for V_{OC} will be high but the value for J_{SC} becomes low. Thus, there should be an optimal amount of protonation of the sensitizer required, so that the product of both J_{SC} and V_{OC} can determine the conversion efficiency of the cell as a maximum. And thus, deprotonation levels of N3, N719, and N712 in solar cells were investigated, where the doubly protonated salt form of N3 or N719 showed higher PCE as compared to the other two sensitizers. The effect of dye protonation on the *I–V* characteristics of TiO_2 photoanode sensitized with different Ru dyes as N3 (4 protons), N719 (2 protons), N3[TBA]$_3$ (1 proton), and N712 (0 protons) dyes, measured under AM 1.5 were shown. However, the main limitations of N3 sensitizers are their relatively low molar extinction coefficient and less of absorption in the red region of the visible spectrum.

π-System Extension (N945, Z910, K19, K73, K8, K9)

As compared to the other organic dyes, standard Ru complexes have significantly lower absorption coefficient and thus a thick layer of TiO_2 was required, which results in the higher electron recombination probability. Thus, two carboxylic acid groups of N3 can be replaced by the ligands containing conjugated π-systems to enhance the absorption and the cell efficiency, simultaneously. Thus, the reason behind the π-system extension in dyes is to create sensitizers with higher molar extinction coefficients (ε), so that the LUMO of the dye can be tuned to get directionality in the excited state and to introduce hydrophobic side chains that repel water and triiodide from the TiO_2 surface. Recently, Rawashdeh et al. have demonstrated an efficiency of 0.45% by modifying the photoanode as graphene-based transparent electrode sensitized with 0.2 mM N749 dye in ethanolic solution.

Styryl-ligands attached to the bipyridil ring showed the utmost results. The $\varepsilon = 1.69 \times 10^4\ M^{-1}\ cm^{-1}$ for the Z910 dye , $\varepsilon = 1.82 \times 10^4\ M^{-1}\ cm^{-1}$ for the K19 dye, and $\varepsilon = 1.89 \times 10^4\ M^{-1}\ cm^{-1}$ for the N945 dye have been found, which were at least 16% more as compared to the standard N3 dye. An efficiency of 10.2% was demonstrated by Wang et al. for Z910 dye. 10.8% of the efficiency was observed for the N945 dye in 2007, on thick electrodes and with volatile electrolytes which was about the same as for the N3 as reference, but, when applied on thin electrodes and with non-volatile electrolytes, the observed PCE was significantly higher. At the same time, a remarkable stability at 80 °C (in darkness) and 60 °C temperature (under AM 1.5) was observed, and between − 0.71 V and − 0.79 V vs. normal hydrogen electrode (NHE), the excited state of these dyes has been reported and was observed sufficiently more negative than the conduction band of TiO_2 (ca. − 0.1 V vs. NHE) to ensure the complete charge injection. In terms of higher molar extinction coefficient, Nazeeruddin et al. synthesized K8 and K9 dyes that showed even better results as compared to the previous ones. K8 and K9 complexes showed broad and intense absorption bands between 370 and 570 nm. In DMF solution, the K9 complex showed the maxima at 534 nm (λ_{max}) with a $\varepsilon = 14{,}500\ M^{-1}\ cm^{-1}$ which was blue shifted by 22 nm compared to K8 complex which showed maxima at 556 nm with a $\varepsilon = 17{,}400\ M^{-1}\ cm^{-1}$, respectively. Thus, due to the substitution of 4, 4′-bis (carboxylvinyl)-2, 2′-bipyridine by 4,4′- dinonyl-2,2′-bipyridine, ε observed for K9 complex was ~ 20% less than that of the K8 complex. The overall PCE observed for K8 and K9 complexes were 8.46% with $J_{SC} = 18\ mA/cm^2$ and $V_{OC} = 640$ mV and 7.81% with $J_{SC} = 16\ mA/cm^2$ and $V_{OC} = 666$ mV, respectively. Grätzel group synthesized K19 as a second amphiphilic dye and demonstrated that K19 shows 18,200 $M^{-1}\ cm^{-1}$ M extinction coefficient, 7.0% overall conversion efficiency and a low energy metal-to-ligand transition (MLCT) absorption band at 543 nm, which was higher than the corresponding values for the first amphiphilic dye Z907 with a molar extinction coefficient of 12,200 $M^{-1}\ cm^{-1}$, 6.0% overall conversion efficiency, and standard N719 dye with a molar extinction coefficient of 14,000 $M^{-1}\ cm^{-1}$ with 6.7% overall PCE under the same fabrication and evaluation conditions. They appraised the performance of the device using N719, Z907, and K19 as sensitizers during thermal aging at 80 °C and observed a lower stability for N719 dye may be due to the desorption of the sensitizer at higher temperature; however, K19 and Z907, both retained over 92% of their initial performances under the thermal stress at 80 °C for 1000 h .

Thiophene ligands containing Ru sensitizers also showed good efficiencies. In 2006, Yanagida et al. reported a Ru complex, by replacing a phenylvinyl group of K19 by thienylvinyl group in HRS-1 and an improved stability along with respectable LHE in vis-NIR and a reversible one electron oxidation process was reported. They found a η up to 9.5% for HRS-1 (substituted thiophene derivatives). Several thiophene containing sensitizers have been developed without conjugation, such as C101 and CYC-B1. After the development of C101 dye, Ru (II) thiophene compounds gained special attention as having set a new DSSC efficiency record of 11.3–11.5% and became the first sensitizer to triumph over the well-known N3 dye.

Amphiphilic Dyes with Alkyl Chains

Two of the four carboxylic groups of N3 dye are replaced by long alkyl chains because the ester linkage of the dye to the TiO_2 was prone to hydrolyze, if water gets adsorbed on the TiO_2 surface, thus resulting in usually lower absorption spectrum in these sensitizers due to the smaller conjugated π-system of the bipyridil-ligand. Even though the PCE offered by these sensitizers were appreciable, ranging from 7.3% for Z907 (with 9 carbon atoms) to 9.6% for N621 (with 13 carbon atoms) and were highly stable, Z907 sensitized DSSCs passed 1000 h at 80 °C in darkness and at 55 °C under illumination without any degradation. It has been found that by coadsorption of decylphosphonic acid on the TiO_2 NPs, the hydrophobicity of the surface could be even enhanced and, thus, stable cells have been demonstrated.

Different Anchoring Groups

Most of the sensitizers in DSSCs have carboxylic acid groups as an anchor on the surface of TiO_2. But the dye molecules get desorbed at the semiconductor surface at a pH > 9, due to the shifting of the equilibrium towards the reactant side. Thus, dyes with different anchoring groups are needed. Again, most of the research focuses on phosphonic acid and the credit goes to its binding strength to a metal oxide surface, as the binding strength to a metal oxide surface decreases in the order, phosphonic acid > carboxylic acid > ester > acid chloride > carboxylate salts > amides. Z955 is a Ru-complex containing phosphonic acid as an anchoring group and demonstrated a η = 8% accompanied by good stability under prolonged light soaking for about 1000 h at AM 1.5 and 55 °C. Triethoxysilane and boronic acid are some other anchoring groups. π-Extended ferrocene with varied anchoring groups (–COOH, –OH, and –CHO) has been applied as

photosensitizers in DSSCs. Chauhan and co-workers has synthesized and characterized two new compounds as $FcCH{=}NC_6H_4COOH$ (1) and $FcCH{=}NCH_2CH_2OH$ (2), where $Fc = C_5H_4FeC_5H_5$ and FcCHO are used as the starting material. By cyclic voltammetry (CV) in dichloromethane solution and using density functional theory (DFT) calculations, they have explained the quasi-reversible redox behavior of the dyes. The redox-active ferrocenyl group exhibited a single quasi-reversible oxidation wave with $E' = 0.34$, 0.44, and 0.44 V for 1, 2, and 3, respectively. In 2017, a study was carried out to inspect the influence of a cyano group in the anchoring part of the dye on its adsorption stability and the overall PV properties like electron injection ability to the surface and V_{OC}. The results indicated that the addition of the cyano group increased the stability of adsorption only when it adsorbs via CN with the surface and it decreased the photovoltaic properties when it was not involved in binding.

However, in the race of improved efficiency and efficient DSSCs, Ru (II) dyes are still an ace. The most vital reason following usage of Ru dyes in DSSCs is their extraordinary stability when being absorbed on the TiO_2 surface. N749 and Z907 are the two important Ru dyes, although N749 which shows broad absorption and high efficiency, in contrast, has low absorption coefficient about $\sim 7000\ M^{-1}\ cm^{-1}$ and the stability of this dye was not so good as compared to other Ru sensitizers. PCE of 10.4% has been observed for black dye, under AM 1.5 and full sunlight. It achieved sensitization over the whole visible range extending into the NIR up to 920 nm with 80% IPCE and 10.4% overall efficiency, when anchored on TiO_2 nanocrystalline film. At NREL, black dye (N749)-sensitized DSSC showed efficiency of 10.4% with $J_{SC} = 20.53\ mA/cm^2$, $V_{OC} = 0.721$ V, and FF = 0.704, where the active area of the cell was $0.186\ cm^2$. Nazeeruddin et al. reported a comparative study between the spectral response of the photocurrent of the two dyes, N3 and N749. In the vis-range, both chromophores showed very high. IPCE values. The response of N749 dye was observed to be extended 100 nm further into the IR compared to that of N3. The recorded photocurrent onset was close to 920 nm and there on the IPCE rose gradually until at 700 nm it reached to a plateau of ca. 80%. From overlap integral of the curves with the AM 1.5 solar emission, it could be predicted that J_{SC} of the N3 and black dye-sensitized cells to be 16 and $20.5\ mA/cm^2$, respectively. In Z907 sensitizer, one of the dicarboxy bipyridine ligands in N3 molecule was replaced by a nonyl bipyridine, which resulted in the formation of a hydrophobic environment on the device. However, the dye has set a precedent for hundreds of tris-heteroleptic Ru complexes with isothiocyanate

ligands that were developed in the last 15 years, but provides efficiencies rarely comparable to N719.

Metal-Free, Organic Dyes

Despite the capability to provide highly efficient DSSCs, the range of application of Ru dyes are limited to DSSCs, as Ru is a rare and expensive metal and, thus, not suitable for cost-effective, environmentally friendly PV systems. Therefore, development and application of new metal-free/organic dyes and natural dyes is much needed. The efficiency of DSSCs with organic dyes has been increased significantly in the last few years and an efficiency of 9% was shown by Ito and co-workers.

Table 4 The efficiency for DSSCs based on different metal-free organic dyes

Thus, metal-free organic dyes are developing at a fast pace to overcome the limitations discussed above and especially promising is the fast learning curve, which raises hope of the further synthesis of new materials with higher stability and, thus, designing highly efficient DSSCs at much lower prices. Though the efficiencies offered by these dyes are less comparable to those by Ru dyes, their application is vast as they are potentially very cheap because of the incorporation of rare noble metals in organic dyes; thus, their cost mainly depends on the number of synthesis steps involved. Other advantages associated with organic dyes are their structure variations, low cost, simple preparation process, and environmental friendliness as compared to Ru complexes; also, the absorption coefficient of these organic dyes is typically one order of magnitude higher than Ru complexes which makes the thin TiO_2 layer feasible. Thus, there is a huge demand to develop new pure organic dyes, so that the commercialization of DSSCs becomes easier.

However, there are certain limitations associated with these dyes too, as under high elevated temperatures the observed stability of the organic dyes were not as good as expected. Therefore, to get a larger photocurrent response for newly designed and developed organic dyes, it is essential to attain predominant light-harvesting abilities in the whole visible region and NIR of dyes, with a sufficiently positive HOMO than I^-/I^-_3 redox potential and sufficiently negative

LUMO than the conduction band edge level of the TiO_2 semiconductor, respectively. In 2008, Tian et al. fabricated DSSCs based on a novel dye (2TPA-R), containing two triphenylamine (TPA) units connected by a vinyl group and rhodanine-3-acetic acid as the electron acceptor to study the intramolecular energy transfer (E_nT) and charge transfer (ICT). They found that the intramolecular E_nT and ICT processes showed a positive effect on the performance of DSSCs, but the less amount of dye was adsorbed on TiO_2 which may make it difficult to improve the efficiency of DSSCs. An efficiency of 2.3% was attained for the DSSC used 2TPA-R dye and an imidazolium iodide electrolyte, whereas $\eta = 2\%$ was achieved for TPA-R dye. This improved efficiency for 2TPA-R device was possibly due to the contribution of the E_nT and ICT. They studied the effect of 2TPA-R via absorption spectrum and found that the two absorption bands, i.e., λ_{abs} at 383 nm and 485 nm obtained for 2TPA-R, are almost the same as those observed for 2TPA (λ_{abs} at 388 nm) and TPA-R (λ_{abs} at 476 nm) in CH_2Cl_2 solution (2×10^{-5} M). Thus, the study on intramolecular E_nT and ICT could help in the design and synthesis of efficient organic dyes. Hence, a suitable anchoring group which can chemically bind over the TiO_2 surface with a suitable structure and effective intramolecular E_nT and ICT processes, is also required for synthesis.

The construction of most of the organic dyes is based on the donor- acceptor (D-A)-like structure linked through a π-conjugated bridge (D–π–A) and usually has a rod-like configuration. Moieties like indoline, triarylamine, coumarin, and fluorine are employed as an electron donor unit, whereas carboxylic acid, cyanoacrylic acid, and rhodamine units are best applicable as electron acceptors to fulfill the requirement. The linking of donor and acceptor is brought about by adding π spacer such as polyene and oligothiophene. This type of the structure results in a higher photoinduced electron transfer from the donor to acceptor through linker (spacer) to the conduction band of the TiO_2 layer, where the π-conjugation can be extended either by increasing the methine unit or by introducing aromatic rings such as benzene, thiophene, and furan or in other words by adding either electron donating or withdrawing groups, which results in the enhanced light harvesting ability of the dye, and by using different donor, linker, and acceptor groups, the photophysical properties of the organic dyes can also be tuned. Whereas the photophysical properties change with the expansion of π-conjugation due to the shift of the both HOMO and LUMO energy levels, thus, D–π–A structure was considered to be the most promising class of organic

dyes in DSSCs as they can be easily tuned. Moreover, in 2010, the encouraging efficiency up to 10.3% was reported using organic dyes. Fuse et al. demonstrated a one-pot procedure to clarify the structure–property relationships of donor–π–acceptor dyes for DSSCs through rapid library synthesis. Four novel organic dyes IDB-1, ISB-1, IDB-2, and ISB-2, based on 5-phenyl-iminodibenzyl (IDB) and 5-phenyliminostlbene (ISB) as electron donors and cyanoacrylic acid moiety as an electron acceptor connected with a thiophene as a π-conjugated system, were designed by Wang et al. in 2012. The highest efficiencies for the devices based on ISB-2 were observed due to the larger red shifts of 48 nm for ISB-2, indicating the more powerful electron-donating ability due to the increased linker conjugation. The absorption peaks for IDB-1, ISB-1, IDB-2, and ISB-2 were obtained at 422, 470, 467, and 498 nm in dichloromethane-diluted solution, respectively.

Tetrahydroquinolines ,yrolidine diphenylamine, triphenylamine (TPA), coumarin, indoline, fluorine, carbazole (CBZ), phenothiazine (PTZ), phenoxazine (POZ) , hemicyanine dyes, merocyanine dyes, squaraine dyes, perylene dyes, anthraquinone dyes, boradiazaindacene (BODIPY) dyes, oligothiophene dyes, and polymeric dyes are widely used in DSSCs and are still under development. Jia et al. designed quasi-solid-state DSSCs employing two efficient sensitizers FNE55 and FNE56, based on fluorinated quinoxaline moiety, i.e., 6, 7-difluoroquinoxaline moiety, and an organic dye FNE54 without fluorine was designed for comparison. From the studies, it was concluded that the absorption properties of the dye enhanced bathochromically from 504 nm for FNE54 to 511 nm and 525 nm for FNE55 and FNE56 sensitizers upon the addition of fluorine into the dye. The addition of fluorine resulted in the improved electron-withdrawing ability of the quinoxaline and, thus, enhanced the push–pull interactions and narrowed the energy band gap. Due to the high polarizability, spectroscopically and electrochemically tunable properties and high chemical stability, π-conjugated oligothiophenes were well applied as spacers in DSSCs. To induce a bathochromic shift and augment the absorption, a number of thiophene units could be increased in the spacers, and by controlling the length of these thiophene units or chain, higher efficiencies up to two to three units can be achieved, as the π-conjugated spacers used previously were thiophenes linked directly or through double bonds to the donor moiety.

As good electron injection is one of the parameters for higher efficiency in the DSSCs, cyanoacetic acid and cyanoacrylic acid are well employed as acceptor

units due to their strong electron withdrawing capability. Yu et al. concluded cyanoacrylic acid as a strong electron acceptor for D–π–A-based dyes because the dye incorporating cyanoacrylic acid as an electron acceptor showed the best results and, due to the maximum absorption spectrum and the highest molar excitation coefficient, the DSSC achieved $\eta = 4.93\%$. Wang and co-workers designed organic dyes based on thienothiophene as π conjugation unit, where they used triphenylamine as donor and cyanoacetic acid as an acceptor. They substituted different alkyl chains on the triphenylamine unit and found the best efficiency of about 7.05% for the sensitizers with longer alkoxy chains due to the longer electron lifetime. Acceptors based on rhodanine-3-acetic acid were also used as an alternative, but due to the low lying molecular LUMO, the results obtained were not pleasing.

Coumarin Dyes

Coumarin is a synthetic organic dye and is a natural compound found in many plants like tonka bean, woodruff, and bison grass (molecular structure. In 1996, Grätzel et al. found the efficient electron injection rates of 200 fs from C343 into the conduction band of the TiO_2, where for the first time the transient studies on a coumarin dye in DSSCs were performed. But the narrow absorption spectrum of C343, i.e., lack of absorption in the visible region, resulted in the lower conversion efficiency of the device. This can be altered by adding more methane groups that result in expanding the π-conjugation linkers and an increased efficiency of the DSSC. Giribabu and co-workers synthesized RD-Cou sensitizers and obtained the conversion efficiency of 4.24% using liquid electrolyte, where coumarin moiety was bridged to the pyridyl groups by thiophene, which resulted in the extended π-conjugation and broadening of the metal-to-ligand charge transfer spectra. They found that the absorption spectrum of RD-Cou dye was centered at 498 nm with a $\varepsilon = 16{,}046\ M^{-1}\ cm^{-1}$. Despite the lower efficiency offered by these cells, the thermal stability of the sensitizer makes its rooftop applications possible because the dye showed stability of up to 220 °C during thermal analysis.

Molecular Structure of metal-free organic dyes

Indole Dyes

Indole occurs naturally as a building block in amino acid tryptophan, and in many alkaloids and dyes too. It is substituted with an electron withdrawing anchoring group on the benzene ring and an electron donating group on the nitrogen atom,

and these dyes have demonstrated good potential as a sensitizer. Generally, the D–A structure of an indole dye is such that the indole moiety acts as an electron donor and is connected to a rhodanine group that acts as an electron acceptor. Also by introducing the aromatic units into the core of the indoline structure, the absorbance in the infrared (IR) region of the visible spectra as well as the absorption coefficient of the dye can be enhanced significantly. An efficiency of 6.1% was demonstrated for DSSCs with D102 dye, and by optimizing the substituents, 8% of the efficiency was attained with D149 dye. Another dye "D205" was synthesized by controlling the aggregation between the dye molecules, as an indoline dye with an n-octyl substituent on the rhodanine ring of D149. They investigated that n-octyl substitution increased the V_{OC} without acknowledging the presence of CDCA too much. However, the increase in the V_{OC} of D205 due to the CDCA was approximately 0.054 V but showed little effect on D149 with an increase of 0.006 V only. But the CDCA and n-octyl chain (D205) together improved the V_{OC} by up to 0.710 V significantly, which was 0.066 V higher (by 10.2%) than that of D149 with CDCA.

Further in 2012, $\eta = 9.4\%$ was shown by Wu et al. with the observed $J_{SC} = 18$ $mAcm^{-2}$, $V_{OC} = 0.69$ V, and FF = 0.78, by employing indoline as an organic dye in the respective DSSC. Suzuka et al. fabricated a DSSC sensitized with indoline dyes in conjunction with the highly reactive but robust nitroxide radical molecules as redox mediator in a quasi-solid gel form of the electrolyte. They obtained an appreciable efficacy of 10.1% at 1 sun. To suppress a charge-recombination process at the dye interface, they introduced long alkyl chains, which specifically interact with the radical mediator. Recently in 2017, Irgashev et al. synthesized a novel push-pull thieno[2,3-b]indole-based metal-free dyes and investigated their application in DSSC. They designed IK 3–6 dyes based on the thieno[2,3-b]indole ring system, bearing various aliphatic substituents such as the nitrogen atom as an electron-donating part, several thiophene units as a π-bridge linker, and 2-cyanoacrylic acid as the electron-accepting and anchoring group. An efficiency of 6.3% was achieved for the DSSCs employing 2-cyano-3-{5-[8-(2-ethylhexyl)-8H-thieno[2,3-b]indol-2-yl]thiophen-2-yl}acrylic acid (IK 3), under simulated AM 1.5 G irradiation (100 $mWcm^{-2}$), whereas the lower values of $\eta = 1.3\%$ and 1.4%, respectively, were shown by the dyes IK 5 and IK 6. The LUMO energy levels are more negative than the conduction edge of the TiO_2 (− 3.9 eV), and their HOMO energy levels of all four dyes were found to be more positive than the I^-/I_3^- redox couple (− 4.9 eV), making possible regeneration of oxidized dye molecules after injection of excited electrons into

TiO_2 electrode. The less efficiency of other dyes was contributed by the intermolecular π-stacking and aggregation processes in these dyes, proceeding on the photoanode surface.

Porphyrins

Porphyrin shows strong absorption and emission in the visible region and has a long lifetime in its excited singlet state (> 1 ns), very fast electron injection rate (femtosecond range), millisecond time scale electron recombination rate, and tunable redox potentials. In 1987, the first paper was published on DSSCs based on efficient sensitization of TiO_2 with porphyrins. This led researchers in the direction to make efforts for the synthesis of novel porphyrin derivatives with the underlying idea to mimic nature's photosystems I and II, so that the large molar extinction coefficient of the Soret bands and Q bands can be exploited. In 2007, a Zn-porphyrin dye-based DSSC was fabricated by Campbell et al. and has given the exceptional PCE of 7.1%. Krishna and co-workers investigated the application of bulky nature phenanthroimidazole-based porphyrin sensitizers in DSSCs. The group designed a novel D–π–A-based porphyrin sensitizer having strong electron-donating methyl phenanthroimidazole ring and ethynylcarboxyphenyl group at meso-position of porphyrin framework (LG11). They have attached the hexyl phenyl chains to the phenanthroimidazole moiety to reduce the unwanted loss of V_{OC} caused by dye aggregation and charge recombination effect, thus achieving an increase in V_{OC} to 460 and 650 mV.

Wang et al. have synthesized zinc porphyrins in a series bearing a phenylethynyl, naphthalenylethynyl, anthracenylethynyl, phenanthrenylethynyl, or pyrenylethynyl substituent, namely LD1, LD2, LD3a, LD3p, and LD4, as photosensitizers for DSSCs. The overall efficiencies of the corresponding devices resulted as LD4 (with$\eta = 10.06\%$) > LD3p > LD2 > LD3a > LD1. The higher value of η and $V_{OC} = 0.711$ V was achieved for LD4 due to the broader and more red-shifted spectral feature; thus, the IPCE spectrum was covered broadly over the entire visible region. Later for a push–pull zinc porphyrin DSSCs, changes in the structural design were carried out and structures with long alkoxyl chains enveloping the porphyrin core were built. By following the process, a $\eta = 12.3\%$ was achieved by Yella et al. for DSSC with cobalt as the mediator.

Giovannetti et al. investigated the free base, Cu(II) and Zn(II) complexes of the 2,7,12,17-tetrapropionic acid of 3,8,13,18-tetramethyl-21H,23H porphyrin (CPI) in solution and bounded to transparent monolayer TiO_2 nanoparticle films to

determine their adsorption on the TiO_2 surface, to measure the adsorption kinetics and isotherms, and to use the obtained results to optimize the preparation of DSSC PVCs (photovoltaic cells). The absorption spectra study of CPI, CPIZn, and CPICu molecules onto the TiO_2 surface revealed the presence of typical strong Soret and weak Q bands of porphyrin molecules in the region 400–450 nm and 500–650 nm, which were not changed with respect to the solution spectra. They observed no modification in the structural properties of the adsorbed molecules.

Triarylamine Dyes

Due to the good electron as well as transporting capability and its special propeller starburst molecular structure with a nonplanar configuration, the triarylamine group is widely applied as a HTM in various electronic devices. Triarylamine derivative distributes the π–π stacking and, thus, improves the cells performance by reducing the charge recombination, minimizing the dye aggregation and enhancing the molar extinction coefficient of the organic dye. By the addition of alkyl chains or donating groups, the structural modification of the triarylamine derivatives could be performed. The performance of a basic D–π–A organic dye can be improved by simply binding donor substitutions on the π-linker of the dye. Thus, Prachumrak and co-workers have synthesized three new molecularly engineered D–π–A dyes, namely T2–4, comprising TPA as a donor, terthiophene containing different numbers of TPA substitutions as a π-conjugated linker and cyanoacrylic acid as an acceptor. To minimize the electron recombination between redox electrolyte and the TiO_2 surface as well as an increase the electron correction efficiency, the introduction of electron donating TPA substitutes on the π-linker of the D–π–A dye can play a favorable game, leading to improved V_{OC} and J_{SC}, respectively. In 2006, Hagberg et al. published a paper on TPA-based D5 dye, where the overall PCE demonstrated for D5 dye was 5.1% in comparison with the standard N719 dye with an efficiency of 6.40% under the similar fabrication conditions. Thus, D5 appeared as an underpinning structure to design the next series of TPA derivatives.

In 2007, a series L0-L4 of TPA-based organic dyes were published by extending the conjugation in a systematic way . By increasing the π conjugation, the absorption spectra and molar extinction coefficients of L0-L4 were increased. The observed IPCE spectra for L0 and L1 dyes were high, but the spectra of these dyes were not broad; as a result, lower conversion efficiencies were obtained for L0 and L1, whereas the broad absorption spectrum as well as the broad IPCE was

obtained for L3 and L4 by the augmentation of linker conjugation, but the efficiencies observed were less than the L0 and L1 due to the amount of dye loading, i.e., with the increase in the size of dye there appears a decrease in the dye amount. Thus, the lower IPCE obtained for longer L3 and L4 may be accredited to unfavorable binding with the TiO_2 surface. Higher efficiencies were obtained for solar cells based on L1 and L2, 2.75% and 3.08%, respectively. Baheti et al. synthesized DSSCs based on nanocrystalline anatase TiO_2 and simple triarylamine-based dyes containing fluorene and biphenyl linkers. They reported that the fluorene-based dyes showed better solar cell parameters than those of the biphenyl analogues. In 2011, Lu et al. reported the synthesis and photophysical/electrochemical properties of three functional triarylamine organic dyes (MXD5-7) as well as their application in dye-sensitized solar cells. They used the nonplanar structures of bishexapropyltruxeneamino as an electron donor and investigated the impact of addition of chenodeoxycholic acid (CDCA) in the respective dyes, as MXD5-7 without CDCA showed lower photocurrent and efficiency as compared to the dyes MXD5-7 with 3 mM CDCA. However, the highest efficiency of 6.18% was observed for MXD7 (with 3 mM CDCA) with electron lifetime (τ) = 63 ms, under standard global AM 1.5 solar conditions (molecular structure is given in Table 4, where R = propyl).

Using furan as a linker, different TPA-based chromophores were studied by Lin and co-workers. When D5 and its furan counterpart were compared, the results were exciting, still the light harvesting abilities observed for D5 were higher (λ_{abs} = 476 nm with ε = 45,900 M^{-1} cm^{-1} in ACN) than those for the furan counterpart (λ_{abs} = 439 nm with ε = 33,000 M^{-1} cm^{-1} in ACN). However, the performance of the solar cells based on the furan counterpart (η_{max} = 7.36%) was better as compared to the one based on D5 (η_{max} = 6.09%) because of the faster recombination lifetimes in D5. Again, the tendency of trapping of charge from the TPA moeity was higher in thiophene than the furan. In 2016, Simon et al. reported an enhancement in the photovoltage for DSSCs that employed triarylamine-based dyes, where halogen-bonding interactions existed between a nucleophilic electrolyte species (I^-) and a photo-oxidized dye immobilized on a TiO_2 surface. They found larger rate constants for dye regeneration (k_{reg}) by the nucleophilic electrolyte species when heavier halogen substituents were positioned on the dye. Through the observations, they concluded that the halogen-bonding interactions between the dye and the electrolyte can boost the performance of DSSC. However, the most efficient metal-free organic dye-based DSSC has shown PCE of 10.3% in combination with a cobalt redox shuttle, by

using the phenyl dihexyloxy-substituted triphenylamine (TPA) (DHO-TPA) Y123 dye. In 2018, Manfredi and group have designed di-branched dyes based on a triphenylamino (TPA) donor core with different aromatic and heteroaromatic peripheral groups bonded to TPA as auxiliary donors. Thus, due to the improved strategic interface interactions between the dye sensitized titania and the liquid electrolyte, better optical properties were achieved.

Phenothiazine (PTZ) Dyes

Phenothiazine is a heterocyclic compound containing electron-rich sulfur and nitrogen heteroatoms, with a non-planar and butterfly conformation in the ground state, which can obstruct the molecular aggregation and the intermolecular excimer formation. Thus, PTZ results as a promising hole transport semiconductor in the organic devices, presenting unique electronic and optical properties.

Tian and co-workers investigated the effect of PTZ as an electron-donating unit in DSSCs, and because of the stronger electron donating tendency of PTZ unit than the TPA unit (0.848 and 1.04 V vs. the normal hydrogen electrode (NHE), respectively), they found efficient results for the sensitizers based on PTZ rather than those based on the TPA. In 2007, a new series of PTZ-based dyes as T2–1 to T2–4 was demonstrated. In these dyes, PTZ unit acted as an electron donor, cyanoacrylic acid or rhodanine-3-acetic acid was used as an electron acceptor, and alkyl chains were used to increase the solubility. They found a red shift in the absorption spectra of T2–3 ($\eta = 1.9\%$) and T2–4 ($\eta = 2.4\%$) dyes with low IPCE values for rhodanine-3-acetic acid as an anchoring group, as compared to T2–1 ($\eta = 5.5\%$) and T2–2 ($\eta = 4.8\%$) dyes with cyanoacrylic acid as an anchoring group. This proved the use of the cyanoacrylic acid is more viable than a rhodanine-3-acetic acid. In 2010, Tian et al. reported modified phenothiazine (P1-P3) dyes with the molecular structure containing the same acceptor and conjugation chain but different donors. Due to the presence of two methoxy groups attached to TPA, a red shift was observed in the absorption spectra of P1 as compared to P2 and P3. This resulted in an increment in the extent of electron delocalization over the whole molecule and, thus, a little red shift in the maximum absorption peak was observed. Xie et al. synthesized two novel organic dyes (PTZ-1 and PTZ-2) using electron-rich phenothiazine as electron donors and oligothiophene vinylene as conjugation spacers. They employed 13 µm transparent and 1.5 µm scattering TiO_2 electrode and used an electrolyte composed of 0.6 M butylmethylimidazolium iodide (BMII), 0.03 M I_2, 0.1 M

GuSCN, 0.5 M 4-tert-butylpyridine in acetonitrile (TBP in ACN), and valeronitrile. They demonstrated that the (2E)-2-cyano-3-(5-(5-((E)-2-(10-(2-ethylhexyl)-10H-phenothiazin-7-yl)vinyl)thiophen-2-yl)thiophen-2-yl)acrylic acid (PTZ-1) and (2E)-3-(5-(5-(4,5-bis((E)-2-(10-(2-ethylhexyl)-10Hphenothiazin-3-yl)vinyl)thiophen-2-yl)thiophen-2-yl)thiophen-2-yl)-2cyanoacrylic acid (PTZ-2)-based DSSC showed $V_{OC} = 0.70$ V, $J_{SC} = 11.69$ mAcm^{-2}, FF = 65.3, and $\eta = 5.4\%$ and $V_{OC} = 0.706$ V, $J_{SC} = 7.14$ mAcm^{-2}, FF = 55.6, and $\eta = 2.80\%$ under AM 1.5100 mWcm^{-2} illumination, respectively. The effect of hydrophilic sensitizer PTZ-TEG together with an aqueous choline chloride-based deep eutectic solvent (used as an electrolyte) has been reported. In the study, glucuronic acid (GA) was used as a co-absorbent because it as has a simple structure and polar nature and is also able to better interact with hydrophilic media and components and possibly participates to the hydrogen bind interaction operated in the DES medium. PCE of 0.50% was achieved for the 1:1 dye/coabsorbent ratio.

Carbazole Dyes

It is a non-planar compound and can improve the hole transporting ability of the materials as well as avert the dye aggregate formation. Due to its unique optical, electrical, and chemical properties, this compound has been applied as an active component in solar cells. Even with the addition of carbazole unit into the structure, the thermal stability and glassy state durability of the organic molecules were observed to be improved significantly. Tian et al. reported an efficiency of 6.02% for the DSSCs using S4 dye as a sensitizer, with an additional carbazole moiety to the outside of the donor group and found that the additional moiety facilitated the charge separation thereby decreasing the recombination rate between conduction band electrons and the oxidized sensitizer.

A series of MK-1, MK-2, and MK-3 dyes based on carbazole were reported by Koumura et al., where MK-1 and MK-2 have alkyl groups but MK-3 had no alkyl group. They showed that the presence of alkyl groups increased the electron lifetime and consequently V_{OC} in MK-1 and MK-2, and due to the absence of alkyl groups, lower electron lifetime values could be responsible for the recombination process between the conduction band electrons and dye cations in MK-3. New structured dyes, i.e., D–A–π–A-type and D–D–π–A-type organic dyes, have been developed by inserting the subordinate donor–acceptor such as 3,6-ditert-butylcarbazole-2,3-diphenylquinoxaline to facilitate electron migration, restrain dye aggregation, and improve photostability. Thus, by further

extending the π conjugation of the linkers, mounting the electron-donating and electron-accepting capability of donors and acceptors, and substituting long alkyl chains, more stable DSSCs with lower dye aggregation and higher efficiency can be achieved.

Phenoxazine (POZ) Dyes

Phenoxazine is a tricyclic isoster of PTZ. The PTZ and POZ units display a stronger electron donating ability than the TPA unit (0.848, 0.880, and 1.04 V vs. normal hydrogen electrode (NHE), respectively). However, DSSCs based on POZ dyes show better cell performance as compared to PTZ dye-based DSSCs . In 2009, two POZ-based dyes were demonstrated by Tian et al., i.e., a simple POZ dye TH301 and triphenylamine attached to TH301, named as TH305. Due to the insertion of TPA unit in TH305, a red shift in the absorption band was seen because of the higher electron donating capability of POZ. The efficiencies obtained for TH301 and TH305 were 6.2% and 7.7%, respectively, where standard N719 sensitizer showed an efficiency of 8.0% under similar conditions. Thus, in 2011, Karslson reported a series of dyes MP03, MK05, MK08, MK12, and MK13, based on POZ unit, to increase the absorption properties of the sensitizers. Further, two novel metal-free dyes (DPP-I and DPP-II) with a diketopyrrolopyrrole (DPP) core were synthesized for dye-sensitized solar cells (DSSCs) by Qu et al.. They demonstrated the better photovoltaic performance with a maximum monochromatic IPCE of 80% and $\eta = 4.14\%$ with $J_{SC} = 9.78$ mAcm^{-2}, $V_{OC} = 605$ mV, and FF = 0.69, for the DSSC based on dye DPP-I.

Singh et al. have demonstrated nanocrystalline TiO_2 dye-sensitized solar cells with PCE of 4.47% successfully designed two metal-free dyes (TPA–CN1–R2 and TPA–CN2–R1), containing triphenylamine and cyanovinylene 4-nitrophenyls as donors and carboxylic acid as an acceptor.

Semiconductor quantum dots (QDs) are another attractive approach to being sensitizers. These are II–VI and III–V type semiconductor particles whose size is small enough to produce quantum confinement effects. QD is a fluorescent semiconductor nanocrystal or nanoparticle typically between 10 and 100 atoms in diameter and confines the motion of electrons in conduction band, holes in valence band, or simply excitons in all three spatial directions. Thus, by changing the size of the particle, the absorption spectrum of such QDs can be easily varied. An efficiency of 7.0% has been recorded by collaborating groups from the

University of Toronto and EPFL. This recorded efficiency was higher than the solid-state DSSCs and lower than the DSSCs based on liquid electrolytes. A high performance QDSSC with 4.2% of PCE was demonstrated by Li et al. This cell consisted of TiO_2/$CuInS_2$-QDs/CdS/ZnS photoanode, a polysulfide electrolyte, and a CuS counter electrode. In 2014, a conversion efficiency of 8.55% has been reported by Chuang et al.. Recently, Saad and co-workers investigated the influence on the absorbance peak on N719 dye due to the combination between cadmium selenide (CdSe) QDs and zinc sulfide (ZnS) QDs. The cyclic voltammetry (CV) of varying wt% of ZnS found that the 40 wt% of ZnS is an opposite combination for a DSSC's photoanode and has produced the higher current. However, 50 wt% of ZnS was found to be the best concerto to increase the absorbance peak of the photoanode.

Natural dyes

New dye materials are also under extensive research, due to the intrinsic properties of Ru(II)-based dyes, and as a result to replace these rare and expensive Ru(II) complexes, the cheaper and environmentally friendly natural dyes overcome as an alternative.

Natural dyes provide low-cost and environmentally friendly DSSCs. There are various natural dyes containing anthocyanin, chlorophyll, flavonoid, carotenoid, etc. which have been used as sensitizers in DSSCs. Table 5 provides the general characteristics of these dyes, i.e., their availability and color range.

Table 5 Availability and color range for the natural dyes (anthocyanin, carotenoid, chlorophyll, and flavonoid)

Molecular Structure

Anthocyanin: In anthocyanin molecule, the carbonyl and hydroxyl groups are bound to the semiconductor (TiO_2) surface, which stimulates the electron transfer from the sensitizer (anthocyanin molecules) to the conduction band of porous semiconducting (TiO_2) film. Anthocyanin can absorb light and transfer that light energy by resonance energy transfers to the anthocyanin pair in the reaction center of the photosystems.

Molecular structures of LD porphyrins

Flavonoid: Flavonoid is an enormous compilation of natural dyes which shows a carbon framework (C_6–C_3–C_6) or more particularly the phenylbenzopyran functionality. It contains 15 carbons with two phenyl rings connected by three carbon bridges, forming a third ring, where the different colors of flavonoids depend on the degree of phenyl ring oxidation (C-ring). Its adsorption onto mesoporous TiO_2 surface is quite fast by displacing an OH counter ion from the Ti sites that combines with a proton donated by the flavonoid.

Carotenoid: Andanthocyanin, flavonoids, and carotenoids are often found in the same organs. Carotenoids are the compounds having eight isoprenoid units that are widespread in nature. Beta-carotene dye has an absorbance in wavelength zones from 415 to 508 nm, has the largest photoconductivity of 8.2×10^{-4} and $28.3 \times 10^{-4}\ (\Omega.m)^{-1}$ in dark and bright conditions, and has great potential as energy harvesters and sensitizers for DSSCs.

Cholorophyll: Among six different types of chlorophyll pigments that actually exist, Chl α is the most occurring type. Its molecular structure comprises a chlorine ring with a Mg center, along with different side chains and a hydrocarbon trail, depending on the Chl type.

In 1997, antocyanins extracted from blackberries gave a conversion efficiency of 0.56%. The roselle (*Hibiscus sabdariffa* containing anthocyanin) flowers and papaw (*Carica papaya* containing chlorophyll) leaves were also investigated as natural sensitizers for DSSCs. Eli et al. sensitized TiO_2 photoelectrode with roselle extract ($\eta = 0.046\%$) and papaw leaves ($\eta = 0.022\%$), respectively and found better efficiency for roselle extract-sensitized cell because of the broader absorption of the roselle extract onto TiO_2. Tannins have also been attracted as a sensitizer in DSSCs due to their photochemical stability. DSSCs using natural dyes tannins and other polyphenols (extracted from Ceylon black tea) have given photocurrents of up to 8 $mAcm^{-2}$. Haryanto et al. fabricated a DSSC using annato seeds (*Bixa orellana Linn*) as a sensitizer . They demonstrated V_{OC} and J_{SC} for 30 g, 40 g, and 50 g as 0.4000 V, 0.4251 V, and 0.4502 V and 0.000074 A, 0.000458 A, and 0.000857 A, respectively. The efficiencies of the fabricated solar cells using annato seeds as a sensitizer for each varying mass were 0.00799%, 0.01237%, and 0.05696%. They observed 328–515 nm wavelength

range for annato seeds with the help of a UV-vis spectrometer. Hemalatha et al. reported a PCE of 0.22% for the *Kerria japonica* carotenoid dye-sensitized solar cells in 2012.

In 2017, a paper was published on DSSCs sensitized with four natural dyes (viz. Indian jamun, plum, black currant, and berries). The cell achieved highest PCE of 0.55% and 0.53%, respectively, for anthocyanin extracts of blackcurrant and mixed berry juice. Flavonoid dye extracted from Botuje (*Jathopha curcas Linn*) has been used a sensitizer in DSSCs. Boyo et al. achieved $\eta = 0.12\%$ with the $J_{SC} = 0.69$ mAcm^{-2}, $V_{OC} = 0.054$ V, and FF = 0.87 for the flavonoid dye-sensitized solar cell. Bougainvillea and bottlebrush flower can also be used as a sensitizer in DSSCs because both of them show a good absorption level in the range of 400 to 600 nm as a sensitizer, with peak absorption at 520 nm for bougainvillea and 510 nm for bottlebrush flower. A study of color stability of anthocyanin (mangosteen pericarp) with co-pigmentation method has been conducted by Munawaroh et al. They have found higher color retention for anthocyanin-malic acid and anthocyanin-ascorbic acid than that of pure anthocyanin. Thus, the addition of ascorbic acid and malic acid as a co-pigment can be performed to protect the color retention of anthocyanin (mangosteen pericarp) from the degradation process. The *I–V* characteristics of DSSCs employing different natural dyes are shown in Table 6.

Table 6 PV characteristics for different natural dye-sensitized solar cells

Organic Complexes of Other Metals

Os, Fe and Pt complexes are considered to be some other promising materials in DSSCs. Besides the fact that Os complexes are highly toxic, they are applied as a sensitizer in DSSCs due to its intense absorption (α811nm = 1.5 × 103 M− 1 cm− 1) and for the utilization of spin forbidden singlet-triplet MLCT transition in the NIR. Higher IPCE values were obtained in this spectral region; however, the overall conversion efficiency was only 50% of a standard Ru dye. Pt complexes have given modest efficiencies of ca. 0.64% and iron complexes, which are very interesting due to the vast abundance of the metal and its non-toxicity; the solvatochromism of complexes like [FeIIL2(CN)2] can be used to adjust their ground and excited state potentials and increase the driving force for electron

injection into the semiconductor conduction band or for regeneration of the oxidized dye by the electrolyte couple.

Thus, a number of metal dyes, metal-free organic dyes, and natural dyes have been synthesized till today. Many other dyes like K51, K60, K68; D5, D6 (containing oligophenylenevinylene π-conjugated backbones, each with one *N*,*N*-dibutylamino moiety); K77 ; SJW-E1 ; S8 ; JK91 and JK92 ; CBTR, CfBTR, CiPoR, CifPoR, and CifPR ; Complexes A1, A2, and A3 ; T18 ; A597 ; YS-1–YS-5 ; YE05 ; and TFRS-1–3 were developed and applied as sensitizers in DSSCs.

Latest Approaches and Trends

However, a different trend to optimize the performance of the DSSCs has been started by adding the energy relay dyes (ERDs) to the electrolyte [57, 304]; inserting phosphorescence or luminescent chromophores, such as applying rare-earth doped oxides [58,59,60] into the DSSC; and coating a luminescent layer on the glass of the photoanode [61, 62]. In the process of adding the ERDs to the electrolyte or to the HTM, some highly luminescent fluorophores have to be chosen. The main role of ERD molecules in DSSCs is to absorb the light that is not in the primary absorption spectrum range of the sensitizing dye and then transfer the energy non-radiatively to the sensitizing dyes by the fluorescence (Forster) resonance energy transfer (FRET) effect [305]. An improvement in the external quantum efficiency of 5 to 10% in the spectrum range from 400 to 500 nm has been demonstrated by Siegers and colleagues [306]. Recently, Lin et al. reported the doping of 1,8-naphthalimide (N-Bu) derivative fluorophore directly into a TiO_2 mesoporous film with N719 for application in DSSCs [307], in which the N-Bu functioned as the FRET donor and transferred the energy via spectral down-conversion to the N719 molecules (FRET acceptor). An improvement of the PCE from 7.63 to 8.13% under 1 sun (AM 1.5) illumination was attained by the cell. Similarly, Prathiwi et al. fabricated a DSSC by adding a synthetic dye into the natural dye containing anthocyanin (from red cabbage) in 2017 [308]. They prepared two different dyes at different volumes, i.e., anthocyanin dye at a volume of 10 ml and combination dyes at a volume of 8 ml (anthocyanin): 2 ml (N719 synthetic dye), respectively. They observed an enhancement in conversion efficiency up to 125%, because individually the anthocyanin dye achieved a conversion efficiency of 0.024% whereas for the combination dye 0.054% conversion efficiency was achieved. This

enhancement was considered due to the higher light absorption. Thus, greater photon absorption took place and the electrons in excited state were also increased to enhance the photocurrent. Thus, cocktail dyes are also developing as a new trend in DSSCs. Chang et al. achieved a $\eta = 1.47\%$ when chlorophyll dye (from wormwood) and anthocyanin dye (from purple cabbage) as natural dyes were mixed together at volume ratio of 1:1 [309], whereas the individual dyes showed lower conversion efficiencies. Puspitasari et al. fabricated different DSSCs by mixing the three different natural dyes as turmeric, mangosteen, and chlorophyll. The highest efficiency of 0.0566% was attained for the mixture of the three dyes, where the absorbance peak of the mixed dyes was observed at 300 nm and 432 nm [106]. Similarly, Lim and co-workers have achieved a 0.085% of efficiency when mixing the chlorophyll and xanthophyll dyes together [310]. In 2018, Konno et al. studied the PV characteristics of DSSCs by mixing different dyes and observed highest $\eta = 3.03\%$ for the combination dye "D358 + D131," respectively [311].

UV-vis spectra and in insert Q-band magnification for CPI, CPICu, and CPIZn incorporated into the TiO_2 films [237]

An approach used to enhance the performance of DSSCs is plasmonic effect. Surface plasmon resonance (SPR) is resonant oscillation of conduction electrons at the interface between negative and positive permittivity material stimulated by incident light. In 2013, Gangishetty and co-workers synthesized core-shell NPs comprising a triangular nanoprism core and a silica shell of variable thickness. SPR band centered at ~ 730 nm was observed for the nanoprism Ag particles, which overlapped with the edge of the N719 absorption spectrum very well. They found the incorporation of the nanoprism Ag particles into the photoanode of the DSSCs yielded a 32% increase in the overall PCE [312]. Hossain et al. used the phenomenon of plasmonic with different amounts of silver nanoparticles (Ag NPs) coated with a SiO_2 layer prepared as core shell $Ag@SiO_2$ nanoparticles ($Ag@SiO_2$ NPs) and studied the effect of SiO_2-encapsulated Ag nanoparticles in DSSCs. They found the highest PCE of 6.16% for the photoanode incorporated 3 wt% $Ag@SiO_2$; the optimal PCE was 43.25% higher than that of a 0 wt% $Ag@SiO_2$ NP photoanode [313]. However, a simultaneous decrease in the efficiency with further increases in the wt% ratio, i.e., for 4 wt% $Ag@SiO_2$ and 5 wt% $Ag@SiO_2$, was observed. This decrease for the excess amounts of $Ag@SiO_2$ NPs was attributed to three

reasons: (i) reduction in the effective surface area of the films, (ii) absorption of less amount of the dye, and (iii) an increase in the charge-carrier recombination [314]. After analyzing the nyquist plots (as shown in Fig. 25), they have found a decreased diameter of Z_2 monotonically as the Ag@SiO_2 NP content increased to 3 wt% and R2 decreased from 10.4 to 6.64 Ω for the conventional DSSC to the 3 wt% Ag@SiO_2 NPs containing DSSC. Jun et al. used quantum-sized gold NPs to create plasmonic effects in DSSCs [315]. They fabricated the TiO_2 photoanode by incorporating the Au nanoparticles (Au NPs) with an average diameter of 5 nm into the commercial TiO_2 powder (average diameter 25 nm) and used N749 black dye as a sensitizer. Thus, due to the SPR effect, the efficiency for the DSSC (incorporating Au NPs) was enhanced by about 50% compared to that without Au nanoparticles. Effect of incorporating green-synthesized Ag NPs into the TiO_2 photoanode has been investigated in 2017 [316]. Uniform Ag NPs synthesized by treating silver ions with *Peltophorum pterocarpum* flower extract at room temperature showed the Ag NPs as polycrystalline in nature with face centered cubic lattice with an approximate size in the range of 20–50 nm [316]. The PCE of the device was improved from 2.83 to 3.62% with increment around 28% after incorporation of the 2 wt% of the Ag NPs due to the plasmonic effect of the modified electrode. Bakr et al. have fabricated Z907 dye-sensitized solar cell using gold nanoparticles prepared by pulsed Nd:YAG laser ablation in ethanol at wavelength of 1064 nm [63]. The addition of synthesized Au NPs to the Z907 dye increased the absorption of the Z907 dye, thus achieving $\eta = 1.284\%$ for the cell without Au NPs and 2.357% for the cell incorporating the Au NPs. Recently, in 2018, a novel 3-D transparent photoanode and scattering center design was applied as to increase the energy conversion efficiency from 6.3 to 7.2% of the device [317] because the plasmonics plays an important role in the absorption of light and thus, the application is developing at a very fast pace and grabbing a lot of attention worldwide in the last few years. Recently, a study on incorporation of Mn^{2+} into CdSe quantum dots was carried out by Zhang and group [318]. An improved efficiency from 3.4% (CdS/CdSe) to 4.9% (CdS/Mn-CdSe) was achieved for the device upon the addition of Mn^{2+} into CdSe because when Mn^{2+} is doped into the CdSe (as shown in Fig. 26), the QDs on the surface of the film became compact and the voids among the particles were small, thus reducing the recombination of photogenerated electrons. Also with the loading of Mn^{2+} into the CdSe, the size of the QD clusters was increased. However, in QDSCs (quantum dot-sensitized solar cells), there is an inefficient transfer of electrons through the mesoporous semi-conductor layer [319], because their application

on a commercial level is still far off. Thus, Surana et al. reported the assembling of CdSe QDs, tuned for photon trapping at different wavelengths in order to achieve an optimum band alignment for better charge transfer in QDSC [319]. TiO_2 hollow spheres (THSs) synthesized by the sacrifice template method was reported as a scattering layer for a bi-layered photoanode for DSSCs by Zhang and co-workers [320]. They used the mixture of multi-walled carbon nanotubes with P25 as an under layer and THSs as an overlayer for the photoanode which showed good light scattering ability. The cross-sectional FESEM images revealed the disordered mecroporous network for the scattering layer containing THSs which was supposed to be responsible for the enhanced light absorption and the transfer of electrolyte. Thus, $\eta = 5.13\%$ was achieved for P25/MWNTs-THSs, whereas 4.49% of efficiency was reported for a pure P25 photoanode-based DSSC. Also, the electron lifetime (τ_e) estimated for pure P25 by Bode phase plots of EIS spectra was 5.49 ms; however, 7.96 ms was shown for P25/MWNTs-THSs.

Chemical structures of **a** anthocyanin, **b** flavonoid, **c** β,β-carotene, and **d** chlorophyll
IPCE of mixed pigment and single pigments, where single pigment were Eosin Y, D131, and D358 and mixed pigments were D358 and Eosin Y; D358 and D131; D131 and Eosin Y [311]

SEM images of **a** CdS/CdSe and **b** CdS/Mn:CdSe QD sensitization on TiO^2 surface. **c** TEM image of CdS/Mn:CdSe QDs [318]

John and group reported the synthesis and application of ZnO-doped TiO_2 nanotube/ZnO nanoflake heterostructure as a photoanode in DSSCs for the first time in 2016 [321]. They used different characterization techniques to investigate the layered structure of the novel nanostructure. The Rutherford backscattering spectroscopy revealed that during the doping process, a small percentage of Zn was doped into TONT in addition to the formation of ZnO nanoflakes on the top, which led to a preferential orientation of the nanocrystallites in the tube on annealing. Back in 2017, Zhang et al. reported paper on low-dimensional halide perovskite and their applications in optoelectronics due to the ~ 100% of photoluminescence quantum yields of perovskite quantum dots [322]. The main emphasis of their paper was on the

study of halide perovskites and their versatile application, i.e., in optoelectronics in spite of PV applications only. The main role of perovskite nanoparticles in solar cells is being applied as sensitizers. Similarly, in the queue of developing highly efficient DSSCs, Chiang and co-workers fabricated DSSCs based on PtCoFe nanowires with rich {111} facets exhibiting superior I^-_3 reduction activity as a counter electrode, which surpassed the previous PCE record of the DSSCs using Ru(II)-based dyes [323]. Recently, in accordance with enhancing the charge collection efficiencies (η_{coll}) as well as PCE of DSSCs, Kunzmann et al. reported a new strategy of fabricating low-temperature (lt)-sintered DSSC and demonstrated the highest efficacy reported for lt-DSSC to date [324]. They have integrated TiO_2-Ru(II) complex (TiO_2_Ru_IS)-based hybrid NPs into the photoelectrode. Due to a better charge transport and a reduced electron recombination, devices with single-layer photoelectrodes featuring blends of P25 and TiO_2_Ru_IS give rise to a 60% η_{coll} relative to a 46% η_{coll} for devices with P25-based photoelectrodes. Further, for usage of a multilayered photoelectrode architecture with a top layer based on TiO_2_Ru_IS only, devices with an even higher η_{coll} (74%) featuring a $\eta = 8.75\%$ and stabilities of 600 h were shown. The two major rewards obtained for such devices were the dye stability due to its amalgamation into the TiO_2 anatase network and, secondly, the enhanced charge collection yield due to its significant resistance towards electron recombination with electrolytes.

Conclusions

The main aim of this study was to put a comprehensive review on new materials for photoanodes, counter electrodes, electrolytes, and sensitizers as to provide low-cost, flexible, environmentally sustainable, and easy to synthesize DSSCs. However, a brief explanation has been given to greater understand the working and components of DSSCs. One of the important emphases in this article has been made to establish a relation between the photosensitizer structure, the interfacial charge transfer reactions, and the device performance which are essential to know as to develop new metal and metal-free organic dyes. In terms of low stability offered by DSSCs, two major issues, i.e., low intrinsic stability and the sealing of the electrolytes (extrinsic stability), have been undertaken in this study. To fulfill huge demand of electricity and power, we have two best possible solutions: this demand should be compensated either by the nuclear fission or by the sun. Even so, the nuclear fission predicted to be the best alternative has great environmental issues as well as a problems associated with

its waste disposal. Thus, the second alternative is better to follow. DSSCs are developed as a cheap alternative but the efficiency offered by DSSCs in the field is not sufficient. Thus, we have to do a wide research on all possible aspects of DSSCs. We proposed to develop DSCCs based on different electrodes viz. graphene, nanowires, nanotubes, and quantum dots; new photosensitizers based on metal complexes of Ru or Os/organic metal-free complexes/natural dyes; and new electrolytes based on imidazolium salts/pyridinium salts/conjugated polymers, gel electrolytes, polymer electrolytes, and water-based electrolytes. In summary, so far, extensive studies have been carried out addressing individual challenges associated with working electrode, dye, and electrolytes separately; hence, a comprehensive approach needs to be used where all these issues should be addressed together by choosing appropriate conditions of electrolyte (both in choice of material and structure), optimum dye, and the most stable electrolyte which provides better electron transportation capability.

In terms of their commercial application, a DSSC needs to be sustainable for > 25 years in building-integrated modules to avoid commotion of the building environment for repair or replacement and a lifespan of 5 years is sufficient for portable electronic chargers integrated into apparel and accessories [325]. However, DSSCs are being quite bulky due to their sandwiched glass structure, but the flexible DSSCs (discussed elsewhere) that can be processed using roll-to-roll methods may came as an alternative but then has to compromise with the shorter lifespan. Although the stability and lifetime of a DSSC most probably depend on the encapsulation and sealing as discussed above. Apart from the usage of expensive glass substrates in the case of modules and panels, one of the biggest hurdles is to manufacture glass that is flat at the 10 μm length scale over areas much larger than 30×30 cm^2 [326] and the humidity. Another challenge is to choose which metal interconnects in the cells that are more or less corroded to the electrolyte, and high degree of control over cell-to-cell reproducibility is required to achieve same current and/or voltage for all the cells in the module. If the abovementioned challenges would be overcome, then there is no roadblock for the commercial applications of DSSCs, which has been restricted up to an amicable extent. G24i has introduced a DSC module production of 25 MW capacity in 2007 in Cardiff, Wales (UK), with extension plans up to 200 MW by the end of 2008 (http://www. g24i. com), and afterwards, many DSSC demonstration modules are now available. However,

the maximum outdoor aging test of DSSCs is reported for 2.5 years up to now [327].

Abbreviations

ACN: Acetonitrile; ***Ag NPs:*** Silver nanoparticles; ***AM 1.5:*** Air mass 1.5; ***Au NPs:*** Gold nanoparticles; ***BODIPY:*** Boradiazaindacene; ***BPI:*** 4,5-Bis(4-methoxyphenyl)-1H-imidazole; ***CBZ:*** Carbazole; ***CDCA:*** Chenodeoxycholic acid; ***CNF:*** Carbon nanofiber; ***CNT:*** Carbon nanotube; ***CPEs:*** Conjugated polymer electrolytes; ***CV:*** Cyclic voltammetry; ***DPP:*** Diketopyrrolopyrrole; ***DSSCDB:*** Dye-sensitized solar cell database; ***DSSCs:*** Dye-sensitized solar cells; ***EC:*** Ethylene carbonate; ***EIS:*** Electron impedance spectroscopy; ***EPFL:*** Ecole Polytechnique Fédèrale de Lausanne; ***ERDs:*** Energy relay dyes; ***FF:*** Fill factor; ***FRET:*** Fluorescence (Forster) resonance energy transfer; ***FTO:*** Fluorine-doped tin oxide; ***GA:*** Glucuronic acid; ***GBL:*** γ-Butyrolactone; ***GuSCN:*** Guanidinium thiocyanate; ***HTMs:*** Hole transport materials; ***IL:*** Ionic liquid; ***IMVS:*** Intensity-modulated photovoltage spectroscopy; ***IPCE:***Incident photon to current conversion efficiency; ***ITO:***Indium-doped tin oxide; J_{sc} **:**Short circuit current; ***LCs:***Liquid crystals; ***LHE:*** Light harvesting efficiency; ***MePN:*** 3-Methoxypropionitrile; ***MLCT:*** Metal to ligand charge transfer; ***nc:*** Nanocrystalline; ***NHE:*** Normal hydrogen electrode; ***NIR:***Near-infrared region; ***NMBI:*** *N*-Methylbenzimidazole; ***NMP:*** *N*-Methylpyrrolidine; ***NPs:*** Nanoparticles; ***PANI:*** Polyaniline; ***PC:*** Propylene carbonate; ***PCE:*** Power conversion efficiency; ***PEO:***Poly(ethylene oxide); ***PET:*** Polyethylene terephthalate; P_{max} **:** Maximum power output; ***POZ:*** Phenoxazine; ***PTZ:*** Phenothiazine; ***PV:*** Photovoltaic; ***QDs:*** Quantum dots; ***QSSE:*** Quasi-solid-state electrolyte; ***RT:*** Room temperature; ***SCE:*** Saturated calomel electrode; ***SCs:*** Solar cells; ***SPR:*** Surface plasmon resonance; ***SSE:*** Solid-state electrolyte; ***TBP:*** 4-Tert-butylpyridine; ***TCO:*** Transparent conducting oxide; ***TPA:*** Triphenylamine; V_{oc} **:** Open circuit voltage; ***WE:*** Working electrode; ***η :*** Efficiency;

References

1. Tributsch H, Calvin M (1971) Electrochemistry Of Excited Molecules: Photo-Electrochemical Reactions Of Chlorophylls. Photochem Photobiol 14:95–112.

2. Tsubomura H, Matsumura M, Nomura Y, Amamiya T (1976) Dye sensitised zinc oxide: aqueous electrolyte: platinum photocell. Nature 261:402–403.

3. O'Regan B, Gratzel M (1991) A low-cost, high-efficiency solar cell based on dye-sensitized colloidal TiO_2 films. Nature 353:737–740.

4. Nazeeruddin K, Baranoff E, Gratzel M (2011) Dye-sensitized solar cells: A brief overview. Sol Energy 85:1172–1178.

5, Altobello S, Bignozzi C (2004) A, Caramori S, Larramona G, Quici S, Marzanni G, Lakhmiri R; Sensitization of TiO_2 with ruthenium complexes containing boronic acid functions. J Photochem Photobiol A Chem 166:91–98.

6, Kunzmann A, Valero SE, Sepúlveda A, Rico-Santacruz M, Lalinde ER, Berenguer J, García-Martínez JM, Guldi D, Serrano ED, Costa R (2018) Hybrid Dye-Titania Nanoparticles for Superior Low-Temperature Dye-Sensitized Solar Cells. Adv Energy Mat 8:121–212.

7. Snaith HJ (2010) Estimating the Maximum Attainable Efficiency in Dye-Sensitized Solar Cells. Adv Funct Mater 20:13–19.

8. Frank AJ, Kopidakis N, De Lagemaat JV (2004) Electrons in nanostructured TiO2 solar cells: Transport, recombination and photovoltaic properties. Coord Chem Rev 248:1165–1179.

9. Anandan S (2007) Recent improvements and arising challenges in dye-sensitized solar cells. Sol Energy Mater Sol Cells 91:843–846.
10.Anandan S, Madhavan J, Maruthamuthu P, Raghukumar V, Ramakrishnan VT (2004) Synthesis and characterization of naphthyridine and acridinedione ligands coordinated ruthenium (II) complexes and their applications in dye-sensitized solar cells. Sol Energy Mater Sol Cells 81:419–428.

11. Bose S, Soni Vand Genwa KR (2015) Recent Advances and Future Prospects for Dye Sensitized Solar Cells: A Review. Int J Sci Res Pub:5(4).

12. Shalini S, Balasundaraprabhu R, Satish Kumar T, Prabavathy N, Senthilarasu S, Prasanna S (2016) Status and outlook of sensitizers/dyes used in dye sensitized solar cells (DSSC): a review: Sensitizers for DSSC. Int J Energy Res 40:1303–1320.

13. Wu J, Lan Z, Lin J, Huang M, Huang Y, Fan L, Luo G, Lin Y, Xie Y, Wei Y (2017) Counter electrodes in dye-sensitized solar cells. Chem Soc Rev 46:5975–6023.

14. Kakiage K, Aoyama Y, Yano T, Oya K, Fujisawab J, Hanaya M (2015) Highly-efficient dye-sensitized solar cells with collaborative sensitization by silyl-anchor and carboxy-anchor dyes. Chem Commun 51:15894–15897.

15. Yeoh ME, Chan KY (2017) Recent advances in photo-anode for dye-sensitized solar cells: a review. Int J Energy Res 41:2446–2467.

16. Fan K, Yu J, Ho W (2017) Improving photoanodes to obtain highly efficient dye-sensitized solar cells: a brief review. Mater Horiz 4:319–344.

17. Mehmood U (2014) Rahman S, Harrabi K, Hussein IA, Reddy BVS, Recent advances in dye sensitized solar cells. Advances in Materials Science and Engineering Article ID 974782:1–12.

18. Andualem A, Demiss S (2018) Review on Dye-Sensitized Solar Cells (DSSCs). Edelweiss Appli Sci Tech 2:145–150.

19.

Table 1 Parameters of Photovoltaic dye sensitized solar cells using different WEs and CEs.

WE / CE	V_{OC}(mV)	J_{SC} (mA/cm^2)	FF (%)	η (%)
WE TiO_2 doped with tungsten	730	15.10	67	7.42
WE TiO_2 doped with Scandium	752	19.1	68	9.6
WE TiO_2 Doped with Indium	716	16.97	61	7.48

WE TiO_2 doped with Boron	660	7.85	66	3.44
WE TiO_2 doped with Fluorine	754	11	76	6.31
WE TiO_2 doped with carbon	730	20.38	57	8.55
WE CNT/FTO	700	10.65	70	5.32
WE G-TiO_2/TiO_2NTs	690	16.59	56	6.29
WE TiO_2 doped with Cu	591	6.84	56	2.28
WE 25%SnO_2 doped TiO_2	790	14.53	58	6.7
WE Nb_2O_5	738	6.23	68.3	3.15
WE nanographite-TiO_2	720	1.69	35	0.44
CE PtCo	717	16.96	66	7.64
CE Cu_2O	680	11.35	47	3.62
CE PtMo	697	15.48	62	6.75
CE Ni-Pani-G	719	11.56	64	5.32
CE PANI nanocarbons	720	17.92	56	7.23
CE PtCuNi	758	18.30	69	9.66
CE g-C_3N_4/G	723	14.91	66	7.13
CEFeN/N-doped graphene	740	18.83	78	10.86
CE MoS_2 Nanofilm	740	16.96	66	8.28
CE $CoSe_2$	809	17.65	71	10.17
CE electrochemically deposited Pt	750	17.16	60	7.72
CE SS Graphene	524	1.46	26	1.96

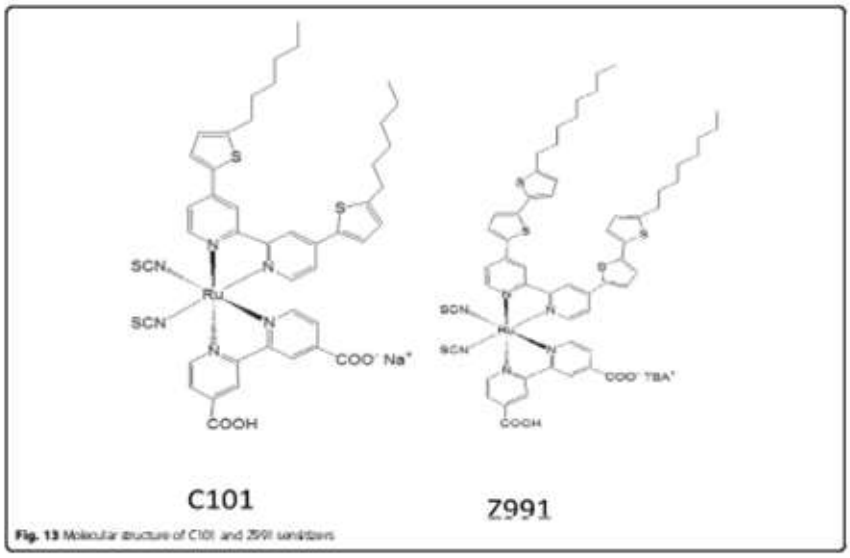

Fig. 13 Molecular structure of C101 and Z991 sensitizers

Table 2 Efficiencies for different dyes and electrolytes

Dye	Redox couple (RC)—(a)/HTM—(b)	FF (%)	η (%)
LEG4 + ADEKA-1	[a] $Co^{III/II}$	77	14.3
D358	Tetra-n-propyl ammonium iodide	60	2.37
N719	[a] I_3^-/I^-	71	8.35
Y123	[a] $Co^{III/II}$	74	8.81
Eosin Y	[a] $Co(bpy)_3$	72	3.85
YD2-o-C8	[a] $Co^{III/II}$	68	8.07
Kojic acid-Azo-4	[a] I_3^-/I^-	75	1.54
N719	[a] I_3^-/I^-	72	8.57
N719	[a] $Co^{III/II}$	71	10.42
N719	[a] I_3^-/I^-	67	7.88
N719	[a] I_3^-/I^-	72	9.96
C106	[a] T_2^-/T^-	70	7.60
C106TBA	[a] I_3^-/I^-	74	9.54
YA423	[a] $Co^{III/II}$	74	10.65
SM315	[a] $Co^{III/II}$	78	13
Y123	[a] $Co^{III/II}$	71	10.30
Z907	[a] T_2^-/T^-	72	7.90
N3	[a] I_3^-/I^-	71	9.25
Y123	[a] $Co^{III/II}$	78	9.90
FNE29	[a] $Co^{III/II}$	70	8.24
CYC-B11	[a] I_3^-/I^-	67	9
3-TPA-R	[a] I_3^-/I^-	72	2.3
T1	[a] I_3^-/I^-	60	5.73
PTZ-1	[a] I_3^-/I^-	65.3	5.4
Y123 (OD)	[b] Spiro-OMeTAD	76	7.2
N719	[b] VM3	43	0.075
Z907	[b] A-537	62	2.48
N3	[b] Pentacene	49	0.8
D102 (OD)	[b] 4-d	32	0.54
SQ (OD)	[b] TVT	64	0.19
D102 (OD)	[b] VMSC9	38	0.47
N719	PET membrane	83	10.24
N719	LC-9% doped	61	4.61
Mangosteen	PEG liquid electrolyte (Type I)	27	0.015
Mangosteen	PEG liquid electrolyte (Type II)	14.5	0.010